Radiation sensitivity and the DNA damage response in planarian stem cells

Thesis submitted for the degree of Doctor of Philosophy in Zoology

Sounak Sahu

Keble College

University of Oxford

Michaelmas Term, 2018

Declaration

I hereby declare that this thesis entitled "*Radiation sensitivity and the DNA damage response in planarian stem cells"* has been originally carried out by me under the supervision of Professor Aziz Aboobaker. This work has not formed the basis for award of any degree or diploma previously. The particulars given in the thesis are true to the best of my knowledge.

Sounak Sahu
Department of Zoology
Keble College
University of Oxford

Acknowledgements

I would like to thank my supervisor Professor Aziz Aboobaker for accepting me as a graduate student to work in his laboratory. He has always been very patient and encouraging throughout the entire course of this D. Phil, giving me lots of freedom and with a willingness to help in all possible ways. I would like to extend my gratitude to Clarendon fund (University of Oxford), Sloane-Robinson Scholarship (Keble College) for funding my D. Phil studies, Zoology Department for the D. Phil completion grant and a research grant from Elizabeth Hannah Jenkinson Fund. A special mention to the Keble Association and many different societies that have supported me in presenting my research in international conferences.

I would also like to express my gratitude to all current and past members of the Aboobaker Lab for all the fun we have had in the last four years. I am grateful to Dr. Nobuyoshi Kosaka and Dr. Prasad Abnave who helped me with timely advice and with optimisation of several techniques described here along with Anish Dattani, Dr. Yuliana Mihaylova, Dr. Alvina Lai, Dr. Natalia Pouchkina-stantcheva, Dr. Damian Kao, Divya Sridhar, Alessia Di-donfrancesco for all their assistance, experimental advice and for intellectual discussions. I would also like to thank my thesis advisory committee members Prof. Peter Holland and Prof. Conrad Nieudszynski for challenging my hypotheses and providing advice on the project.

I would also like to thank our collaborators Dr. Mark. A. Hill, Dr. James Thompson, Luke Bird and Amy Elliott for helping me to use the irradiation facility at the Oncology Department, Mick Woodcock for his assistance in FACS sorting of planarian cells, Dr. Alan Wainman for his help in confocal microscopy, Samuel Hume for his help in COMET assay imaging, Prof. Scott Hawley (Stowers Institute, USA), Dr. Jelena Vermezvoic (IFOM, Italy), Dr. Ian Gibbs Seymour and Prof. Nick Lakin (Oxford Biochemistry) for providing reagents and advice on the project, Dr. Manisha Jalan, Dr. Shifali Shishodia and Dr. Kokil Tandon for proof-reading. A special mention to the undergraduate students (Nazli Akilli, Evangeline Guitard, Erica Boston, Matthew Mcloughlin) and Post-graduate students (Talal Syed) associated with this project. A special mention to all the staff at the Zoology Department and to the Sir William Dunn School of Pathology (during the closure of Tinbergen building) for day-to-day support with general laboratory related reagents and apparatus.

I would like to specially thank my parents for always extending their unconditional love and support and providing with the foundation to stand where I am today. And last but not the least, huge thanks to all my friends for scientific discussions, here in Oxford for their help in my scientific and social life, and supporting me in every possible way to feel home-away home at Oxford.

Abstract

Radiation sensitivity and the DNA damage response in planarian stem cells

Ionizing radiation (IR) can inflict various types of DNA lesions which if not repaired, can induce genomic instability and subsequent oncogenic transformation. Potentially immortal and highly regenerative animals are hypothesized to have enhanced genome maintenance mechanisms to protect their stem cells. One such example, the freshwater planarian, *Schmidtea mediterranea,* contains a large population of collectively pluripotent adult stem cells called neoblasts that are completely ablated following exposure to lethal doses of IR (30 Gy). We identified a non-lethal dose of IR (15 Gy) that leads to a significant decrease in neoblasts but where full recovery of the stem cell number occurs over time. However, there is no evidence that DNA repair is required during regeneration and normal neoblast function. Here we show, exposure to 15 Gy of IR following knockdown of DNA repair gene is lethal, proof of principle that well-known DNA damage response (DDR) genes have a role in stem cell survival and repopulation post IR.

We provide evidence that a new non-canonical role of DDR is to combat DNA damage during stem cell migration and that in the absence of a fully functioning DDR machinery, stem cells fail to migrate. Using an *in-vivo* shielded-irradiation assay, that allows cell migration to be tracked, we observed that neoblasts pre-exposed to IR migrate much slower, in a dose dependent manner, but eventually reach the wound. Migrating neoblasts were also more sensitive to IR than stationary cells suggesting that the mechanical stress due to changes in nuclear shape during migration represents a significant load on repair mechanisms. Our results provide an *in vivo* demonstration that a major novel role of DNA repair mechanisms may be to allow stem cell migration.

Despite enormous efforts to treat cancer, radiotherapy is still the major treatment to kill cancerous cells. There is growing evidence that tumour-initiating cancer stem cells survive and adapt to repeated rounds of IR eventually leading to cancer-recurrence. This radio-tolerance is dependent on an efficient DDR signalling. However, the molecular basis of variations in IR resistance is not well understood. The extraordinary capacity of neoblasts to tolerate high doses of IR offer an opportunity to get novel mechanistic insights into radiation resistance. Using RNA-sequencing we delineate the transcriptional response to IR in planarian stem cells. We identified genes that were differentially expressed in

response to IR and characterized the role of transcription factors (FHL-1) and a tetraspanin family of genes in stem cell repopulation post IR. We further extended our investigation by comparing the transcriptome of irradiated planarian stem cells with a human fibrosarcoma cell line, HT1080. We identified conserved transcriptional responses to IR providing a rich resource to identify radiation responsive genes. Given the conservation between pASCs and mammalian stem cells these conserved genes may include novel druggable targets for combining with radiotherapy.

Key words: Adult stem cells, Cancer, Cell migration, DNA damage response, Genome stability, Ionizing radiation, Neoblast, Planarian, Radiotherapy.

Abbreviations

ASC	adult stem cell
ATM	ataxia-telengiectasia mutated
ATR	ATM and RAD3 related
BSA	bovine serum albumin
bp	Base pair
^{0}C	degree Celsius
cDNA	complementary deoxyribonucleic acid
CSC	cancer stem cell
ChIP	chromatin immuno-precipitation
DDR	DNA damage response
DIG	digoxigenin
DMSO	dimethylsulphoxide
DNA	deoxyribonucleic acid
DNA-PKcs	DNA-protein kinase (catalytic subunit)
dNTP	deoxyribonucleotide triphosphate
dT	deoxythymine
DTT	dithiothreitol
EDTA	ethylenediaminetetraaceticacid
EGFR	epidermal growth factor receptor
ESC	embryonic stem cell
FACS	fluorescence associated cell sorting
FGFR	fibroblast growth factor receptor
FISH	Fluorescence in situ hybridization
FITC	fluorescein isothiocyanate
GFP	green fluorescent protein
Gy	Gray
HR	homologous recombination
HRP	horseradish peroxidase
HSP	heat shock protein
ICL	inter-strand crosslink
IR	irradiation
LB	Luria bertini
MMS	methyl methane sulfonate
MMR	mismatch repair
MMEJ	microhomology mediated end joining
NAC	N-Acetyl-L-cysteine
NB	neoblast
NHEJ	non-homologous end joining
nM	nanomolar
MW	molecular weight
PBS	phosphate buffered saline
PCR	polymerase chain reaction
PI	propidium iodide
PIKK	phosphatidylinositol 3-kinase-like protein kinase
POD	peroxidase
PTEN	phosphatase and tensin
PVDF	polyvinylidene fluoride
rNTP	ribonucleotide phosphate
RNA	ribonucleic acid
RNAse	ribonuclease

rpm	revolutions per minute
RPKM	reads per kilobase million
SC	stem cell
SSC	Saline sodium citrate
SSA	single strand annealing
SDS-PAGE	sodium dodecyl sulphate polyacrylamide gel electrophoresis
SDSA	synthesis-dependent strand annealing
SMG-1	suppressor of Male Genitalia-1
Sec	second(s)
Taq	*Thermus aquaticus*
TNF	tumour necrosis factor
TOR	target of rapamycin
TRAF	TNF receptor associated factor
TSA	tyramide signal amplification
TSG	tumour suppressor gene
Tm	melting temperature
TNT	Tris-NaCl-Tween20
µg	Microgram(s)
µl	Microlitre (s)
VNC	ventral nerve cord

Table of contents

Declaration…………….……………………………………………………….……..i
Acknowledgements……….………………………………………………………ii
Abstract…………………………………..……………………………………iii
Abbreviations……………………..………………………………………….…v

Chapter 1. Introduction……………………………………………....1

1.1 Regeneration and stem cells ……………………………………………….. 2

1.2 An overview of planarian stem cells, tissue homeostasis and regeneration……………………………………………………………………………. 6

1.2.1 The experimental accessibility of planarians and their stem cells 6
1.2.2 Neoblast heterogeneity and lineage commitment in planarians 7

1.3. Planarians as a model for stem cell biology to study genome maintenance mechanisms……………………………………………………………………… 10

1.3.1 The immortality of the stem cell population and regenerative mechanisms act together to maintain genome stability in planarians 11
1.3.2. Protection against stem cell transformation and cancer in stem cells. 12
1.3.3. Guarding the genome against endogenous DNA damage and mutational processes. 16
1.3.4. High resistance to exogenous damaging agents suggests highly efficient DNA repair mechanisms 18

1.4. DNA damage response: the evolutionary trade-off between regeneration and tumour suppression……………………………………………………………….

1.4.1 DNA damage response in embryonic stem cells (ESCs) and induced pluripotent stem cells (iPSCs) 20
1.4.2. DNA damage response in tissue-specific adult stem cells 23
1.4.2. 1. Stem cells in the intestine 23
1.4.2.2. Hematopoietic stem cells (HSCs) 24
1.4.2.3. Epidermal stem cells/Hair follicle stem cells 24

1.4.3. DNA damage response in germline stem cells 27
1.4.4. DNA damage response in cancer stem cells (CSC) 30
1.4.5. DNA damage response in post-mitotic cells 33

1.5. Thesis aim and outline 36

Chapter 2. Material and methods……………………………………....

2.1. Planarian culture 39

2.2. Total RNA isolation 39

2.3. cDNA synthesis and amplification of planarian genes 39

2.4. Cloning into pPR-T4P vector 40

2.5. RNA interference for gene knockdown in planarians

2.5.1. Generation of double-stranded RNA (dsRNA) 41

2.5.2. Microinjection 42

2.6. Riboprobe synthesis 42

2.7. *In situ* hybridization 43

2.8. Immunostaining 44

2.9. Sectioning of planarian worms 45

2.10. Cell dissociation and fluorescence activated cell sorting (FACS) 46

2.11. RNA isolation from dissociated cells for library preparation 47

2.12. Library preparation for RNA sequencing 47

2.13. RNA-sequencing data analysis (planarian and human dataset) 48

2.14. COMET Assay (Single cell gel electrophoresis) 49

2.15. Western blotting 50

2.16. Generation of *Schmidtea* H2AX antibody 51

2.17. Cell culture of HT1080 cells 51

2.18. Immunostaining of HT1080 cells for γ-H2Ax assay 52

2.19. Gamma Irradiation 52

2.20. Shielded irradiation assay 53

2.21. Dosimetry 53

2.22. Measurement of cell migration in shielded irradiation assay 54

2.23. Image processing and data analysis 54

2.24. Statistical analysis 54

Chapter 3. Radiation sensitivity and the DNA damage response in planarian stem cells……………………………………………………………

3.1. Introduction………………………………………………………………………
3.1.1. The DNA damage response pathway 56
3.1.2. DNA repair pathway choices 57
3.1.2.1. End resection and cell cycle phase 57
3.1.2.2. DSB in repetitive sequence and in microhomologies 60
3.1.2.3. Throughout the cell cycle: canonical NHEJ 61
3.1.3. DSB repair and genome plasticity 61
3.2. Aim of this chapter……………………………………………………… 62
3.3. Results and discussion……………………………………………………… 63
3.3.1. Planarians can resist a high dose of 15 Gray (Gy) γ-irradiation 63
3.3.2. Methods to study the DNA damage response in planarian stem cells 68
3.3.2.1. Immunostaining to detect DNA damage in stem cells 68
3.3.2.1.1. H2Ax in planarians 68
3.3.2.1.2. RAD51 and Poly-ADP-Ribose (PAR) formation after DNA damage 71
3.3.2.2. COMET assay 75
3.3.3. Identification of DNA repair genes in the planarian genome 77
3.3.4. Identification and understanding the role of transducers of DNA DSB repair 80
3.3.5. Identification of BRCA2 genes in *Schmidtea mediterranea* 81
3.3.6. Role of Microhomology mediated end-joining (MMEJ/Alternative NHEJ) repair pathway in *Schmidtea mediterranea* 88
3.3.7. p53 binding proteins: 53BP1 and 53BP2 in planarians 93
3.3.8. Double knockdown of *atr, atm, brca2* and *parp1* suggest a synergistic interaction to maintain planarian stem cells. 96
3.3.9. Role of the Fanconi Anaemia pathway in radiation sensitivity 98
3.3.10. The Mismatch Repair (MMR) pathway in planarians. 101
3.4. Conclusion………………………………………………………………. 103

Chapter 4. Role of DNA damage response during stem cell migration………………………………………………………………………..

4.1. Introduction…………………………………………………………………………..
4.1.1. Cell migration 105
4.1.2. Cell migration in health and disease 107

4.2. Aim of this chapter………………………………………………………………… 108

4.3. Results and discussion……………………………………….……………….
4.3.1. Overview of the X-ray-shielded irradiation assay to study cell migration 109

4.3.2. Role of the nucleus during stem cell migration 111

4.3.3. Effect of ionizing radiation in stem cell migration 114

4.3.4. Migrating cells are sensitive to a low dose of ionizing radiation 117

4.3.5. RNAi of conserved DNA repair genes impairs stem cell migration to wound sites 120

4.4. Conclusion…………………………………………………………………….... 123

Chapter 5. Transcriptional response of planarian stem cells to ionizing radiation…………………………………………………………………

5.1. Introduction…………………………………………………………………………. 125

5.1.1. Interplay between transcription and DNA repair 125
5.1.2. The transcriptional response to IR in different organism 126

5.2. Aim of this chapter……………………………………..……………………….. 128

5.3. Results and discussion………………………………………………………… 128

5.3.1. The transcriptional response to γ-irradiation in planarian stem cells. 129
5.3.2. Functional characterization of IR-responsive genes 136
5.3.3. Evolutionarily conserved responses to ionizing radiation in human cancer cells 140
5.3.3.1. γ-H2AX immunostaining show IR-induced DNA damage in HT1080 cells. 140
5.3.3.2. IR induces DNA protective proteins, anti- 142

apoptotic and matrix remodeling proteins in HT1080 cells
5.3.3.3. Evolutionarily conserved responses between planarian stem cell and HT1080 fibrosarcoma cell line. 146
5.4. Conclusion………………………………………………………………………….. 147

Chapter 6. Discussion and future directions.............……..…….

6.1. Discussion………………………………………………………………………... 150

6.2. Future directions………………………………………………………………. 156

Chapter 7. Appendix………………………………………………..…

7.1. Appendix A: Details of the reagents used in this study 161
7.2. Appendix B: Details of the plasmid used in this study 165
7.3. Appendix C: Amino-acid sequences of DDR genes used in this study 166
7.4. Appendix D: Publications from D.Phil 172

References…………………………………………………….……….. 173

Table of figures

Chapter 1. Introduction

1.1 A simplified overview of planarian regeneration, different cell types and reproductive strategy. 4
1.2 A simplified diagram of neoblast heterogeneity and lineage commitment in planarian stem cells. 9
1.3. Evolution of a high regenerative capacity can protect against the pathology caused by cancer. 14
1.4. Schematic showing the effect of different exogenous and endogenous sources leading to DNA damage in induced pluripotent stem cells (iPSCs). 22
1.5. Schematic showing the role of different DNA repair pathways employed by tissue-specific adult stem cells. 26
1.6. DNA damage response in germline stem cells. 29
1.7. DNA damage response in cancer stem cells. 32
Chapter 3. DNA damage response and radiation sensitivity in planarian stem cells
3.1. Schematic showing the different DNA repair pathway choice in eukaryotic cells. 59
3.2. Planarian stem cells can resist doses up to 15 Gy of γ-irradiation. 64
3.3 Dynamics of stem cell proliferation after different dose of IR. 66
3.4. Flow cytometry data showing the survival of planarian stem cells at different phases of cell cycle to different doses of IR. 67
3.5. H2AX in planarians. 70
3.6. RAD51 foci and Poly ADP-Ribose (PAR) polymer formation in planarian stem cells. 73
3.7. Optimisation of Anti-PAR antibody to detect DNA damage in planarian stem cells. 74
3.8. Single cell gel electrophoresis (COMET assay) to detect irradiation-induced DNA damage in planarian cells. 76
3.9. Evolutionary conservation of DNA repair genes in planarians. 79
3.10. The identification of key proteins involved in homologous recombination. 84
3.11. The role of HR-related genes in stem cell maintenance and during repopulation post irradiation. 86
3.12. Alternative NHEJ/Microhomology-mediated end-joining (MMEJ) pathway in planarians. 90
3.13. The role of Alternative NHEJ/Microhomology-mediated end-joining (MMEJ) pathway in stem cell maintenance and during repopulation post IR. 91

3.14. The role of p53 binding proteins in planarians. 95
3.15. Combination knockdown of *atr, atm, brca2* leads to defects in stem cell maintenance. 97
3.16. The role of Fanconi anaemia (FA) genes in stem cell maintenance post IR. 100
3.17. The role of mismatch repair proteins in planarians. 102

Chapter 4. Role of DNA damage response during stem cell migration

4.1. An overview of different types of cell migration 106
4.2. Shielded irradiation assay to study stem cell migration 110
4.3. Changes in nuclear aspect ratio during stem cell migration. 113
4.4. Stem cells pre-loaded with damage before wounding show delays in migration. 115
4.5. Radiation sensitivity of stem cells during migration 118
4.6. Active DNA repair machinery is necessary for continued migration in response to wounding. 122

Chapter 5. Transcriptional response of planarian stem cells to ionizing radiation

5.1. The fate of transcription near double-stranded break is dependent on the DNA damage sensing mechanism. 127
5. 2. Experimental strategy to understand the transcriptional response to γ-irradiation in planarian stem cells. 131
5.3. Transcriptional response to γ-irradiation in planarian stem cells. 132
5.4. Expression pattern of tetraspanin group genes in planarians 138
5.5. Role of FHL and tetraspanin in stem cell repopulation post IR. 139
5.6. γ-H2AX immunostaining show IR-induced DNA damage in HT1080 cells 141
5.7. Transcriptional response of HT1080 fibrosarcoma cells in response to γ-irradiation. 144
5.8. Gene Ontology analysis of differentially expressed genes in HT1080 fibrosarcoma cell line after exposure to 2 Gy of γ -irradiation 145

Chapter 1

Introduction

Part of this chapter has been published in *“Secrets from Immortal worms: What can we learn about biological ageing from the planarian model system?”* S. Sahu, A. Dattani, A. A. Aboobaker; Seminars in Cell and Developmental biology; 2017; **70,**108-121. Some recent references have been updated.

1. Introduction

1.1 Regeneration and stem cells

A fundamental feature of multicellular organisms is the ability to respond to injury and regenerate missing body parts to restore tissue integrity. In recent years, great strides have been made in our understanding of how stem cells (SCs) govern tissue homeostasis, repair and regeneration. For example, human skin constantly regenerates to heal from wounds and deal with daily wear and tear (Fuchs, 2016). Other cells that contribute to regeneration can be found in many human tissues like heart, skeletal muscle, bone and liver (Carlson, 2005). Compared to most vertebrates, adult mammals have a very limited regenerative capacity (Iismaa et al., 2018; Simkin et al., 2015). This has led to modern regeneration biologists focussing on highly regenerative species in the animal kingdom. Animals that have robust regenerative abilities throughout their life history include Hydra (Galliot, 2012), Hydractinia (Gahan et al., 2016), ascidians (Brown et al., 2009), echinoderms (Kondo and Akasaka, 2010), annelids (Bely et al., 2014; Özpolat and Bely, 2016; Yoshida-Noro and Tochinai, 2010), planarians (Reddien and Sánchez Alvarado, 2004), macrostomum (Wudarski et al., 2017) crustaceans (Grillo et al., 2016) and urodele amphibians (like newts and salamanders (Brockes and Gates, 2014; Nacu and Tanaka, 2011)) [for reviews on regeneration in non-model organisms; refer to (Lai and Aboobaker, 2018; Tanaka and Reddien, 2011; Yun, 2015)]. Some of these regenerating animals like Hydra (Schaible et al., 2015; Tomczyk et al., 2015) and planarians (Aboobaker, 2011; Mouton et al., 2009; Rink, 2013; Tan et al., 2012; Valenzano et al., 2017) seem to avoid the physiological decline that characterises ageing. These can even be referred to as somatically immortal, based on the observation of a species life cycle that does not involve either sexual reproduction (and meiosis) or development from a zygote, but instead uses only regeneration to reproduce.

Recent efforts to understand stem cell biology and the widespread nature of regenerative process have focused on freshwater planarians, in particular, *Schmidtea mediterranea* [Fig 1.1 A and B]. In this chapter, we focus on discussing

planarian flatworms, that have been formally studied as a research system for well over a century and were recognised as potentially immortal (Dalyell, 1814; Reddien and Sánchez Alvarado, 2004). These animals are famous for their amazing powers of regeneration; capable of regenerating all organs and tissues of the body starting from small fragments. This ability is fuelled by a population of collectively pluripotent adult stem cells called neoblasts (NBs) capable of making all body tissues and undergoing indefinite self-renewal [Fig 1.1 C and D] (Elliott and Sánchez Alvarado, 2013; Newmark and Sánchez Alvarado, 2002).

The extent of regenerative ability varies greatly across flatworms (Egger et al., 2007) and even within the Triclad planarians where head regeneration can be reactivated by genetic manipulation (Liu et al., 2013b; Sikes and Newmark, 2013). Planarians generally reproduce sexually, however, in many cases, such as the laboratory model species *Schmidtea mediterranea*, an asexual species that reproduces by exploiting regeneration has also evolved from the sexual state [Fig. 1.1 E and F] (Solana, 2013). In these scenarios, reproduction has become entirely a collective function of the stem cell population, which as well as powering regeneration effectively take on the role of the germline. For these asexual species to persist as a continuous adult population these somatic stem cells must be collectively immortal and underpin ever-ongoing homeostatic maintenance of healthy adult tissues.

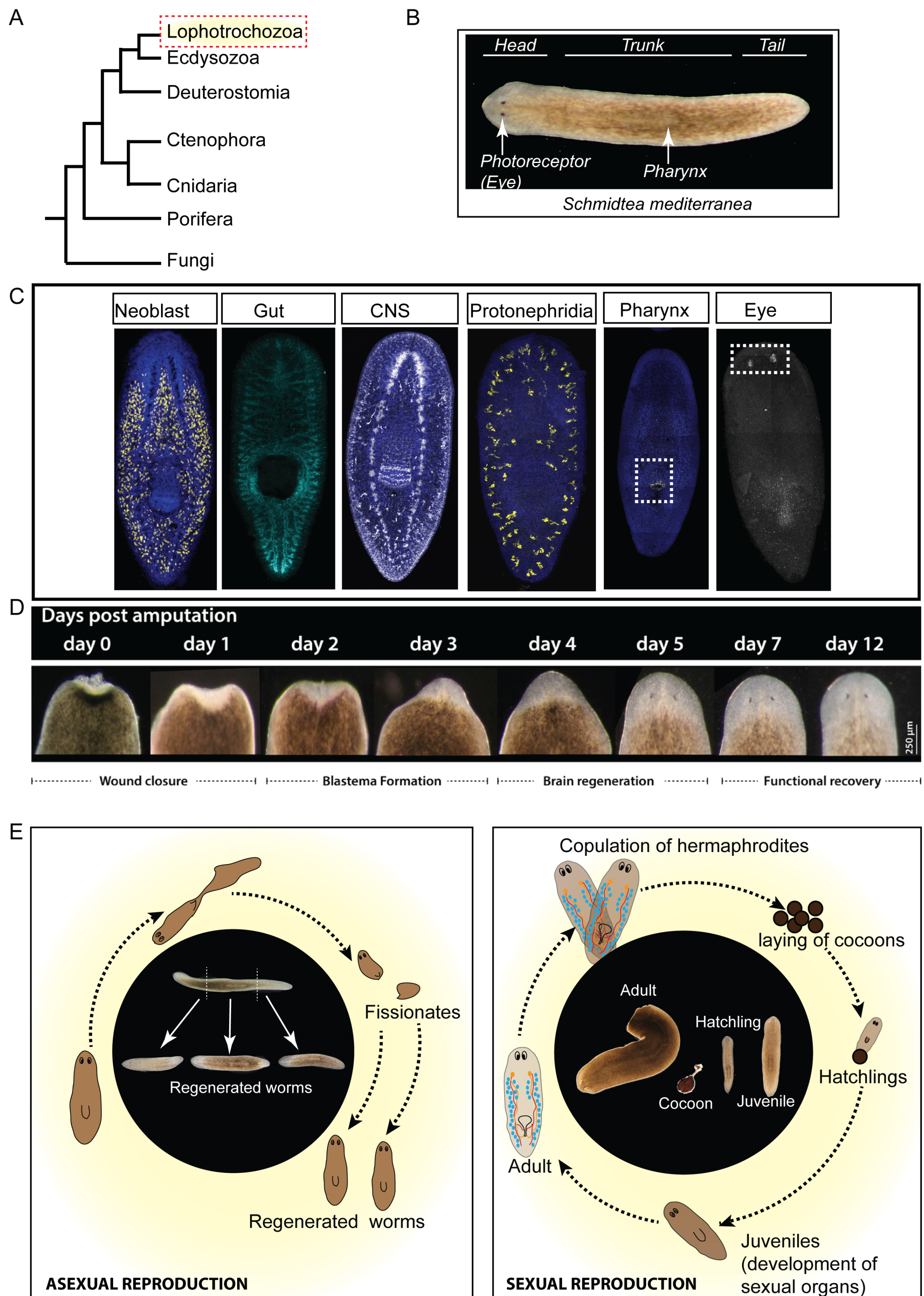
A
Lophotrochozoa
Ecdysozoa
Deuterostomia
Ctenophora
Cnidaria
Porifera
Fungi
B
Head
Trunk
Tail
Photoreceptor (Eye)
Pharynx
Schmidtea mediterranea
C
Neoblast
Gut
CNS
Protonephridia
Pharynx
Eye
D
Days post amputation
day 0
day 1
day 2
day 3
day 4
day 5
day 7
day 12
250 µm
Wound closure
Blastema Formation
Brain regeneration
Functional recovery
E
Fissionates
Regenerated worms
Regenerated worms
ASEXUAL REPRODUCTION
Copulation of hermaphrodites
laying of cocoons
Adult
Hatchling
Cocoon
Juvenile
Hatchlings
Adult
Juveniles (development of sexual organs)
SEXUAL REPRODUCTION

Figure 1.1 A simplified overview of planarian regeneration, different cell types and reproductive strategy. (A) Molecular phylogeny places planarian within the Lophotrochozoans. (Branch lengths of the phylogenetic tree are not drawn to scale).

(B) Bright field image of a live planaria (Model: *Schmidtea mediterranea*), showing photoreceptor (eyes) on the anterior side and with pharynx in the trunk (feeding organ).

(C) Fluorescence *In Situ* Hybridisation (FISH) showing the distribution of planarian stem cells, neoblasts (*Piwi-1*), gut, central nervous system (Immunostaining with Anti-SYNAPSIN) showing bilobed brain and ventral nerve cord, protonephridia (*Carbonic anhydrase VII*), pharynx (*Laminin*), photoreceptors (*Tyrosine hydrolase, TPH*) [mRNA are *italicized* and protein names are in BOLD].

(D) The robust regenerative ability of a decapitated planarian (*Schmidtea mediterranea)*. Regeneration in planarians involves a rapid wound closure by the adjacent epithelial cells (0-1 dpa), formation of unpigmented blastema (2-3dpa), regeneration of the brain and formation of photoreceptors (3-7dpa) followed by a phase of morphallaxis to maintain body proportion. [dpa: days post amputation]

(E) Mode of reproduction in *Schmidtea mediterranea.* Asexually reproducing planarians stretch their body post-pharyngeal and split into two pieces. Each piece regenerates the missing parts resulting in two worms, thus exploiting regeneration as a mode of reproduction. Sexually mature hermaphrodites copulate and lay cocoons. These cocoons give rise to hatchlings, which eventually develop the germline and become sexually mature. Sexually reproducing planarians are also capable of whole-body regeneration but use the germline as their mode of reproduction.

1.2. An overview of planarian stem cells, tissue homeostasis and regeneration

1.2.1. The experimental accessibility of planarians and their stem cells

While a substantial amount of research has been conducted on planarians throughout the late nineteenth and twentieth century (Dalyell, 1814; Elliott and Sánchez Alvarado, 2013; Johnson, 1822; Morgan, 1898, 1901), it was the discovery of RNAi that catalysed a major rejuvenation in planarian research (Fire et al., 1998; Newmark et al., 2003; Reddien et al., 2005a; Sánchez Alvarado and Newmark, 1999). Over the last twenty years, the ability to study gene function in planarians has allowed the growing research community to advance our understanding of the biology of these exciting animals (Aboobaker, 2011; Adler and Sánchez Alvarado, 2015; Elliott and Sánchez Alvarado, 2013; Reddien, 2018; Rink, 2013). Improvements in sequencing technology have also benefited planarian research leading to the sequencing of the *S. mediterranea* genome (Grohme et al., 2018; Robb et al., 2015), many transcriptome studies (Blythe et al., 2010; Brandl et al., 2016; Kao et al., 2013; Labbé et al., 2012; Önal et al., 2012; Rozanski et al., 2018; Solana et al., 2012; Swapna et al., 2018), single cell expression profiling (van Wolfswinkel et al., 2014) and RNA sequencing (Molinaro and Pearson, 2016; Wurtzel et al., 2015, 2017), single cell transcriptome atlases (Fincher et al., 2018; Plass et al., 2018) and genome-wide epigenetic studies (Dattani et al., 2018a; Duncan et al., 2015; Mihaylova et al., 2018). The ability to accurately FACS-sort stem cells at different stages of the cell-cycle and undifferentiated progenitor cells from differentiated cells, based on nuclear to cytoplasmic ratios, has provided essential access to these cells to apply genome-wide analysis (Hayashi et al., 2006; Romero et al., 2012). These ‘omic approaches, combined with an ever-growing list of cell and tissue markers and improved protocols of visualising gene expression in whole animals, provides a powerful set of tools for planarian researchers (Brown and Pearson, 2015; Currie et al., 2016; King and Newmark, 2013; Newmark and Sánchez Alvarado, 2000). One notable absence is an approach to deregulate gene function or exploiting genome editing tools, and this deficit needs urgent attention to improve

the depth of mechanistic insight that can be achieved in this model organism.
Due to these developments and some elegant experimental designs, we now understand some fundamental aspects of regeneration. One emerging theme is that well-known signalling pathways conserved in embryogenesis have conserved roles and interactions during regeneration (Almuedo-Castillo et al., 2011; Hill and Petersen, 2015; Petersen and Reddien, 2008, 2009, 2011; Rink et al., 2009; Roberts-Galbraith and Newmark, 2013; Tejada-Romero et al., 2015). Additionally, many similarities between planarian stem cells and mammalian embryonic and germ-line stem cells have been discovered (Aboobaker and Kao, 2012; Dattani et al., 2018a; Önal et al., 2012; Solana, 2013). This, along with other studies across metazoans (Alié et al., 2011, 2015; Juliano et al., 2010) , has contributed to an appreciation of surprising levels of molecular conservation across animal stem cells and the mechanisms that underpin “stemness’. This molecular conservation suggests that many discoveries made in planarians and other highly regenerative animals will be directly relevant to understand human diseases related to dysfunction of stem cell population.

1.2.2. Neoblast heterogeneity and lineage commitment in planarians

Planarians are somewhat unusual in having adult stem cells that are collectively, and in at least some cases individually, pluripotent (Wagner et al., 2011; Zeng et al., 2018). Currently the consensus is that planarian stem cells (SCs) are the cycling cells that express transcripts considered to be pan-stem cell markers, with the most widely used being the *smedwi-1* (coding for a PIWI family ortholog) (Reddien et al., 2005b) and *Smed-Histone 2B* (encoding a Histone 2B protein) (Guo et al., 2006; Solana et al., 2012) (Fig 2 A - B). The injection of single NBs into a lethally irradiated hosts, where all cycling cells have been killed, has been shown to rescue individual planarians. It was also possible to establish new populations from these rescued individual (Wagner et al., 2011). While the main conclusion from this work is that individual SCs can be pluripotent, it also provides compelling evidence that a ‘individual’ somatic stem cell and its descendants generated by self-renewal are immortal.

Sampling expression in individual planarian SCs has revealed some heterogeneity in the population at both, the level of gene expression and at the level of potency. These experiments reveal a stem cell population (called *sigma*) that gives rise to *zeta* and *gamma* SC [Fig 1.2. A – B]. Each of these three classes is enriched for expression for specific transcription factors. Functional experiments have revealed that *zeta*-SCs are committed to the epidermal lineage, which is currently the best-described lineage in planarians [Figure 1.2. A – B]. (van Wolfswinkel et al., 2014). The expression profile of markers of the *gamma* sub-population suggests that these SCs are very likely committed to making the gut and endodermal lineages. Both *zeta* and *gamma* SCs do not appear to have any self-renewing capacity. Once transiting from the *sigma*-SC class to *zeta* or *gamma* during S-phase they appear to go through mitosis and leave the cell cycle. This observation is based on gene expression, so it is possible they switch off *zeta* and *gamma* marker expression and reactivate *sigma* marker expression to stay in the cell cycle. However, recent analyses of condensin knockdown phenotypes, which block mitosis and can result in endocycling, revealed that only the *sigma*-SCs have increased DNA content indicative of having attempted multiple rounds of division. These data suggest that only sigma-SCs are capable of self-renewal (Lai et al., 2018). Another single cell RNA-seq. study has suggested the existence of a *smedwi-1*$^{-ve/low}$ population of *nu*-neoblasts, committed to neural fate (Molinaro and Pearson, 2016). To date, the use of *piwi1* expression to identify SC subclasses has been qualitative and recent quantitative methods to simultaneously measure piwi1 mRNA and PIWI1 protein expression resolved some heterogeneity of the SC compartment. Single-cell RNA-sequencing of Piwi1^{high} cells revealed a SC cluster marked by a tetraspanin family integral membrane protein (TSPAN1). We now can prospectively isolate pluripotent stem cells using an antibody to TSPAN-1 and single cell transplantation of TSPAN1^{+} cells can rescue and repopulate a lethally irradiated planarian, suggesting the existence of a truly pluripotent stem cell cluster. (Zeng et al., 2018). However, the authors did not directly address whether or not other cells are also pluripotent.

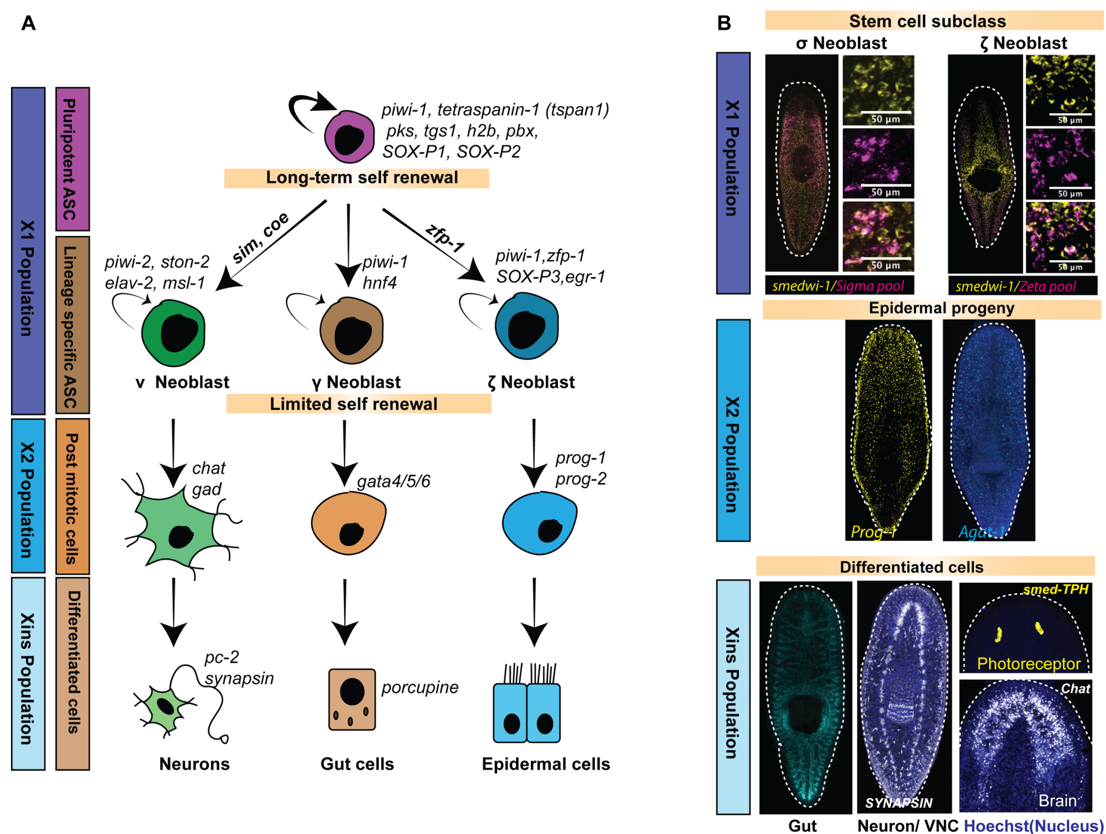

Figure 1.2. A simplified diagram of neoblast heterogeneity and lineage commitment in planarian stem cells. (A) Stem cells/Neoblasts (NBs) in planarians express *smedwi-1* (coding for a PIWI family ortholog) and *Smed-Histone2B* (encoding a Histone 2B protein) transcripts. *Smedwi-1*$^{+}$ cells are considered to be collectively pluripotent and contain a population of clonogenic neoblasts expressing tetraspanin-1 *(tspan-1)*, polyketide synthetase (*pks-1*) and tetraspanin group specific gene *(tgs-1)* that can self-renew and collectively give rise to other stem cell lineages/ progenitors. Sigma class NBs (expressing relatively high levels of SRY-box family genes *SoxP1, SoxP2*) give rise to Zeta (expressing Zinc finger protein family genes *Zfp1, SoxP3, egr1*) NBs, Gamma NBs (expressing *hnf4*) and nu NBs (expressing *smedwi-2, elav2, ston2, but with low/no smedwi-1*). This subset of lineage committed NBs differentiate to give rise to epidermis, gut and the neuronal cell types.

(B) Representative FISH images showing the different subclasses of cycling stem cells (Sigma class represented by *piwi-1* in yellow, Sigma pool consisting of *SOX-P1, SOX-P2*, in magenta; Zeta class represented by *piwi-1* in yellow, Zeta pool consisting of Zfp-1, *SOX-P3, egr-1*, in magenta). This represents the X1 (stem cells in S/G2/M phase of the cell cycle) fraction in a FACS plot. X2 Fraction is a mixture of stem cells in G1 phase and post-mitotic progenies. The epidermal progeny is characterized by *Prog-1* (Yellow) marking the early epidermal progenitors and *Agat-1* (Cyan) marking the late epidermal progenitors. Xins fraction in a FACS plot represents the X-ray insensitive cells comprising of differentiated cells, marking the Gut, Ventral Nerve Cord (SYNAPSIN), Photoreceptors (*TPH*), and brain (*Choline Acetyl Transferase,ChAT*)

We now know that many aspects of stem cell biology in planarians are conserved with vertebrates and mammals. These include the overall molecular expression profile of stem cells (Önal et al., 2012; Wang et al., 2010b), control of splicing and intron retention (Solana et al., 2016), epigenetic regulation (Dattani et al., 2018a; Duncan et al., 2015; Mihaylova et al., 2018) and the mechanisms controlling stem cell migration (Abnave et al., 2017; Guedelhoefer and Sánchez Alvarado, 2012). Together this body of work has established planarians as a powerful model system for studying stem cells and fundamental aspects of regeneration.

1.3. Planarians as a model for stem cell biology to study genome maintenance mechanisms

If planarians are to be a useful model organism we first need to establish which specific causes of genome instability are relevant to an animals' life history and have been solved by the evolution of appropriate cellular and molecular mechanisms. If we consider what are currently thought to be the likely causes of genome instability in humans, we can see that many of the primary molecular causes must also be relevant to planarians. For example, the immortal life history of planarian SCs is aided by their ability to protect their DNA against both endogenous and exogenous mutagenic agents as well as circumvent the issue of telomere attrition common to all eukaryotic cells with linear chromosomes (Tan et al., 2012). In addition to avoiding mutation to the genome sequence itself, SCs must avoid adverse effects from other necessary cellular activities such as the maintenance of a tightly regulated genome-wide epigenetic state (Pal and Tyler, 2016; Sen et al., 2016) and correct cellular proteostasis (Kaushik and Cuervo, 2015; Steffen and Dillin, 2016), both of which can have long-term effects on cellular function. Another relevant fundamental cause of genome instability is mitochondrial dysfunction leading to increased production of mutagenic and damaging reactive oxygen species (ROS) (Finkel and Holbrook, 2000; López-Otín et al., 2013). It may be that planarian SCs have evolved efficient and/or novel pathways for dealing with these harmful processes.

Stem cell pools can eventually become exhausted as cells undergo senescence as a result of elevated levels of DNA damage or simply due to reaching the end of their normal replicative lifespan (Burkhalter et al., 2015; Sperka et al., 2012). Alternatively, transformation of stem cells leads to over-proliferation and cancer. Poorly functioning stem cells will produce poorly functioning differentiated cells in tissues and organs that can affect broader physiological function. This can also feedback to the stem cell pool through poor stem cell niche signalling affecting both stem cell self-renewal and differentiation (Oh et al., 2014; Schultz and Sinclair, 2016). Investigating the underlying processes bestowing the ability to maintain genome stability in stem cells will be informative for developing anti-cancer strategies in the future.

1.3.1 The immortality of the stem cell population and regenerative mechanisms act together to maintain genome stability in planarians

We might predict those mechanisms that maintain genome integrity would be very efficient and play a core part of stem cell function, and that high-risk processes (like ROS forming energy production) would be limited or removed. We now know that SCs appear to be able to avoid telomere attrition in some contexts, have powerful protection against endogenous sources of genome instability and are remarkably resistant to exogenous sources of DNA damage (Tan et al., 2012). This suggests that, as has been found in other long-lived animals like the naked mole rat (Buffenstein, 2008; Valenzano et al., 2017), that mechanisms to maintain genome integrity and reduce errors in other cellular processes have been optimised during evolution compared to animals that do age (Gorbunova et al., 2014; Kim et al., 2011; Lagunas-Rangel and Chávez-Valencia, 2017). Currently, there is little known about the regulation of mitochondrial function in SCs, except that planarian SCs have a very few immature mitochondria (Brubacher et al., 2014; Morita et al., 1969). This suggests that one-way SCs protect from endogenous DNA damage is by avoiding ROS production, instead generating energy by other means or perhaps importing it from other shorter-lived differentiated cells where the effects of ROS are less critical.

Another level at which planarian stem cells can protect from DNA damage is through regeneration itself. As previously mentioned a constant process of homeostasis replaces all differentiated tissues at a regular rate, meaning that no individual differentiated cell is old. All of these processes are controlled by an interplay of nutritional and positional signals in the animals that regulate the pluripotent SC population (González-estévez et al., 2012). This means that if any single SC does acquire mutations that might lead to genome instability, will eventually trigger a response from those SCs that are still fully functional. While the damaged SC and its progeny may not survive, the remaining SCs are more than sufficient to maintain the organismal function. For the rest of this discussion, I focus on what is currently known about the mechanisms to maintain genome stability in planarian SCs and how it protects from oncogenic transformation.

1.3.2. Protection against stem cell transformation and cancer

One major risk associated with longevity (and size) is the balance between having the proliferative capacity for extensive tissue homeostasis (and growth) and the risk of proliferative cells becoming transformed leading to the formation of tumours (Campisi, 1997; Gorbunova et al., 2014; Rodier and Campisi, 2011; Seluanov et al., 2008). The highly proliferative nature of SCs and the constant homeostatic process offer an opportunity to study this balance in a highly accessible context. It is tempting to hypothesize that planarians will have evolved very effective tumour suppressive mechanisms and although SCs are amazingly proliferative they are also kept under strict control. For example, SC proliferation increases upon wounding with two characteristic peaks, before returning to basal levels (Wenemoser and Reddien, 2010), demonstrating fine temporal control that is able to both accelerate and brake SC proliferation as necessary. This control makes planarians an excellent model system to study the mechanism controlling stem cell activity relevant to cancer (see below). However, while molecular mechanisms to control SC activity are crucial to prevent hyper-proliferation, planarians are protected against the occurrence of cancers by the very fact they are highly regenerative. This can be demonstrated by a simple thought experiment that walks through what would happen when a SC first becomes transformed and cycles out of control [Fig. 1.3].

Imagine a single SC becomes transformed through the acquisition of mutations that allow it to avoid both proliferative control and any cell death mechanisms normally triggered by genome instability. Subsequently, a clone of cells potentially consisting of both self-renewing and post-mitotic cells will form. As this clone of cells begins to cause any physiological damage, for example by disturbing the integrity of an epithelial layer or an organ, this damage would be sensed by regenerative mechanisms.

As a result of this, normally functioning SCs would be mobilised to repair the damaged tissue and eventually a fragment containing the tumour like tissue would separate from healthy tissue [Figure 1.3]. Given it is highly unlikely that a large proportion of SCs would be transformed simultaneously we can assume that naturally occurring cancers are not a major concern in a highly regenerative system. Other highly regenerative animals may benefit from the same protection against mutation and transformation of their stem cell populations. The chances that cancer can arise through the transformation of stem cells obviously increases with age and the primary function of some of the mechanisms that lead to ageing through senescence is to prevent cancers. Intuitively planarians and their SCs could be an excellent model system to study fundamental aspects of stem cell activity that are common to both regeneration and cancer. While the control of proliferation is central to this, mechanisms that regulate migration and differentiation (or failure to differentiate) are also important. As planarian SCs are always proliferating both potentially oncogenic drivers of proliferation and tumour suppressive mechanisms are likely key to allow proper NB regulation and provide protection against neoplasia (Pearson and Sánchez Alvarado, 2008; Sánchez Alvarado, 2012). Use of RNAi allows a direct method to screen for both oncogenic and tumour suppressor gene (TSG) function in *S. mediterranea*. These studies have revealed both conservation and divergence of function between planarians and mammals and have clearly demonstrated planarians can be used to make novel insights relevant to cancer (González-Estévez et al., 2012; Mihaylova et al., 2018; Pearson and Sánchez Alvarado, 2008, 2010; Van Roten et al., 2018; Sánchez Alvarado, 2012).

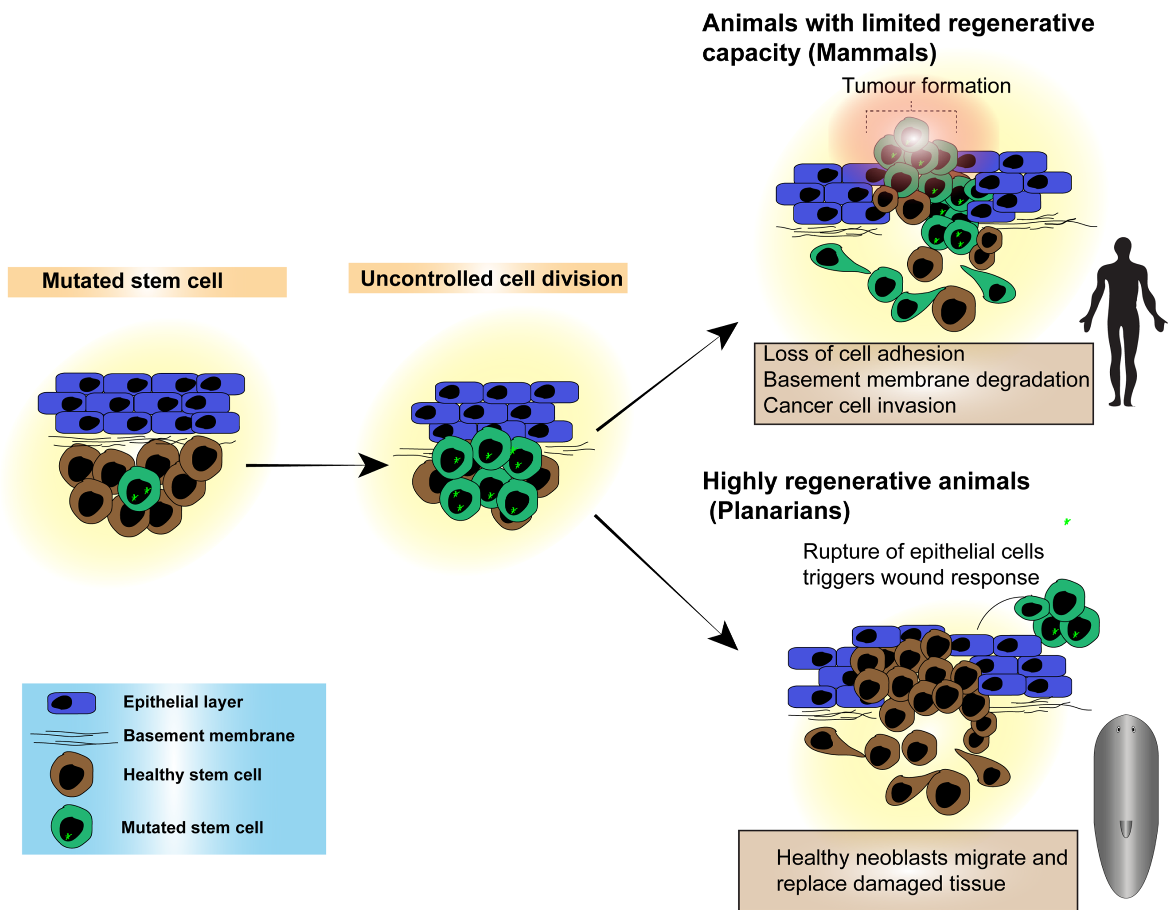

Figure 1.3. Evolution of a high regenerative capacity can protect against the pathology caused by cancer. A single stem cell (neoblast; brown cell) acquires mutations that cause it to escape the proliferative control and avoid cell death mechanisms that are ordinarily triggered by genome instability (green cell). As these cancer-like cells begin to grow in number, this colony may disrupt normal tissue patterning, for example disrupting the epithelial layer (blue cells). This damage will be sensed by a currently unknown signalling mechanism that triggers a regenerative response. As a consequence, neoblasts are mobilised to the damaged site, where they repair tissue and eliminate the over-proliferative NBs. Conversely, in mammals, a regenerative response is not able to resolve the tissue pathology caused by a tumour.

The first conservation of tumour suppressor function was demonstrated for PTEN (Phosphatase and tensin homolog), a frequently mutated TSG in most human cancers, that governs a plethora of biological processes including cellular proliferation, migration and differentiation (Song et al., 2012). Combined RNAi of two homologs of PTEN in planarians (*Smed-PTEN1 and 2*) resulted in a hyper-proliferative phenotype with ectopic cellular outgrowths (Oviedo et al., 2008). This RNAi approach can also be used to implicate novel tumour suppressors. Knockdown of the planarian ortholog of SMG-1 (Suppressor of male genitalia) , a member of Pi3k family with similarity to TOR (Target Of Rapamycin), was found to increase SC proliferation and lead to ectopic outgrowths providing evidence that SMG-1 was a novel tumour suppressor (González-Estévez et al., 2012). Rapamycin treatment reduced cellular proliferation in both PTEN or SMG-1 RNAi worms suggesting that for these phenotypes planarian tumorigenesis is driven by over-activity of the canonical Pi3k-AKT-mTOR signalling pathway (González-Estévez et al., 2012; Oviedo et al., 2008). Another recent study has also shown potential conservation of genome-wide epigenetic regulation of SC proliferation. Knockdown of the planarian orthologs of the histone methyltransferases human MLL3 (*Mixed Lineage Leukaemia*) and MLL4 leads to ectopic outgrowths caused SC over-proliferation (Mihaylova et al., 2018). Combined RNA-seq. and ChIP-seq. of FACS-sorted stem cells after MLL3/4 knockdown reveal a selection of conserved oncogenes and TSGs are epigenetically mis-regulated, and this likely drives the tumour-like phenotype in planarians (Mihaylova et al., 2018).

The function of other tumour suppressor pathways in planarians is not clearly conserved, and this may be a necessary adaption to allowing the high rates of SC proliferation that underpin their regenerative life history. For example, planarians have a single homolog of the p53/63/73 gene family and of the Retinoblastoma (Rb) gene, which are amongst the most commonly mutated TSGs in human cancer (Pearson and Sánchez Alvarado, 2010; Zhu and Pearson, 2013). Studies of these two genes suggest that in planarians they have a minor, if any role, in limiting stem cell proliferation. The planarian p53/63/73 ortholog is mainly expressed in the early post-mitotic progeny of SCs, rather than in cycling SCs. Knockdown of *Smed-p53* results in loss of both SCs and post-mitotic progeny after a brief initial increase in

proliferation, which is perhaps compensatory response for the disappearance of progeny. The loss of SC progeny and potential defects in differentiation are lethal (Pearson and Sánchez Alvarado, 2010). The *Smed- Rb* gene is mostly expressed in NBs and knockdown of Rb showed hypo-proliferation of mitotic cells leading to stem cell depletion, suggesting conservation of a role in cell division but not a role analogous to tumour suppressor function (Zhu and Pearson, 2013).

Overall, our present understanding of the role of different oncogenes and TSGs is still rather limited. What we know so far suggests that SCs can efficiently regulate proliferation to ensure regeneration. A balance exists between the anti-aging effects of a constant homeostatic SC activity and anti-cancer pathways to maintain genome stability. While all metazoans must achieve this balance as appropriate to their normal lifespan, this will be most extreme in animals that have high regenerative potential.

1.3.3. Guarding the genome against endogenous DNA damage and mutational processes

Genome sequencing has revealed that transposable elements (TEs) constitute a large portion of eukaryotic genomes (Cordaux and Batzer, 2009; Levin and Moran, 2011). As active TEs are highly mutagenic and may target protein-coding genes for insertion, their repression is necessary for the maintenance of genomic stability. This is particularly true of germline stem cells (GSCs), which must repress TE activity in order to maintain a long-term ability to proliferate and produce both new stem cells (self-renew) and differentiating progeny. To combat the invasion and expansion of these selfish elements in the germline, metazoans have evolved a novel class of small RNA molecules called piwi interacting RNAs (piRNAs), that are typically 24-31nt long and that bind to members of the PIWI (*P-element-induced wimpy testis*) subclass of the Argonaute superfamily of proteins. These PIWI-piRNA effector complexes bind to complementary TEs and silence them both epigenetically, by the recruitment of H3K9me3 chromatin marks and/or DNA methylation (Aravin et al., 2008; Huang et al., 2013; Sienski et al., 2012; Le Thomas et al., 2013; Walter et al., 2016) and through post-transcriptional mechanisms, via

direct cleavage of TE transcripts in a self-amplifying ‘ping-pong’ cycle (Aravin et al., 2008; Brennecke et al., 2007; Gunawardane et al., 2007; Weick and Miska, 2014).

Although the PIWI-piRNA pathway has been best characterized in the germline of classical model systems, observations in other organisms suggest that PIWI proteins are present in somatic stem cells and in many cases are necessary for stem cell function. Moreover, phylogenetic analysis suggests an intriguing correlation between the presence of multipotent and pluripotent stem cells that confer the ability for extensive regeneration, and the level of PIWI expression (van Wolfswinkel, 2014). Sponges (Funayama et al., 2010), acoels (De Mulder et al., 2009), cnidarians (Juliano et al., 2014; Lim et al., 2014), and tunicates (Rinkevich et al., 2013; Rosner et al., 2009) are all capable of whole-body regeneration, and contain pluripotent adult stem cells that express one or more PIWI proteins. The correlation between PIWI and potency can be explained by the fact that these stem cells must protect their genome from the malevolent effects of endogenous TEs in order to maintain a long-lived stem cell program consisting of differentiation and self-renewal.

TEs are predicted to constitute in excess of 31% of the planarian asexual genome (Friedländer et al., 2009), and studies have identified three major planarian PIWI proteins: SMEDWI-1, SMEDWI-2, and SMEDWI-3 in *Schmidtea mediterranea* (Palakodeti et al., 2008; Reddien et al., 2005b) and their respective orthologs Dj-PIWIA, Dj-PIWIB, and Dj-PIWIC in *Dugesia japonica* (Shibata et al., 2016). The transcripts for all three of these genes are highly expressed in SCs, and inhibition of *smedwi-2* and *smedwi-3* (but not *smedwi-1*) causes significant reductions in organismal piRNA levels, and results in regenerative defects and lethality (Palakodeti et al., 2008). This phenotype was investigated in greater detail by Shibata et al (2016) who showed that following RNAi of DjpiwiB, SCs are able to proliferate normally and TEs continue to be silenced in DjpiwiB depleted SCs 7 days post-RNAi. By contrast, TEs were de-repressed at the onset of differentiation, as observed by the up regulation of a gypsy element in differentiated somatic cells. Unlike DjPIWIA and DjPIWIC that have cytoplasmic expression patterns restricted to neoblasts, DjPIWIB is expressed at the protein level in the neoblast

nuclei and continues to be expressed in neoblast progeny and differentiated cells. This suggested that DjPIWIA and DjPIWIC compensate for the loss of DjPIWIB to maintain genome integrity in SCs, but since only DjPIWIB is inherited by the SC descendants, knockdown of DjPIWIB results in a loss of SC progeny during the differentiation process. Since DjPIWIB expression is nuclear, whereas DjPIWIA and DjPIWIC are cytoplasmic, a convincing parallel may be drawn between the planarian and Drosophila/mouse germline PIWI-piRNA pathways. DjPIWIB may be the counterpart of Drosophila Piwi, transcriptionally silencing TEs in the nucleus via epigenetic processes, while cytoplasmic DjPIWIA and DjPIWIC might be the counterparts of Drosophila cytoplasmic Piwi proteins Aub and Ago3 and implement transposon silencing at the post-transcriptional level by functioning as part of the 'ping-pong' pathway.

The hypothesis that PIWI is necessary for the maintenance of genomic integrity and cellular longevity is not restricted to stem cell systems. For example, the presence of a functional somatic PIWI-piRNA pathway in differentiated cells has been discovered in the adult Drosophila fat body, where loss of this pathway leads to TE mobilization and DNA damage in these cells and manifests in mutants being starvation sensitive, immunologically compromised, and short-lived (Jones et al., 2016).

1.3.4. High resistance to exogenous damaging agents suggests highly efficient DNA repair mechanisms

Defects in DNA repair mechanisms in adult stem cells leads to genome instability that causes ageing, stem cell exhaustion and carcinogenesis (Kenyon and Gerson, 2007). They must act to repair damage from endogenous sources (e.g replicative error or damage by ROS) and exogenous damage from environmental sources (Jackson and Bartek, 2009). Planarians SCs can withstand relatively high doses of ionizing radiation (IR), suggesting they have very efficient DNA repair mechanisms. Very little is known about the DNA damage response (DDR) in normal adult stem cells *in vivo* and planarians provide a potential system to study this.

While doses of IR around 60 Gray (Gy) kill all SCs by 24 hours after exposure and are therefore lethal to planarians, lower doses of up to 17.5 Gy have been reported to be non-lethal as the animal can rescue its SC population from the few remaining stem cells that survive (Wagner et al., 2011, 2012; Zhu et al., 2015). These surviving SCs are able to repair any damage and repopulating the animal. Planarians are not exposed to high levels of IR, UV or genotoxic agents in their natural environment at the bottoms of lakes and rivers. Animals that do experience highly stressful environment or conditions, like tardigrades, tend to have even higher IR resistance (>200 Gy) (Beltrán-Pardo et al., 2015; Hashimoto et al., 2016; Horikawa et al., 2013). Based on this it seems highly likely that the relative resistance to IR of planarian SCs compared to mammalian cells in culture is an emergent property of having highly efficient DNA repair and other cellular machinery to avoid genome instability over long time periods. This would also help to explain how planarians avoid ageing.

A survey of the planarian genome shows that they possess many members of the different DNA repair pathways for different types of damage (Discussed in Chapter 2). So far relatively little is known about repair mechanisms or genes associated with DNA repair in planarians. For example, RNAi of *Smed-msh2*, the ortholog of the mismatch repair gene MSH2, was able to confer SC resistance to a cytotoxic DNA alkylating agent compared to control worms (Hollenbach et al., 2011). While, Knockdown of a Rad51, a core component in homologous recombination mediated DNA repair leads to stem cell defects and also induced genome instability in *S. mediterranea* (Peiris et al., 2016), it is not known yet whether other components of DDR also play a major role in genome maintenance in planarians.

1.4. DNA damage response: the evolutionary trade-off between regeneration and tumour suppression.

Both exogenous and endogenous agents constantly threaten genome integrity and cells have evolved with mechanisms to counteract these various forms of DNA damage (Hoeijmakers, 2001; Tubbs and Nussenzweig, 2017). Efficient DNA repair mechanisms, in particular, to counteract the effects of replication stress, are therefore hypothesized to be central to avoiding both premature ageing and cancer. However, the relationship between the biology of ageing and cancer has been well documented, the functional interplay between ageing processes and cancer still remain a complex problem. DNA damage, and genome instability increases with age and deleterious mutation accumulate in stem cell compartments. Accumulated genotoxic damage, particularly in stem cells, is thought to underpin both ageing and the development of cancer (Goodell and Rando, 2015; Mandal et al., 2011; Vitale et al., 2017). The accumulation of mutations coupled with the longevity of stem cells makes them a "mutation reservoir" and they are often considered to be "precancerous units" (Mandal et al., 2011). Here we discuss a systematic, in-depth understanding of exogenous/endogenous sources of DNA damage and how different stem cells maintain genome integrity in response to DNA damage. Given that asexual planarians show negligible signs of ageing, it is important to know how planarian SCs can maintain genome stability and can proliferate throughout their life.

1.4.1 DNA damage response in embryonic stem cells (ESCs) and induced Pluripotent stem cells (iPSCs)

ESCs are totipotent cells with a key role in the process of development and a potential tool for regenerative medicine. The high proliferation rate in ESCs make them prone to replication-induced DNA breaks and are mostly repaired by homologous recombination (HR)-based DNA repair (Ahuja et al., 2016). Moreover, failure to repair DNA breaks can lead to apoptosis or senescence or suppress the pluripotency factors and pushed to differentiate (Li et al., 2012; Lin et al., 2005; Liu et al., 2013a). Thus, ESCs can efficiently avoid propagation of

mutations to the next generation by employing error free HR to accurately repair DNA lesions or block cell-cycle progression when damage is unresolvable.

On other hand, somatic cells can be reprogrammed into induced pluripotent stem cells (iPSCs), a breakthrough in modern biology and a promising resource for drug discovery, stem cell therapy and regenerative medicine (Robinton and Daley, 2012). However multiple studies highlighting genome instability in iPSCs during reprogramming raises concerns about the safety of its clinical application. For example, iPSCs generated from aged donors could exhibit genome instability compared to young donors, thus, mutational profiling and understanding the DDR status are important parameters for the clinical application of iPSCs (Kang et al., 2016; Lo Sardo et al., 2017).

During cellular reprogramming, iPSCs undergo a metabolic shift from an oxidative to glycolytic stage leading to increased ROS production that causes DNA damage and poor iPSC generation [Fig. 1.4.] (Apostolou and Hochedlinger, 2013; Chen et al., 2013; Esteban et al., 2010; Yoshida et al., 2009). Another critical factor is telomere maintenance in stem cells as shortened telomere affects both reprogramming efficiency and also exhibit DDR leading to genomic instability in iPSC (Marion et al., 2009; Marión et al., 2017; Melguizo-Sanchis et al., 2018). Replicative stress due to prolonged *in vitro* culturing of iPSCs is considered to be one of the major sources of DNA damage (Liang and Zhang, 2013; Mayshar et al., 2010; Ruiz et al., 2015) that leads to chromosomal aberrations and aneuploidy (Felgentreff et al., 2014; Lamm et al., 2016) [Fig.1.4.]. In response to reprogramming-induced DNA damage, iPSCs can efficiently resolve DSBs by overexpressing DDR factors and eliciting a robust antioxidant response to ROS (Dannenmann et al., 2015; Momcilovic et al., 2010). Although studies are currently ongoing to understand DDR during reprogramming to efficiently generate viable iPSCs for biomedical research, we can focus on experimentally accessible animal models with pluripotent adult stem cells like planarians to understand how stem cells can maintain their pluripotent state in response to genotoxic assaults.

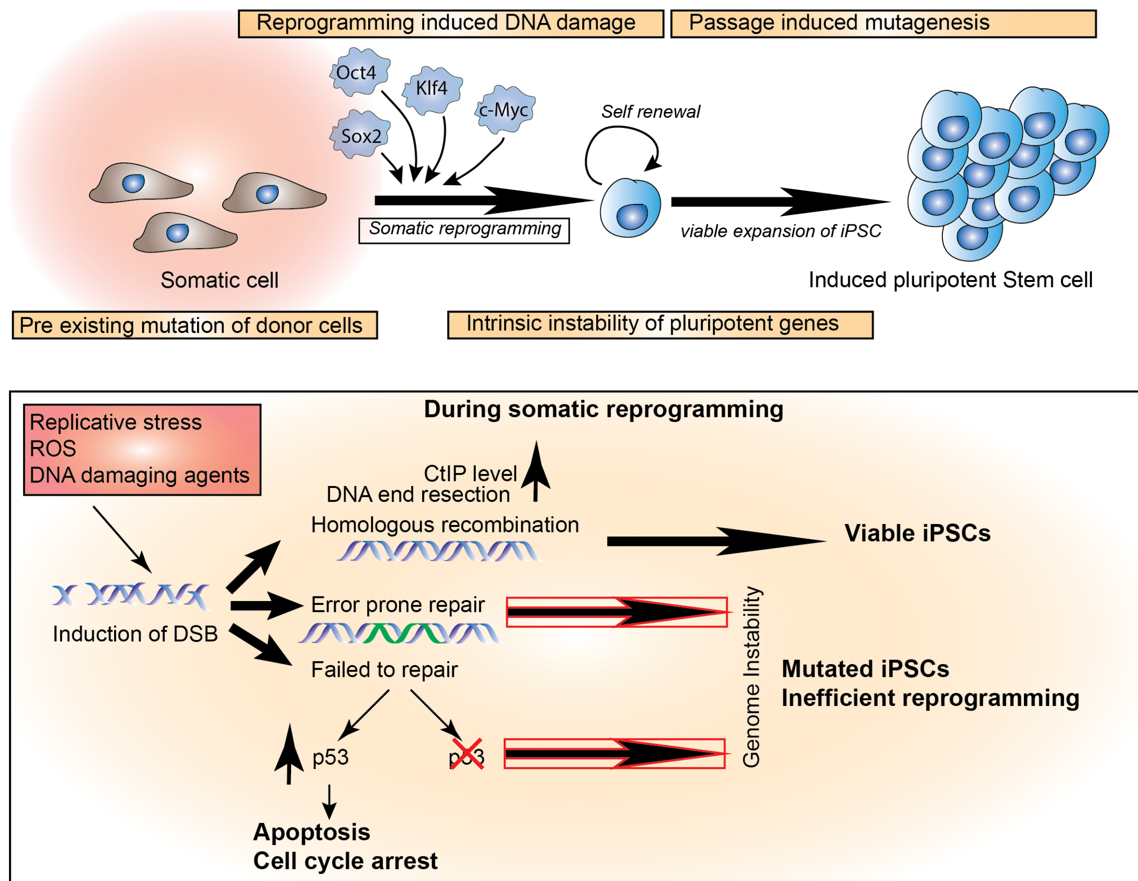

Figure 1.4. Schematic showing the effect of different exogenous and endogenous sources lead to DNA damage in induced pluripotent stem cells (iPSCs). The pre-existing mutation of the donor cells may induce DNA damage to reprogrammed stem cells. Indeed, somatic reprogramming also lead to genome instability. Different DNA repair pathways have evolved to deal with these physical assaults during somatic reprogramming (due to replicative stress and ROS generation). Homologous recombination undergoes error-free DNA repair thus producing viable iPSCs. On the other hand, Error prone-repair pathway (mostly via NHEJ) leads to mutated iPSCs that are inefficient in reprogramming and often lead to apoptosis/cell cycle arrest.

1.4.2. DNA damage response in tissue-specific adult stem cells

Most adult tissues, including the epidermis, the hematopoietic system and the intestine undergo constant wear and tear to ensure tissue homeostasis (Morrison and Spradling, 2008). Adult stem cells (ASCs) play a major role in replenishing these damaged/dead cells and in regeneration after wounding. The lifelong regenerative capacity demands tight control of genome maintenance in ASCs. Unlike ESCs, ASCs can exist in a low metabolic state called quiescence or G_0 phase. For example, ASCs in the hair follicle, gut and bone marrow can coexist in a dynamic pool of actively dividing and quiescent cells (Li and Clevers, 2010). ASCs reside and self-renew in adult tissues for extended periods and thus are prone to higher risk of DNA damage. On contrary, non-cycling quiescent stem cells minimize DNA lesion by limiting metabolic activity and making them less prone to endogenous DNA damage (Tothova et al., 2007; Yamazaki et al., 2006). Here we will discuss how adult stem cells residing in a particular tissue maintain genome stability in response to different DNA damage. The DNA repair mechanism and the outcome of DDR varies greatly between different tissue-specific ASCs and here we will discuss how ASCs residing in intestine, epidermis, lungs and mammary gland respond to DNA damaging agents.

1.4.2.1. Stem cells in the intestine

The human intestine is very sensitive to IR and whole-body exposure (<6Gy) lead to defects in the intestinal lining (consists of proliferative (crypt) and differentiated (villi) cells). Intestinal stem cells (ISCs, small intestine) coexist with cycling and quiescent ISCs (Barker, 2014). The cycling ISCs (crypt) resolve DSBs via HR (Barry et al., 2013; Gregorieff et al., 2015; Hua et al., 2012) and quiescent ISCs by promoting Ligase IV mediated NHEJ (Gong et al., 2016; Jun et al., 2016; Saha et al., 2016; Yousefi et al., 2016) [Fig. 1.5. A]. There are conflicting lines of evidence as to whether cycling ISCs are more sensitive to IR than quiescent ones or vice versa. It is interesting to note that colon (large intestine) stem cells can resist higher doses than ISCs due to overexpression of pro-apoptotic genes like Bcl2 and down regulation of p53. This induction of cell death in ISCs has been

correlated to frequent colon cancer (large intestine) compared to intestinal neoplasia (small intestine), despite higher cellular turnover in the small intestine, although this hypothesis needs more experimental investigation (Blanpain et al., 2011).

1.4.2.2. Hematopoietic stem cells (HSCs)

Hematopoietic stem cells (HSCs) divide asymmetrically to undergo haematopoiesis throughout our life. These stem cells also exist in an active cycling state to undergo haematopoiesis and in a quiescent phase to ensure HSC preservation (Crane et al., 2017). HSCs are considered to be the most radiosensitive cells in human and are one of the first organs to fail after whole body radiation (Milyavsky et al., 2010; Mohrin et al., 2010). The outcome of DDR varies from the developmental stage of HSCs, for example, foetal HSCs induce apoptosis, but adult HSCs (quiescent in bone marrow) induce cell survival and DNA repair (Mohrin et al., 2010). This can be achieved because proliferating HSCs repair DSBs via HR but quiescent cells preferentially activate the error-prone NHEJ pathway (Moehrle et al., 2015). This often leads to genomic rearrangement and mutations in HSC clones leading to haematological malignancies (Adams et al., 2015). It may also explain the rapid occurrence of haematological disorders (leukaemia and lymphoma) in cancer patients treated by radiotherapy or other DNA damaging agents (Blanpain et al., 2011). Overall, a robust DDR mechanism is required for efficient haematopoiesis and to limit haematological malignancies.

1.4.2.3. Epidermal stem cells/Hair follicle stem cells

The epidermis protects our body from the external environment and is constantly assaulted by genotoxic stresses such as UV irradiation. Different classes of epidermal stem cells maintain tissue homeostasis in humans (Blanpain and Fuchs, 2009). In fact, skin epidermis in human is considered to be radio-resistant and increased survival is linked to up-regulation of FGF2 that increases DNA repair (Harfouche et al., 2010) [Fig. 1.5. C]. Hair follicle bulge stem cells in aged

mice could not self-renew due to impaired DDR leading to stem cell exhaustion and eventual loss of hair follicles (Matsumura et al., 2016). Conditional deletion of BRCA1 in mice leads to hairless epidermis suggesting its role in the development of hair follicle and hair follicle bulge stem cells (Sotiropoulou et al., 2013), suggesting that DNA repair machinery in mammals has evolved not only to deal with genotoxic assaults but also to promote development and regeneration. Another kind of tissue-specific stem-cells that reside in the hair follicle bulge (melanocyte stem cells) are involved in body hair/skin pigmentation. Despite sharing the similar niche, DDR mechanisms vary a lot in melanocyte SCs compared to hair follicle bulge SCs as melanocyte SCs undergo terminal differentiation to eliminate precancerous stem cells from the hair follicle in response to IR/DNA damaging agents (Blanpain et al., 2011) [Fig. 1.5. C]. This suggests the existence of a complex and intricate relationship between stem cells and its response to DNA repair that can be modulated depending on their niche.

Other tissue-specific ASC includes the mammary stem cells (MaSC) that are involved in the development of mammary gland and to maintain breast tissue homeostasis during pregnancy and lactation (Shackleton et al., 2006; Stingl et al., 2006; Yang et al., 2017). The long-term maintenance of these multipotent SCs during glandular tissue remodelling demands an efficient genome maintenance mechanism. Human mesenchymal stem cells show a ATM-dependent resistance to DNA damaging agents (Oliver et al., 2013). Skeletal muscle stem cells (Satellite cells) accurately resolve DSBs induced by radiation via a DNA-PKcs dependent NHEJ (Vahidi Ferdousi et al., 2014). Collectively, these studies underpin the functional significance of DDR in adult stem cells and how their deregulation leads to stem cell exhaustion. The generalized view of the complex DDR in mammals is to promote cellular senescence or activate premature differentiation to prevent propagation of mutagenic genetic lesions. Although hematopoietic stem cells, epidermal stem cells and intestinal stem cells, can maintain tissue functionality by repairing their DNA via error prone NHEJ pathway this can also lead to genomic rearrangements that could be precancerous. Thus NHEJ in adult stem cells is considered to be a “double edged sword” (Blanpain et al., 2011; Soteriou and Fuchs, 2018).

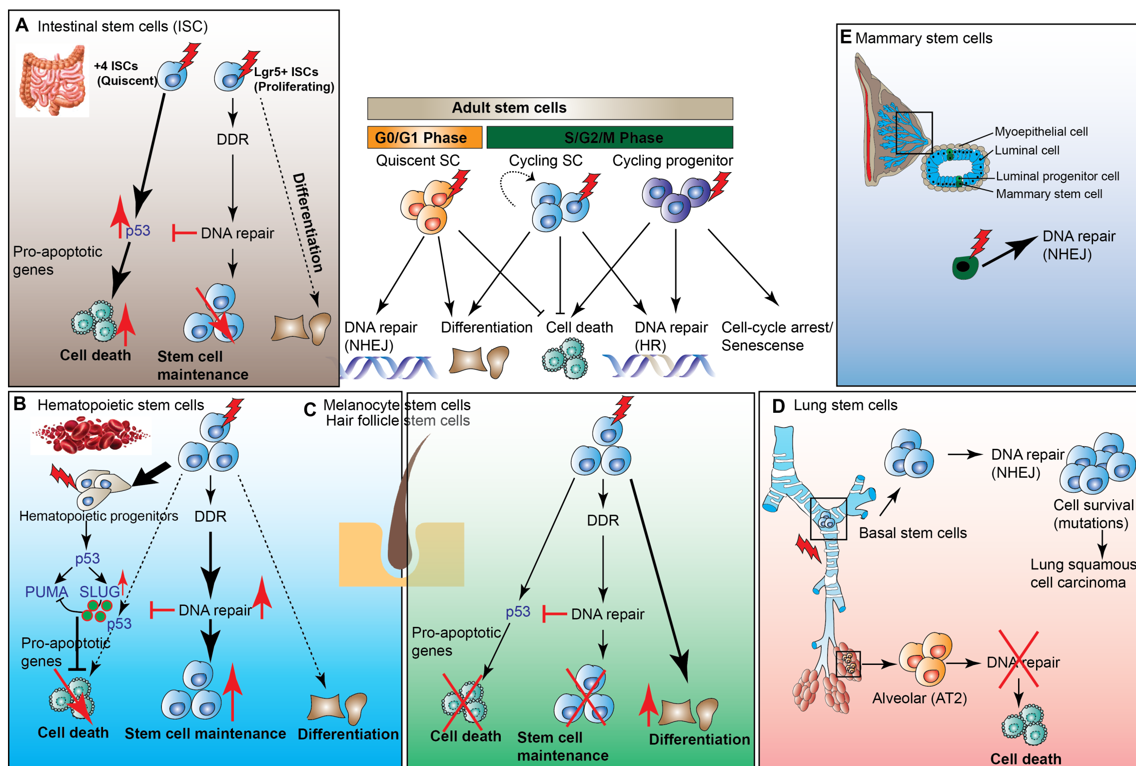

Figure 1.5. Schematic showing the role of different DNA repair pathways employed by tissue-specific adult stem cells. Stem cells in G2/M phase mostly undergo HR due to the availability of the sister chromatid and if unrepaired undergo apoptosis. Most adult stem cells in human exist in a niche and in a quiescent phase and when pushed to divide undergo NHEJ in G1 phase. Individual cartoons depict the DNA repair choice in intestinal stem cells, hematopoietic stem cells, hair follicle/melanocyte stem cells and lung stem cells.

1.4.3. DNA damage response in germline stem cells

Germline stem cells play a pivotal role as carriers of genetic information from one generation to the next. Primordial germ cells (PGCs) are transient precursors of germline stem cells that give rise to either sperm or egg. Spermatogonia remain quiescent until puberty and then require coordination of mitosis and meiosis to produce mature gametes (sperm). In contrast, a pool of oogonia is established during embryogenesis and females are born with finite number of egg (Lehmann, 2012; Spradling et al., 2011). Mutations in the germline lead to several hereditary diseases like breast, ovary and pancreatic cancer that necessitates maintaining the genome integrity of the immortal germline. Several DNA repair proteins that are involved in HR also play a major role during meiosis to produce fertile gametes. Therefore the occurrence of meiotic DSBs are very frequent in the germline and this requires the activity of highly conserved kinases like ATR, ATM and other checkpoint regulators (Sasaki et al., 2010). For example, ATM and ATR deficient undifferentiated spermatogonia show higher levels of DNA damage and G1- arrest (Takubo et al., 2008) and impaired spermatogenesis in mice (Ruzankina et al., 2007). Thus, maintenance of genome stability in germ line is very crucial to limit transmission of heritable mutations to the next generation.

The vast majority of studies focusing on DDR rely on the use of *in-vitro* experiments on the cultured cell or single-celled organisms. It is well known that DNA damage response varies from cell type and their response on individual tissues *in-vivo.* Studies using germline stem cells of *C. elegans* and *Drosophila melanogaster* have provided mechanistic insights to understand the stem cell response to DNA damaging agents *in vivo*. (Ma et al., 2016). These studies provide our fundamental understanding of how the decrease in proliferative capacity, accumulation of DNA damage and loss of stem cells eventually lead to organismal ageing. The *C. elegans* germline consists of mitotic stem cells that proliferate in the distal tip and undergo meiosis as it descends towards the uterus. The proliferating and the meiotic germ cells preferentially use HR over NHEJ to repair DSB in order to limit heritable mutations (Clejan et al., 2006). In response to IR, the mitotic germline stem cells undergoes cell cycle arrest whereas meiotic

germ cell undergo apoptosis (Gartner et al., 2000; Stergiou and Hengartner, 2004). [Fig. 1.6.] Multiple other DNA repair pathways (NER, BER, ICL repair) work in order to maintain genome stability in germ cells and reduce replicative stress in mitotic cells (Dengg et al., 2006; Lee et al., 2010; Stergiou et al., 2011; Youds et al., 2008). The presence of active DDR in the germline and absence of checkpoint signalling in somatic cells is an evolutionary strategy to minimalize the maintenance of the soma and to support efficient DNA repair in the immortal germline (Vermezovic et al., 2012). DNA damage in the worm's germline induces the activation of ERK- MAPK signalling that enhances stress resistance in somatic tissue. This altruistic behaviour of germ cells promotes somatic tissues to delay progeny production when germ cells are compromised due to genomic instability (Ermolaeva et al., 2013). A similar phenomenon is observed in spermatogonia within *Drosophila* testis that die synchronously to protect the genome integrity of the gamete to be passed on to the next generation(Lu and Yamashita, 2017). The genetic tractability and defined lineage commitment in *C. elegans* have improved our understanding of how germline stem cells cope with DNA damaging agents *in vivo.*

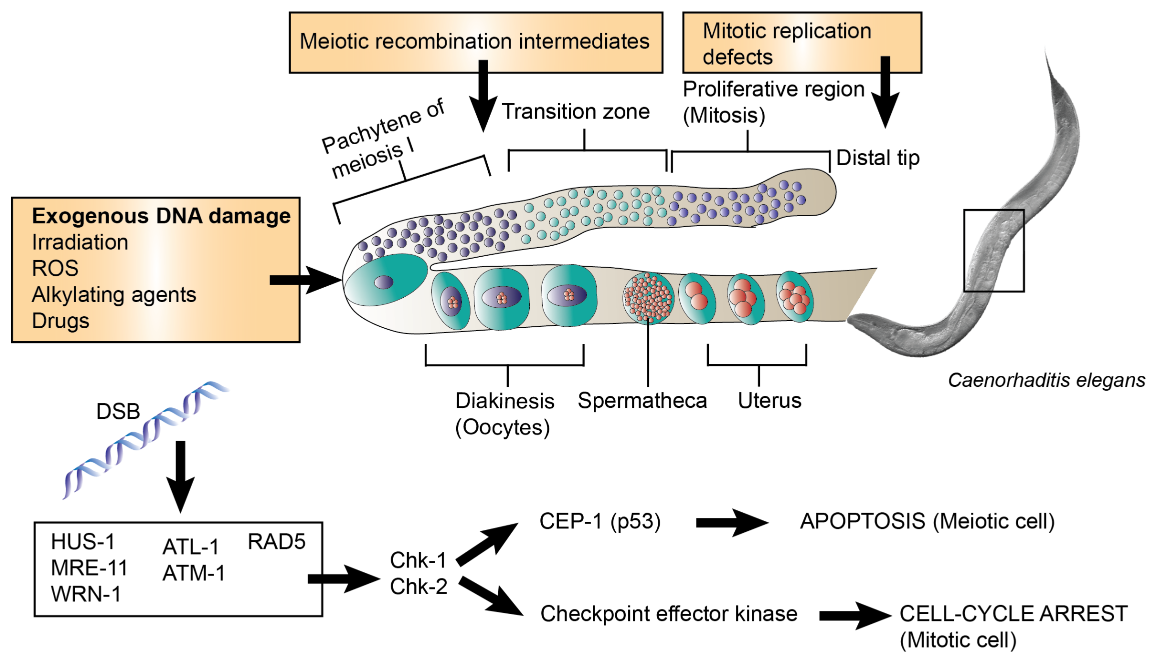

Figure 1.6. DNA damage response in germline stem cells. The germline of the nematode worm *C. elegans* provide insights on how exogenous DNA damage lead to double stranded breaks that upregulate checkpoint kinases to either lead to cell cycle arrest of mitotic cells or apoptosis in meiotic cells. The proliferating meiotic germline cells preferentially use HR to inhibit error-prone mutations to be transmitted to the next generation.

1.4.4. DNA damage response in cancer stem cells (CSC)

Most neoplasms contain multipotent stem cells with a high degree of genotypic and functional heterogeneity that have an efficient DNA repair pathway to promote tumorigenesis and block senescence. Thus DNA damage response (DDR) is often considered to be a double-edged sword, that promotes self-renewal in healthy stem cells by repairing DNA breaks and is detrimental by promoting survival/resistance in cancer stem cells (Mandal et al., 2011). These highly debated "cancer stem cells (CSC)" coexist in proliferative and quiescent phase (G_0/dormant) and have an extraordinary resistance to genotoxic agents and efficient DNA repair mechanism (Kreso and Dick, 2014) [Fig. 1.7. A]. Multiple lines of experimental evidence using cultured cancer stem cell models proved efficient HR plays a major role in DDR in CSCs compared to their progenitors (Desai et al., 2014; Lim et al., 2012; Yuan et al., 2014). Currently, CSCs are identified based on the expression of cell surface markers (namely CD24, CD44, CD117 or CD133) and are abundant in 3-40% of total population of cancer cells (Kreso and Dick, 2014). Although radiotherapy is considered to be an effective non-surgical strategy to treat solid tumour, gliomas are highly radioresistant with frequent relapse after radiotherapy. This is because CSCs can efficiently repair their DNA post IR. For example, glioblastomas show increased PARP1 activity that repairs single-stranded DNA breaks and contributes to radiation resistance (Ahmed et al., 2015; Bao et al., 2006; Desai et al., 2014). To counteract this effect, PARP inhibitors have been developed to selectively target glioblastomas (Venere et al., 2014). PARP inhibitors (PARPi) has been shown to be synthetic lethal to BRCA mutants (Bryant et al., 2005) but not all breast cancers respond to PARPi. For example, triple negative breast cancers that do not express genes for oestrogen and progesterone receptor and Her2 ($ER^{-}PR^{-}Her2^{-}$TNBC) shows high resistance to PARPi. TNBC accounts for 10-17% of all breast cancers and often needs combinatorial therapies as most of the hormonal therapies do not work. A recent study has shown knockdown of Rad51 sensitizes BRCA1-mutant TNBC to PARPi (Liu et al., 2017) [Fig. 1.7. B]. This could potentially lead to an improved therapeutic response in TNBC patients. The concept of synthetic lethality and the development of PARPi to cure BRCA-mutant cancer is a

breakthrough in cancer research but multiple studies now suggests that the stabilization of replication fork in BRCA mutants confers increased resistance to PARPi (Ding et al., 2016; He et al., 2018; Ray Chaudhuri et al., 2016). This suggest the clinical application of PARPi may be limited to few BRCA-mutated cancer patients and studies are currently ongoing to identify synthetic lethality with other DDR genes.

Another efficacious treatment for cancer is to inhibit checkpoint kinases like ATM or ATR signalling. Recently checkpoint inhibitors have been shown to sensitize CD133+glioblastomas, lung CSCs and pancreatic CSCs (Al-Ejeh et al., 2014; Bao et al., 2006; Bartucci et al., 2012). Epigenetic drugs like DNA methyltransferase (DNMT1) inhibitor (5-azacytidine) and histone deacetylase (HDAC) inhibitor (butyrate) are also used to selectively target CSCs (Pathania et al., 2016) and hematopoietic stem cells (Zhou et al., 2015). Hypomethylating agents in combination with HDAC and PARP inhibitors have been shown to induce apoptosis in human leukaemia and lymphoma (Valdez et al., 2018). [Fig. 1.7. B]. Abrogation of multiple signalling pathways that modulate DDR also sensitizes CSCs to chemotherapy or radiotherapy. For example, induction of BMP signalling forces colorectal CSCs to differentiate and increase their sensitivity to drugs (Lombardo et al., 2011). Similarly, Notch signalling increases sensitivity of ovarian CSCs (McAuliffe et al., 2012), glioma stem cells (Hovinga et al., 2010; Wang et al., 2010a) and melanoma stem cells (Kaushik et al., 2015) to IR, inhibition of TGF- β signalling sensitizes CSCs (Hardee et al., 2012), abrogation of AKT signalling increases radio-sensitivity of breast cancer cells (Zhang et al., 2010), mTOR signalling sensitize glioblastoma by inhibiting DDR (Kahn et al., 2014) [Fig. 1.7. B]

Although much of our understanding comes from studying DDR in cells *in vitro* but studying how the microenvironment modulates DDR in CSCs *in vivo* is still limited. Therefore, studies focussed at the whole-organism level with evolutionary conserved mechanisms will provide insights to understand genome instability and can be used to better understand cancer stem cells.

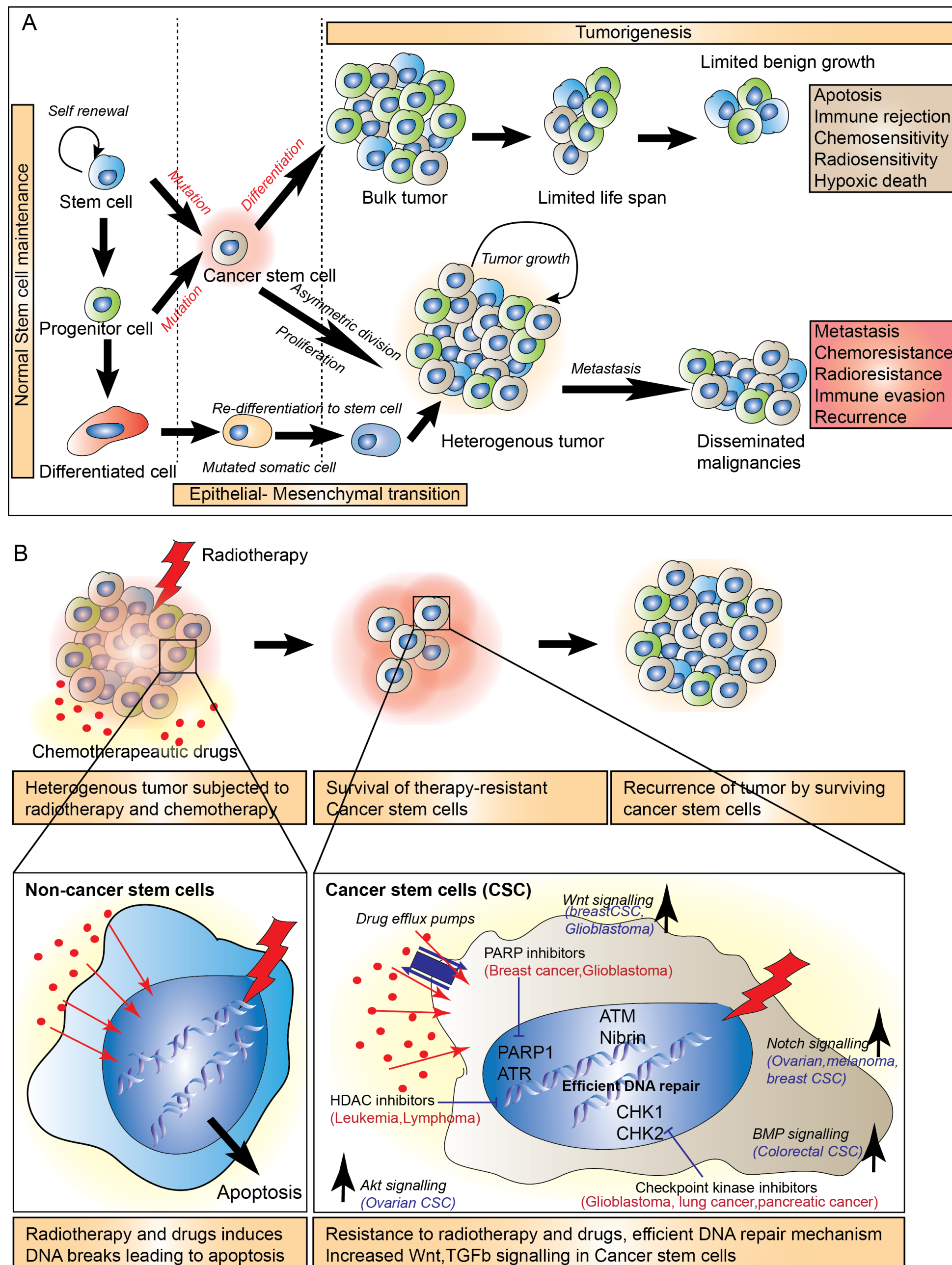

Figure 1.7. DNA damage response in cancer stem cells.

(A) Mutations in stem/progenitor cells lead to defects in checkpoint kinase which either lead to hyper proliferation by asymmetric division or undergo differentiation to form tumour. The heterogeneous tumour is difficult to treat by normal therapies and eventually lead to metastasis.

(B) Radiotherapy and chemotherapy are routinely used to treat solid tumour, but survival of some radiation-resistant cells often leads to relapse of tumour. The radiation resistant cells are termed as cancer stem cells that have efficient DNA repair machinery, increased Wnt and TGF- β signalling. CSCs are also resistant to multiple drugs including PARP, HDAC and different checkpoint kinase inhibitors.

1.4.5. DNA damage response in post-mitotic cells

We have already discussed how the DNA damage response varies depending on the cell cycle stage and proliferative capacity of stem cells. DDR in cycling cells (pluripotent SC) is different from their progenitors (lineage committed multipotent/ unipotent SCs), which differs again from post-mitotic progenies (terminally differentiated cells). Compared to neurons or adipocytes, highly dividing cells like blood and skin can efficiently deal with genome instability. The majority of human cells are terminally differentiated that are derived from self-renewing somatic stem cells. Dysfunctional DDR machinery is often correlated with the occurrence of many neurodegenerative disorders and neurological abnormalities (Madabhushi et al., 2014). Therefore, understanding how post-mitotic cells deal with genotoxic assaults will have a broader implication in the pathogenesis of several degenerative diseases. A general notion is terminally differentiated cells down-regulate DDR, as removal of damaged cells can be replenished by stem cells and thus functional restoration is possible. But how do post mitotic cells respond to DNA damaging agents despite not showing efficient DNA repair is clinically relevant. A major application to understand DDR in post-mitotic cells is to design specific therapeutic targets for several neurodegenerative or muscle related disorders. break will lead to apoptosis or senescence leading to neurodegenerative diseases.

Pioneering studies suggest the role of nucleotide excision repair (NER) and base excision repair (BER) in modulating DDR in post-mitotic /terminally differentiated cells (Narciso et al., 2007). Differentiated cells mostly rely on NHEJ to repair DSBs. Myotubes have been shown to down-regulate genes responsible for NHEJ (Ligase 1 and XRCC1) compared to post-mitotic neural cells, whereas XRCC1 protects neuronal cells from oxidative damage (Kulkarni et al., 2008; Lee et al., 2009). Moreover, myotubes that lack ATR and Chk1 upregulates ATM-Chk2 axis in response to DNA damaging agents/IR (Fortini et al., 2012a; Latella et al., 2004). The high resistance to DNA damaging agents in myotubes and astrocytes is also linked with the lack of p53 phosphorylation after DDR activation, thereby limiting cell death. Another study revealed ATM is transcriptionally downregulated

in astrocytes (predominant cells in the brain) and DNA-PKcs mediates H2Ax phosphorylation to initiate the DDR signalling (Schneider et al., 2012). Adipocytes also up-regulate DNA-PKcs in response to DNA damaging agents/IR. Not many studies have been done to understand the DDR in post-mitotic cells due to experimental limitations. Planarians possesses a distinct pluripotent stem cell and a differentiated cell compartment and therefore establishing these non-model organisms to understand the DNA damage response will be useful.

We have explained in detail on what is currently known on DDR in different stem cells and summarised these in Table-1. Overall, this literature will be our foundation to explore DDR mechanisms in a model organism that is currently understudied in the field of cancer, DNA damage and radiation biology.

Table 1. Summarised table showing the differences in physiological status and response to DNA damage between stem cells and post-mitotic/somatic cells. Adapted from (Fortini et al., 2012b)

Process	**Cell type**			
	ESC	**ASC**	**Post-mitotic cells**	**Germline cells**
Proliferation	Yes	Quiescent	Irreversible exit from cell cycle	Yes
ROS level	Low	Low	High	High
Mutation rate	Low	High	–	Low
Turnover	High	Persistence of damaged cells	Restricted apoptosis	High
DNA repair	Efficient	Efficient/less efficient	Downregulated	Efficient
DSB repair	HR	NHEJ*	NHEJ	HR
DDR	Lack of G1 checkpoint	Tissue-specific and cell-cycle phase dependent	Not fully active	Active

* When ASC are stimulated to replicate.

(ESC: Embryonic stem cell, ASC: Adult stem cells, ROS: Reactive Oxygen Species, DSBR: Double stranded break repair, NER: Nucleotide Excision Repair, BER: Base Excision Repair, DDR: DNA damage response)

1.5. Thesis aim and outline

The inherent longevity of planarian stem cells raises the possibility that unique protective mechanisms may exist to balance the trade-off between stem cell ageing and oncogenic transformation. In highly regenerative contexts, the cost of accumulating deleterious mutations is high because mutations inherited by progeny will eventually lead to genome instability with an increased risk of cancer occurrence. This raises an important question how do stem cells handle these genotoxic assaults? Much of our understanding of DDR pathways originates from elegant genetic studies in the yeasts *Saccharomyces cerevisiae* and *S. pombe.* These studies, together with work performed in *Aspergillus, C. elegans, Drosophila* and various mammalian species have revealed much conservation, but also some surprising changes in DNA damage response pathways through evolution.

Chapter 1 has given a brief outline of the state-of-art in today's planarian stem cell biology and DNA damage response mechanism in different types of stem cells. The highly regenerative planarian *Schmidtea mediterranea* has a population of collectively pluripotent adult stem cells and potentially avoids both ageing and cancer. A lethal ionizing radiation (IR) dose of 30 Gray (Gy) is required to kill these cycling stem cells but radiation resistance up to 15 Gy suggests they might have an efficient DNA damage response (DDR) machinery. **Chapter 2** describes all the material and methods used in the subsequent results chapters presented in this thesis. In **Chapter 3,** I have identified the different DNA repair pathways and their role in stem cell maintenance post-IR and elucidating the potential to use a flatworm stem cell model to study DDR in the context of stem cells.

The impact of mechanical stress during cell migration may be a previously unappreciated source of genome instability but to what extent this happens *in vivo* remains unknown. Our lab has generated a novel system whereby planarian stem cells are required to migrate over long distances to a distal wound site, thus enabling the interplay between DNA damage and migration to be studied during

regeneration. In **chapter 4,** I have discussed how mechanical stress during migration due to changes in nuclear shape affects the sensitivity of SCs to DNA damaging agents. I have also demonstrated a non-canonical role of DDR is to combat DNA damage during stem cell migration and in the absence of fully functioning DDR machinery stem cells fail to migrate.

Improvements in sequencing technology have benefited planarian research in the last few years. With an aim to understand the transcriptional response to IR, we used RNA sequencing on planarian stem cells after irradiation. We have identified some novel targets that are up-regulated in response to IR and a loss of function strategy to understand their role in radiation response and stem cell maintenance is described in **chapter 5.** We have extended our findings by identifying a conserved response to IR between planarian stem cells and human fibrosarcoma model (HT1080 cell line).

Chapter 6 gives a summary of this thesis. I discuss the key findings of all the studies mentioned here, state of art of ongoing research and future perspectives to understand DNA damage response in stem cells.

Chapter 2

Material and methods

2.1. Planarian culture

Asexual freshwater planarians of the species *Schmidtea mediterranea* were used in this study. The culture was maintained in 0.5% Instant Ocean, fed with organic calf liver twice a week and cultured in the dark at 20^0C. Planarians were starved for 7 days prior to each experiment and also throughout the duration of each experiment.

2.2. Total RNA isolation

1-2 worms (~5 mm size) were added in a micro-centrifuge tube and 500 µl of TRIZOL was added, snap-frozen in dry ice for 1 hour (or overnight). After homogenization, samples were incubated for 15 minutes at -20^0C. 100 µl of chloroform were added and samples were shaken vigorously for 15 seconds and incubated at room temperature for 5 minutes. The sample was centrifuged at 12000g for 15 minutes at 4^0C and the aqueous phase was carefully transferred to a fresh new micro-centrifuge tube. 250 µl of isopropanol and 3M sodium acetate was added, vortex and incubated for 15 minutes at -20^0 C. Sodium acetate was added to remove the pigments from planarian samples. The sample was centrifuged at 12000g for 15 minutes at 4^0C followed by 70% ethanol (chilled and freshly prepared) wash and centrifuged at 7500g for 7 minutes at 4^0C. The pellet was carefully air-dried and suspended in RNAse free water. The quality of RNA was checked using nanodrop and quantity was estimated and approximately 1 µg of RNA was used for cDNA synthesis. The samples were kept at -80^0 C for long-term storage.

2.3. cDNA synthesis and amplification of planarian genes

1 µg of RNA was used for 20 µl of cDNA synthesis using Oligo-dT primers and Superscript IV-Reverse Transcriptase polymerase (Invitrogen). Total RNA along with 50 µM Oligo-dT, 10mM dNTPs was incubated at 65^0C for 5 minutes to denature RNA/primer sample and chilled on ice for 2 minutes. The first strand buffer mix, 0.1M DTT, Superscript IV polymerase (200 U/ µl), RNAse OUT inhibitor (40U/ml) were added to the reaction mix and incubated at 50^0C for 90 minutes and at 85^0C for 20 minutes. 1 Unit (U) of RNAse-H was added to the

reaction mix and incubated at 37^{0}C for 20 minutes. The cDNA was stored at -20^{0}C.

Primer designing was performed using Primer 3 plus https://primer3plus.com/cgi-bin/dev/primer3plus.cgi with the following parameters: product size range 600-800bp, GC content: 50 %, Tm: 60^{0}C. The following adapter sequences were added to individual primer sets:

Forward primer adapter: 5'-CATTACCATCCCG-3'

Reverse primer adapter: 5'-CCAATTCTACCCG-3'

The PCR cycling parameters used for amplification were as follows: initial denaturation - 94^{0}C for 1 minute, 35 cycles of [94^{0}C for 45 seconds, annealing temp 55^{0}C for 30 seconds, 72^{0}C for 45 seconds]; final extension 72^{0}C for 10 minutes and 4^{0}C hold. The PCR product was gel extracted using the Wizard ® SV Gel and PCR Clean-Up kit (Promega) as per the manufacturer's guideline. The product was visualized using 1 % agarose gel before any downstream experiments.

2.4. Cloning into pPR-242 vector

Planarian genes were cloned into the pPR-242 plasmid vector containing opposable T7 promoters (a kind gift from Dr. Jochen Rink, Max Planck Institute, Dresden). PCR products were cloned directly into a T7/T7 pPR-242, vector which can be utilized to generate PCR-product templates for riboprobe synthesis (using PR244 and AA18 primers) and double-stranded RNA generation (using the universal M13 forward and reverse primers) followed by *in vitro* transcription using T7 polymerase. Since this is a directional cloning procedure, the forward and reverse sequences are different, such that PCR products always ligate in the same orientation. This makes it easy to simply use T7 polymerase to make antisense riboprobe.

pPR-242 vector was linearized using the *SmaI* restriction enzyme overnight at room temperature and the digested vector was gel eluted. The linearized vector

and the purified insert were put in a thermo-cycler for the T4-Polymerase (T4P) reaction using T4 DNA polymerase and dGTP (for vector) and dCTP (for the insert). T4 DNA polymerase is very unstable and small aliquots should be ordered to prevent degradation of the enzyme. T4P reaction should be performed fresh during every cloning procedure. 2 µl of the T4P-insert PCR product was added into tubes containing T4P-digested vector for ligation at 4^0C overnight. The vector to insert ratio is very critical for efficient ligation. 15 µl of high-efficiency competent cells (Bioline) were added to the ligation mixture and transformed into pre-warmed kanamycin containing LB plates. The LB plates were incubated at 37^0C overnight. There is no possibility of self-ligation due to the T4P reaction and all colonies in kanamycin$^+$ LB plates should be containing the gene of interest. The following day, the colonies were screened with T7 promoter primer using the following PCR cycling parameter: initial denaturation at 94^0C for 1 minute, 25 cycles of [94^0C for 45 seconds, annealing temp 55^0C for 30 seconds, 72^0C for 45 seconds]; final extension 72^0C for 10 minutes and 4^0C hold. A successful amplification using T7 promoter primer indicates that the flanking T7's was intact. The flanking T7 promoters in this vector decides the orientation of the gene sequence thus making it easier for the generation of antisense riboprobes and also making double-stranded RNA by using T7 polymerase only. The positive colonies (with gene of insert) were incubated for an overnight liquid culture for plasmid isolation. Plasmids were isolated using Wizard ® plus SV Miniprep kit (Promega) according to the manufacturer's guideline. Plasmids were quantified using a nanodrop and sent for sequencing to check the insert of our gene of interest.

2.5. RNA interference for gene knockdown in planarians

2.5.1. Generation of double-stranded RNA (dsRNA)

The M13 amplified template was used for *in-vitro* transcription reaction using T7 polymerase and 20mM rNTPs for 6 hours at 37^0C. The sample was treated with DNAse (Ambion) for 30 minutes at 37^0C to remove any residual DNA in the sample. The product was then precipitated using 3M Sodium acetate and chilled 100% Ethanol at -20^0C overnight. The following day the sample was centrifuged

at 13000 g for 30 minutes at 4^0C. The pellet was washed using 300 µl of 70% ethanol (fresh and chilled) at 10000g for 10 minutes and air-dried. The ds-RNA was eluted in RNAse free water and the sample was annealed at 68^0C for 15 minutes followed by 37^0C incubation for 45 minutes. The sample was mixed and 2 µl of dsRNA was loaded in a 1% agarose gel and the remaining was stored at -20^0C.

2.5.2. Microinjection

dsRNA was delivered via microinjection using Nanoject II apparatus (Drummond Scientific) with 3.5’’ Drummond Scientific (Harvard Apparatus) glass capillaries pulled into fine needles on a Micropipette Puller (Sutter instrument company). The needle was filled with mineral oil and dsRNA was loaded into the needle. Worms were placed on a piece of black card in an ice-filled petridish (to limit worm movement). The worms were turned with their ventral side up (less pigmented) for the ease of injection. Each worm was injected in the middle of the anterior gut branch with 32nl of dsRNA (thrice per day) 6 times over 2 weeks. A 1-day gap was kept between the last injection and irradiation experiments (as described in individual experiments).

2.6. Riboprobe synthesis

The template for riboprobe synthesis was amplified from the plasmid using PR244 and AA18 primer. This makes it easy to simply use T7 polymerase to generate antisense riboprobe. The PCR parameters used were: 94^0C for 5 minutes, 35 cycles of (94^0C for 45 seconds, 55^0C for 30 seconds, 72^0C for 1 minute), 72^0C for 10 minutes. The PCR product was column purified using Wizard SV gel and PCR clean up kit (Promega) according to the manufacturer’s guidelines and checked in 1 % agarose gel for the correct size of the PCR product.

In-vitro transcription reaction was performed using the purified template, T7 polymerase along with its buffer, and either DIG-labelled rNTPs or FITC-rNTPs and RNAse-OUT inhibitor for 3 hours at 37^0C. The sample was treated with DNAse for 30 minutes at 37^0C. The reaction mix was transferred to a new micro-

centrifuge tube and lithium chloride, glycogen, ethanol was added for overnight precipitation at -20^{0}C. The sample was centrifuged at 13000g for 30 minutes at 4^{0}C, followed by 70% ethanol wash. The pellet was air-dried and re-suspended using hybridization buffer followed by incubation at 68^{0}C for 15 minutes. 2 µl of probes were checked in 1% agarose gel and stored at -20^{0}C for long-term storage. Probes were re-suspended in hybridization buffer and can be stored >1 year at -20^{0}C.

2.7. *In situ* hybridization

Fluorescent *In situ* hybridization (FISH) was performed as described previously (King and Newmark, 2013). Worms are killed using 5% NAC solution (should not be more than 5 minutes to reduce epidermal peeling) and fixed with freshly prepared 4% formaldehyde solution for 30 minutes. The worms are dehydrated in 50 % methanol solution and can be stored at -20^0 C for a month. The worms were then rehydrated in 50% methanol followed by rinsing in PBSTx (0.3% Triton-X). Worms were bleached in 6% bleaching solution (formamide-H_2O_2-SSC) for 2 hours under white light. Animals were then digested with Proteinase K for 10 minutes followed by fixation using 4% formaldehyde for 20 minutes. Optimization with proteinase K and the concentration of riboprobes are both important for better *in-situ* signals and to detect lowly expressed genes. Insufficient digestion result in a diminished hybridization signal and excess riboprobes leads to background non-specific signals. After two washes in PBSTx (5 minutes each), worms were then placed in a pre-hybridization buffer at 56^0 C for 2 hours followed by hybridization solution (containing the desired DIG/FITC labelled riboprobe in 5% dextran sulfate) at 56^0 C for >15 hours. After riboprobe incubation, a series of washes using 2x SSC (3 times) and 0.2x SSC (4 times) were performed with 30 minutes per wash. SSC washes shouldn't be prolonged more than those recommended in the protocol. Animals were then rinsed in TNTx for 5 minutes followed by blocking solution (TNTx, Horse Serum and western blocking reagent) for 1 hour in room temperature. Secondary antibody solution (Anti-DIG-POD or FITC-POD antibody diluted in blocking solution; 1:2000 dilution) was added and incubated overnight at 4^0 C. The following day, animals were rinsed 6 times using TNTx, for 20 minutes per wash. The samples were developed using tyramide

signal amplification (TSA) and a fluorophore of choice (TAMRA, Alexa Fluor 488; 1:500 dilution). For double FISH, the samples were washed in PBSTx after development with a single fluorophore and followed by Sodium Azide treatment for 1 hour to eliminate the peroxidase activity. The sodium-azide treatment was necessary if immunostaining (developed using TSA) has to be performed after *in-situ* hybridization. This step is not required if a conjugated fluorophore antibody is used for visualization. The samples were washed thrice in PBSTx for 15 minutes, per wash and blocked for the secondary antibody of choice. After an overnight incubation, the samples were rinsed 6 times using TNTx, for 20 minutes per wash. The samples were developed using tyramide signal amplification and the second fluorophore of choice. After a couple of PBSTx washes, the samples were incubated with Hoechst 33242 (1: 5000 dilution) for nuclear labelling overnight. The animals were rinsed in 0.3% PBSTx followed by fixation with 4% formaldehyde and two washes using PBS. The samples were kept in 70% glycerol overnight and mounted in a clean slide for confocal microscopy.

2.8. Immunostaining

The worms were killed using 2% HCl in 5/8 Holtfreter's solution for 5 minutes. Followed by fixation using Carnoy's solution (freshly prepared using Ethanol, Chloroform, Acetic acid in the ratio 6:3:1) for 2 hours at 4^0C. Alternatively, worms can be fixed in 4% formaldehyde solution. The worms were then bleached in 5% H_2O_2-methanol solution overnight and can be stored (if needed) in 100% methanol for 1 month. The samples were dehydrated through a gradient of 75%-50%-25% methanol washes followed by PBSTx (0.3% Triton-X) washes. The samples were blocked using 1% BSA (dissolved in PBSTx and western blocking reagent) for 1 hour at room temperature. The primary antibodies were diluted in the blocking reagent and the samples were incubated at 4^0C overnight. The following day samples were washed in 0.3% PBSTx [7 - 8 times, 30 minutes per wash at room temperature]. The samples were blocked in 1% BSA-PBSTx solution for 1 hour followed by an overnight incubation with the respective secondary antibody (1: 2000 dilution). The following day samples were washed in 0.3% PBSTx, 7 - 8 times, 30 minutes per wash at room temperature and if HRP-based secondary antibodies were used the samples were developed using

tyramide signal amplification (TSA) and a fluorophore of choice (similar to *in-situ* hybridization). After a couple of PBSTx washes, the samples were incubated with Hoechst 33242 (1: 5000 dilution) for nuclear labelling overnight. The following day, the animals were rinsed in PBSTx followed by fixation with 4% formaldehyde and two washes using PBS. The samples were kept in 70% glycerol overnight and mounted in a clean slide for confocal microscopy.

Primary antibodies used were: anti-H3-pSer10 (phosphorylated serine 10 on histone H3; Millipore; 09-797; 1:1000 dilution), anti-SMED-RAD51 (1:500; kind gift from Scott Hawley, Stowers Institute USA), anti-Poly (ADP) Ribose (PAR) monoclonal antibody (1:500) (Santacruz) and the secondary antibodies used were Anti-Rabbit-HRP, anti-Guineapig-HRP and anti-mouse-HRP respectively (1:2000 dilution).

2.9. Sectioning of planarian worms

1-week starved planarians were killed in 2% HCl and Holtfreter solution and fixed with 4% formaldehyade for 2 hours. The worms were then washed in PBST (0.3% Triton-X) and dehydrated with an increasing gradient of methanol washes and stored at -20^{0}C. The following day worms were re-hydrated with a decreasing gradient of Methanol and PBS, Xylene washes (2 washes of 7 minutes each) and put into molten paraffin for 1 hour. Individual worms were then aligned (sagittal or transverse) in paraffin moulds followed by trimming and sliced into 10 μm sections using a microtome. Individual ribbons of planarian sections were put in a 37^{0}C water bath and aligned to have the entire worm on each Poly-lysine coated slide.

2.9.1. Immunostaining and FISH on sections

Planarian sections were deparaffinized using Xylene substitute (2 washes of 7 minutes each) and washed with PBS-Tx0.3 (0.3% Triton-X). The sections were subjected to antigen retrieval with proteinase K (37^{0}C) or sodium citrate buffer at 37^{0}C or Trilogy (Cell Marque) at 90^{0}C. Trilogy was used for RAD51 immunostaining, and Proteinase K-based antigen retrieval method was used for PAR immunostaining. Sodium citrate buffer was found to be harsh that reduces

the efficiency of FISH/immunostaining. The slides were then fixed in 4% fixative for 15 mins followed by two washes of PBS-Tx0.5 (0.5% Triton-X) for 30 mins and transferred to a blocking solution (0.5% BSA and PBS-Tx0.5). 150 µl of primary antibody (diluted in blocking solution) was added to individual slides and a Parafilm was placed on top for uniform spreading of the antibody solution. After an overnight antibody incubation at 4^0C, the slides were washed with alternating changes of PBS-Tx0.5 and PBS+0.1% Tween-20. The secondary antibodies were diluted in blocking solution and incubated overnight. Slides were washed again with alternating changes of PBS-Tx0.5 and PBS+0.1% Tween-20. After two 10 minutes washes slides were developed with Tyramide/other fluorophores (according to the *in-situ* protocol described in section 2.8). For double FISH and immunostaining, FISH was performed followed by immunostaining. Extreme care was taken during the entire procedure and Sodium-Azide based peroxide inactivation was performed after the development of each probe/antibody. After two 10 min washes with PBS-TW, slides were stained with DAPI for nuclear staining overnight. Slides were mounted and imaged in Olympus FV1000 confocal microscope with the appropriate fluorescent laser.

2.10. Cell dissociation and fluorescence-activated cell sorting (FACS)

Planarians were cut into small pieces with a scalpel and transferred into 1.5 ml low-binding tubes with $CMFHE^{2+}$ solution (calcium-magnesium free buffer supplemented with 0.1% BSA, 0.5% glucose 15 mM HEPES and 3mM EDTA). Repeated wiping of the scalpel is recommended during cutting planarians to get rid of the mucus. The worms were gently diced to reduce any mechanical stress to the cells (mostly for Comet assay). The tissue pieces were digested using Papain (Sigma Aldrich) (15 U/ml) for 1 hour at 25^0C. 10X CMF, HEPES and EDTA can be stored as a stock solution at 4^0C for 6 months, but $CMFHE^{2+}$ and the digestion solution should be made fresh. The pieces were mechanically dissociated using a P1000 pipette to form single cell suspension and filtered through 100µm followed by 35 µm cell strainer (BD Falcon). This step preferentially enriches the stem cell population by reducing the cellular debris. The filtered cells were collected and stained with a nuclear marker Hoechst 34580 (1mg/ml stock concentration) at a final concentration of 20µg/ml.

Cytoplasmic staining was performed using calcein AM (1mg/ml stock concentration) at a final concentration of 0.5 µl/ml. Staining was performed at least for 1 hour at room temperature and protected from being exposed to light. Prior to FACS acquisition, 1 µl/ml of propidium iodide (Sigma) solution was added to the cells to exclude dead/apoptotic cells. FACS was performed with the BD FACS Aria III instrument with Hoechst 34580 signal at 450 nm while calcein AM signal at 488 nm. Appropriate gating was performed based on forward vs. side scatter and excluding PI positive cells. Cells were finally collected based on their nuclear vs. cytoplasmic content into individual tubes containing either CMFHE2+ buffer or into "RNAlater" (invitrogen) (for RNA-sequencing experiments). The final volume of cell suspension should be around 1 ml (from 50 worms). This reduces the sorting time (around 30 mins when sorted using 80 µm nozzle) and multiple samples can be processed in a day to reduce batch effects. Dissociating 60 worms will give roughly around > 350,000 X1 cells, > 1million X2 cells and >1 million Xins cells.

2.11. RNA isolation from FACS sorted planarian cells for library preparation

The cells were collected directly into "RNAlater" (Invitrogen) stabilization solution and centrifuged at 5000g for 25 minutes at 4^0C. The RNAlater was replaced with 1 ml of TRIZOL and stored at -80^0C. RNA was isolated as described in section 2.2. To increase the purity of the sample, the RNA was column purified using "RNA clean and concentrator" (Zymo) kit. The total RNA was quantified using "Qubit broad range Assay" (Invitrogen) kit. Around 0.8 - 1µg of RNA was used for library preparation. It is important to note that around 400,000 X1 cells give around 1.2 µg of total RNA and 1 million X2 cells will give approximately 1 µg RNA. 600 ng of RNA has given a good quality of library for RNA-seq.

2.12. Library preparation for RNA sequencing

Around 1 µg of RNA was used for library preparation using Illumina TruSeq stranded mRNA LT kit, as per manufacturers guideline. The adapters were diluted 1:1 using re-suspension buffer to reduce the chance of getting adapter-dimers. The libraries were quantified using "Qubit High sensitivity" kit (Invitrogen)

and the quality, size of the libraries was checked in “Agilent 4200 Tapestation” system. The libraries were individually quantified using KAPA qPCR library quantification kit and multiple libraries were then pooled together to 4nM concentration. The pooled libraries with different indices were sequenced on an Illumina NextSeq machine. Two biological replicates per condition per sample were prepared and sequenced paired end to generate high quality, alignable sequence data.

2.13. RNA-sequencing data analysis (Planarian and human dataset)

Raw paired-end reads were trimmed with Trimmomatic 0.32 and the reads were imported to CLC genomics (Qiagen) workspace. The reads were mapped to a set of asexual transcripts downloaded from the publicly available *S. mediterranea* transcriptome dd_Smed_v6.pcf.contigs.fasta.zip or human genome and transcriptome (downloaded from Uniprot) with the following mapping parameters (mismatch cost = 2, insertion cost = 2, deletion cost = 3) The RNA-seq. algorithm produces expression tracks one for each transcripts mapped and were used and expression value was calculated as TPM (Transcripts per million) and RPKM (Reads Per Kilobase per Million mapped reads). The differential expression was analysed from two replicates of each condition using Walds Test. Each gene is modelled by a separate Generalized Linear Model (GLM) and fold changes are calculated from the GLM, which corrects for differences in library size between the samples and the effects of confounding factors. The statistical comparison plots were used to represent the relationship between the p-values of the statistical test and fold changes among the samples as a volcano plot. Heat maps were generated to cluster expression values (Euclidean distance and complete linkage) of each transcript that are differentially expressed. The hierarchical clustering feature in CLC workspace uses the TMM normalization to make samples comparable and perform a Z-score normalization to make features comparable. The Gene Set Test tool for HT1080 RNA-seq. dataset was performed to identify the Gene Ontology (GO) terms that were over-represented in a set of differentially expressed genes (from a statistical test) using hypergeometric test. GO annotations were downloaded from Gene Ontology database for humans.

2.14. COMET Assay (Single cell gel electrophoresis)

Frosted microscope slides were coated with 700µl of 1% Normal Melting Point Agarose (NMPA) in 1X PBS. A coverslip was placed on top to make a uniform layer and kept for overnight drying in a hybridization oven (~55^{0}C). The thickness of the first layer of NMPA (800 µl of 1% NMPA) should be optimum and dried completely, to avoid peeling off from the slide during the entire procedure. Planarian worms were dissociated into single cell suspension (as described in section 2.10.) and re-suspended in 80µl of CMFHE$^{2+.}$ Equal amount of 1.5% Low Melting Point Agarose was added and mixed uniformly. 40 µl of the cell-agarose suspension was added onto NMPA coated slides and allowed to solidify at 4^{0}C until the agarose is solidified (~30 mins and should not be prolonged as keeping embedded cells in the fridge induce cellular stress). Slides were incubated overnight (~15 hours) in a coplin jar at 4^{0}C with 89% Lysing solution [(2.5 M Nacl, 100mM EDTA, 10 mM Trizma base, 8g pelletized NaOH in dH2O, filter and pH 10.0) and freshly added 1% Triton x-100]. The solution was then replaced with neutralization buffer (0.4M Tris base in dH2O, pH to 7.5) for 15 mins and kept at 4^{0}C. The neutralization buffer was then removed, and slides were placed into an electrophoresis chamber at 4^{0}C filled with freshly prepared 1X electrophoresis buffer (10N NaOH and 200 mM EDTA in dH2O, pH = 13). The slides were allowed to equilibrate for 15 minutes followed by an alkaline electrophoresis. The current was adjusted to 20 V for 20 minutes at 4^{0}C. Next, slides were transferred back into the coplin jar and equilibrated for 5 minutes in neutralization buffer. The slides were stained with SYBR Green I (1:10000 dilution) into 1X TE buffer (10mM Tris-HCl and 1mM EDTA, pH 7.5). For long term storage the slides were fixed with cold 100% ethanol for 5 minutes and kept for drying. After drying the comets were at the same plane making it easy for automated imaging. 50 comets per slides were analysed using KOMET software (Andor) and the % of tail DNA was measured after different doses of gamma irradiation. Individual comets were analysed from the centre of the coverslip, due to variation in comet formation towards the edges (because of varied thickness of cell-agarose and overflowing of cells).

2.15. Western blotting

Total protein was extracted by homogenizing 5-7 worms in a solution containing 1XPBS, protease and phosphatase inhibitors. 2X Laemmli buffer (Invitrogen) and DTT were added and the samples were denatured at 80^0C. The protein samples were immediately used for western blotting or stored at -80^0C for long term storage.

The protein sample from each irradiated condition was run on a NuPAGE® 4-12 % Bis-Tris gel (Life technologies) in 1X NuPAGE® MES SDS running buffer using Xcell SureLock™ electrophoresis chamber (Invitrogen) at 200V/125mA for 1 hour until the protein ladder was resolved. The proteins were transferred to PVDF membrane (activated in methanol for 1 minute) using a Mini trans-Blot Electrophoretic Transfer Cell (Biorad) for 1.5 hours in chilled conditions at 125V/300mA. The PVDF membrane was washed with distilled water and stained with Ponceau-S to ensure successful transfer of proteins. The membrane was then washed with PBSTx (0.1% TritonX) and blocked for 1 hour in freshly prepared 3% skimmed milk in PBSTw (0.05%-Tween20). The blocking solution was replaced with the respective antibody solution (diluted in blocking solution) and the samples were left at 4^0C overnight on a rocker. The following day, the membrane was washed with PBSTw (0.05%-Tween20) for 3 hours followed by incubation with respective HRP-based secondary antibody (1:4000 dilution) for 1.5 hours on the rocker at room temperature. The membrane was washed for 45 minutes in PBSTw (0.05%-Tween20) and developed with “Clarity Western ECL substrate” (Biorad) as per manufacturer’s guidelines. Exposure times varied depending on the signals. All the washes were changed to TBS instead of PBS to detect any phosphorylated antibodies in a western blot. Tubulin was used as a loading control for all western blots and H3-pSer10 as a technical control to detect phosphorylated proteins. The western blots presented in this thesis using RAD51 were exposed for 1 minute, H3P-Ser10 for 3 minutes, Smed-H2Ax (non-phosphorylated) for 5 minutes and Smed-H2Ax (phosphorylated) for 1 to 10 minutes and Tubulin for 30 seconds.

2.16. Generation of *Schmidtea* H2AX antibody

A putative H2AX was identified after aligning the 6 H2A variants of *S. mediterranea* (described in chapter 3, section 3.3.2.1.1). A synthetic peptide was designed to the C-terminal of Schmidtea H2Ax (phosphorylated peptide: Cys-NKENRAPKVIE[pS]QEF and Non-phosphorylated peptide Cys-NKENRAPKVIESQEF) to immunize two rabbits (serial number: S4527-1 and S4527-2). A test bleed was taken after 2 booster doses followed by the first production bleed (serum volume:13 ml) after 3rd boost and a second production bleed (serum volume: 15 ml) after 4th boost. The ELISA result of the test bleed titer was 1:100,000. 60 ml of final bleed was taken from individual rabbits and both the phosphorylated and non-phosphorylated antibody was affinity purified. The ELISA titer for the purified phosphorylated antibody from two rabbits was 1:2000 and 1:10,000 and for the non-phosphorylated was 1:10000 and 1:10000 respectively. The antibody concentration was estimated by SDS-PAGE and 1 ml (150 μg/ml) of phosphorylated H2AX and 0.9 ml (300 μg/ml) of non-phosphorylated H2AX antibody was purified from 1st rabbit and 0.9 ml (200 μg/ml) of phosphorylated H2AX and 3 ml (350 μg/ml) of non-phosphorylated H2AX antibody was purified from 2nd rabbit. The immunization of rabbits and subsequent purification of antibody was performed by Proteintech Group (Manchester).

2.17. Cell culture of HT1080 cells

HT1080 cells were cultured using High Glucose DMEM (Dulbecco's modified Eagle's medium) supplemented with 10% Fetal Bovine Serum (FBS), Penicillin/Streptomycin, 7.5% $NaHCO_3$ and 20mM HEPES, and grown in a humid incubator at 37^0C with 5% CO_2. HT1080 cells were grown in a tissue culture treated T-75 flasks (Corning) and upon reaching 75% confluency (visually determined using inverted light microscope), the cell culture media in each flask was changed to fresh medium. Cells were passaged every three days using a standard Tryp-LE based cell trypsinization protocol. HT1080 cells were a generous gift by Prof. Geoffrey Higgins (Department of Oncology, Oxford) and cell culture was performed in the laboratory of Prof. Paul Fairchild (Dunn School

of Pathology, Oxford). For irradiation experiments, cells were plated with equal number and once attached after 48 hours, flasks were irradiated with 2 Gy, 4Gy or 6Gy of ^{137}Cs gamma rays. The cells were incubated at 37^{0}C and 5% CO_2 and fixed for immunostaining after defined time points.

2.18. Immunostaining of HT1080 cells for γ-H2Ax assay

HT1080 cells were grown on tissue-culture treated coverslips in a 6-well culture plates until they reached 75% confluency. Confluent HT1080 cells were irradiated and incubated for 2 hours, following which the coverslips were washed in PBS and fixed in 4% fixative in 1X PBST for 10 minutes at room temperature. Coverslips were then washed in 0.3%PBS-Triton for 10 minutes at room temperature. The cells were blocked for 30 minutes in 1% BSA/PBST (0.1% Tween 20). Following blocking and incubation, HT1080 cells on coverslips were incubated with mouse anti-human γ-H2Ax monoclonal antibody (*Santacruz SC-517348*) at a dilution of 1:250 overnight at 4^{0}C. Following 3 washing for 10 mins each in 0.1 % PBS-Tween, the coverslips were incubated with goat anti-mouse Alexa Fluor 568 secondary antibody in 1% BSA in PBST (0.1% Tween 20) for 1 hour at room temperature at a dilution of 1: 2000. The coverslips were then washed and carefully mounted onto 1.5 mm glass slides using the DAPI-containing mounting medium Fluorshield (Thermos Fisher). HT1080 cells were imaged using Olympus Fluoview FV1000 Confocal laser microscope. The images were processed and γ-H2AX foci were manually counted using *Fiji* software (cell counter plugin).

2.19. Gamma Irradiation

Radiation is considered to be ionizing, if the energy of radiation exceeds the amount needed to eject a single electron from and therefore ionize a target atom. The dose (D) delivered by IR is the energy (E) absorbed per mass unit (m) and is represented by the unit Gray (Gy) [D = E/m; Joule/kilogram] named after Louise Harold Gray. 1Gy = 100 rad. This thesis will use the dose of radiation as Gy.

Animals were starved for at least 7 days and exposed to 1.5,5,10,15,20 and, 30 Gray (Gy) of ^{137}Cs gamma rays using a GSR D1 Gsm (Gamma service GmbH,

serial number: A0108) gamma irradiator at a dose rate of 1.9 Gy/min. The irradiations were performed using a 50 ml falcon tubes with worms settled at the bottom with minimal amount of planarian water (~2 ml).

2.20. Shielded irradiation assay

X-ray irradiation and design of shield Irradiations were performed using a Comet MXR-321 X-ray set operated at 225 kVp and 17 mA with a 0.5 mm aluminium filter. The X-ray field is collimated to 40×20 mm with a 6.1 mm thick lead disc positioned centrally, directly above the X-ray tube focal spot and supported within an aluminium frame. The removable central shielded area is achieved using a 0.8 mm wide, 6.1 mm thick lead strip spanning the long axis of the collimated field; this sits slightly proud of the main lead collimator so that it is in contact with the base of the Petri dish. When in position, the worms are irradiated at a dose rate of 23 Gy/min, reducing to ~1 Gy/min underneath the shielded region. The circular hole in the top aluminium plate corresponds to the outside diameter of the Petri dish and enables dishes to be positioned quickly and reproducibly. Thin strips of materials such as tungsten or tantalum could be used to replace the lead strip to achieve thinner shielded regions if required. The details of the apparatus including the dimensions are available in (Abnave et al., 2017).

2.21. Dosimetry

Dosimetry for all irradiation experiments were performed by Dr. James Thompson and Dr. Mark. A. Hill at ORCRB, Department of Oncology, Oxford. A Gafchromic EBT3 film (International Specialty Products, Wayne, NJ, USA) was placed in the base of an empty 60 mm petri dish to measure the dose rate. The EBT3 film was scanned after 24 hours post exposure in transmission mode at 48-bit RGB (16 bits per colour) with 300 dots per inch resolution using a flatbed scanner (Epson Expression 10000XL). A template was used to position the film within the scanner and the scanning direction was kept constant with respect to the film orientation, as recommended in the manufacturer’s guidelines. The dose was calculated using the optical density of the red channel and corrected using the optical density of the blue channel in order to compensate for small non-uniformities in the film, which cause false apparent variations in dose.

2.22. Measurement of cell migration in shielded irradiation assay

Lack of posterior migration of cells during the experimental timeframe allowed us to define the posterior boundary of the shield. This posterior boundary was used as reference for all distance measurements. Usually, cells in the posterior boundary are confined in a straight lateral line. Next, we defined the anterior boundary of the shield at 0.8 mm in front of the posterior boundary (thickness of shield). By knowing both the posterior and anterior boundary of the shielded region we moved on to measure distances migrated by individual cells. The distance between cells and the anterior boundary gave a direct measurement of the distance migrated by cells.

2.23. Image processing and data analysis

Bright field images were captured using the Zeiss SteREO Discovery V8 microscope attached with a Canon EOS 1200D digital SLR camera. The images were processed in Adobe photoshop and the background was changed into black. Whole worm confocal imaging was done with Olympus FV1000 and Zeiss 880 Airyscan microscope using 63X Oil objective lens and taken as Z-stacks (slices of 4 µm each D/V axis) stitched and then processed as maximum projection using Fiji software. The intensity of the DAPI channel is manually increased to make it uniform without deleting any biological information. All measurements and quantifications were done with Fiji https://fiji.sc/ (using cell counter plugin) and normalized to the area. Images are processed/cropped/pseudo-coloured in Fiji software. The background was changed into black for better visualization and cropping/rotating of images were performed using Adobe Photoshop. All figures are prepared using Adobe illustrator v6.

2.24. Statistical analysis

Results are expressed as mean ± standard deviation (SD). Statistical analyses were performed using Prism, GraphPad Prism version 6.0 (https://www.graphpad.com/). Student's t-test and Tukey's multiple comparison test was used for statistical significance at $p<0.05$.

Chapter 3

Radiation sensitivity and the DNA damage response in planarian stem cells

3.1. Introduction

All cells must accurately maintain their DNA to ensure faithful transmission of their genetic material to the next generation. DNA replication allows the duplication of genome, whereas DNA repair maintains the integrity in response to a myriad of exogenous and endogenous genotoxic agents. For example, DNA replication errors, transposition, spontaneous chemical reactions, reactive metabolic bi-products, exogenous environmental agents, and anti-cancer therapeutics cause DNA damage resulting ~1 million molecular lesions per cell per day (Ciccia and Elledge, 2010; Hoeijmakers, 2009; Lodish et al., 2004). Single strand DNA lesions are the most common and it has been estimated approximately 1% of endogenous single-strand DNA breaks are converted to around 50 Double stranded breaks (DSBs) per cell after each round of cell cycle (Vilenchik and Knudson, 2006).

Two principal recombinant repair pathways to repair DNA lesions have been described, homologous recombination (HR) and non-homologous end joining (NHEJ). HR requires an undamaged template molecule that contains a homologous DNA sequence, typically on the sister chromatid in the S and G2 phase of the cell cycle. In contrast, NHEJ may occur in all cell cycle phases, and does not require an undamaged partner or any homology between recombining ends. It is important to note that DSBs are required for programmed genome rearrangements necessary for antibody generation (class-switch recombination or V(D)J recombination). So not all DSBs are harmful but a vital component of the immune system in jawed vertebrates (Alt et al., 2013; Arya and Bassing, 2017). In this chapter we will discuss the functional significance of DSBs caused by ionizing radiation (IR) and how adult stem cells (SCs) deal with these harmful DNA lesions.

3.1.1. The DNA damage response pathway

DNA double-strand breaks (DSBs) are cytotoxic lesions generated due to exposure to IR, UV radiation, clastogenic (chromosome breakage) agents, and other endonucleases (Jackson and Bartek, 2009; Khanna and Jackson, 2001). Unrepaired DSBs lead to apoptosis or senescence of cells whereas errors in DSB

repair can often lead to genome instability and carcinogenesis (Davis and Chen, 2013). The generalised view for Double stranded break (DSB) repair is described by the Access-Repair-Restore (ARR) model (Smerdon, 1991). In this model the damaged chromatin first becomes accessible to enable DNA repair, followed by restoration of chromatin organization. DNA damage response (DDR) machinery is a cascade of signal transduction processes consisting of multiple interconnected pathways which sense and transduce the damage signals and trigger cellular responses (for example cell cycle arrest, DNA repair or apoptosis). This is primarily mediated by proteins of the phosphatidylinositol 3-kinase-like protein kinase (PIKKs) family- ATM, ATR, and DNA-PK and by members of the poly (ADP-ribose) polymerase (PARP) family (Ciccia and Elledge, 2010). An early event after a DSB is encountered involves recruitment of MRN (Mre11-Rad50-Nbs1) complex that eventually recruits ataxia-telengiectasia mutated (ATM), DNA protein kinase (DNA-PKcs) and ATR (ATM and RAD3 related). Activated ATM phosphorylates the C-terminal tail of the histone variant H2AX at ser139 (also known as γH2AX) that recruits MDC1 (mediator of DNA damage checkpoint protein 1) and other checkpoint mediators like 53BP1 (p53 binding protein-1) and BRCA1 (breast cancer 1, early onset) (Soria et al., 2012). The downstream effects of DDR signalling are mediated by the kinases CHK1 and CHK2 that execute p53 dependent cell cycle arrest and promote cell survival or activate apoptosis /senescence.

3.1.2. DNA repair pathway choices

DSBs are resolved by four possible repair mechanisms depending on the cell cycle stage, extent of resection, presence of a sister chromatid, chromatin compaction and extent of the damage [Fig. 3.1].

3.1.2.1. Role of end resection and cell cycle phase in DNA repair

During DNA replication a chromosome gets untangled for successful cell division and the chromatin gets compacted which eventually lead to changes in the substrate of DNA repair. Thus the cell cycle stage at which a DSB is encountered

plays a major role for the repair pathway choice (Hustedt and Durocher, 2017). Nuclease-mediated end resection is activated by the phosphorylation of C-terminal binding protein-interacting protein (CtIP or Rbbp8 (Sae2 in Yeast)) to generate recombinase-coated single-stranded overhangs (Huertas and Jackson, 2009; Sartori et al., 2007). The end resection leads to the formation of ssDNA varying from few hundred nucleotides to few kilobases long, depending on the availability of the homologous template (Chung et al., 2010). The ssDNA is first bound by RPA (Replication Protein-A), which is replaced by RAD51 forming a nucleo-filament through a concerted action of BRCA1-PALB2-BRCA2 recombination mediator complex [Fig. 3.1. A].

Cells in G1 phase also show limited end resection due to reduced CDK (cdc28) activity and thereby activates Ku-dependent NHEJ/Classical NHEJ (C-NHEJ). C-NHEJ is a blunt end ligation that is independent of any sequence homology and can occur throughout the cell cycle but predominantly by cells in G0/G1 phase (Chiruvella et al., 2013; Karanam et al., 2012). In contrary, HR uses a sister/homologous chromatid and requires a strand invasion mediated by the recombinase RAD51. This process is generally error free and cells mostly use HR in mid-S phase (4N stage) [Fig. 3.1. A]. 3’ end resected DNA can also be repaired either by single stranded annealing (SSA) or by the Alternative NHEJ (alt-NHEJ) repair pathway [Fig. 3.1. B-C]. Overall, the extent of resection is the critical factor that decides SSA, Alt-NHEJ or HR and C-NHEJ. 53BP1 (end resection inhibitor) is the major regulator that monitors the balance between HR and SSA (Ochs et al., 2016).

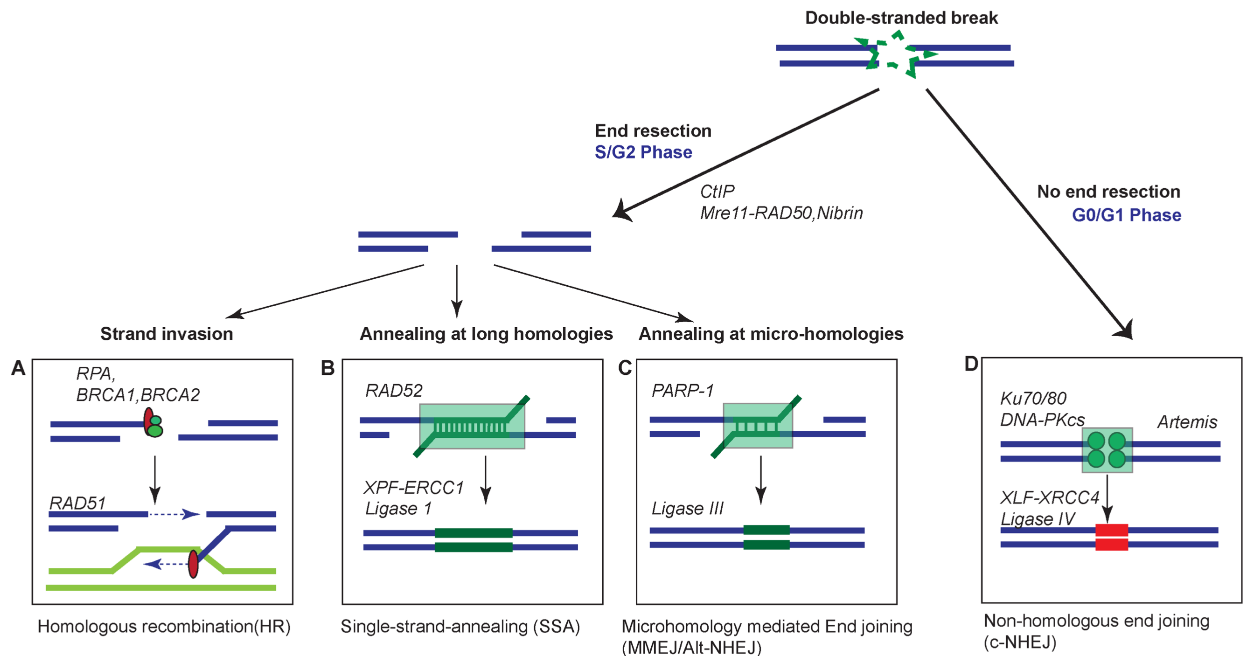

Figure 3.1. Schematic showing the different DNA repair pathway choice in eukaryotic cells. Nuclease-mediated end-resection is specifically activated in S/G2 phase of the cell cycle. **(A)** Proteins that help in strand invasion to undergo homologous recombination (HR) bind the ssDNA. **(B, C)** 3' end resected DNA can also be repaired by SSA or Alt NHEJ depending on the homology search and mostly in the repetitive sequences. **(D)** C-NHEJ does not require end resection and is active throughout the cell cycle but is mostly used to repair DSBs in G0/G1 phase of cell cycle. [Adapted from (Ceccaldi et al., 2016)]

3.1.2.2. DSB repair in repetitive sequence and in microhomologies

DSB encountered between a tandemly repeated sequences may expose complementary sequences after end resection. This can lead to the annealing of homologous repeat sequences flanking a DSB without undergoing strand exchange. The outcome is often mutagenic and error prone due to the deletion of sequences and rearrangement between the repeats. Therefore, a competition always exists to supress the mutagenic repair pathways and activate error free HR, as both involves end-resection via phosphorylation of CtIP.

CtIP mediates the end resection to form 3’ ssDNA flanking the homologous repeats that are annealed together to form a synapsed intermediate. The non-homologous 3’ ssDNA tails are eventually cleaved off by endonucleases and polymerase ligates the end gaps [Fig. 3.1. B]. Another recombinase RAD52 re-anneals the Replication-protein A (RPA) bound ssDNA (homologous sequences flanking the DSB) leading to deletion of intervening sequence and thus considered to be a mutagenic repair process (Bhargava et al., 2016). RAD52 plays a major role in SSA in yeast (Lee et al., 2003; Shinohara and Ogawa, 1998) , however vertebrate RAD52 does not seem to be crucial for DSB repair. This is based on the observation that RAD52 knockout mice do not show any DSB repair defects or increased sensitivity to IR (Rijkers et al., 1998). In contrary, BRCA2 plays the major role in loading RAD51 on RPA-coated ssDNA, thus making RAD52 redundant. However, RAD52 deficiencies are synthetic lethal with BRCA1 and BRCA2 deficient mammalian cells (Feng et al., 2011; Lok et al., 2013) suggesting RAD52 may act as a back-up to BRCA1 or BRCA2 containing organisms.

CtIP dependent end joining is not only restricted to DSB repair in S/G2 phase but also required for Alt-NHEJ in G1 cells (Yun and Hiom, 2009). Alternative NHEJ anneals short (6-20 bp) homologous repeats (microhomology) flanking the DSBs, hence also termed as microhomology-mediated End joining (MMEJ). This repair pathway can also lead to deletion of fragments and is therefore considered to be mutagenic like SSA. Although both SSA and Alt-NHEJ involves annealing of

flanking homologous repeats, the intermediate factor responsible to mediate synapsis and annealing appear to be distinct. For example, RAD52 plays a conserved mediator for SSA, while PARP and DNA-Polymerase theta is important for Alt-NHEJ (Sfeir and Symington, 2015; Wang and Xu, 2017).

3.1.2.3. DSB repair throughout the cell cycle: canonical NHEJ

C-NHEJ does not require an intact homologous template or end resection to bridge the DSB and is therefore active throughout the cell cycle but preferentially in G0/G1 phase and in some post-mitotic cells. Both ends of the DNA break are bound by the Ku70/80 heterodimer, which recruits the catalytic subunit of DNA-dependent protein kinase (DNA-PKcs) (Chang and Lieber, 2016) . The ends can be either trimmed by nucleases (like Artemis) or filled by DNA polymerases lambda and mu to create compatible ends (Lieber, 2008, 2010). The ligation complex (Ligase IV, X-ray cross-complementation group 4 (XRCC4), XRCC4 like factor (XLF) and paralog of XRCC4 and XLF (PAXX)) ligates the ends (Ahnesorg et al., 2006) [Fig. 3.1. D].

3.1.3. DSB repair and genome plasticity

SSA may restore broken chromosome with DSBs that have undergone extensive end resection and cannot be resolved by HR or Alt-NHEJ (Bhargava et al., 2016). The presence of large numbers of highly repetitive sequences in the DNA also affects the DSB repair choice and is a major source of genome plasticity. Any DSB encountered in the repetitive element gives the HR machinery to either recombine with allelic sequences on sister chromatid/homologous chromosome or to recombine with non-allelic repeats. This often makes HR between homologous repeats prone to misalignment leading to extensive chromosomal rearrangements between repetitive DNA sequences. Therefore, a balance between genome size and genome instability exists in higher eukaryotes like humans (large genome with high repetitive elements). For example, NHEJ generally dominates over HR in higher eukaryotes to reduce misalignment of homologous sequences (Brandsma and Gent, 2012). On the other hand, HR

dominates in organisms with a small genome and with low abundance of repetitive sequences. A recent study reported a complete loss of C-NHEJ and instead relies on mutagenic Alt-NHEJ/MMEJ repair pathway in larvaceans *Oikopleura*. The consequence of MMEJ is deletion of larger gene fragments which would contribute to extensive genome compaction and a relatively smaller genome size in *Oikopleura dioica* (<70Mb) compared to other larvacean genomes (~1 Gb) (Deng et al., 2018). Non-allelic HR between repetitive DNA sequences such as transposable elements have also played a major role in reshaping the genome (Argueso et al., 2008; Kidd et al., 2008; Korbel et al., 2007; Sharp et al., 2006).

3.2. Aim of this Chapter

IR leads to DNA damage by creating double-stranded breaks (DSBs) which if not repaired, can lead to cell death or oncogenic transformation. We lack the complete understanding of the molecular processes that lead to cell transformation, tissue hyperplasia and tumour formation that would allow us to design more effective personalised therapies for cancer. Understanding both the broad properties of stem cells that are related to cancer pathology and how stem cells survive and adapt to anticancer therapies is therefore a key goal and any suitable new model is of potentially very high biomedical value.

In this chapter, we want to exploit the potential of the planarian model for understanding the radiation sensitivity and the DNA damage response in SCs. Planarians contain a large population of pluripotent adult stem cells, which are required for their celebrated powers of regeneration and homeostatic plasticity. We have discussed the role of many conserved pathways that regulate stem cell renewal, differentiation and proliferation in planarians and like cancer cells, the planarian SCs show a heterogenous dose dependent sensitivity to IR (Wagner et al., 2011). The aim of this chapter is to identify different DNA repair genes in planarians and to characterize the pathways that repair DNA breaks in SCs.

3.3. Results and discussion

3.3.1. Planarians can resist a high dose of ionizing irradiation

Planarian stem cells can be selectively ablated following exposure to lethal dose (>30 Gy) of IR (Wagner et al., 2011, 2012). In order to understand, the maximum dose a planarian can survive, planarians were exposed to an increasing gradient dose of γ-irradiation. The survival curve suggests asexual planarians (~ 5 mm size) were capable of resisting doses up to 15 Gy**.** The worms initially show head regression and tissue lesion, but eventually resolve this damage normally [Fig. 3.2. A-B]. Using Fluorescent *In-Situ* Hybridisation (FISH) of *smedwi-1* mRNA transcript on planarians exposed to different dose of γ-irradiation, we observed decrease in SC number (*smedwi-1*$^{+}$ cells) concomitant with an increase in dose of irradiation ranging from 5 to 30 Gy [Fig. 3.2. C]. SCs that survive after exposure to doses below 15 Gy can repopulate and rescue the entire worm within 21-days post irradiation (dpi) [Fig. 3.2. C-D]. On the other hand, SCs that survived after exposure to 20 Gy of IR failed to repopulate. This led us to use 15 Gy as a non-lethal dose of IR that reduces the SCs number but does not affect worm survival. The number of cells in mitosis undergoes a dose-dependent decrease post-IR [Fig. 3.3. A] and the repopulation of mitotic cells suggests the worms irradiated with doses up to 15 Gy can eventually proliferate back to wild type worms [Fig. 3.3. B]. The number of stem cells in M phase was greatly reduced as early as 1.5 hours post 15 Gy exposure. This suggests that IR exposure induces a cell-cycle checkpoint block in most of the cycling cells, that only start to proliferate after 72 hours post IR [Fig. 3.3. B]. To study if clonal repopulation of SCs after exposure to 15 Gy of IR leads to complete recovery without any long-term physiological defects, we amputated the rescued animals to check regenerative capacity. We did not observe any discernible regeneration defects after amputation of the rescued worms (27 days post 15 Gy exposure) [Fig. 3.3. C-D]. Using FISH, we also verified that stem cell (*smedwi-1*), early epidermal progenitor (*prog-1*) and later epidermal progenitor (*Agat-1*) counts were as in wildtype worms [Fig. 3.3. E].

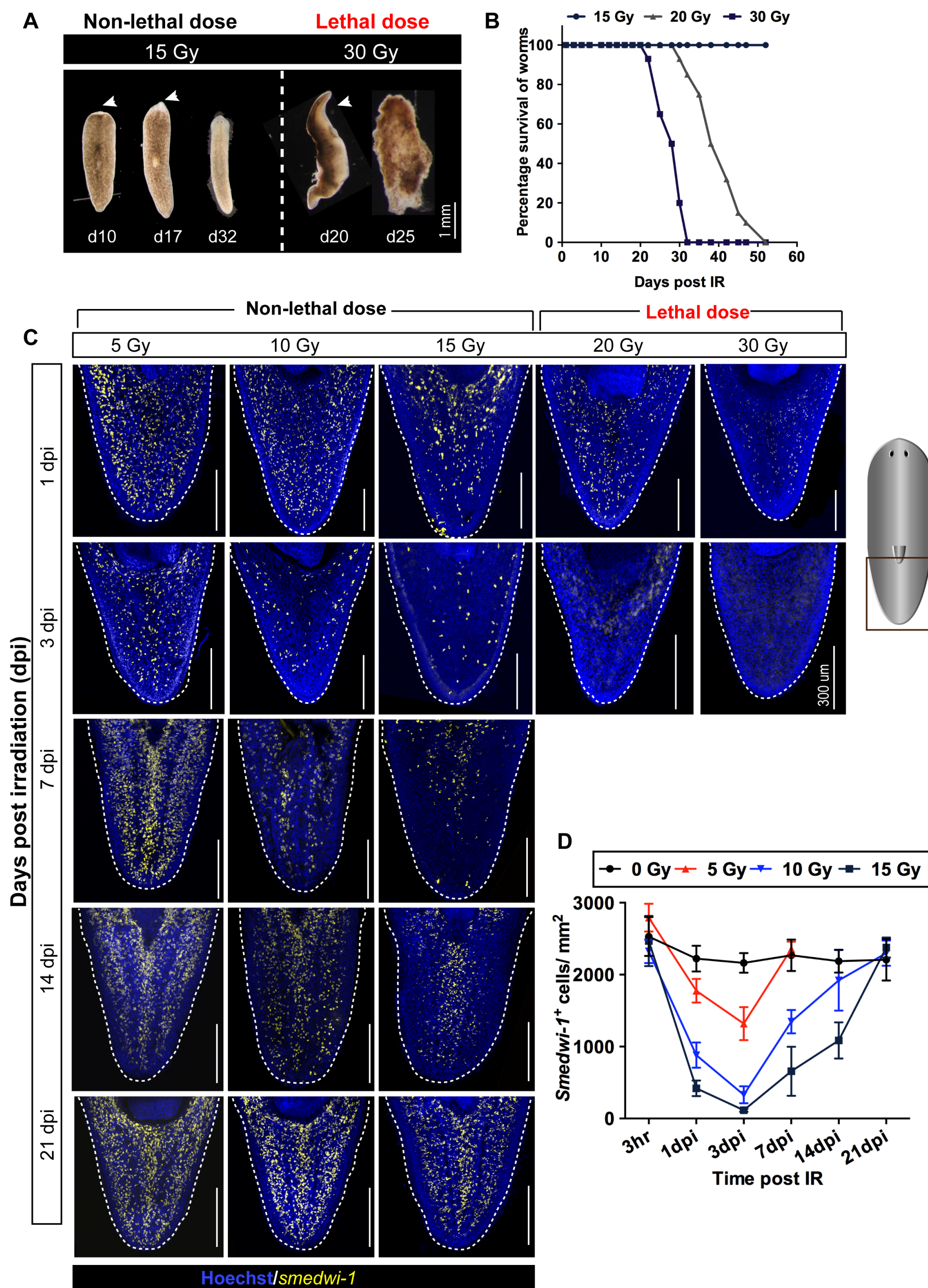

Figure 3.2. Planarian stem cells can resist doses up to 15 Gy of γ-irradiation. (A) Brightfield images of wild type planarians exposed to 15 Gy of IR (non-lethal dose) and 30 Gy of IR (lethal dose). **(B)** Survival curve showing the percentage of worms survived after different dose of IR. **(C)** *smedwi-1* FISH of planarians exposed to different doses of gamma IR (5,10,15,20 and 30 Gy) after 1,3,7,14 and 21 days post IR (dpi) showing a dose dependent decrease in stem cell number. Scale bar: 300 µm. The nucleus is stained with Hoechst (Blue). **(D)** Quantification of *smedwi-1*$^{+}$ cells/mm^2 (yellow) showing the repopulation kinetics of surviving stem cells after different doses of IR post IR (n = 5 per dose, per time point). Results are expressed as mean ± SD

We also checked the proportion of cells at different phase of cell cycle that survive post-IR. Using flow-cytometry, we observed cells in S/G2/M-phase (X1 population) were most sensitive to IR and are completely ablated after lethal dose of 30 Gy [Fig. 3.4]. The stem cells in G1 phase (X2 population with post mitotic progenies) were present after irradiation, that led us to hypothesize that G1 stem cells are mostly radio-resistant and can repopulate the whole worm [Fig. 3.4]. Our previous data using immunohistochemistry with H3-pSer10 (mitotic marker) showed the existence of very few mitotic cells after 24 hours post 15 Gy IR [Fig. 3.3. A], which we cannot detect by flow-cytometry suggested an accumulated effort of cells in G1 (X2 population) and G2/M phase eventually repair and proliferate. Future studies using antibodies to mark G1 cells (currently unavailable in planarians) will provide more insights to understand radiation tolerance in a particular cell cycle phase. Overall our data suggests that animals can tolerate a high dose of 15 Gy IR and the surviving stem cells can repopulate and rescue the entire animals with no long-term physiological defects in stem cell proliferation and differentiation.

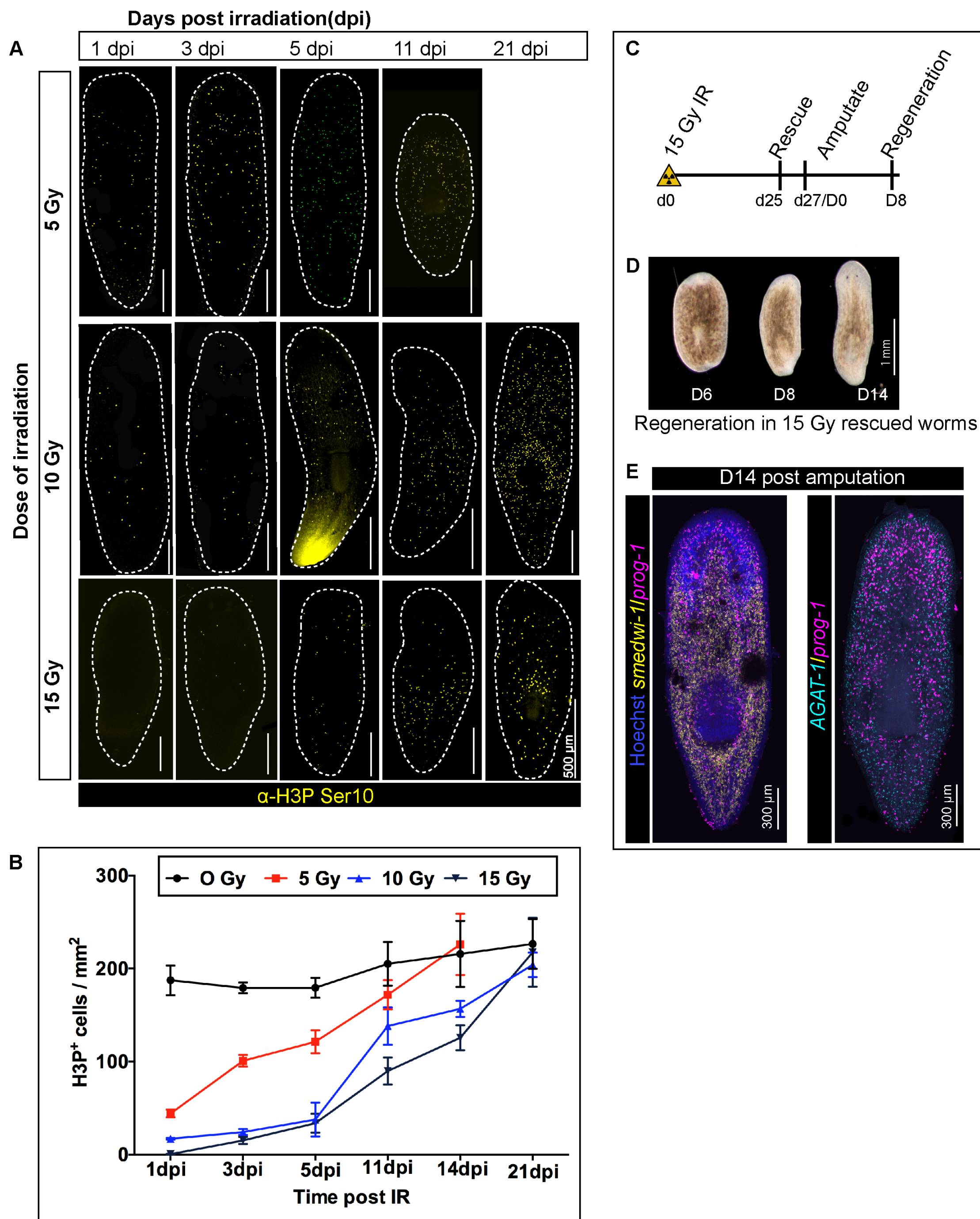

Figure 3.3 Dynamics of stem cell proliferation after different doses of IR. (A) Immunostaining with mitotic marker Anti-H3 phosphorylated-ser10 (H3-pSer10) showing the repopulation of mitotic cells (yellow) after exposure to different doses of gamma IR (5,10,15 Gy) at indicated days post IR (dpi). Scale: 500 µm (B) Quantification shows the repopulation kinetics of mitotic cells at different doses of irradiation (n = 5 per condition). Results are expressed as mean ± SD. (C-D) Brightfield images showing the worms rescued after exposed to 15 Gy IR undergo normal regeneration within 7 days post amputation. (E) FISH using *smedwi-1* (stem cell marker) and *prog-1* (Early epidermal progeny marker) and *AGAT1* (Late epidermal progeny marker) show normal distribution of cell after 14-day post amputation in rescued planarians.

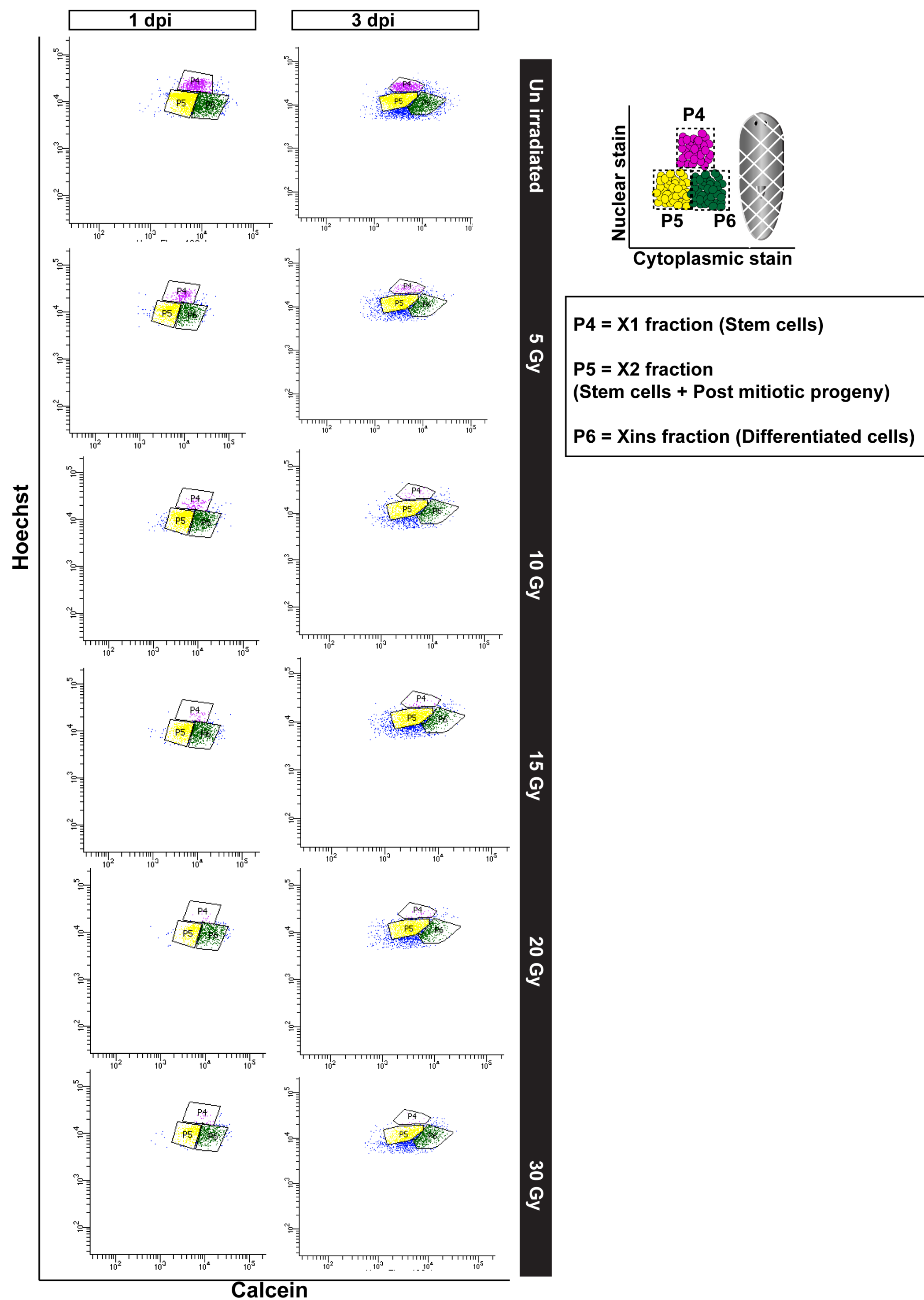

Figure. 3.4. Flow cytometry data showing the survival of planarian stem cells at different phases of cell cycle to different doses of IR. Planarian cells were dissociated and stained with Hoechst 34580 (Nuclear) and Calcein (Cytoplasmic). Three different population of cells were detected using FACS based on the nuclear to cytoplasmic content. X1 fraction (containing stem cells in S/G2/M phase), X2 fraction (containing stem cells in G1 phase and post-mitotic progenies) and Xins fraction (containing differentiated cell types). The X1 stem cell fraction decreases over the time with increasing dose of IR.

3.3.2. Methods to study DNA damage response in planarian stem cells

IR induces DNA breaks and we focussed to develop markers/assay to detect DNA damage and understand the kinetics of IR-induced DNA break repair in planarian stem cells.

3.3.2.1. Immunostaining to detect DNA damage in stem cells

3.3.2.1.1. H2Ax variants in *Schmidtea mediterranea*

Double stranded breaks (DSBs) result in the phosphorylation of histone H2A variant at Ser139 by kinases such as ataxia telangiectasia mutated (ATM) and ATM-Rad3-related (ATR). This phosphorylated protein, also known as γ-H2AX is the first step in recruiting and localizing DNA repair proteins and initiate a cascade of biochemical events to repair double stranded breaks (DSBs) (Bonner et al., 2008). Intriguingly, the phylogeny of nucleosome suggest H2AX variants have arisen multiple times (Malik and Henikoff, 2003; Thatcher and Gorovsky, 1994) and is the minor variant of H2A gene family. Although exceptions include, *S. cerevisae* genome that contains only H2AX (no canonical H2A gene) and *C. elegans* lacks H2AX.

The consensus signature sequence specific to H2Ax proteins and not present in canonical H2A proteins in mammals is SQEY. The presence of serine in the C-terminal is conserved in all metazoans that gets phosphorylated in response to DNA damage (Rogakou et al., 1998). Although variation in SQ {xx} exist in metazoans hinting an important role for this amino acid change. For example, Xenopus H2AX encodes 1 protein with SQEY motif and 2 distinct genes encoding SQEF motifs. H2AX with SQEF motifs were also identified in goldfish, zebrafish and in Arabidopsis and chickpea (Shechter et al., 2009). Interestingly, two H2Ax variants have been identified in another highly regenerative model, *Hydractinia.* H2Ax.1 [SQEY] is a replication-independent variant expressed in the feeding polyps in both the sexual strains. On the other hand H2Ax.2 [SQAY] is a *Hydractinia* variant expressed only in the female germ cells and could be involved in regulating DNA repair (Török et al., 2016). To understand the DDR mechanism in planarians we looked for H2A variants in the *Schmidtea mediterranea* genome

to identify a putative H2AX. We found 6 H2A variants and identified a putative H2Ax with a signature SQEF motif at the C-terminal [Fig. 3.5. A-B]. Some commercially available Human H2Ax antibodies have been published to cross-react in planarians (Barghouth et al., 2018; Thiruvalluvan et al., 2017; Yin et al., 2016), but failed to give a specific staining to detect DSBs in planarians in our laboratory. This led us to try and develop a *Schmidtea* specific H2Ax antibody near the C-terminal [NKENRAPKVIE {pS} QEF]. [Fig. 3.5. C]. The predicted molecular weight of H2Ax in Schmidtea is 16 kDa. We performed a western blot using whole protein lysate from irradiated worms to detect the specificity of this antibody. Our data showed the Non-phospho antibody can detect proteins at 16 kDa and phosphorylated one at 17 kDa (probable H2AX) and other stronger bands at 25, 37 and 50 kDa. The molecular weight (MW) of Ubiquitin is 8.5 kDa and the MW of SUMO is 11 kDa. The higher bands in our western blot could be ubiquitinated H2AX (24 kDa) and SUMOylated H2AX (37 kDa) [Fig. 3.5. D]. Although this requires further verification by an immunoprecipitation followed by mass-spectrometric analysis to detect the protein modifications. But the phospho-specific antibody (γ-H2AX) failed to give any signals in western blot or immunohistochemistry [Fig. 3.5. E]. We used a phosphorylated H3-Ser10 antibody in our western blot/immunohistochemistry as a positive control to detect a phospho-specific protein in planarians. The planarian H2Ax seem to be more conserved with the Drosophila H2Av. We tried the Drosophila H2Av antibody (DSHB) (Lake et al., 2013) but failed to detect any specific signals in western blot/immunohistochemistry.

A

```
               1         10         20         30         40         50         60         70         80         90
SMU15017658                   MSAKG--KTGKTTKFQSKIRSSRTGLQFPVGRIHRKLRKGNLTERVGAVAPVYLASVLEYLATEVLELAGNAA
SMU15035011              MCLDKMSGKAG-KAGKTSRNQSKTRSSRAGLQFPVGRIHRKLRKGNFAERVGAGAPVYLAAVLEYLAAEVLELAGNAA
SMU15005266                   MSAKG--KAGKTTKSQSKTRSSRAGLQFPVGRIHRKLRKGNFAERVGAGAPVYLAAVLEYLAAEVLELAGNAA
SMU15005267    FSRACSIKSMISVQELTSFNMSTKR--KAGKTNKSQSRIRSTRAGLHFLVVRIHRKLRKGNFAERVGAGAPVYLAAVLEYLAAEVLELAGNAA
SMU15010840                   MSGKA--GKA-LKKSQSKTRSSRAGLQFPVGRIHRKLRKGNFAERIGAGAPVYMAAVLEYLAAEVLELAGNAA
SMU15026988                  EMSGKA--GKAKITKTKSQTRSSRAGLQFPVGRLHRKLRKGNFAERVGAGAPVYMAAVLEYLAAEVLELAGNAA
SMU15037275           WVTLIIIMSGRG--KSGGKTRTKAKTRSSRAGLQFPVGRIHRKLRKGNYAERIGAGAPVYLAAVLEYLAAEVLELAGNAA
SMU15040137                   MSGRG--K-GGKSRNKAKSRSVRAGLQFPVGRIHRWLRKGNYAERVGSGAPVYLAAVLEYLAAEVLELAGNAA
SMU15013108               MSTTGKGGKAKGKTASSKQVSRSARAGLQFPVGRISRFLKNGRYSERIGTGAPVYLAAVLEYLAAEVLELAGNAA
Smed_H2Ax                     MTKKENIGAHGKVKKLQNSRSSRAGLTFPVGRVHRLLRKGKFGERIGHGAPVYMSAILEYLTAEILELAGNAA

               100        110        120        130        140        150        160     167
SMU15017658    RDNKKSRIIPRHLQLAIRNDEELNKLLGGVTISQGGVIPNIQSALLPKKTEEKPAK*
SMU15035011    RDNKKSRIIPRHLQLAIRNDEELNKLLGGVTISQGGVIPNIQSALLPKKTEEKPAKGNLLKITSISSSVRDSP*
SMU15005266    RDNKKSRIIPRHLQLAIRNDEELNKLLGKVTIAQGGVLPNIQISLLPKKAEEKKRDLEARN*
SMU15005267    RDNKKSRIIPRHLQLAIRNDEELNKLLGKVTIAQGGVLPNIQISLLPKKAEEKK*
SMU15010840    RDNKKSRIIPRHLQLAIRNDEELNKLLGHVTISQGGVLPNIQNSLLPKKAEEKDK*
SMU15026988    RDNKKSRIIPRHLQLAIRNDEELNKLLGHVTISQGGVIPNIQASLLPKKTEEKEK*
SMU15037275    RDNKKTRIIPRHLQLAIRNDEELNKLLGGVTIAQGGVLPNIQAILLPKKTPKESS*
SMU15040137    RDNKKTRIIPRHLQLAIRNDEELNKLLGSVTIAQGGVLPNIQSVLLPKKTSNDKKKNKIQYFFYNINI*
SMU15013108    KDNKKTRIVPRHILLAIRNDEELNKLMANTTIADGGVLPNINPMLLPSKTKKSTEPEH*
Smed_H2Ax      RDNKKSRIAPRHILLAIKNDSELSELLKSVTISQGGVMPNIQNTLLPKTPNKPVANKENRAPKVIESQEF*
```

H2Ax variant in *S.mediterranea*

B

```
             1        10        20        30        40        50
Hsap_H2Ax    MSGRGKTG--GKARAKAKSRSSRAGLQFPVGRVHRLLR-KGHYAERVGAGAPVYLAA
Smed_H2Ax    MTKKENIGAHGKVKKLQNSRSSRAGLTFPVGRVHRLLR-KGKFGERIGHGAPVYMSA
Dmel_H2Av    MAGGKAGKDSGKAKAKAVSRSARAGLQFPVGRIHRHLKSRTTSHGRVGATAAVYSAA

             60        70        80        90        100       110
Hsap_H2Ax    VLEYLTAEILELAGNAARDNKKTRIIPRHLQLAIRNDEELNKLLGGVTIAQGGVLPN
Smed_H2Ax    ILEYLTAEILELAGNAARDNKKSRIAPRHILLAIKNDSELSELLKSVTISQGGVMPN
Dmel_H2Av    ILEYLTAEVLELAGNASKDLKVKRITPRHLQLAIRGDEELDSLIK-ATIAGGGVIPH

             120       130       140   147
Hsap_H2Ax    IQAVLLPKKTSATVGPKAPSGGKKATQASQEY
Smed_H2Ax    IQNTLLPKTPNKPVANKENRAPK--VIESQEF*
Dmel_H2Av    IHKSLIGKK-ETVQDPQ-RKGN--VILSQAY
```

Millipore 05-63...

Smed Ab; Domain

Hawley H2Av Ab; Domain

Serine 139 gets phosphorylated after DNA damage and termed as gamma H2Ax

C

Phosphopeptide

Cys-NKENRAPKVIESQEF

Non-Phosphopeptide

Cys-NKENRAPKVIESQEF

D

30 Gy-72 hr | 15 Gy-6 hr | 0 Gy

250 kDa, 150 kDa, 100 kDa, 75 kDa, 50 kDa, 37 kDa, 25 kDa, 20 kDa, 15 kDa, 10 kda

1:500 dilution
(5%BSA/0.05% TBSTween)
Non-Phospho H2Ax

E

30 Gy-72 hr | 15 Gy-6 hr | 0 Gy

250 kDa, 150 kDa, 100 kDa, 75 kDa, 50 kDa, 37 kDa, 25 kDa, 20 kDa, 15 kDa, 10 kda

1:1000 dilution
(5%BSA/0.05% TBSTween)
Phospho H2Ax

F

Post-regeneration: 6h, 12h, 24h, 48h, 72h, d5
Irradiation: 5 Gy, 10 Gy, 15 Gy

H3-pSer10 — 17 kDa

RAD51 — 37 kDa

Tubulin — 50 kDa

Figure. 3.5. H2AX in planarians. (A) Multiple sequence alignment of the different H2A variants identified in *Schmidtea* genome. H2AX is identified by its unique C-terminal containing [SQ] motif. (shown by an arrow) **(B)** Multiple sequence alignment of Human H2AX, Drosophila H2Av variant and Smed-H2AX, showing a strong conservation in H2A along with C-terminal containing [SQ] motif. The highlighted region represents the region used for generating commercial antibodies. **(C**) The peptide used for generating the *Schmidtea* H2AX specific antibody by "Proteintech Group (Manchester)". The antibody recognising the phosphorylated region is in red and the Non-phosphorylated region is in Black. The non-phosphorylated antibody (Black) detects the phosphor and un-phosphorylated peptides. However, the red only detects the phosphor peptide thus specific interaction. **(D-E)** Western blot showing the specificity of the non-phosphorylated and the phosphorylated antibody to detect H2AX in planarians. **(F)** Western blot (technical controls) using a DNA damage repair protein (Smed-RAD51) and a phospho-specific antibody (H3-pSer10) during regeneration time course and after different dose of IR.

3.3.2.1.2. RAD51 and Poly-ADP-Ribose (PAR) formation detects DNA damage in stem cells.

We have performed a time course of DSB repair kinetics using a *S. mediterranea* specific RAD51 antibody (kind gift by Prof. Scott Hawley, Stowers Institute, USA) previously used to detect meiotic DSBs in the germline. (Xiang et al., 2014). We checked the specificity of this antibody in a western blot using whole worm lysate and it gives an intense band around 37 kDa (molecular weight of full length smed-RAD51) and some non-specific bands (>110 kDa, faint bands) [Fig. 3.6.A]. We checked the expression of RAD51 in planarian cells after exposed to a non-lethal dose of IR (15 Gy) by western blot. Although RAD51 protein expression is not induced after irradiation, we observed a clear decrease in expression after 5- and 9-days post 15 Gy IR due to the presence of very few stem cells at that time-point [Fig. 3.6. A]. We next investigated to detect DSBs in stem cells but failed to see any specific Rad51 staining in whole mount immunohistochemistry (IHC) after multiple attempts and using different optimisations (antigen retrieval, fixation, permeabilization methods). So, we used dissociated cells to perform a time course of RAD51 localization to nucleus after irradiation. We observed an increase in the number of Rad51 stained nuclei as early as 6 hours post IR [Fig. 3.6. B-C] that return to pre-irradiation levels by 72 hours post IR. The surviving

stem cells at 72 hours start to proliferate and this data correlates with our stem cell survival and repopulation kinetics data [Fig. 3.2 and 3.3]. This suggests cells enter M phase and start dividing after DNA repair. We could not detect any staining in whole mount IHC and tried to see if this antibody works on planarian paraffinized sections. We detected some staining in irradiated worms (using Trilogy based antigen retrieval method) [Fig. 3.6. D] and future experiments should focus on detecting RAD51 co-localization with smedwi-1 stem cells, to detect DSBs in planarian stem cells.

Apart from DSBs, IR also leads to the generation of single-stranded breaks (SSBs) that induce polymerisation of poly-ADP-ribose (PAR). An antibody to detect PAR polymer formation has been previously used as a marker for DNA damage in planarians (Shibata et al., 2016) and in human cells (Gibbs-Seymour et al., 2016). We used the Anti-PAR mouse monoclonal antibody (Santacruz, clone 10H) and detected nuclear localization in TUD-1$^+$ cells [Fig. 3.6. E]. Our lab has developed an antibody to the Tudor-1 homologue in *Schmidtea* (Smed-TUD1) that detects perinuclear RNA-granules (also known as chromatoid bodies) in neoblasts (Solana et al., 2009). We therefore checked for the intense perinuclear staining of Tud1 antibody to mark the stem cells and PAR antibody to detect DNA damage in neoblasts [Fig. 3.6. F]. Smed-TUD1 antibody detects some of the early stem cell progenies and therefore we used PAR antibody immunostaining along with *smedwi-1* FISH (pan-stem cell marker) but observed a strong background epidermal staining of Anti-PAR with no staining in the stem cell plane [Fig. 3.7. B]. This could be due to lack of permeabilization and performing these experiments in paraffin sections might reduce the background staining. Although some of the Tud1$^+$ cells have strong PAR signals in unirradiated controls, an optimised protocol and analysis of these staining is important to confirm the antibody specificity. Optimising these antibodies to detect DNA damage in stem cells is currently ongoing in the lab and due to lack of any commercial antibodies to cross-react in planarians, we looked for other molecular techniques to detect DNA breaks.

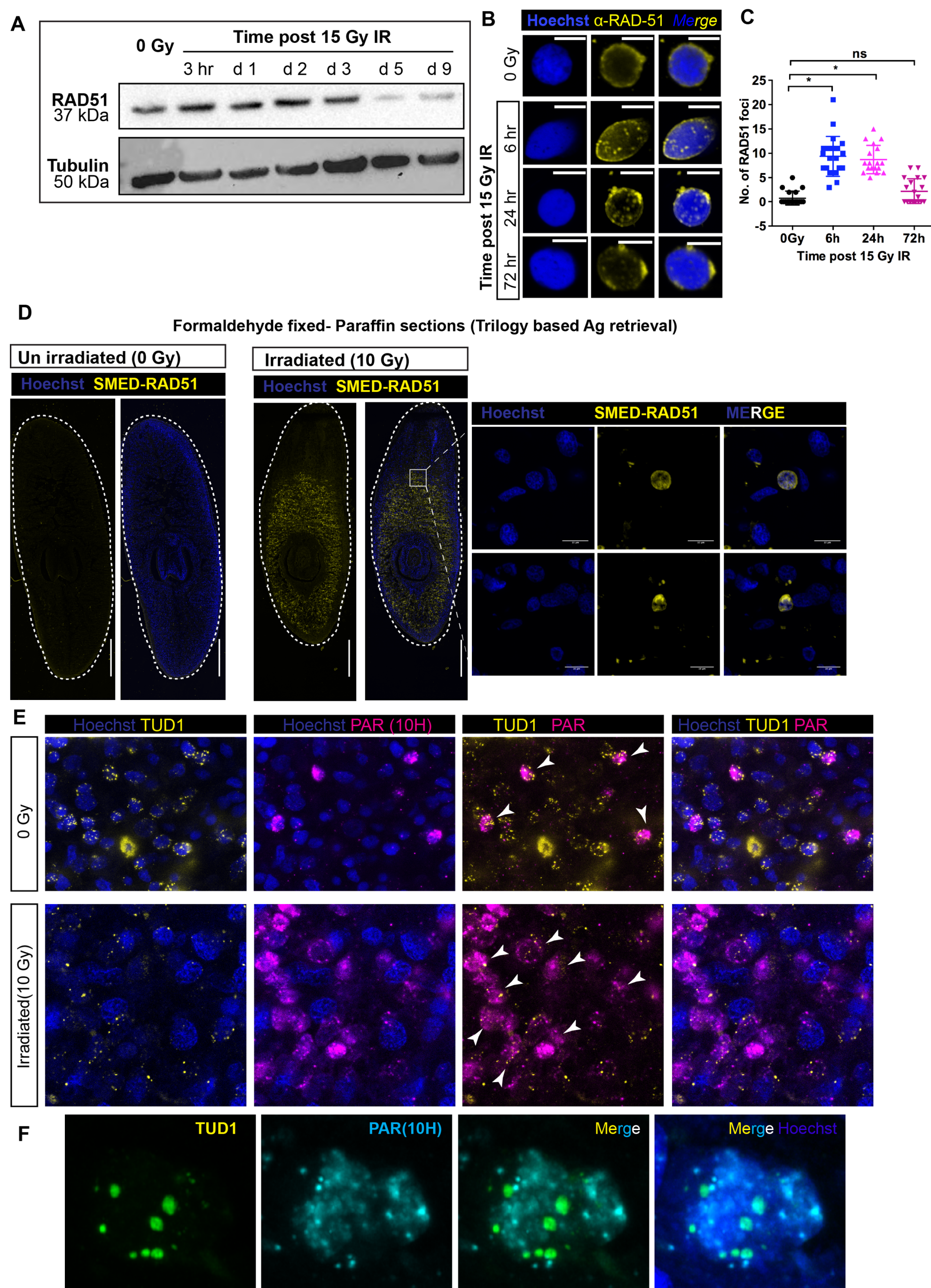

Figure. 3.6. RAD51 foci and Poly ADP-Ribose (PAR) polymer formation in planarian stem cells. (A) Western blot using whole planarian cell lysate showing the specificity of RAD51 antibody (37 kDa), and a time course showing protein kinetics post 15 Gy IR. Tubulin was used as a control. **(B)** Time course showing RAD51 foci formation in dissociated planarian cells after irradiation **(C)** Quantification of RAD51 foci in individual planarian cells (ns=not significant, *p-value<0.05, Students unpaired t-test). **(D)** Optimisation of RAD51 immunostaining in planarian sections with a magnified image to visualise single cells showing RAD51 staining. **(E)** Double immunostaining using anti-TUD1 and anti-PAR antibody to detect DNA damage in planarian stem cells post-IR. **(F)** A representative high resolution Airyscan imaging of PAR staining in TUD1+planarian cells.

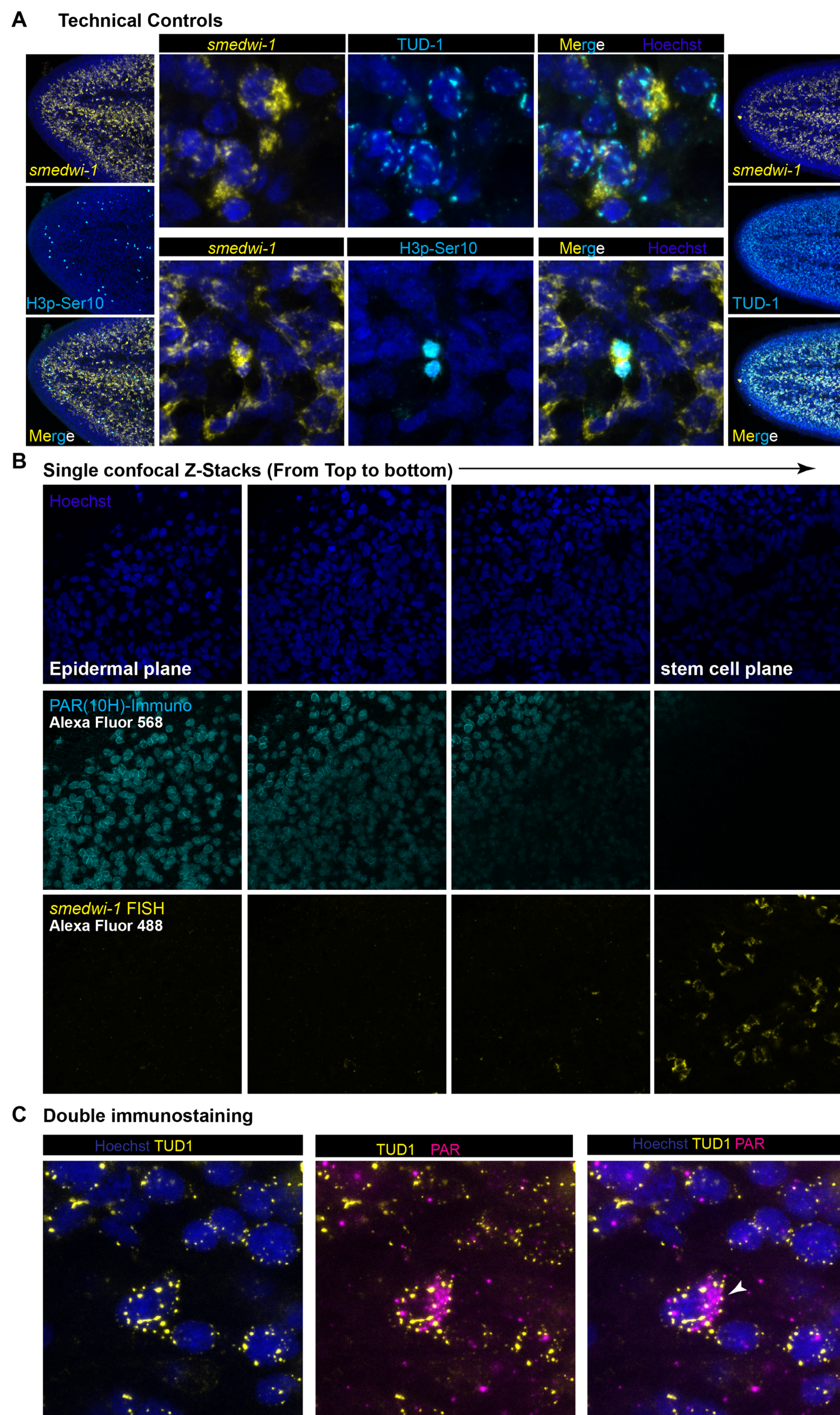

Figure. 3.7. Optimisation of Anti-PAR antibody to detect DNA damage in planarian stem cells. (A) Technical controls for double FISH and immunostaining showing Anti-H3-pSer10 immunostaining in *smedwi-1*+ stem cells and Anti-TUD1 immunostaining in *smedwi-1*+ stem cells. **(B)** Optimisation of anti-PAR antibody after *smedwi-1* FISH, showing intense epidermal background staining of PAR antibody and no signals in *smdewi-1* (stem cell plane). **(C)** Double immunostaining with anti-PAR and anti-TUD1 in whole mount planarians.

3.3.2.2. COMET assay in planarians

Single cell gel electrophoresis (SCGE; also known as comet assay) is a classical method to detect DNA breaks (single/double stranded breaks) base damage, DNA-protein crosslinks. The advantage of comet assay is its sensitivity to detect various kinds of DNA damage at a single cell resolution, and any eukaryotic cell is amenable to analysis. Cells were embedded in agarose on a microscope slide and lysed with detergent and high salt. The aqueous salt disrupts the RNA, proteins within the cell and the detergent dissolves the cell membrane. The cellular debris diffuse into the agarose matrix leaving only the concentrated DNA (also known as nucleoids). Under electrophoresis at high pH (>13), the DNA fragments (strand breaks) migrate in a “comet” like pattern compared to intact DNA strands. Therefore, the amount of damage is measured as the percentage of DNA in the comet tail relative to the intact head (Singh et al., 1988) [Fig. 3.8. A]. We optimised this protocol for planarian cells, including the concentration and thickness of the low-melting agarose, voltage and timing of electrophoresis (discussed in detail in chapter 2, material and methods). The slides were carefully handled after embedding of cells and were protected from light. Previous studies utilising comet assay in planarians used a manual visualisation-based scoring methods (Peiris et al., 2016; Thiruvalluvan et al., 2017) which can often be biased or have manual error in interpreting the data. In this study, the following parameters were analysed using Andor KOMET 5.5 image analysis software (Oxford instruments) attached to Nikon Eclipse 90i microscope.

Head % DNA = (Head Intensity / (Head Intensity + Tail Intensity)) *100.

Tail % DNA = 100 – Head % DNA.

We observed a significant increase in Tail % DNA in cells exposed to 5, 15 and 30 Gy as early as 2 hours post-IR. Our data revealed few cells have a baseline damage after 5 and 15 Gy suggesting the possibility that these cells were either resistant to DNA damage or have not been hit by IR [Fig. 3.8. B-C]. We observed reduction in comet formation in 5 Gy exposed cells at 7-day post IR suggesting successful repair of DNA breaks.

A

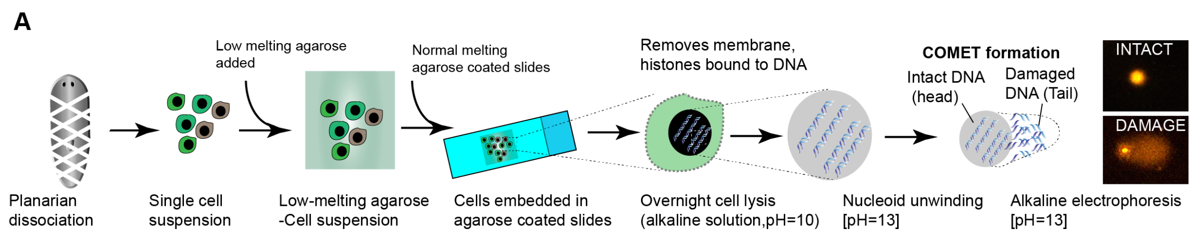

B

Dose of irradiation

	0 Gy	5 Gy	15 Gy	30 Gy
2 hour				
24 hour				
72 hour				
Day 7				

Time post-irradiation

C

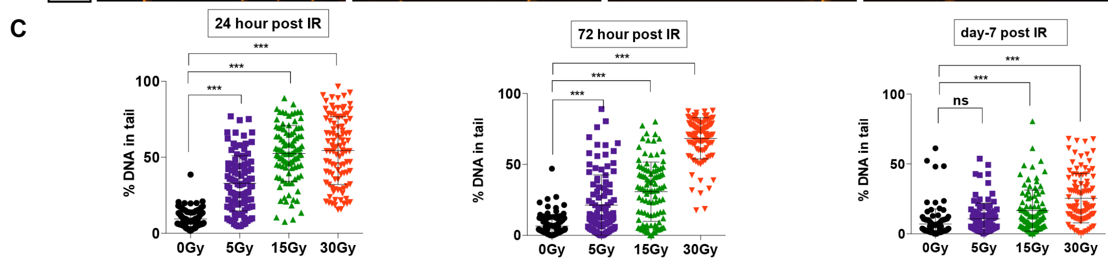

Figure. 3.8. Single cell gel electrophoresis (COMET assay) to detect irradiation-induced DNA damage in planarian cells. (A) Schematic showing the procedure of COMET assay in planarians. Worms were dissociated into single cells and embedded in low-melting-agarose. The cells were lysed overnight with detergent and high salt followed by electrophoresis in an alkaline buffer. **(B)** Representative images showing the extent of comet formation in planarian cells irradiated with 5, 15 and 30 Gy compared to un-irradiated controls after different time post IR. **(C)** The percentage of DNA in the tail compared to head in individual comets were analysed and plotted in the graph, where each dot represents the value from individual comet. At least 100 comets were analysed per slide per condition. (ns = not significant, p-value>0.01; ***p-value<0.0001, Unpaired Students t-test with welch correction).

It is difficult to discriminate between highly damaged cells and apoptotic nuclei in a comet assay as both show increased DNA fragmentation. The comet formation in some cells after 30 Gy at 7-day post IR (no stem cells but only differentiated cells are present) may be due to increased rate of apoptosis. Since the comet assay was performed on dissociated cells containing stem cells, progeny and differentiated cells, we cannot comment if there is any difference in the induction of DNA damage and repair specifically in stem cells versus progenies. We performed comet assay on FACS sorted X1 (stem cells) and X2 (progenies) population, but we observed a huge variation in comet formation indicative of DNA damage in unirradiated (control) cells. This could be due to the sorting of the cells, increased Hoechst exposure or increased incubation of dissociated cells on ice leading to cell death during the whole procedure and therefore requires further optimisation in future.

3.3.3. Identification of DNA repair genes in the *S. mediterranea* genome

The seemingly endless regenerative capacity and well-controlled SC maintenance in planarians would be underpinned by efficient DNA repair mechanisms to maintain genome stability during proliferation and differentiation of the pluripotent SC population. This led us to identify the DDR genes from the *Schmidtea mediterranea* genome that are essential to repair DNA breaks in other metazoans [Fig. 3.9]. It is interesting that planarians have lost many genes thought to be essential for DNA repair (Grohme et al., 2018). For example, BRCA1 (regulates end resection during HR) is present in nematodes and

molluscs but is absent in *Schmidtea* and other dipteran insects (Drosophila). It is currently unknown how BRCA2 facilitates RAD51 homology search without BRCA1.

Moreover, the recently sequenced *Schmidtea* genome has revealed a repetitive fraction of 61.7% (Grohme et al., 2018) that raises the question how are DSBs repaired if encountered between a tandemly repeated sequence? End resection in a repetitive region may expose complementary sequences leading to single-strand annealing (SSA) without homology search (Bhargava et al., 2016). The repair strategy involving SSA is studied in yeast and is mainly regulated by Rad52 (Lee et al., 2003; Shinohara and Ogawa, 1998) but is not a critical factor in vertebrates (Rijkers et al., 1998). But the loss of RAD52 is synthetic lethal with loss of BRCA1 or BRCA2 in human cells (Feng et al., 2011; Lok et al., 2013) indicating RAD52 act as a backup to BRCA1 or BRCA2 containing organism. Interestingly, *Drosophila* and *Schmidtea* have lost both RAD52 and BRCA1, compared to other arthropods and nematodes that have retained at least one of them (Liu and Heyer, 2011; Sekelsky, 2017). This led us to hypothesize that BRCA2 may be the major regulator for RAD51 mediated homology search or planarians may undergo PARP-mediated micro-homology-end joining (Alt-NHEJ/MMEJ). This has been recently reported in *Oikopleura* that have lost all the c-NHEJ genes and employ the mutation-prone MMEJ to repair DSBs (Deng et al., 2018). Although orthologs of the Lig3 gene were not found in *Schmidtea*, its role in MMEJ may be played by Lig1, as reported in other organisms lacking Lig3 (Paul et al., 2013). In this chapter we focussed on characterizing in detail the role of HR and MMEJ repair pathway genes in planarian stem cells.

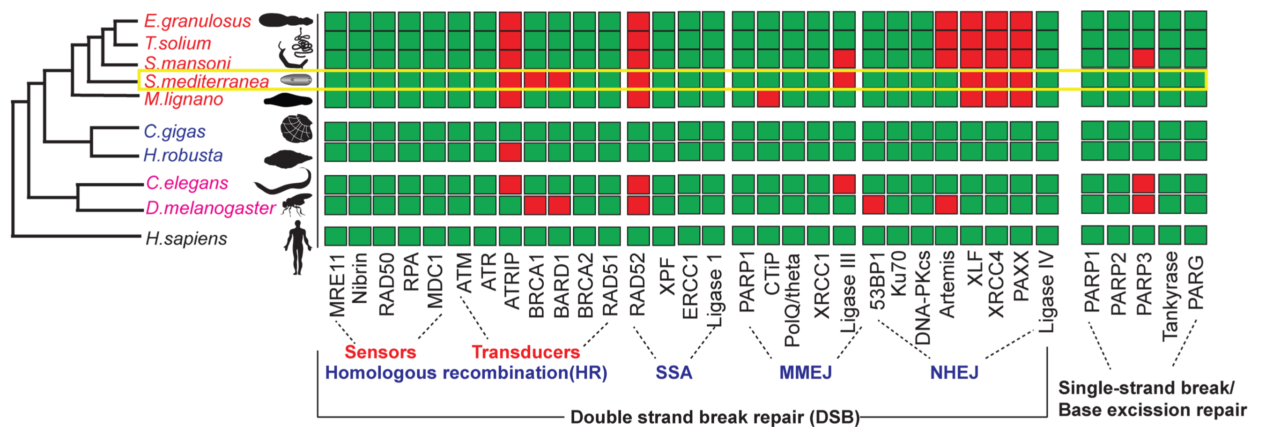

Figure. 3.9. Evolutionary conservation of DNA repair genes in planarians. Phylogenetic conservation of genes involved in double stranded break repair. The presence (Green) or absence (Red) of different DNA repair genes showing the conservation in Ecdysozoa, lophotrochozoans with humans. The yellow box denotes the conservation of DDR genes in planarian *Schmidtea mediterranea.*

3.3.4. Identification and understanding the role of transducers of DNA DSB repair

DSBs in mammalian cells activate the kinases like ATR and ATM that mediates DNA repair signalling via HR. One of the key steps in HR is end-resection of the broken DNA by the Mre11-Rad50-Nbs1 (MRN) complex to generate a single-stranded DNA (ssDNA). Replication protein A (RPA) binds to this ssDNA tail and activates ATR dependent signalling and checkpoint kinase I (Chk1) phosphorylation. BRCA2 mediates the replacement of RPA by RAD51, to form a nucleoprotein filament for homology search. Using the homologous strand, Rad51 undergoes strand invasion and forms a holliday junction to repair the broken DNA strand (Pardo et al., 2009).

ATM and ATR belong to class-IV phosphoinositide 3-kinase (PI3K)-related kinase (PIKK) and mainly act as transducers of DNA repair. For example, ATM is primarily activated due to double-strand breaks (Álvarez-Quilón et al., 2014) and regulates CHK2 to signal P53 and BRCA1 (Falck et al., 2001). On the other hand, ATR initiates the signalling pathway involving CHK1 to P53 and BRCA2 (Zou and Elledge, 2003). ATR forms a heterodimer with ATR-interacting protein (ATRIP) (Cortez et al., 2001) that interacts directly with ssDNA-bound RPA leading to ATR activation (Awasthi et al., 2015; Yazinski and Zou, 2016; Zou and Elledge, 2003). ATM exists as a multimer and upon DNA damage undergoes auto-phosphorylation and dissociation into ATM homodimers (Bakkenist and Kastan, 2003) leading to the activation of the ATM-MRN signalling axis. Apart from CHK2, ATM-dependent DDR also involves direct phosphorylation of other DNA repair factors like MRE11, RAD50, p53, NBS1, DNA-PKcs, CtIP (RBBP8) (Shiloh and Ziv, 2013).

We have identified ATM and ATR in the *Schmidtea* genome, which belongs to PI3K family together with mammalian target of rapamycin (mTOR), human suppressor of morphogenesis in genitalia-1 (SMG-1), PRKDC (DNA-PKcs) and TRRAP. ATM and ATR, mTOR and SMG-1 have been previously identified in *S. mediterranea* but only the role of mTOR and SMG-1 have been previously

identified and characterized in planarians to regulate stem cell proliferation and act as a tumour suppressor (González-Estévez et al., 2012; Pearson and Sánchez Alvarado, 2010; Peiris et al., 2012). *Smed-atm* and *Smed-atr* consists of FRAP-ATM-TRRAP (FAT) domain in the N-terminal, PIKK-regulatory domain (PRD) and FAT carboxy-terminal (FATC) domains, a characteristic feature shared among the PIKK enzymes [Fig. 3.10. A-B] (Lovejoy and Cortez, 2009) that are crucial for ATM and ATR gene activation (Awasthi et al., 2015).

3.3.5. Identification of BRCA genes in *Schmidtea mediterranea*

Another important protein family that plays a major role in DDR signalling are BRCA1 and BRCA2 that are frequently mutated in hereditary breast cancer. BRCA proteins maintain genome stability but the two proteins BRCA1 and BRCA2 work at different stages in DDR with different chemo resistant mechanism in BRCA-mutant cancers (Jiang and Greenberg, 2015). BRCA1 regulates checkpoint activation and DNA repair, whereas BRCA2 acts as a mediator of HR (Venkitaraman, 2014).

BRCA1 possess a N-terminal RING (really interesting new gene) domain (Zinc finger C3HC4) (interacts with E2 enzymes); a coiled-coiled serine rich domain near its C terminus (interacts with PALB2), and two BRCA1 C terminal (BRCT) repeats (binds to phospho-peptides) [Fig. 3.10. A]. The 95-100 residue BRCT repeats are present in other proteins involved in DDR and the crystal structure of two BRCT domains in XRCC1 revealed the presence of four-stranded parallel β-sheet surrounded by three α-helices with a secondary structural element ordered as βαββαβα. BRCT domains in BRCA1 can bind to phosphorylated proteins with a signature sequence motif pS-X-X-F (P-Phosphorylated, X-any residue).

We performed a tBLASTN in *Schmidtea* genome and transcriptome using human BRCA1 sequence but failed to identify a putative BRCA1 in *Schmidtea.* The best hit encodes for an E3 Ubiquitin ligase Ring finger protein 2 (dd_smed_v6_8989_0_1). Despite the presence of a conserved ring finger domain, the absence of BRCT domains suggest a possible loss of BRCA1 in

Schmidtea [Fig. 3.10. C]. Interestingly, *Drosophila* and *Schmidtea* have lost both RAD52 and BRCA1, compared to other arthropods and nematodes that have retained at least one of them (Liu and Heyer, 2011; Sekelsky, 2017). For example, *C. elegans* BRCA1 gene (C36A4.8) consists of a N-terminal RING domain, a nuclear localization signal, and two BRCT repeat domains. Ce-BRC-1 protein (596 aa) shares 24% identity and 52% similarity with human BRCA1delta exon 11 splice variants (721 aa, largest exon comprising of 60% of amino acids that shares very little homology with other proteins.). The alignment with human BRCA1 delta exon 11 variant with the closest hit of Smed-BRCA1 amino acid sequences reveals the conservation of the RING finger domain with a characteristic Zinc finger motif [C(3) HC(4)] but lacks the BRCT domain [Fig. 3.10. D]. Functional characterization of this BRCA1-like gene is required to confirm, if *Schmidtea* has retained a partial BRCA1 or another gene complements its function in HR.

The BRCA1-RING domain interacts with BARD1 that also possess a N-terminal RING domain and BRCT repeats along with ankyrin repeats. BARD1 is present in *C. elegans* (K04C2) (23% identity and 41% similarity with human BARD1) but we cannot find an orthologue in the *Schmidtea* genome and transcriptome. Another interacting partner is PALB2 that acts as a bridge between BRCA1 and BRCA2, and promotes RAD51 nucleofilament formation during HR (Schlacher et al., 2012; Xia et al., 2006). We could not identify any orthologue to BARD1 or PALB2 in the *Schmidtea* genome.

On the other hand, BRCA2 is an evolutionary conserved gene with BRC motifs that facilitates binding to RAD51, a helical domain and OB folds that binds to single-stranded DNA. We have found only one BRCA gene in *Schmidtea* with BRC repeats, a helical domain and 3 OB folds in the C-terminal which is more similar to the BRCA2 in humans. Although the protein sequences of these BRC motifs are very conserved, its number varies among the metazoans [Fig. 3.10. E]. C*. elegans* possess a BRCA2-like protein (*Ce-brc2*) with a single BRC motif that interacts directly with Rad51 and binds to the single-stranded DNA through OB folds (Martin et al., 2005). BRCA2 in fungus, *Ustilago* (Brh2) possesses a

single BRC motif and two OB folds in the C-terminal region. BRCA2 in flies (*Dm-brca2*) lacks the DNA binding/DSS1 interaction domain but knockdown of *Dm-brca2* sensitizes Drosophila embryonic cells to X-ray irradiation or genotoxic agents (Brough et al., 2008). *Ce-brc2* does not have a tower domain, and single OB fold is more related to OB folds in RPA suggesting a BRC-RPA fusion that delivers RAD51 directly to ssDNA (Martin et al., 2005). We have identified 4 BRC repeats that may aid in RAD51 localisation in the absence of BRCA1-BARD1 complex.

We next checked the expression of the DNA repair components in different FACS sorted cell population and found that the components of HR repair genes have enriched expression in the X1-FACS sorted (stem cell) population (Dattani et al., 2018a) [Fig. 3.10. F]. This expression is consistent with the single cell sequencing dataset revealing *atr, atm* and *brca2* are expressed in sigma, zeta, gamma neoblast with very little expression in other cell types (like post-mitotic progenies and differentiated cells) (Wurtzel et al., 2017). This suggest DNA repair genes are important for stem cell regulation. We performed FISH to detect the expression of HR-related genes in stem cells. These genes are very lowly expressed in homeostatic condition. It was difficult to detect a whole-body expression and so we focussed on individual stem cells after whole-mount FISH showing the co-localisation of *atr, atm* and *brca2* expression in *smedwi-1*$^{+}$ stem cells [Fig. 3.10. F].

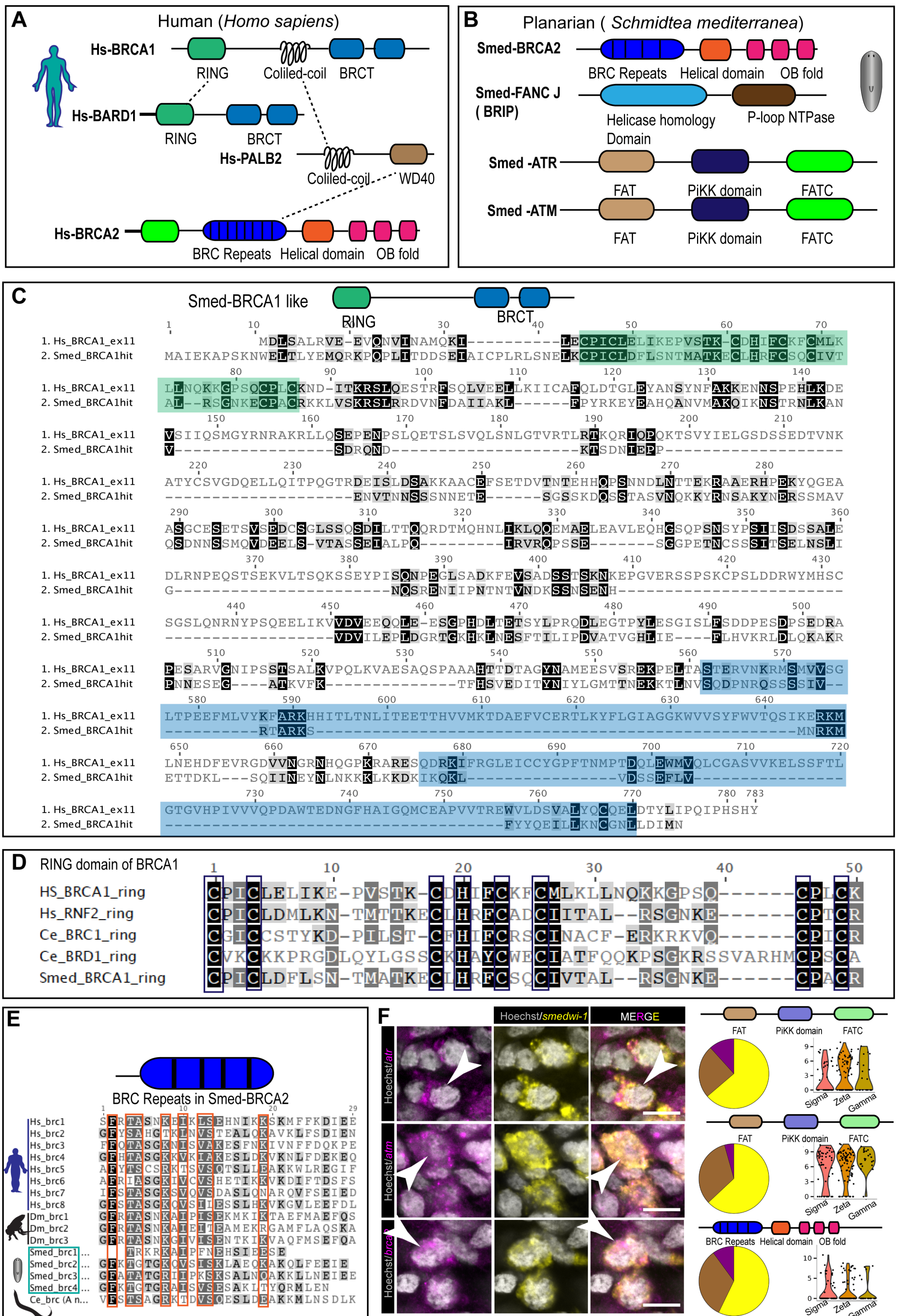
A
Human (Homo sapiens)
Hs-BRCA1
RING
Coliled-coil
BRCT
Hs-BARD1
RING
BRCT
Hs-PALB2
Coliled-coil
WD40
Hs-BRCA2
BRC Repeats
Helical domain
OB fold
B
Planarian (Schmidtea mediterranea)
Smed-BRCA2
BRC Repeats
Helical domain
OB fold
Smed-FANC J
(BRIP)
Helicase homology
Domain
P-loop NTPase
Smed -ATR
FAT
PiKK domain
FATC
Smed -ATM
FAT
PiKK domain
FATC
C
Smed-BRCA1 like
RING
BRCT
1. Hs_BRCA1_ex11
2. Smed_BRCA1hit
D
RING domain of BRCA1
HS_BRCA1_ring
Hs_RNF2_ring
Ce_BRC1_ring
Ce_BRD1_ring
Smed_BRCA1_ring
E
BRC Repeats in Smed-BRCA2
Hs_brc1
Hs_brc2
Hs_brc3
Hs_brc4
Hs_brc5
Hs_brc6
Hs_brc7
Hs_brc8
Dm_brc1
Dm_brc2
Dm_brc3
Smed_brc1
Smed_brc2
Smed_brc3
Smed_brc4
Ce_brc (A n...
F
Hoechst/smedwi-1
MERGE
Hoechst/atr
Hoechst/atm
Hoechst/brca2
FAT
PiKK domain
FATC
Sigma
Zeta
Gamma
BRC Repeats
Helical domain
OB fold

Figure. 3.10. The identification of key proteins involved in homologous recombination. (A) Conserved domain architecture of the components encoding for proteins involved in HR in humans and **(B)** in Planarians. **(C-D)** Alignment with the closest hit of BRCA1 like gene (Ring finger containing) in *Schmidtea* with human BRCA1. **(D)** Conserved Ring finger of human BRCA1 and planarian RNF gene. **(E)** BRC repeats in planarian showing the consensus amino acids (Box) with the 8 BRC repeats in human, 3 in Drosophila, 1 in C. elegans. **(F)** Single confocal stacks of double FISH showing the co-localisation of the expression of *atr, atm* and *brca2* mRNA in *smedwi-1*+ stem cells (left). The conserved domains of the genes encoding for HR in Schmidtea along with its proportional expression in FACS sorted cell population (Dattani et al., 2018) and in different subclasses of stem cells (Sigma, Zeta and Gamma stem cells) Arrows denote double positive cells. [Single cell sequencing data from Wurtzel et al., 2016].

We next tested the role of these genes in stem cell regulation, and its role in DNA damage response in planarians. We performed RNAi of *atr, brca2, RAD51,* BRCA1-interacting protein *(BRIP1/Fanc-J).* Previous research revealed the role of RAD51 in regulating cell-cycle related genes and mediates regional differences in cell proliferation and survival (Peiris et al., 2016). We observed defects in regeneration after *rad51* RNAi [Fig. 3.11. A] but did not observe any phenotypes after *atr* and *brca2* RNAi, consistent with a previous study (Pearson and Sánchez Alvarado, 2010). Immunostaining with H3-pSer10 showed no effect in stem cell proliferation after *atr* and *brca2* knockdown [Fig. 3.11. B-C]. We have previously established a quantitative assay to check stem cell depletion and repopulation that scores *smedwi-1*$^+$ stem cells. Stem cells decrease significantly by 3 days post IR and can clonally repopulate by 7 days post IR (section 3.3.1; Figure 3.1 and 3.2). To understand the role of DNA repair genes in stem cell survival and repopulation post IR, we hypothesized that stem cell number should be comparable and significantly lower in RNAi worms at 7-day post IR. Using this assay (we will term as the “sub-lethal irradiation assay”), we irradiated RNAi animals with a 15 Gy of non-lethal dose of IR and checked for stem cell survival, stem cell proliferation and scoring of lethal phenotypes [Fig. 3.11. D]. We observed 100% lethality in RNAi animals in 2 weeks compared to gfp injected (control) animals [Fig. 3.11 E-F]. When assayed by *smedwi-1* FISH, RNAi of *atr, brca2, rad51, BRIP-1* showed a significant decrease in stem cell density after 7 days post 15 Gy IR compared to the controls [Fig. 3.11. G-H].

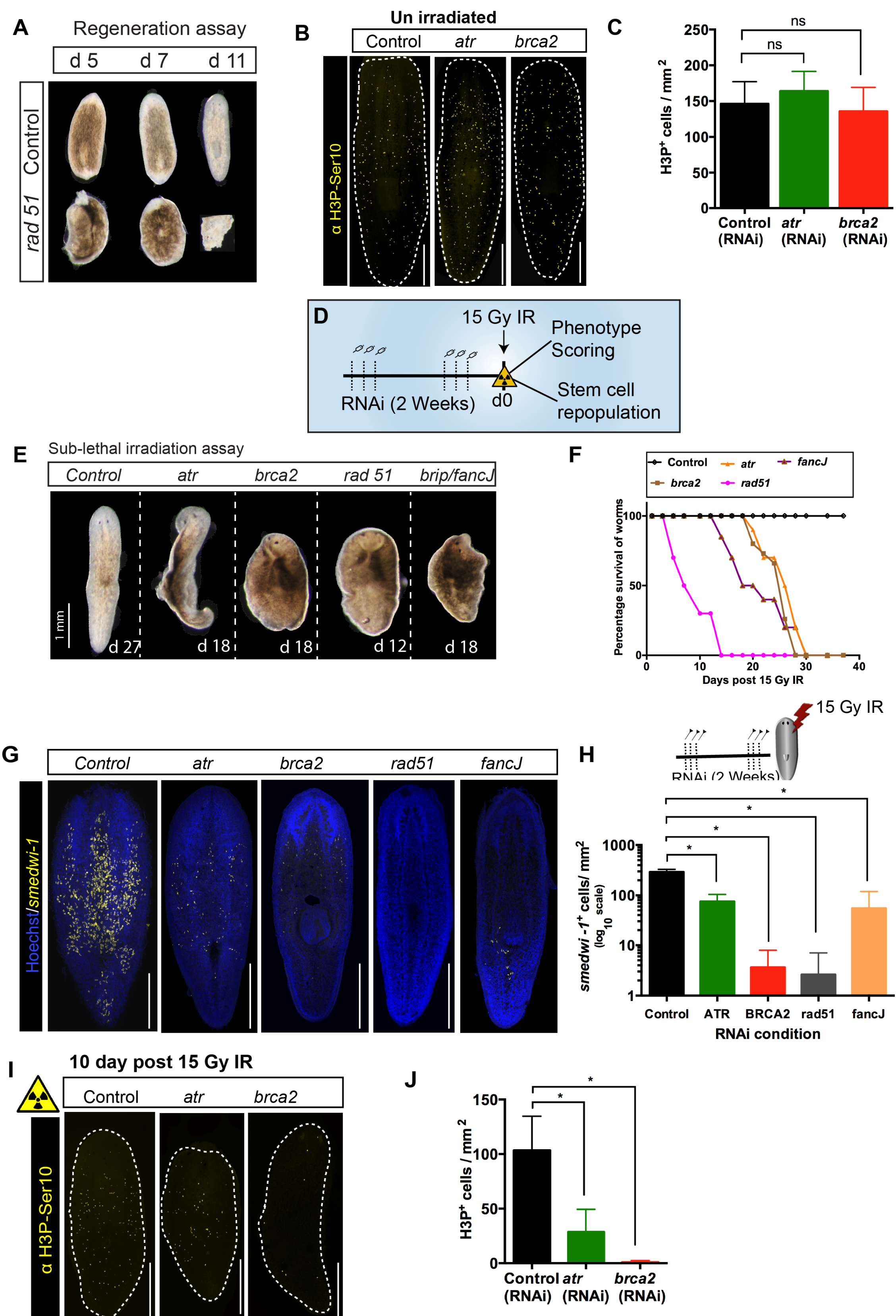
A
Regeneration assay
d 5
d 7
d 11
Control
rad 51
B
Un irradiated
Control
atr
brca2
α H3P-Ser10
C
ns
ns
H3P+ cells / mm2
Control (RNAi)
atr (RNAi)
brca2 (RNAi)
D
15 Gy IR
Phenotype Scoring
Stem cell repopulation
RNAi (2 Weeks)
d0
E
Sub-lethal irradiation assay
Control
atr
brca2
rad 51
brip/fancJ
1 mm
d 27
d 18
d 18
d 12
d 18
F
Control
atr
fancJ
brca2
rad51
Percentage survival of worms
Days post 15 Gy IR
G
Control
atr
brca2
rad51
fancJ
Hoechst/smedwi-1
H
15 Gy IR
RNAi (2 Weeks)
smedwi -1+ cells/ mm2 (log10 scale)
Control
ATR
BRCA2
rad51
fancJ
RNAi condition
I
10 day post 15 Gy IR
Control
atr
brca2
α H3P-Ser10
J
H3P+ cells / mm2
Control (RNAi)
atr (RNAi)
brca2 (RNAi)

Figure. 3.11. The role of HR-related genes in stem cell maintenance and during repopulation post irradiation. **(A)** Regeneration assay showing the failure in regeneration and subsequent lysis after *Rad51* RNAi in planarians. **(B)** Immunostaining with H3-pSer10 antibody (marker for mitotic cells) after *atr* and *brca2* RNAi and **(C)** the quantification showing no change in stem cell proliferation after knockdown compared to the controls. **(D)** The experimental strategy of sub-lethal irradiation assay. Double stranded RNA of the gene of interest will be injected to 1-week starved worms for 2 weeks and then exposed to 15 Gy of IR. Worms will be fixed at 7-day post IR for smedwi-1 FISH/10-day post IR for H3P-immunostaining and scored for lethal phenotype. **(E)** Brightfield images of RNAi animals after days (indicated in the figure) post irradiation. Control animals show know phenotypic defects after day 27 post IR. **(F)** Survival curve showing 100% lethality in RNAi animals compared to the controls. **(G)** *smedwi-1* FISH showing defects in stem cell repopulation at 7-day post 15Gy-IR in RNAi animals compared to controls. **(H)** Quantification showing a significant decrease in stem cell density (number of *smedwi-1*+ stem cells) in RNAi animals compared to the controls. The values are represented in log10 scale (*p-value<0.05, Students t-test, n = 5 animals/RNAi condition). **(I)** Immunostaining with H3-pSer10 antibody after *atr* and *brca2* RNAi ay 10-day post 15 Gy IR. **(J)** Quantification showing a significant decrease in stem cell proliferation (number of $H3P^+$ cells/mm^2) in RNAi animals compared to the controls (*p-value<0.05, Students t-test, n = 5 animals/RNAi condition).

Immunostaining for mitotic cells (using H3-pSer10 antibody) showed a significant decrease in stem cell proliferation after RNAi of *atr* and *brca2* [Fig. 3.11. I-J]. Altogether these data indicate that ATR-BRCA2 signalling cascade plays a major role in repairing IR-induced DNA strand breaks and is required for stem cell repopulation post-IR. Here we also demonstrate the use of sub-lethal irradiation assay to study DDR in adult stem cells *in vivo* and show the components of HR-repair pathway are necessary for stem cell survival post-IR.

3.3.6. Role of Microhomology mediated end-joining (MMEJ/Alternative NHEJ) repair pathway in *Schmidtea mediterranea*

Ku-independent NHEJ (also known as Alternative NHEJ or microhomology mediated end joining (MMEJ)) based DNA repair pathway is active during S and G2 phases of the cell cycle and dependent on poly (ADP-ribose) polymerase 1 (PARP1) signalling. PARPs initiate ADP-ribosylation, a post-translational modification that plays critical role for a wide array of cellular and physiological processes including DNA damage. PARP catalyse the formation of long, branched chains of ADP-ribose known as poly-ADP ribose (PAR) that initiates the nucleation of DNA damage response and recruitment of XRCC1 to DNA strand breaks. [Fig. 3.12. A]. According to domain architecture and conservation of function, PARP family comprises of 17 members (Gibson and Kraus, 2012). DNA damage dependent PARPs (PARP1, PARP2, PARP3) are activated by DNA breaks and involved in DNA repair and chromatin regulation (Boehler et al., 2011; Krishnakumar and Kraus, 2010). 8 types of PARPs (5 conserved with humans) are found in choanoflagellates, 9 types in sponges (7 conserved with humans), 2 types in *Drosophila* (PARP1 and tankyrase), *C.elegans* (PME-1 and PME-2*)* and 15 types of PARPs in fishes suggests that the ancestral eukaryote had at least two PARP enzymes and multiple independent losses and expansions of PARP genes occurred across the eukaryotes (Citarelli et al., 2010; Perina et al., 2014). *Schmidtea* genome shows a wide conservation of PARPs (includes PARP1, 2, 3, *tankyrase1, PARP-9 [Macro H2A]* and *PARP16).* In humans, PARP9, 15 and 16 share the same macrodomain (Macro H2A) and planarians/other invertebrates have only Parp9, suggesting Parp15 and 16 are vertebrate specific and have evolved from its ancestral Parp9 gene. A single PARP gene has been identified in *Drosophila* which is similar to the mammalian *PARP-1* and involved in maintenance of chromatin structure during development (Tulin et al., 2002). Studies on PARP1 and PARP2 knockout mice revealed hypersensitivity to ionizing radiation and embryonic lethality in PARP1/2 double knockout mice (Ménissier de Murcia et al., 2003).

We have identified 3 PARP genes in *S. mediterranea* genome*, PARP1* gene with a conserved Zn finger domain in the N-terminal, BRCT domain and tryptophan-glycine-arginine (WGR) domain in the middle and the catalytic PARP domain in the C-terminal. In contrast to PARP1, PARP2 and PARP3 do not contain the N-terminal Zn finger domain. With their homology to 3 mammalian PARPS, and its phylogenetic conservation with both other lophotrochozoans and vertebrates, we have named them as *Smed-parp1, parp-2* and *parp-3* respectively [Fig. 3.12. B]. We found *Parp1* and *Parp2* are highly expressed in X1-FACS sorted (stem cell) population while Parp3 is mostly expressed in the Xins (differentiated cell) fraction (Dattani et al., 2018a) [Fig. 3.12. C]. The expression is consistent in the single cell sequencing dataset revealing *Parp1* and *Parp2* are expressed in sigma, zeta and gamma neoblast with no expression of *Parp3* in any stem cell subclasses (Wurtzel et al., 2017). We performed double FISH to detect the expression of *Parp1*, *Parp2* and *Parp3*. Individual stem cells showed co-localisation of *parp1* and *parp2* with *smedwi-1* and no detectable expression of *parp3* in stem cells [Fig. 3.12.C].

PARP1 is mainly required for single-strand break (SSB) repair and base excision repair (BER) in mammalian cells. The knockdown of individual Parp genes didn't show any defect in regeneration/ worm survival and immunostaining with H3-pSer10 revealed no significant changes in stem cell proliferation [Fig. 3.13. A-B]. This data suggest knockdown of PARP genes does not affect stem cell proliferation and have no effect on planarian regeneration. Using an established sub-lethal assay, we next checked if RNAi of PARP family genes sensitizes the worms to IR [Fig. 3.13. C]. We observed 100% lethality in *Parp-1, -2, -3* RNAi animals that are exposed to a 15 Gy non-lethal dose of IR. [Fig. 3.13. D-F]. We performed *smedwi-1* FISH and observed a significant decrease in stem cell density at 7 days post 15 Gy-IR compared to the controls and failure to repopulate stem cells post IR [Fig. 3.13. G-H.]. Using H3-pSer10 immunostaining we checked the proliferative capacity was also impaired in RNAi worms post-IR [Fig. 3.13 I-J]. These data demonstrate defects in stem cell repopulation and a lack of mitotic cells to proliferate after irradiation. This leads to lethality in RNAi worms,

suggesting the crucial role of PARP signalling in regulating DDR post-IR in planarian stem cells.

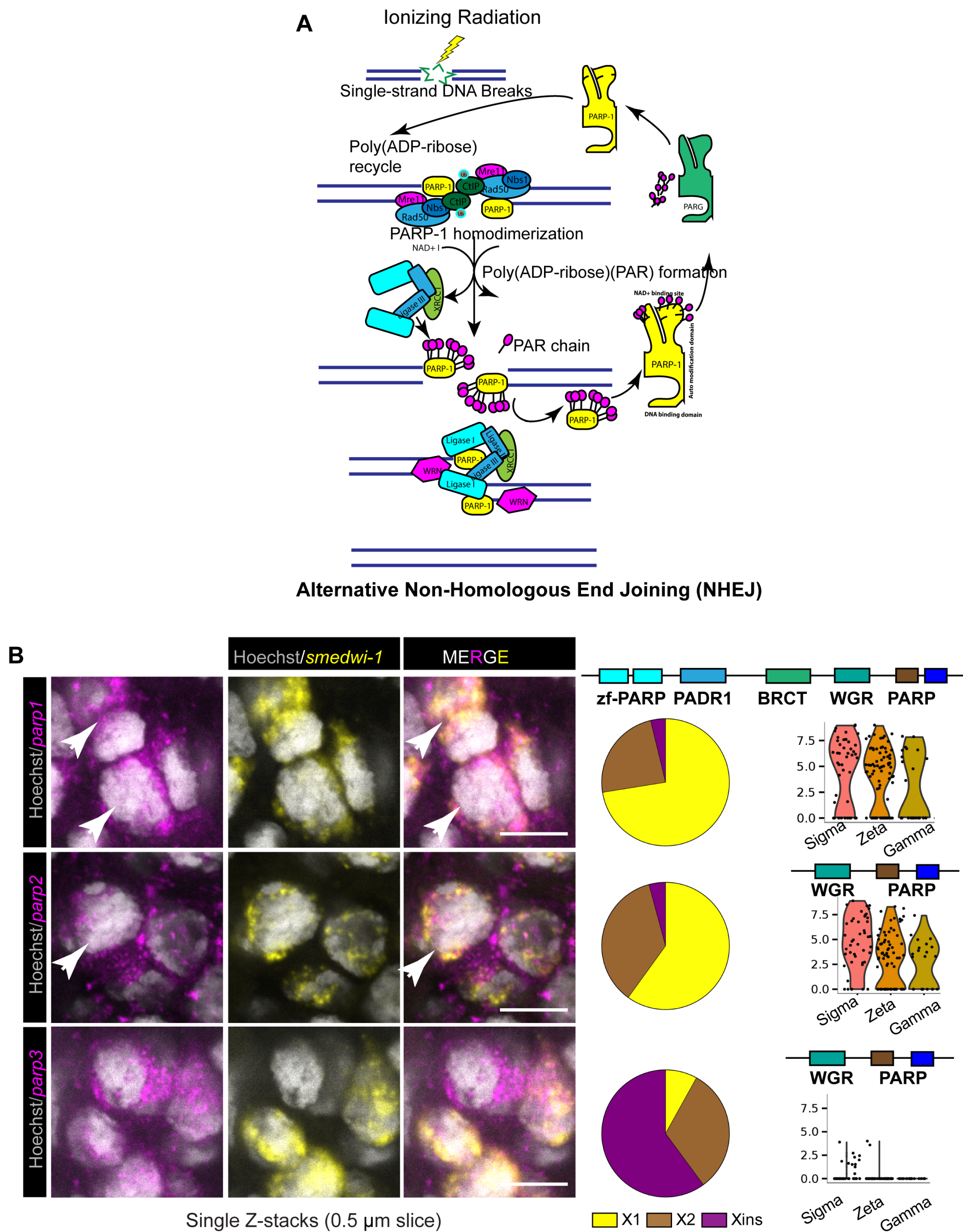

Figure. 3.12. Alternative NHEJ/Microhomology-mediated end-joining (MMEJ) pathway in planarians. (A) Schematic pathway representing the identification of DNA lesion and the role of PARP proteins in transducing the repair pathway to initiate end-joining repair. **(B)** Single confocal stacks of double FISH showing the co-localisation of the expression of *parp-1,-2,-3* mRNA in *smedwi-1*+ stem cells (left). The conserved domains of PARPs in *Schmidtea* along with its proportional expression in FACS sorted cell population (Dattani et al., 2018) and in different subclasses of stem cells (Sigma, Zeta and Gamma stem cells) [Single cell sequencing data from Wurtzel et al., 2016].

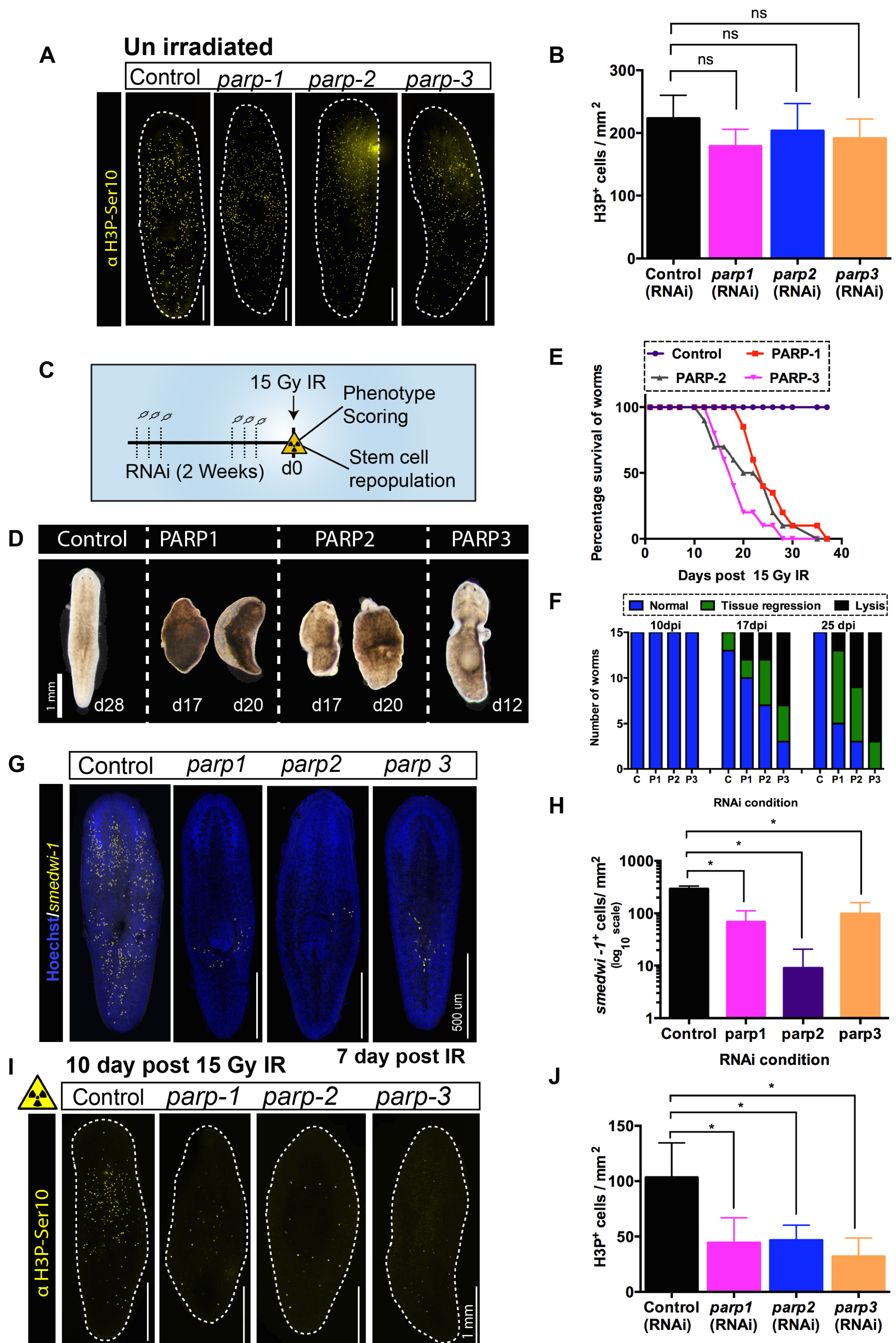
A
Un irradiated
Control parp-1 parp-2 parp-3
α H3P-Ser10
B
ns
ns
ns
H3P+ cells / mm2
300
200
100
0
Control (RNAi)
parp1 (RNAi)
parp2 (RNAi)
parp3 (RNAi)
C
15 Gy IR
Phenotype Scoring
RNAi (2 Weeks)
d0
Stem cell repopulation
D
Control
PARP1
PARP2
PARP3
1 mm
d28
d17
d20
d17
d20
d12
E
Control
PARP-1
PARP-2
PARP-3
Percentage survival of worms
Days post 15 Gy IR
F
Normal
Tissue regression
Lysis
10dpi
17dpi
25 dpi
Number of worms
C P1 P2 P3
RNAi condition
G
Control parp1 parp2 parp 3
Hoechst/smedwi-1
500 um
H
smedwi-1+ cells/ mm2 (log10 scale)
Control parp1 parp2 parp3
RNAi condition
I
10 day post 15 Gy IR
7 day post IR
Control parp-1 parp-2 parp-3
α H3P-Ser10
1 mm
J
H3P+ cells / mm2
Control (RNAi)
parp1 (RNAi)
parp2 (RNAi)
parp3 (RNAi)

Figure. 3.13. The role of Alternative NHEJ/Microhomology-mediated end-joining (MMEJ) pathway in stem cell maintenance and during repopulation post IR. (A) Immunostaining with H3-pSer10 antibody (marker for mitotic cells) after *parp-1, parp-2* and *parp-3* RNAi and **(B)** the quantification showing no significant change in stem cell proliferation after knockdown compared to the controls. **(C)** The experimental strategy of sub-lethal irradiation assay **(D)** Brightfield images of RNAi animals after days (indicated in the figure) post irradiation. Control animals show know phenotypic defects **(E)** Survival curve showing 100% lethality in RNAi animals compared to the controls (n=15) **(F)** Histogram of number of control RNAi versus PARPs RNAi animals showing head regression or lysis at indicated times post IR. (n = 15). **(G)** *smedwi-1* FISH showing defects in stem cell repopulation at 7-day post 15Gy-IR in RNAi animals compared to controls. **(H)** Quantification showing a significant decrease in stem cell density (number of *smedwi-1*+ stem cells) in RNAi animals compared to the controls. The values are represented in Log10 scale (*p-value<0.05, Students t-test, n = 5 animals/RNAi condition). **(I)** Immunostaining with H3-pSer10 antibody after *parp-1, parp-2, parp-3* RNAi ay 10-day post 15 Gy IR. **(J)** Quantification showing a significant decrease in stem cell proliferation (number of *H3P*+ cells) in RNAi animals compared to the controls (*p-value<0.05, ns=not significant, Students t-test, n = 5 animals/RNAi condition).

3.3.7. p53 binding proteins: 53BP1 and 53BP2 in planarians

The p53 binding protein (also known as 53BP1 and 53BP2) was initially discovered to stabilize p53 in response to IR (Iwabuchi et al., 1994; Soussi et al., 2016) and later it was shown to regulate DNA repair choice between HR or NHEJ (Wang et al., 2002). 53BP1 is a chromatin-binding protein that inhibits 5' end resection (necessary for HR), via its interaction with PTIP and RIF1 to promote NHEJ (Chapman et al., 2013; Munoz et al., 2007; Di Virgilio et al., 2013; Zimmermann et al., 2013). 53BP1 protein is characterised by a Tudor domain in the N-terminal and two BRCT domains in the C-terminal. The Tudor domain recognizes symmetrically di-methylated arginine (Sprangers et al., 2003) and a lot of Tudor domain containing proteins have been identified in eukaryotes. But the tandem Tudor domains in 53BP1 specifically recognizes the di-methylated histone H4 at Lys 20 (H4K20me2) to mediate DDR signalling (Botuyan et al., 2006). The formation of 53BP1 foci at the damage site still remains unclear and very recently multiple groups independently identified that 53BP1-RIF1-REV7 forms a complex (known as shieldin) with RINN1, FAM35A (Shieldin2/RINN2) and C20Orf196 (shieldin1/RINN3) and gets recruited to damage sites (Dev et al., 2018; Findlay et al., 2018; Gao et al., 2018; Gupta et al., 2018; Mirman et al., 2018; Noordermeer et al., 2018; Tomida et al., 2018). The 53BP1-RIF1-REV7-RINN complex shields the DSBs from end resection thereby promote NHEJ based DNA repair. Although budding yeast orthologs of 53BP1, RIF1 are involved in DDR but their function is not conserved in DSB repair pathway choice. On the other hand, *C. elegans* germline showed a pan-nuclear staining of HSR9 (53BP1 in human) in response to double stranded breaks but *hsr9* mutants were not hypersensitive to IR (Ryu et al., 2013). In the absence of H2AX in the *C. elegans* genome*,* the localisation of 53BP1 to DSBs could substitute for the H2Ax signalling cascade. Whether 53BP1 in *C. elegans* also play a role in DSB repair pathway choice warrants further investigation. 53BP1- deficient mice show increased DNA damage and are sensitive to IR (Ward et al., 2003). Interestingly, RINN1-3 complex is mostly expressed in vertebrates and not in invertebrates or plants, suggesting the role of 53BP1 in repair pathway choice is a recently evolved function in vertebrates. Compared to other core regulators of NHEJ (like

Ku70/80, Lig1), 53BP1 is not crucial for DNA end joining but essential for vertebrate specific immunoglobulin class-switch recombination (Gupta et al., 2018). Therefore, comparative studies using invertebrates will provide underpinnings to the evolutionary origin of p53 binding proteins and their function in stem cell maintenance.

In this study we have identified 53BP1 and 53BP2 [Fig. 3.14. A-C] which were previously overlooked in the planarian literature (Pearson and Sánchez Alvarado, 2010). 53BP1 in *Schmidtea* contains a conserved Tudor domain [Fig. 3.14. A-B] along with two BRCT domains and 53BP2 is characterized with ankyrin repeats and SH3 domain. To understand the role of 53BP1 and 53BP2 in planarians we performed a RNAi screen followed by a non-lethal dose of 15 Gy IR. We observed 100% lethality in RNAi worms to irradiation within 2 weeks post irradiation [Fig. 3.14. D-E] suggesting a role in regulating DNA damage response in planarian stem cells. It will be interesting to understand if the role of 53BP1 in repair pathway choice is conserved in planarians, but this requires generation of conserved antibodies that can localise to DSB sites. Due to poor conservation of the epitope with commercially available antibodies, future work should aim to develop a planarian specific 53BP1 antibody to see if the protein localizes to DNA-DSBs.

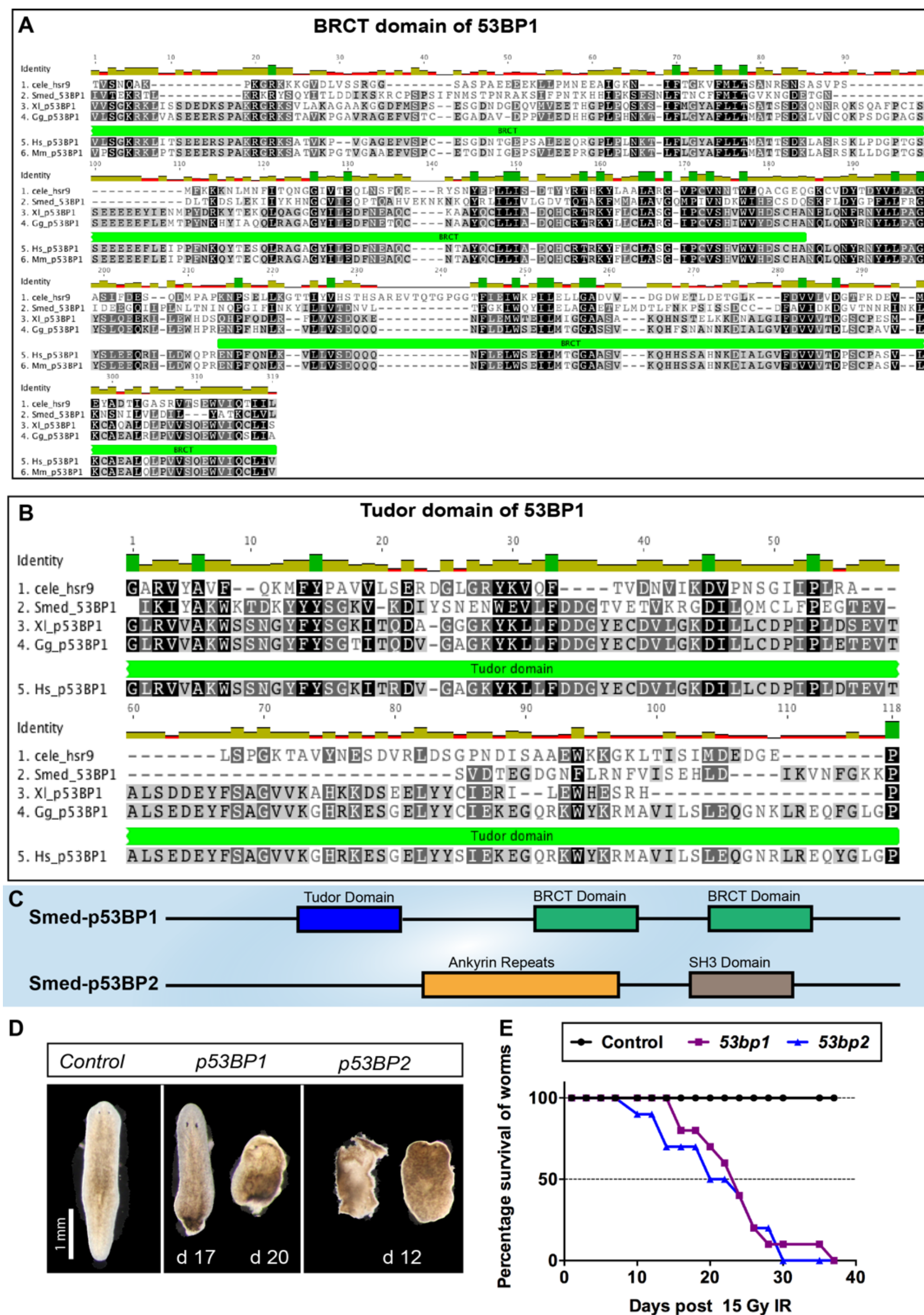

Figure. 3.14. The role of p53 binding proteins in planarians. Multiple sequence alignment showing the amino acid conservation of the BRCT domain **(A)** and the Tudor domain **(B)** in 53BP1 in *C. elegans (*hsr9), *Xenopus laevis, Gallus gallus, Homo sapiens* and *Schmidtea mediterranea.* **(C)** The conservation of domains that are present in 53BP1 and 53BP2 genes in *Schmidtea mediterranea* (from smart.embl.de) **(D)** Sub-lethal irradiation assay after knockdown of 53BP1 and 53BP2 followed by a non-lethal dose of IR showing increased sensitivity to IR (d* represents days post irradiation)

(E) Survival curve after knockdown of 53BP1 and 53BP2 followed by a 15 Gy IR showing 100% lethality after knockdown of worms compared to the controls. (n = 15 worms per RNAi condition).

3.3.8. Double knockdown of *atr, atm, brca2* and *parp1* suggest a synergistic interaction to maintain planarian stem cells.

Our previous data revealed that individual knockdown of the components of HR and Alt-NHEJ does not lead to any defect in stem cell proliferation or whole-body regeneration. We therefore tested whether a functional redundancy in DNA repair machinery exists to maintain stem cell proliferation. To address this, we performed double knockdown with combinations of *atr* and *brca2, atm* and *brca2, parp1* and *brca2.* We also performed single RNAi of these genes (with control gfp ds-RNA as the second gene of RNAi) as a control to our double RNAi experiment. Using *smedwi-1* FISH, we checked the number of stem cells significantly reduced only after double knockdown of DDR genes in homeostatic condition [Fig. 3.15. A and B]. We also exposed the RNAi animals with 15 Gy IR to check its role in stem cell repopulation post IR. Our data is consistent with our previous observation that single knockdown of *atr, atm, brca2* and *parp1* did not affect the homeostasis of stem cell population compared with controls, but robustly impaired repopulation post IR [Fig. 3.15 .C-D]. The failure to recover stem cell number was amplified when double knockdown animals were exposed to 15 Gy irradiation [Fig. 3.15. D]. The double knockdown of DNA repair genes suggests a synergistic interaction exists between the transducers (*atr* and *atm*) and *brca2* that work together to maintain genome stability during normal stem cell turnover.

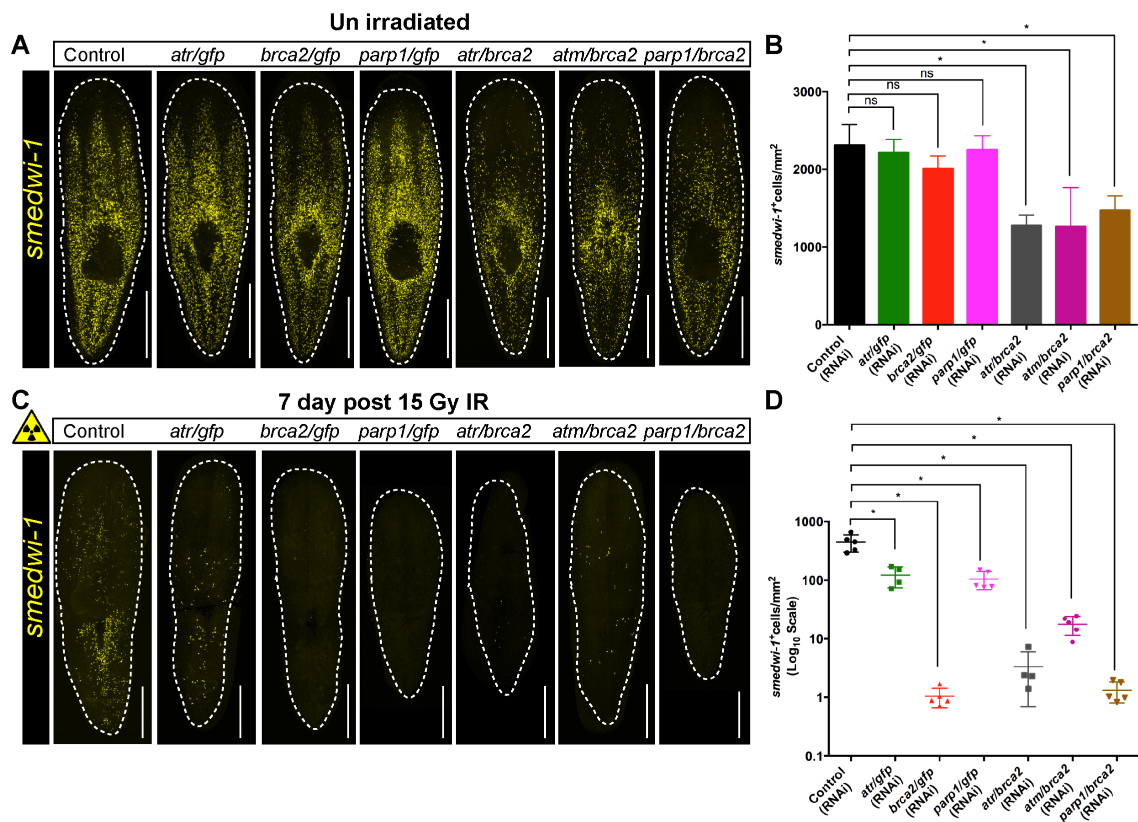

Figure. 3.15. Combination knockdown of *atr, atm, brca2* leads to defects in stem cell maintenance. (A) *smedwi-1* FISH showing defects in stem cell maintenance in *atr/brca2, atm/brca2, parp1/brca2* RNAi worms compared to controls at 10-day post RNAi **(B)** Quantification showing a significant decrease in stem cell density (number of *smedwi-1*+ stem cells) in double RNAi animals compared to the controls and no significant reduction after *atr, brca2* and *parp1* RNAi. (*p-value<0.05, Students t-test, n = 5 animals/RNAi condition). **(C)** *smedwi-1* FISH showing defects in stem cell repopulation in *atr/brca2, atm/brca2, parp1/brca2* RNAi worms compared to controls at 7-day post 15 Gy IR. The values are represented in Log10 scale (*p-value<0.05, Students t-test, n = 5 animals/RNAi condition). **(D)** Quantification showing a significant decrease in stem cell density (number of *smedwi-1*+ stem cells) RNAi animals exposed to IR compared to the controls (*p-value<0.05, Students t-test, n = 5 animals/RNAi condition). gfp dsRNA was injected as a control for double knockdown experiments to match the concentration.

3.3.9. Role of the Fanconi Anaemia pathway in radiation sensitivity.

In the previous section, we have discussed the role of HR, Alt-NHEJ repair pathways in regulating DDR signalling post-IR. Apart from double stranded breaks DNA-protein crosslinks can also induce DNA damage. Interstrand and intrastrand crosslinks (ICL) are caused by exogenous sources like platinum compounds, chemotherapeutic drugs (like Mitomycin-C or cisplatin) and by endogenous sources like ROS and dietary fat like aldehydes. A unique genetic network comprising of 19 gene products (FANCA to FANCT) known as the Fanconi anaemia /BRCA pathway repairs the ICL lesions. Among which FANCA, FANCC, FANCG and FANCD2 are the most frequently mutated genes along with FANCD1 (BRCA2), FANCS (BRCA1), FANCJ (BRIP1), FANCM, FANCN (PALB2) - ovarian and breast cancer susceptibility genes. It has been estimated that every human cell has to repair around 10 ICLs/day and FA-repair pathway is the only mechanism to repair ICLs (Clauson et al., 2013; Grillari et al., 2007). Failure to repair ICLs leads to replication fork stalling, thereby leading to chromosomal rearrangements and DNA breakage.

The initial step of lesion detection is mediated by FA proteins which subsequently co-opt proteins from several other DNA repair pathways. There is increasing evidence of crosstalk between FA-pathway and other repair processes. FANCM is a DNA-binding protein with helicase motifs and plays a major role in ICL lesion recognition in a manner dependent on the phosphorylation of ATR. The FA-core complex proteins are recruited to the DNA damage sites and form nuclear foci (mediated by FANCM, ATR and BRCA1). This complex interacts with multiple other proteins and ubiquitinates two other FA proteins, FANCD2 and FANCI. It forms a heterodimer (named as FANCI-D2 complex) and they are interdependently monoubiquitinated by FANCL [Fig. 3.16. A]. FA proteins also modulate homologous recombination and participate in CtIP-based end resection (Murina et al., 2014; Unno et al., 2014) but antagonize Ku-mediated classical NHEJ (Adamo et al., 2010; Pace et al., 2010) to reduce error prone mutations. FA proteins act as ICL sensors and also co-opt factors from other repair pathways to perform a rapid and robust repair machinery to maintain genome stability.

We have identified the core FA proteins, FANC-I, FANC-D2 and FANC-M in the planarian genome, along with previously described FANCD1 (BRCA2), FANCJ (BRIP1), FANCO (RAD51C), FANCQ (ERCC4), FANCR (RAD51), FAN1 (FancD2 and FancI-associated nuclease 1) [Fig. 3.16. B] Multiple studies using *C. elegans*, chicken DT40 and mammalian cells has revealed the active role of FA-pathway is to suppress NHEJ and promote HR-based repair pathway. We performed knockdown of the core FA-complex, *Smed-FancI*, *Smed-FancD2* and *Smed-FancM* and observed no discernible phenotypes in regeneration assay, suggesting knockdown of FA genes has no effect on stem cell maintenance [Fig. 3.16. C]. We next investigated the role of these genes in radiation sensitivity and checked its role using sub-lethal irradiation assay [Fig. 3.16. D]. The knockdown worms were exposed to 15 Gy of non-lethal dose of IR and few worms after FANCD2 (RNAi) showed head regression but the majority survived up to 30 days post IR. Interestingly, FANCI worms showed IR-sensitivity [Fig. 3.16. D-E] suggesting the possibility that FANCI could play a significant role in FANCI-D2 complex formation and ubiquitination to induce DDR.

Future work should look into the functional redundancy of FANCD2 in the I-D2 complex formation or if FANCI has any other functional role in response to IR. Interestingly, FA deficient cells are mostly sensitive to ICL and not to other DNA damaging agents like IR or drugs. Moreover, with an active DNA repair machinery (ATR-BRCA signalling axis) in planarians to repair DSBs, Fanconi anaemia proteins may be playing other roles in addition to repairing DSBs. Whether FA-deficient planarians that are not sensitive to IR are prone to other DNA damaging drugs warrants future investigation.

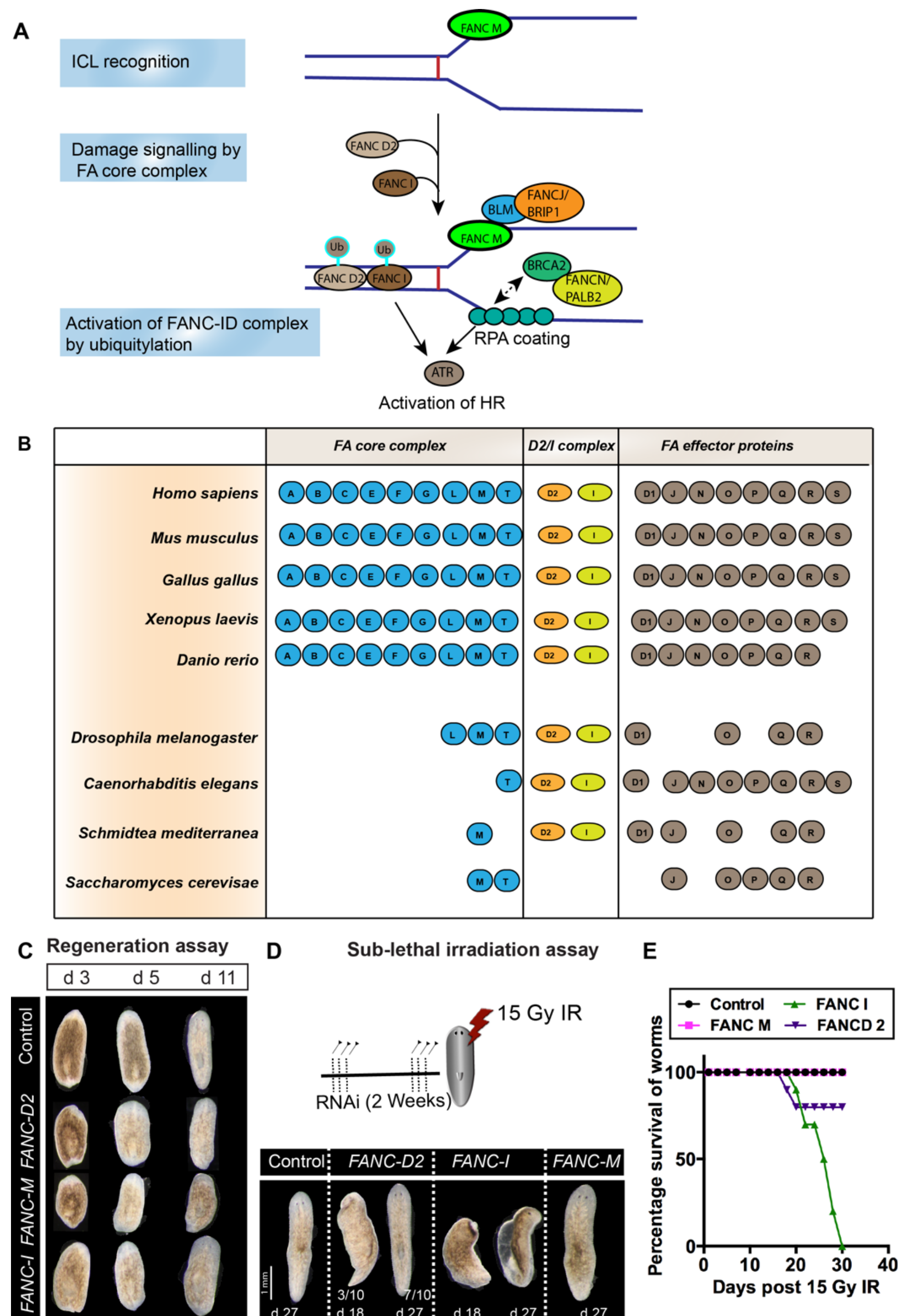

Figure. 3.16. The role of Fanconi anaemia (FA) genes in stem cell maintenance post IR. (A) Schematic representation of the cascade of FA repair pathway in a eukaryotic cell with the key proteins involved in each step. FA proteins are involved intra-strand crosslink repair and subsequently activates homologous recombination to repair the broken DNA strand. **(B)** Evolutionary conservation of FA proteins from the core complex, I/D2 complex and other accessory effector proteins involved in ICL repair. **(C)** Regeneration assay after knockdown of *FancI, FancD2* and *FancM* in planarians showing normal capacity to regenerate from head, trunk and tail pieces. **(D)** Sub-lethal irradiation assay after knockdown of *FancI, FancD2* and *FancM* followed by a 15 Gy non-lethal dose of IR showing *FancI* RNAi animals failed to survive after irradiation. **(E)** Survival curve after knockdown of *FancI, FancD2* and *FancM* followed by a 15 Gy IR showed 100% lethality in *FancI* RNAi animals. (n = 15 worms per RNAi condition).

3.3.10. The Mismatch Repair (MMR) pathway in planarians.

In mismatch repair, detection of mismatches and insertion/deletion loops triggers a single-strand incision that is then acted upon by nuclease, polymerase and ligase enzymes [Fig. 3.17. A]. Other than DDR, mismatch repair pathway is also involved in chromatin assembly, immunoglobulin diversification and recombination. Germline mutations in mismatch repair (MMR) genes allow abnormal proliferation of damaged cells leading to increased risk of tumorigenesis. 3 MMR genes (*Smed-msh2, Smed-msh6, Smed-mlh1)* have been identified in planarians [Fig. 3.17. B]. RNAi of *Msh2* has no characteristic defect in stem cell maintenance, but showed a selective advantage to tolerate DNA alkylating agent (MNNG) compared to controls. (Hollenbach et al., 2011). We checked if loss of MMR genes show any IR induced lethality in planarians. As previously reported we also did not observe any effects on regeneration after RNAi of MMR genes [Fig. 3.17. C]. We next wanted to check if knockdown of MMR genes sensitizes planarians to irradiation. The RNAi animals were exposed to 15 Gy IR to check the repopulation of stem cells post-IR. *msh2* and *msh6* RNAi animals can be rescued and showed no obvious radiation sensitivity phenotype [Fig. 3.17. D-E], suggesting MMR genes may play major role in stem cell survival/repopulation post IR. Although similar to Fanconi anaemia genes, MMR genes may be involved oxidative damage/ DNA damage caused by alkylating drugs. Overall, our data suggests stem cell number in MMR deficient worms can be maintained during regeneration and has the capacity to repopulate post IR.

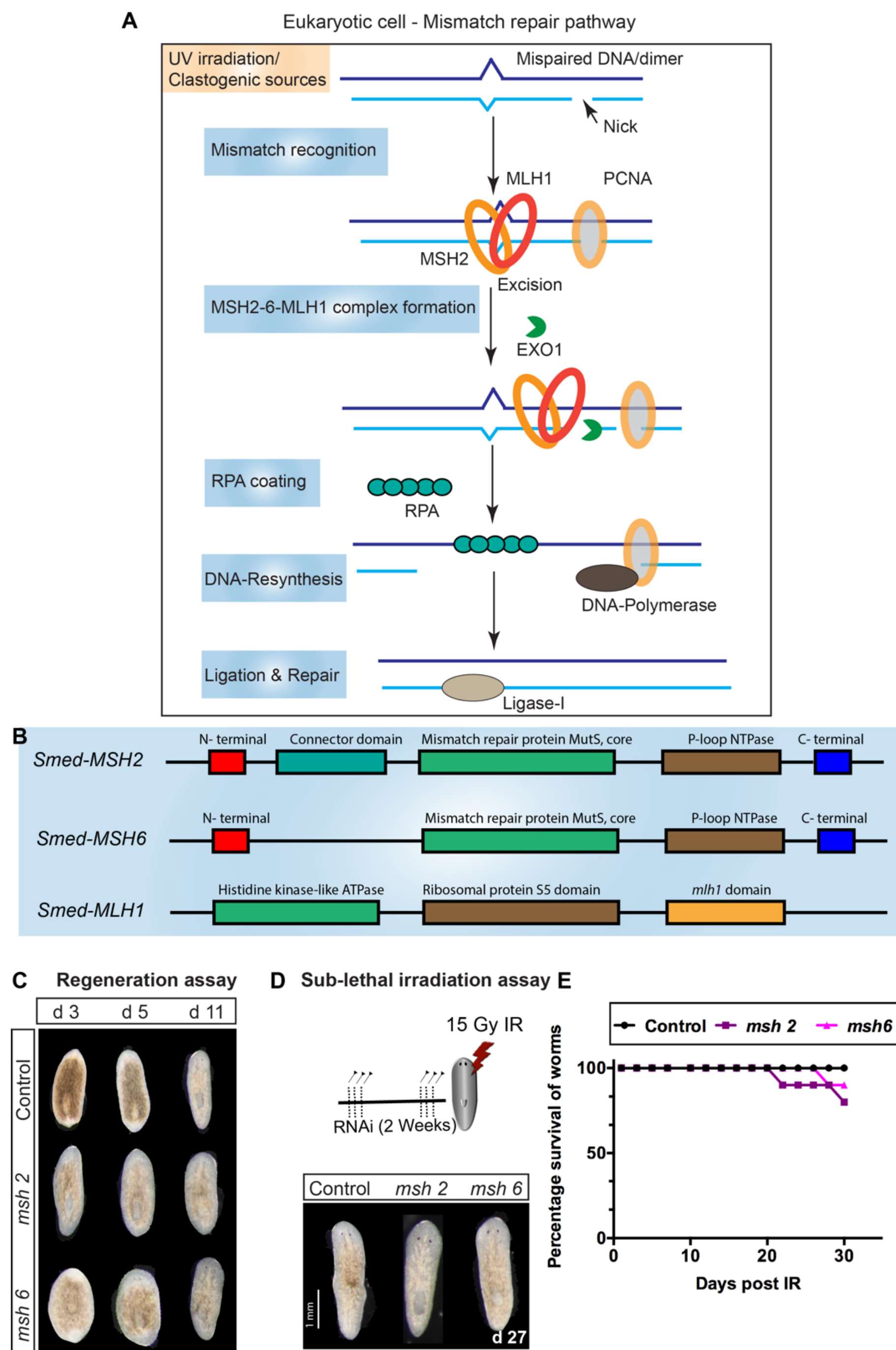

Figure. 3.17. The role of mismatch repair proteins in planarians. (A) Schematic representation of the cascade of mismatch repair pathway in a eukaryotic cell with the key proteins involved in each step. **(B)** The conservation of domains that are present in mismatch repair genes in *Schmidtea mediterranea* (from smart.embl.de) **(C)** Regeneration assay after knockdown of *msh2* and *msh6* in planarians showing normal capacity to regenerate from head, trunk and tail pieces. **(D)** Sub-lethal irradiation assay after knockdown of *msh2* and *msh6* followed by a non-lethal dose of IR showing no effect on survival. **(E)** Survival curve after knockdown of msh2 and msh6 followed by a 15 Gy IR. (n = 15 worms per RNAi condition).

3.4. Conclusion

Overall, this study demonstrates planarians are an experimentally accessible model organism to study DDR in the context of adult stem cells. We confirmed the conservation of the key components of DNA repair pathways in ASCs. However, several key components essential for the DNA repair machinery are absent in flatworms. We cannot exclude the possibility that the sequence homology is too low to identify several DNA repair factors, and any functional redundancy in repair pathways exists in *Schmidtea* requires further experimental evidence. It may be possible that planarian SCs possess some unconventional mechanism to repair DSBs or other cellular responses that stabilize survival while DSBs are repaired. Within the context of our sub-lethal irradiation assay, RNAi of genes encoding for DNA repair pathways led to failure in stem cell repopulation. These data confirm the conserved role of DDR genes in planarian stem cells and suggest that we can use this assay for studying novel DNA repair genes that are important for SC survival post IR.

Chapter 4

Role of DNA damage response during stem cell migration

4.1. Introduction

4.1.1 Cell migration

Cell migration is a crucial physicochemical process involved in tissue surveillance, wound healing, regeneration, immune defence and also in pathological conditions like chronic inflammation and cancer metastasis (Friedl and Gilmour, 2009; Friedl and Wolf, 2010; Friedl et al., 2011; Scarpa and Mayor, 2016). Cells migrate to reach a destination either individually or collectively, respond to mechanical/chemical cues and interact with surrounding cells/tissues.

Primordial germ cells (PGCs), leukocytes and hematopoietic stem cells migrate as individual cells (Friedl et al., 2001) as compared to cells that migrate collectively during border cell migration in the *Drosophila* ovary (Montell, 2003), neural crest cell migration and sensory lateral line development in fish (Aman and Piotrowski, 2010; Ghysen and Dambly-Chaudière, 2004; Kniss et al., 2016; Theveneau and Mayor, 2012; Thiery, 2003; Vasilyev et al., 2009) [Fig. 4.1. A-C]. Cells show a wide diversity in the mechanism by which they migrate and understanding its dynamics with the extra-cellular matrix (ECM) yield new insights into key developmental processes. Migration of individually isolated cells is mainly amoeboid or mesenchymal. For example, embryonic cells and leukocytes migrate as ellipsoid bodies with blebs and without attaching to the cell matrix [Fig. 4.1. E]. On the contrary, neutrophils and dendritic cells form characteristic actin-rich filopodia and migrate with a weak matrix interaction (Charras and Paluch, 2008; Keren et al., 2008). Mesenchymal migration by fibroblasts and tumour cells that undergo epithelial to mesenchymal transition (EMT) are characterised by a strong focal attachment to the matrix and a contractile cytoskeleton (Grinnell, 2003; Thiery, 2002). [Fig. 4.1. F - G]. A dynamic reciprocity exists between the migrating cell and the matrix through which it migrates (Te Boekhorst et al., 2016; van Helvert et al., 2018). This complex process is resilient to several mechanical, physical and chemical signalling assaults that allow cells to defend, remodel and repair on demand. Any defects in cell migration can eventually lead to pathologies ranging from chronic inflammation to cancer metastasis (Te Boekhorst et al., 2016).

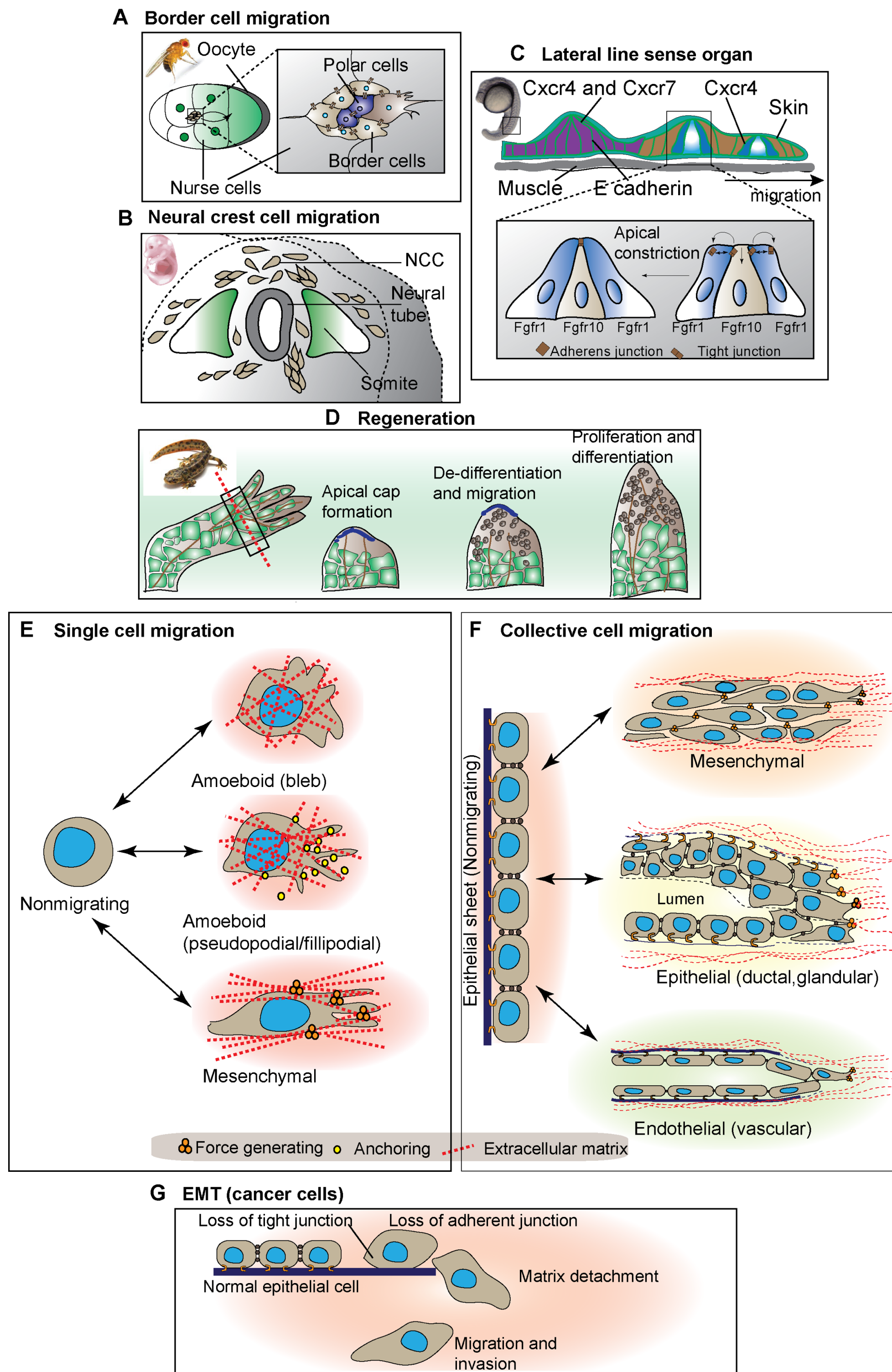

Figure. 4.1. An overview of different types of cell migration. (A) Border cell migration in Drosophila **(B)** Neural crest migration in chick embryo **(C)** Lateral line sense organ regeneration in fish **(D)** Limb regeneration in Salamander **(E)** Different types of isolated single cell migration including amoeboid/fillipodial migration by anchoring to the extra cellular matrix. **(F)** Collective cell migration in mesenchymal, epithelial and endothelial cells. **(G)** Cell migration by cancer cells undergoing Epithelial-Mesenchymal-Transition.

4.1.2. Cell migration in health and disease

The efficient migratory capability of immune cells in our body is important to detect and eliminate foreign pathogens. For example, dendritic cells (DC) are antigen-presenting cells that migrate to maintain tissue homeostasis and also initiate a pro-inflammatory immune response. Malfunctioned or abnormal DC migration can often lead to inflammatory diseases like arthritis, psoriasis and systemic lupus erythematosus (SLE) (Worbs et al., 2017). On the other hand, deregulated migration of cancer cells away from the primary tumour site and extravasation to secondary tissues leads to metastasis. Cancer metastasis and abnormal cell migration is often considered to be the leading cause behind the dissemination of the tumour cells (Herraiz et al., 2016). Metastasis is a multi-step process and involves an invasion from a primary tumour site and cancer cells have evolved with strategies to move through different tissues and organs.

An understanding on cell migration and its consequences will provide insights into new therapeutic strategies for modulating cell migration in a broad range of conditions ranging from cancer invasion to tissue regeneration. Several methods have been employed to study the underlying mechanism of cell migration (Kramer et al., 2013), each of them having their own advantages and limitations. The main advantage of *in vitro* assays is high throughput and easy handling, but it often does not mimic the *in-vivo* context. Our lab has established an *in-vivo* system where the stem cells of potentially immortal and highly regenerative planarian flatworms are required to migrate over long distances to a distal wound site (Abnave et al., 2017). This assay established the conserved role of matrix metalloproteinase (MMP-a) and β1-integrins suggesting planarian stem cell migration requires the dynamic interaction between the cell and the underlying ECM on which it is attached and over which it migrates. It also has implications for the conserved role of EMT-TFs [like the members of the *snail* TF family (*snail-1* and *snail-2*) and an ortholog of the zinc-finger E-box-binding homeobox 1 (*zeb-1*)] that regulate stem cell migration, establishing conservation of this regulatory circuit across bilaterians (Abnave et al., 2017). This work established an experimentally tractable assay for further in-depth study of the processes regulating stem cell migration *in vivo.*

4.2. Aim of this chapter

Recent *in vitro* studies using cancer cell lines and dendritic cells have shown that mechanical stress on nuclei during migration through microcapillaries leads to DNA damage (Denais et al., 2016; Irianto et al., 2017a; Raab et al., 2016). The genotoxicity of cell migration is a potentially an unappreciated source of mutations leading to the stem cell dysfunction underpinning ageing and the development of cancer. The impact of mechanical stress during cell migration has just started to be investigated *in vitro* but to what extent this happens *in vivo* remains unknown. We used the *in-vivo* assay established by Abnave et. al. 2017 to look for a relationship between cell migration and DNA damage during planarian regeneration. The main aim of this chapter is to investigate if SCs experience increased stress owing to changes in nuclear shape during migration. How does a cell with DNA damage migrate *in vivo*? What is the role of different DNA repair genes in stem cell migration?

4.3. Results and discussion

In chapter 3, we have already established the role of conserved DDR genes in maintaining genome stability in stem cells after IR. We next decided to check how cells with DNA damage behave during migration. Although the links between migration and DNA damage has just started to be investigated (Denais et al., 2016; Raab et al., 2016), almost nothing is known about how cells *in vivo* behave during migration with respect to genome instability and the role of DDR in maintaining this crucial process. Planarian stem cells and their progeny must migrate to the site of a wound following injury. Similarly, migration may also be required during reproductive (asexual) fission to form a regenerative blastema (Reddien and Sánchez Alvarado, 2004). To study this phenomenon in planarians, despite the lack of live-cell imaging approaches, our lab has established a robust assay for stem cell migration. This uses a lead shield to perform ‘shielded irradiation’, to leave a stripe of stem cells whose subsequent migration can be unambiguously followed (Abnave et al., 2017).

4.3.1. Overview of the X-ray shielded irradiation assay to study cell migration

Stem cells are sensitive to IR (discussed in chapter 3) and exposing planarians to a lethal dose of IR lead to failure in the formation of a regenerative blastema. Classical studies using a lead shield to partially expose planarians to IR has been shown to slow down its regenerative ability, suggesting the possibility that stem cells have to migrate to repopulate and restore its regenerative ability. Recent studies also show evidence for the migration of eye progenitors (Lapan and Reddien, 2011) and anterior pole cell progenitors (Oderberg et al., 2017) during regeneration. Our lab has developed an *in vivo* assay utilising the lead shielding approach to precisely observe the molecular control of stem cell migration (Abnave et al., 2017). There are several advantages of this assay compared to previously developed ones (Guedelhoefer and Sánchez Alvarado, 2012; Tasaki et al., 2016). For example, multiple animals can be uniformly irradiated with X-rays, except for a thin strip (0.8 mm) of lead that significantly attenuate the X-rays in a pre-determined position along the body axis [Fig. 4.2. A-C]. This apparatus can fit a standard 60 mm Petri dish [Fig. 4.2. A i-iii] and worms are aligned across the diameter after being anaesthetised using 0.2% chloretone for 5 minutes. The worms were then exposed to a normally lethal 30 Gy X-ray dose with the shielded region receiving less than 1.5 Gy. Exposure to 1.5 Gy IR does not affect the survival of stem cells [Fig. 4.2. D-E], thus making it easier to precisely observe SC migration from the surviving band of stem cells. The lack of posterior cell migration during the experimental time frame also allows to appropriately measure the distance migrated by individual stem cells. Details on the apparatus are available in Abnave et al., 2017.

Dr. Prasad Abnave kindly helped in performing the shielded irradiation assay for the experiments described in this chapter.

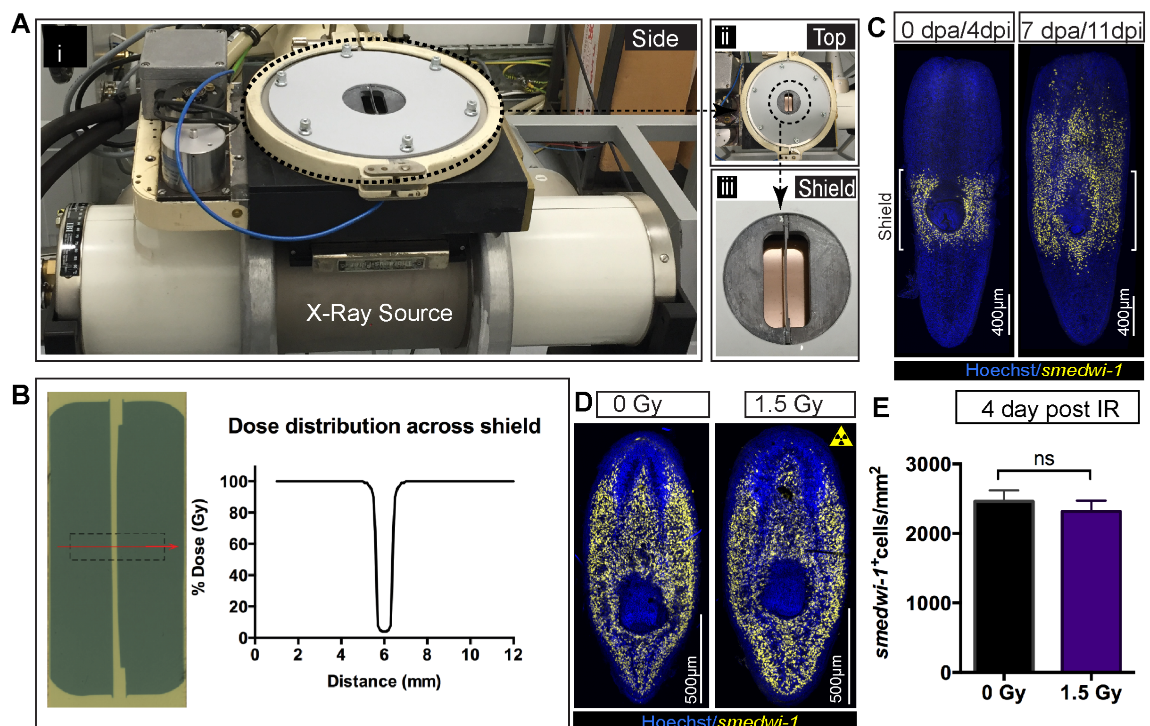

Figure. 4.2. Shielded irradiation assay to study stem cell migration

(A) Experimental set up showing the shielded irradiation assay (i), with a top view showing the position of the shield (ii) and focussing on the shield (iii).

(B) Dose distribution across the lead strip shows > 95% attenuation of X-Ray. An exposure of 30 Gy corresponds to a dose to the cells directly above the shield-protected region of less than 1.5 Gy. [From Abnave et al., 2017]

(C) Representative FISH of *smedwi-1* showing the distribution of stem cells (yellow) after shielded irradiation assay and the migration of stem cells from the shield after 7-day post head amputation. Brackets "[ ] "represents the position of the shield. Scale bar = 400 µm.

(D) Representative *smedwi-1* FISH showing the survival of stem cell after 4-day post 1.5 Gy of IR.

(E) The graph represents *smedwi-1*$^{+}$ cells/mm^{2} showed no significant difference in stem cell maintenance after 1.5 Gy IR. (n = 5, *p<0.05, ns=not significant).

4.3.2. Role of the nucleus during stem cell migration

Nuclear dysmorphia is considered to be a hallmark feature for cancerous cells, but the reason behind increased nuclear envelope (NE) rupture in cancer cells is still unknown (Chow et al., 2012; Zink et al., 2004). Recent studies suggest the physical damage incurred during migration involves nuclear envelope squeezing leading to DNA damage and genome instability (Cho et al., 2017; Irianto et al., 2017b; Pfeifer et al., 2017; Shah et al., 2017; Takaki et al., 2017). The transient loss of NE integrity often leads to DNA rearrangements called chromothripsis (Isermann and Lammerding, 2017; Maciejowski et al., 2015; Zhang et al., 2015). The NE is a double lipid bilayer that acts as a physical barrier between the chromosome and the cytoplasm. Components of NE (inner and outer nuclear membranes, nuclear pore complex, and lamina) work together to protect the genetic material. The NE was initially thought to facilitate nuclear-cytoplasmic trafficking but is in fact a dynamic organelle that gets remodelled during every cell division. During mitosis, physiologically normal cells undergo NE rupture to facilitate chromosome segregation to daughter cells (Smoyer and Jaspersen, 2014). The activation of cyclin-dependent kinase cdk1 leads to phosphorylation of lamins and reseals the envelope to resolve the transient rupture of NE (Güttinger et al., 2009). Apart from lamins, actin filaments and actomyosin contractility are the major determinants that regulate nuclear shape and NE integrity (Vishavkarma et al., 2014). Recent studies also discovered that mechanical forces exerted by the actin cytoskeleton increase the intra-nuclear pressure leading to NE rupture (Denais et al., 2016; Raab et al., 2016).

Planarian stem cells are characterized by a large nucleus and a high nuclear: cytoplasmic ratio (Gehrke and Srivastava, 2016) and the perinuclear actin must protect this stiff organelle from any mechanical damage. Migratory cells in planarians show extended protrusions compared to cells in the shielded region [Fig. 4.3. A] and knockdown of β-integrin and MMPs affect the formation of these extended processes, thus inhibiting cell migration (Abnave et al. 2017). Nuclei in stem cells are more prone to deform compared to differentiated cells (Pajerowski et al., 2007). To determine the changes in nuclear shape during cell migration,

we measured the nuclear aspect ratio (NAR) by taking the ratio of the length and the width of the nucleus of *smedwi-1*$^+$ cells. The nuclear aspect ratio changes significantly in migratory cells compared to cells in the shielded region [Fig. 4.3. B-D] highlighting the possibility of mechanical stress in stem cells. The transient NE rupture in cancer cells also leads to mis-localization of diffusible DNA repair proteins like Ku80, BRCA1, 53BP1 (Pfeifer et al., 2018; Xia et al., 2018) The lack of NE markers and any antibodies to DNA damage proteins (Ku80 or BRCA1) in planarians means that we were unable to test if this stress may lead to defects in the NE integrity and if DNA repair proteins invariably mis localize after migration. The extent of NE rupture also varies based on the pore size of the matrix through which a cell migrates (Pfeifer et al., 2018) and understanding the matrix composition through which planarian stem cells migrate is an outstanding question that needs to be addressed in the future.

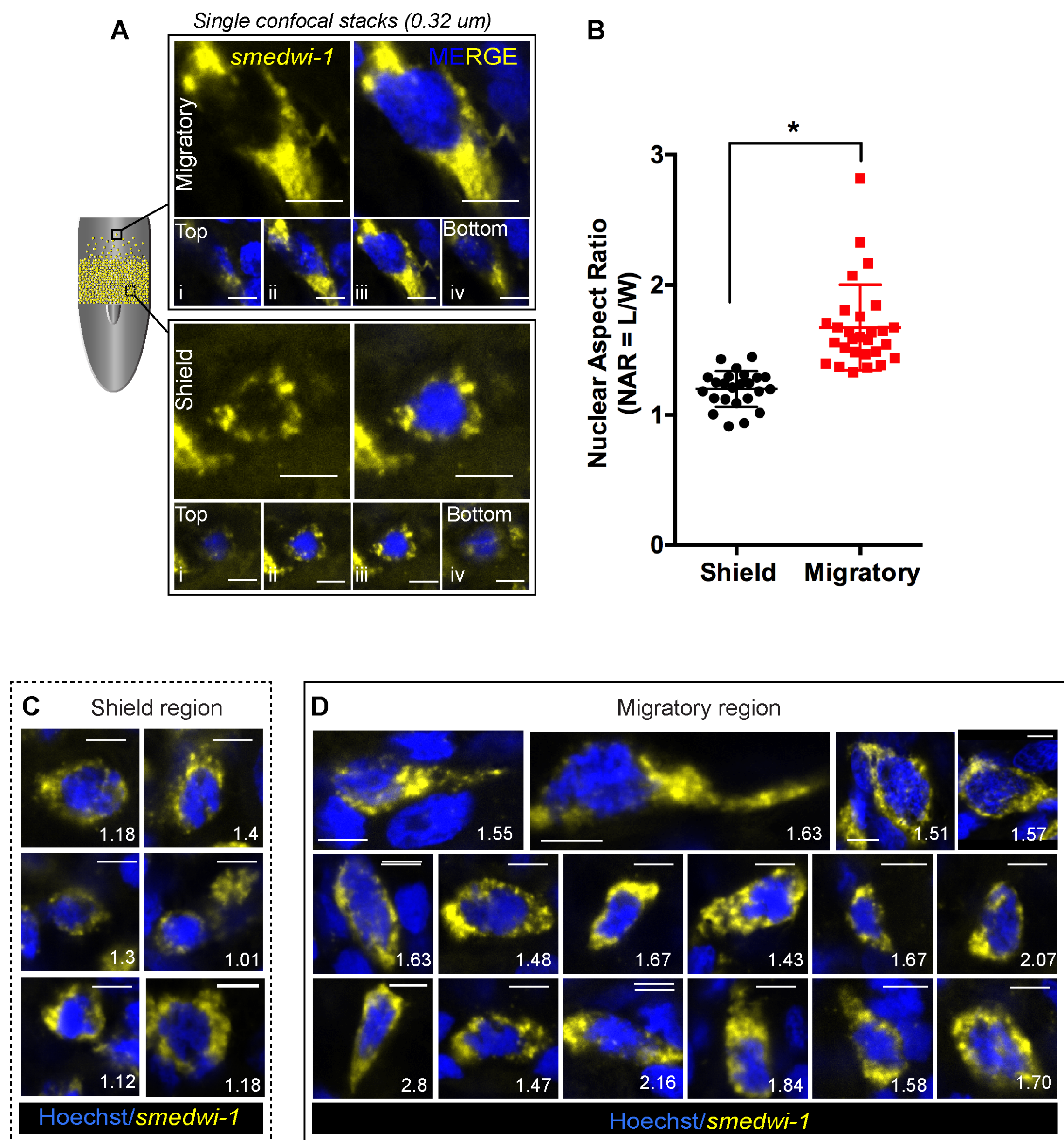

Figure. 4.3. Changes in nuclear aspect ratio during stem cell migration.

(A) Representative FISH showing stem cells (*smedwi-1*$^{+}$) with extended protrusions in migratory cells and stationary cells from the shielded region**.** Nuclei stained with hoechst (blue). Images are shown as single confocal Z-stack (0.32µm). (i-iv) is the single Z-stack from top to bottom. Scale bar: 5 µm. **(B)** Quantification of Nuclear aspect ratio (NAR) in the migratory cells compared to stationary cells (n = 28 cells in migratory region and n = 24 cells from the shield at 7dpa/11 dpi (shielded irradiation assay). Representative images of FISH showing stem cells (*smedwi-1*$^{+}$) with extended protrusions from shielded region **(C)** and migratory region **(D).** Nuclei stained with Hoechst 33342 (blue). Images are shown as single confocal Z-stack (0.32µm). The number represents the NAR value of individual cells, plotted in (B). Scale bar = 5 µm.

4.3.3. Effect of ionizing radiation in stem cell migration

Mechanical stress during immune/cancer cell migration can lead to DNA damage (Denais et al., 2016; Raab et al., 2016) but the interplay between cell migration and DNA damage is currently unknown. Here we looked to what extent does DNA damage impede stem cell migration in planarians. We used IR as a method to induce DNA damage to stem cells and then track for cell migration. Fig. 4.4. A describes the overview of the experimental strategy where we pre-irradiate the whole worms with 5 Gy and 10 Gy IR before following stem cell migratory behaviour using our shielded irradiation assay [Fig. 4.4. B]. With the activation of the DNA damage response, we decapitated the worms after 24 hours post IR to trigger stem cell migration towards the wounded region. The stem cells show a significant delay in migration after 5 days [Fig. 4.4. C] and 7-day post-IR [Fig. 4.4. D] in pre-irradiated worms compared to un-irradiated controls [Fig. 4.4. E]. This data reveals that pre-loading stem cells with damage prevent migration until it has been repaired. Although there is a significant delay in migration, stem cells eventually reach the wound; maintain normal stem cell number, and fuel normal regeneration [Fig. 4.4. F]**.** Taken together this data suggests that genome integrity must be sufficiently restored before migration can proceed. With the current lack of DNA damage markers, it is not yet possible to study the crosstalk between repair of DNA breaks, and subsequent initiation of stem cell migration. It will be essential to develop tools to directly measure DNA damage *in vivo* in stem cells to answer these fundamental questions and is currently ongoing in the lab.

A

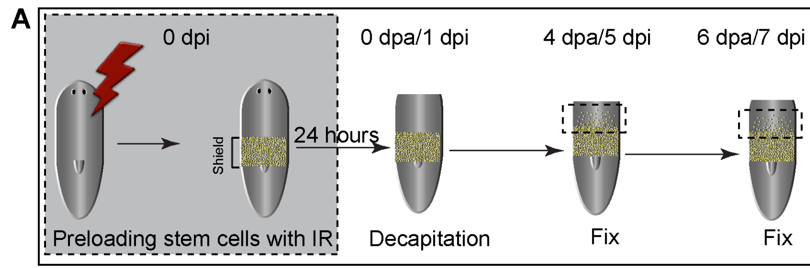

B *Irradiation(i) followed by Shielded Irradiation (3 dpi)*

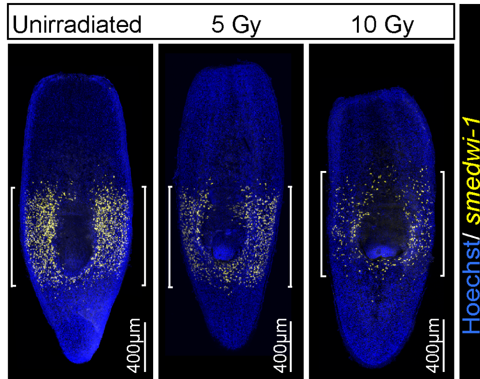

F *Irradiation(i) followed by Shielded Irradiation(25 dpi)*

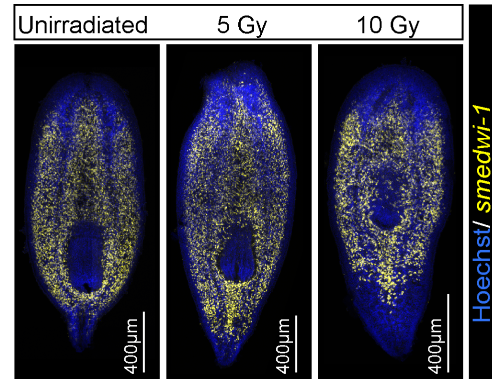

C

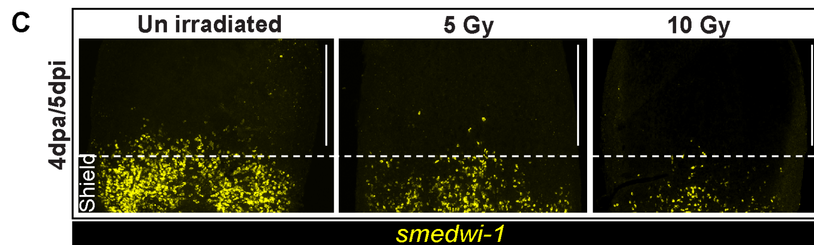

D

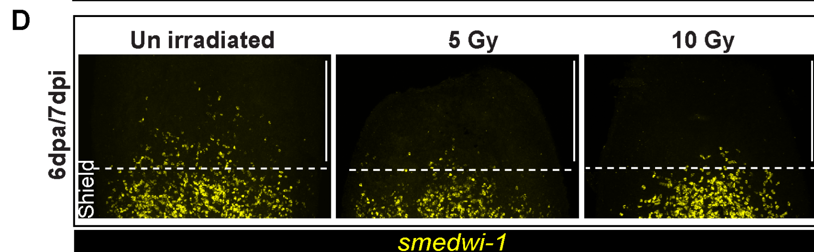

E

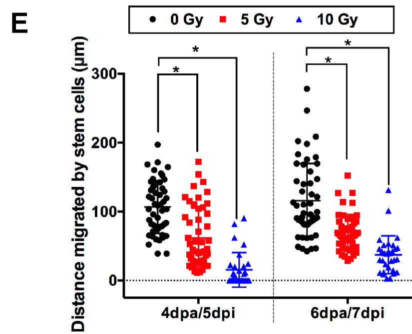

Figure. 4.4. Stem cells pre-loaded with DNA damage before wounding show delays in migration.

(A) Experimental scheme showing worms pre-exposed to irradiation (5 and 10 Gy) followed by shielded irradiation and decapitation after 24 hours. Worms are fixed at 4dpa and 6dpa (dpa = days post-amputation). Box represents the migratory region, represented in the figure below. **(B)** Representative FISH showing the distribution of stem cells in the shield after 5 and 10 Gy of IR followed by the shielded irradiation assay (3-day post-IR). [ ] brackets indicate the shielded area. Scale bar: 400 µm. **(C-D)** FISH showing worms pre-exposed to IR (5 and 10 Gy) show delayed stem cell migration after 4 and 6dpa. The dotted line represents the anterior boundary of the shield. Scale bar: 350 µm **(E)** Distance migrated by 10 most distant cells are counted from individual worms (n = 5 per condition) Results are expressed as mean ± SD. Statistical significance determined by multiple t-test using the Holm-Sidak method, *$p<0.05$ **(F)** The stem cells can eventually migrate and rescue the whole animal. Representative FISH showing the stem cells migrate and reach the wound and rescue the worm (25-day post IR). Scale bar: 400 µm.

4.3.4. Migrating cells are sensitive to a low dose of ionizing radiation

Live cell imaging by monitoring the accumulation of fluorescently labelled DNA damage marker 53BP1 or performing γ-H2AX immunostaining revealed DNA damage occurs near the NE rupture and also within the nuclear interior (Denais et al., 2016; Raab et al., 2016). We still lack a complete understanding of the mechanism behind DNA damage in migrating cells, and multiple hypotheses can be stated (as reviewed in Shah et al. 2017). For example, cytoplasmic nucleases can damage the exposed DNA after nuclear rupture and evidence suggests that the "Three prime repair exonuclease" (TREX1) has a role in cleaving chromosomal DNA outside the nucleus (Maciejowski et al., 2015). Chromatin fragmentation can further contribute to genomic instability, as exposed chromatin is more prone to damage. Recent gene expression studies comparing cells with rupture due to compression also suggest NE rupture results in activation of DNA damage response. A recent study reported heritable changes and chromosome copy number variations in cells migrating *in vitro* through narrow pore matrix (Bennett et al., 2017; Irianto et al., 2017a; Pfeifer et al., 2017). These studies suggested the possibility that genome instability can be induced during migration, but its consequences still remain unknown.

We hypothesized that cells with accumulated DNA damage during migration will either be sensitive to DNA damaging agents due to genome instability or resistant to DNA damaging agents due to increased DNA repair. To understand the effect of IR (DNA damaging agent) on migrating stem cells, we exposed the whole worm to a low dose of 5 Gy γ-irradiation at 7-day post decapitation where a significant number of stem cells are present in the migratory region [Fig. 4.5.A]. SC survival was checked at 24 hours post-IR using *smedwi-1* FISH to assay SC sensitivity to IR. The survival of stem cells in the migratory region after 5 Gy γ-irradiation was significantly less compared to un-irradiated controls [Fig. 4.5. B-G] suggesting stem cells are indeed more sensitive to IR in the migratory region than the cells in the shielded region [Fig. 4.5. H].

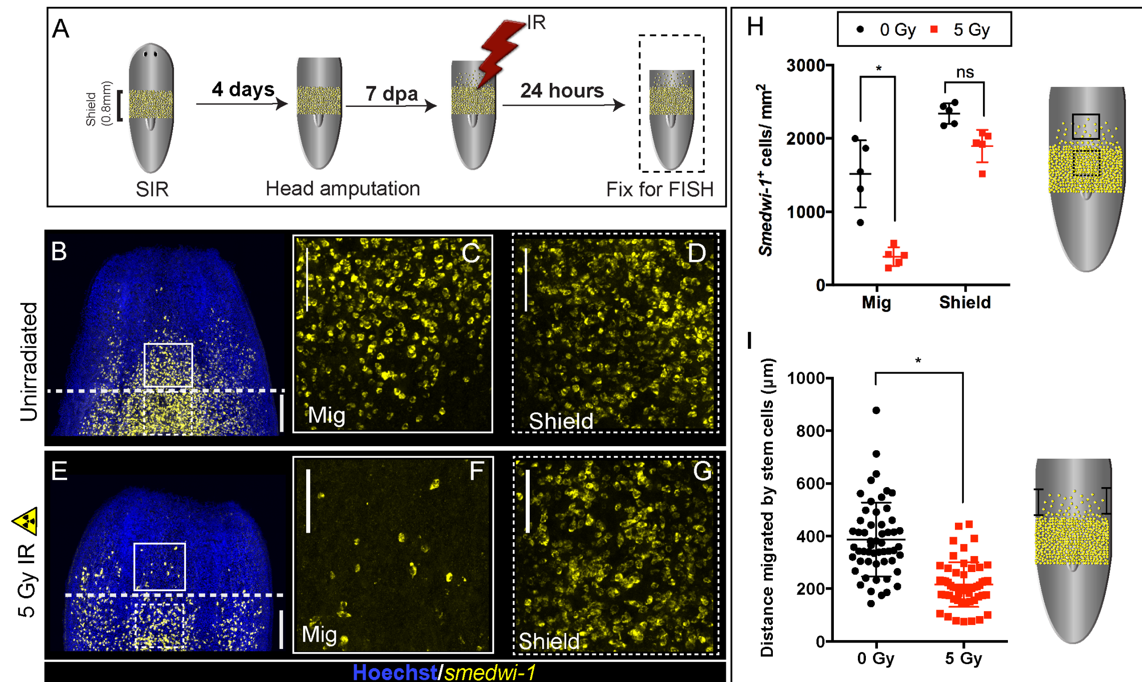
A
Shield (0.8mm)
4 days
7 dpa
IR
24 hours
SIR
Head amputation
Fix for FISH
B
C
D
Unirradiated
Mig
Shield
E
F
G
5 Gy IR
Mig
Shield
Hoechst/smedwi-1
H
0 Gy
5 Gy
Smedwi-1+ cells/ mm2
Mig
Shield
ns
I
Distance migrated by stem cells (µm)
0 Gy
5 Gy

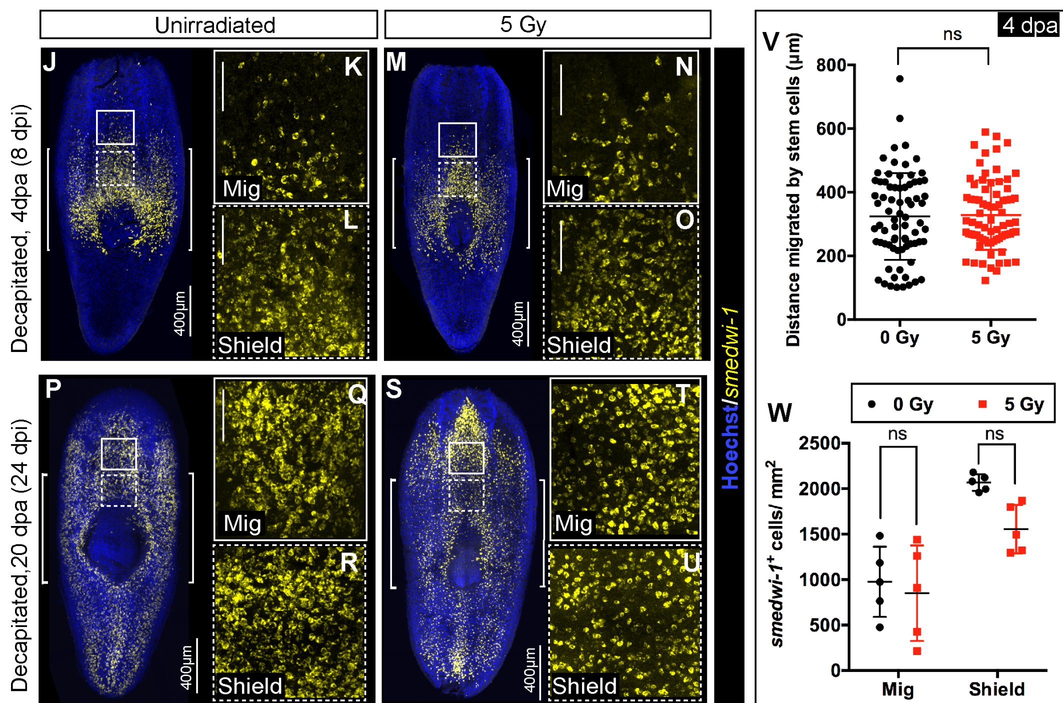
Unirradiated
5 Gy
J
K
L
M
N
O
Decapitated, 4dpa (8 dpi)
Mig
Shield
400µm
P
Q
R
S
T
U
Decapitated,20 dpa (24 dpi)
Hoechst/smedwi-1
V
4 dpa
ns
Distance migrated by stem cells (µm)
0 Gy
5 Gy
W
0 Gy
5 Gy
smedwi-1+ cells/ mm2
Mig
Shield

Figure. 4.5. Radiation sensitivity of stem cells during migration

(A) Schematic of experimental set up to study the sensitivity of migrating cells to IR. In addition to the initial shielded irradiation, the worms were irradiated with a low dose of IR (5 Gy, whole body) at 7dpa and were fixed after 24 hours to check the survival of the migratory stem cells to IR.

(B-G) Representative *smedwi-1* FISH showing migrating cells are more sensitive to IR than the cells in the shielded region. The region counted for analysis is marked with a box (bold: migratory region, dotted: shielded region). [n = 5 per condition, scale bar: 200 µm (B, E), 100 µm (C, D, F, G)].

(H) Quantification of *smedwi-1*$^{+}$ cells/mm^{2} cells in the shielded region and in the migratory region. The decrease in cells/ mm^{2} in the migratory field is significant compared to the decrease in the shielded region indicating that cells in the migratory region are sensitised to IR. Cartoon showing the region counted for analysis. Each dot represents the number of surviving cells from individual worms, n = 5. Statistical significance determined by Tukey's multiple comparison test (*p < 0.05).

(I) Distance migrated by stem cells showing that cells are more sensitive to low dose IR the further they have migrated. Each dot represents the distance migrated by individual cells. Distance migrated by 11 most distant cells are counted from individual worms (n = 5 per condition) Results are expressed as mean ± SD (student's t-test; *p<0.05, ns = not significant).

(J) Worms are irradiated with a low dose of IR (5 Gy) when cells start to migrate (4dpa, **J-O**) and cells reach the wound (20 dpa, **P-U**). Worms are fixed after 24 hours to check the survival of the migratory stem cells. The region counted for analysis is marked with a box (bold: migratory region, dotted: shielded region). [n = 5 per condition]

(V) Distance migrated by stem cells suggests no significant sensitivity of stem cells to IR (at least 10 distant cells are counted from individual worms and plotted in the graph. Results are expressed as mean ± SD and students' t-test used for analysis (*p<0.05, ns=not significant) n = 5 worms/condition.

(W) Quantification of *smedwi-1*$^{+}$ cells/mm^{2} cells (yellow) in the shielded region and in the migratory region. The rate of decrease in the migratory field and in the shielded region is plotted in the graph. The region counted for analysis is marked with a box (bold: migratory region, dotted: Shielded region). Cells are counted by making a 300 x 300 box anterior to the shield (counted as migratory field) and 300 x 300 box posterior to the shield (counted as shielded region). Results are expressed as mean ± SD and Tukey's multiple comparison tests is used to check for significance. Each dot corresponds to *smedwi-1*$^{+}$cells/mm^{2} in individual worm, n=5, *p<0.05, ns = not significant).

There is no significant difference in stem cell survival after low dose IR at 4-days post-amputation, when cells have just started to migrate [Fig. 4.5. J-O, W] or have reached their wound site at 20-days post-amputation [Fig. 4.5. P-U]. The sensitivity of migratory stem cells to IR and the fact that cells that are farthest from the shield are more sensitive to IR at 7 dpa [Fig.4.5. I] is an exciting finding that suggest cells accumulate more damage during the course of migration and are therefore more sensitive to IR.

4.3.5. RNAi of conserved DNA repair genes impairs stem cell migration to wound sites

Mechanical stress at the nuclear envelope activates the well-known checkpoint kinase ATR in mammalian cells and is known to regulate genome integrity (Kidiyoor et al., 2016; Kumar et al., 2014). Moreover, knockdown of another kinase ATM or using an ATM inhibitor has been shown to inhibit migration and invasion of human glioma cells (Chen et al., 2015; Golding et al., 2009; Hall et al., 2016). Although ATR is upregulated in response to mechanical stress, the role of other DNA repair genes in cell migration still remains unknown. The mechanical stress incurred during migration can potentially cause DNA damage in planarian SCs and we hypothesized an active DNA repair machinery is therefore necessary for SCs to migrate and reach the wound site. In chapter 3, we have identified the different DNA repair genes and their role in stem cell survival post-IR. We next investigated the role of some conserved repair specific DDR genes (like *atr, atm, brca2* and *parp1*) in cell migration in the context of shielded irradiation assay. After knockdown of DNA repair genes for two weeks followed by shielded irradiation assay, the worms were decapitated after 4 days to induce cell migration [Fig. 4.6. A]. Knockdown of DDR genes leads to anterior tissue regression ultimately leading to worm lethality, suggesting that stem cells failed to migrate. Then we performed FISH to check the migration of *smedwi-1*$^+$ stem cells, and observed reduced migration in *atr, atm, brca2* and *parp1* RNAi worms compared to migrating cells in the control RNAi worms [Fig. 4.6. B-G]. Stem cell migration was impaired after knockdown of DDR genes but the number of *smedwi-1*$^+$ stem cells was not affected in the shield-protected region [Fig. 4.6.

H]. These data suggest that knockdown of these genes did not affect normal stem cell turnover as previously shown in chapter 3. The significant reduction in distance migrated by stem cells [Fig.4.6. I] suggests DNA repair genes play a pivotal role in regulating genomic integrity during stem cell migration. The role of these genes may be cell-cycle specific and due to the lack of availability of cell-cycle stage-specific antibodies in planarians; it is difficult to study at what stages of the cell-cycle the damage occurs. Here we show that rather than replicative stress, enhanced DDR in planarians is required for stem cell migration and with the lack of DDR machinery, stem cells fail to migrate and reach the wound site.

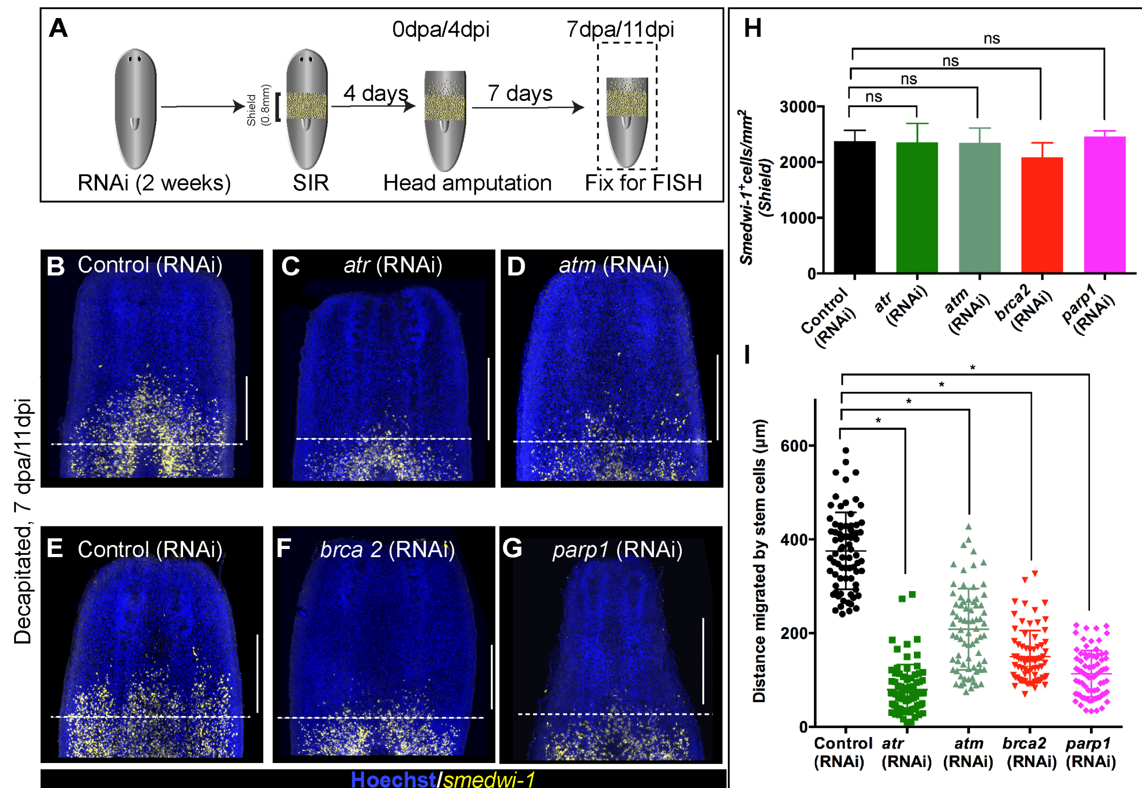

Figure. 4.6. Active DNA repair machinery is necessary for continued migration in response to wounding.

(A) Experimental scheme to study the role of DDR genes in stem cell migration. Worms are injected for 2 weeks (RNAi) followed by the shielded irradiation assay and fixed for FISH 7 days post head amputation (dpa). **(B-G)** Representative *smedwi-1* FISH shows the migration of stem cells (yellow) at 7 dpa in control (RNAi) (B and E) worms, but migration is inhibited in *atr* (C), *atm* (D) *brca2* (F) and *parp1* (G) RNAi worms. (n = 5 per RNAi condition). Scale bar: 400 µm, dotted line represents the anterior boundary of the shielded region. **(H)** Stem cells in the shielded region show no significant changes in the stem cell turnover. (*p<0.05, ns= not significant, n=5 per RNAi condition). **(I)** Quantification showing the distance travelled by stem cells after knockdown of DNA repair genes compared to the control RNAi. Each dot represents the distance migrated by individual cells. Distance migrated by 15 most distant cells are counted from individual worms. Results are expressed as mean ± SD; n = 75 cells, N = 5 worms/RNAi condition (student's t-test; *p<0.05, ns = not significant).

4.4. Conclusion

Both ageing and oncogenic phenotypes thought to be caused by mutations due to replicative stress may also result from genome instability incurred during cell migration. This could be an under-appreciated source of genomic heterogeneity in highly invasive cancer cells that encounter tight spaces in the tissue microenvironment. Using an *in vivo* assay, we revealed DNA repair genes are necessary for normal stem cell migration. Planarian SCs incur mechanical stress during migration *in vivo* that can potentially lead to DNA damage Nonetheless many open questions remain as to whether planarian SCs undergo NE rupture during migration and what are its long-term effects on genome instability. How does NE rupture affect transcriptional regulation and chromatin organization during migration? Future work in planarians can reveal the regulatory interplay between stem cell migration and DNA-repair processes. Understanding these fundamental questions using an experimentally accessible model organism will improve our understanding of cell migration and also provide new avenues for translational cancer research.

Chapter 5

Transcriptional response of planarian stem cells to ionizing radiation

5.1. Introduction

IR is used to treat cancers and increasing the sensitivity and specificity of radiotherapy is a priority. There is growing evidence that tumour-initiating cancer stem cells are resistant to IR and so can be selectively enriched by repeated radiotherapy (Bao et al., 2006; Chiou et al., 2008; Pajonk et al., 2010; Rich, 2007; Woodward et al., 2007). Therefore, identification of biomarkers of radiation survival are critical to understand this process and for developing therapeutic strategies to target cancer cells specifically. In chapter 3, we have identified that planarian stem cells can resist a high dose of 15 Gy (thrice the lethal dose to humans) without any physiological defects. Many organisms can resist high doses of IR, like the bacterium *Deinococcus* that can resist 30,000 Gy, and Tardigrades, which can tolerate up to 5000 Gy (Beltrán-Pardo et al., 2013; Horikawa et al., 2006, 2013; Levin-Zaidman et al., 2003; Zahradka et al., 2006). An understanding of how these organisms can resist such a high dose will help to identify targetable mechanisms contributing to increased radiation resistance.

5.1.1 Interplay between transcription and DNA repair

Broadly, DDR includes the stalling of the cell cycle, initiation of DNA repair, regulation of transcription, translation and ubiquitin-proteasomal system to ensure normal cell physiology. The crosstalk between activation of DDR and transcription is particularly important if a break is encountered in an actively transcribed gene. The prevailing model is that DNA damage elicits phosphorylation and ubiquitination of RNA polymerase II (RNAPII) leading to the global repression of transcription both at sites of DNA damage and even genes that are not damaged (Proietti-De-Santis et al., 2006; Rockx et al., 2000) [Fig. 5.1. A-B]. Depending on the nature of the genetic lesion, cells react differently at the transcriptional level [Fig. 5.1. C] and the advantage of global repression of transcription is to allow efficient DNA repair. With this idea, this chapter aimed to explore the interplay between transcriptional response and IR-induced DDR.

5.1.2. The transcriptional response to IR in different organism

IR induces damage to DNA and cells activate a cascade of biochemical events to modulate gene expression (Radman, 2016). The role of p53 and ATM in modulating IR-induced transcriptional changes have been well documented (Amundson et al., 2005; Jen and Cheung, 2005; Rashi-Elkeles et al., 2014) but one limitation of these studies was the changes in transcript level could be due to alterations in the synthesis or stability of pre-existing RNA. A recent study approached this problem by labelling and isolating the nascent RNA using bromouridine, showed p53 and ATM regulates RNA stability post IR (Venkata Narayanan et al., 2017). Apart from human cells, studies on Bryophyte *Physcomitrella* (Kamisugi et al., 2016) and a radio-resistant bacterium *Kineococcus radiotolerans* (Li et al., 2015) also revealed the role of DNA repair genes as a response to IR-induced DSBs. A comprehensive investigation of the transcriptional response of radiation-resistant species will provide a better understanding of the underlying genetic mechanisms responsible for radiation resistance. Moreover, studying the transcriptional response to IR could also provide insights to identify novel factors that contribute to increased radiation tolerance and stem cell survival in planarians.

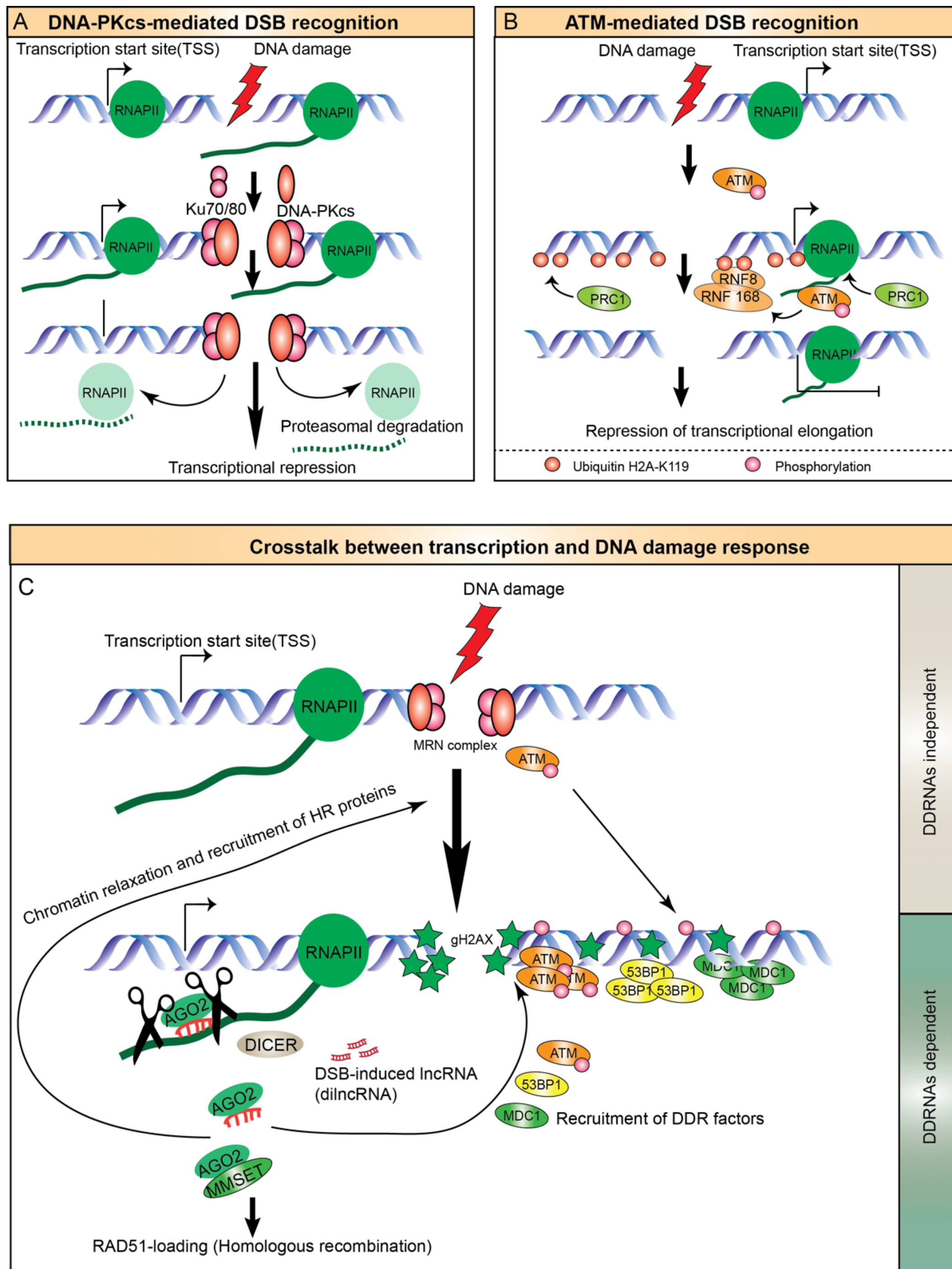

Figure 5.1. The fate of transcription near double-stranded break is dependent on the DNA damage sensing mechanism. (A) KU70/80 sense DSBs and recruit DNA-PKcs that actively removes RNAPII from damaged genes via the proteasomal pathway**.** **(B)** ATM gets phosphorylated leading to monoubiquitylation of H2A-K119 that results in chromatin compaction and inhibition of RNAPII elongation but not degradation of RNAPII. **(C)** Although transcription halts near DSBs, small RNAs are transcribed by RNAPII near the breaks. Dicer/Drosha cleaves the small RNAs to generate DDRNAs that are important for recruitment of secondary DDR factors and also for RAD51 mediated homologous recombination. [Figure adapted from (Capozzo et al., 2017; D'Alessandro and d'Adda di Fagagna, 2017; Michelini et al., 2017)]

5.2. Aim of this chapter

Radiation tolerance (RT) depends on the efficient performance of the DNA damage response (DDR) genes (Bunting et al., 2010; Fokas et al., 2014; Gibson and Kraus, 2012; Panier and Boulton, 2014). An understanding could enable radioresistant cancer patients experiencing tumour relapse to have more effective personalized therapeutic strategies along with radiotherapy or chemotherapy. Currently, there are no clinically predictive markers available to detect cancer cells or to indicate the effective treatment outcome. Planarian SCs can resist a high dose of IR, where the surviving stem cells clonally repopulate and rescue the animal. The aim of this study is to understand the transcriptional response to IR in adult stem cells and identify some novel genes that are responsible for increased RT in SCs. An understanding of the mechanism will be useful for the development of biomarkers for surviving radiation exposure and identify targets for radio-sensitization. We also studied the radiation response of a radioresistant human fibrosarcoma cell line HT1080 to a clinically relevant dose of IR to understand the functional conservation of radiation response between invertebrate adult stem cells and a human cancer cell line. These findings will provide a better understanding of radiation-induced carcinogenesis.

5.3. Results and discussion

Radiation transcriptomics has been effectively utilized to gain mechanistic insights into radiation resistance in tumour or cancer stem cells and also to identify biomarkers for radio-response (Krause et al., 2017; Lu et al., 2014; Rashi-Elkeles et al., 2014). Although much of the DNA repair mechanism operates at a protein level, the cellular transcriptome is also a key modulator of DDR signalling. Lethal doses of IR (>30 Gy) eliminates all stem cells in planarians and transcriptomic analysis after lethal doses have been used to identify neoblast enriched transcripts (Blythe et al., 2010; Cheng et al., 2018; Galloni, 2012; Önal et al., 2012; Solana et al., 2012; Wagner et al., 2012). RNA-sequencing after a sub-lethal dose of IR (12.5 Gy) has also been used to identify markers involved in stem cell repopulation (Lei et al., 2016; Wagner et al., 2012; Zeng et al., 2018).

Our independent analysis of the RNA-Seq datasets from lethally irradiated worm (60 Gy IR) (Cheng et al., 2018) revealed 838 genes were significantly depleted after 24 hours post IR, most of which are associated with stem cell maintenance, such as cell cycle and replication related genes (*PCNA, cyclin-B, mcm2, wee1, cdt1*), RNA-binding proteins (*piwi-1, ddx52*), and genes involved in DDR (*RAD51, RAD54B, RAD50, ERCC6*). Interestingly, many of the DDR related genes were depleted due to stem cell depletion after lethal dose of IR.

The transcriptional response to IR using an entire worm gives a heterogeneous response from different cell types, especially with higher doses of IR (>10 Gy) as very few SCs survive post IR (previously described in chapter 3). Most of the differentially expressed genes will be a mixed response from the very few surviving stem cells (after 12.5 Gy) and mostly from the progeny/differentiated cells (in lethal 60Gy dose). Therefore, using whole worm irradiation dataset is not informative regarding changes in the stem cells.

5.3.1. The transcriptional response to γ-IR in planarian stem cells

Despite the significant advancement of identifying novel stem cell markers using lethal irradiation as a tool, the current literature lacks the understanding of how IR-induced DNA damage can lead to transcriptional changes specifically in stem cells. High dose of IR (including 15 Gy) leads to the survival of few stem cells to be FACS sorted (previously described in chapter 3) and in order to isolate an optimum amount of stem cells for a robust RNA-seq library preparation, we exposed the worms to a low dose of 5 Gy γ-IR. From our comet assay data described in chapter 3, we know exposure to 5 Gy IR causes DNA breaks at 2-hours and 24-hours post-IR and is therefore used to understand the transcriptional response of SCs to IR. The stem cells were FACS-sorted into X1 (containing stem cells in S/G2/M phase of the cell cycle) and X2 (containing stem cells in the G1 phase of the cell cycle and post-mitotic progenies) fractions after 3 hours and 24 hours post-IR [Fig. 5.2. A]. We used an early time point (3-hours post-IR) and a late time point (24-hours post-IR) to understand the DDR signalling. Total RNA was isolated from X1 fraction and X2 fraction followed by

library preparation for sequencing [Fig. 5.2. A – C]. SC heterogeneity exists within the X1 fraction and the present study is aimed to understand the effect of IR on global transcriptional response of SCs at different cell cycle phase.

We used the publicly available *S. mediterranea* transcriptome assembly (Planmine Dresden, dd_smed_v6 transcriptome assembly)(Brandl et al., 2016) to map our raw RNA-seq. FASTQ reads and differential gene expression (DGE) analysis was performed using the Walds test (details on RNA-sequencing analysis is described in chapter 2). DGE analysis revealed 221 genes were upregulated [Fold change (FC) >2, p-value<0.05], 615 genes were downregulated, [FC<-2, p-value<0.05] after 3 hours and 2010 genes were upregulated [$Log_2FC>4$, p-value<0.01] after 24 hours post IR in X1 sorted stem cells. On the other hand, 328 genes were upregulated [FC>2, p-value <0.05], 693 genes were downregulated [FC>2, p-value <0.05] after 3 hour and 644 genes were upregulated [FC>2, p-value <0.05], 592 genes were downregulated [FC>2, p-value <0.05] after 24 hours post IR in X2 sorted cells [Fig. 5.3. A – D]. 42 genes were common to X1 and X2 irradiated cell dataset at 24 hours out of which 23 genes were upregulated that includes cell-death related nuclease, apoptosis and autophagy-related genes.

Genes that are upregulated in X1 stem cells at 24 hours post-IR include genes involved in Reactive Oxygen Species (ROS) signalling, metabolic pathways, stress-related genes, interferon signalling along with genes involved in extracellular matrix remodelling. For example, *ULK1-like* (dd_1620) is autophagy related kinase that was significantly upregulated in planarian stem cells following IR (log_2 FC=4.2). Autophagy plays a significant role in cancer because of its role in tumour suppression and cell-cycle arrest to protect cells from a myriad of genotoxic assaults.

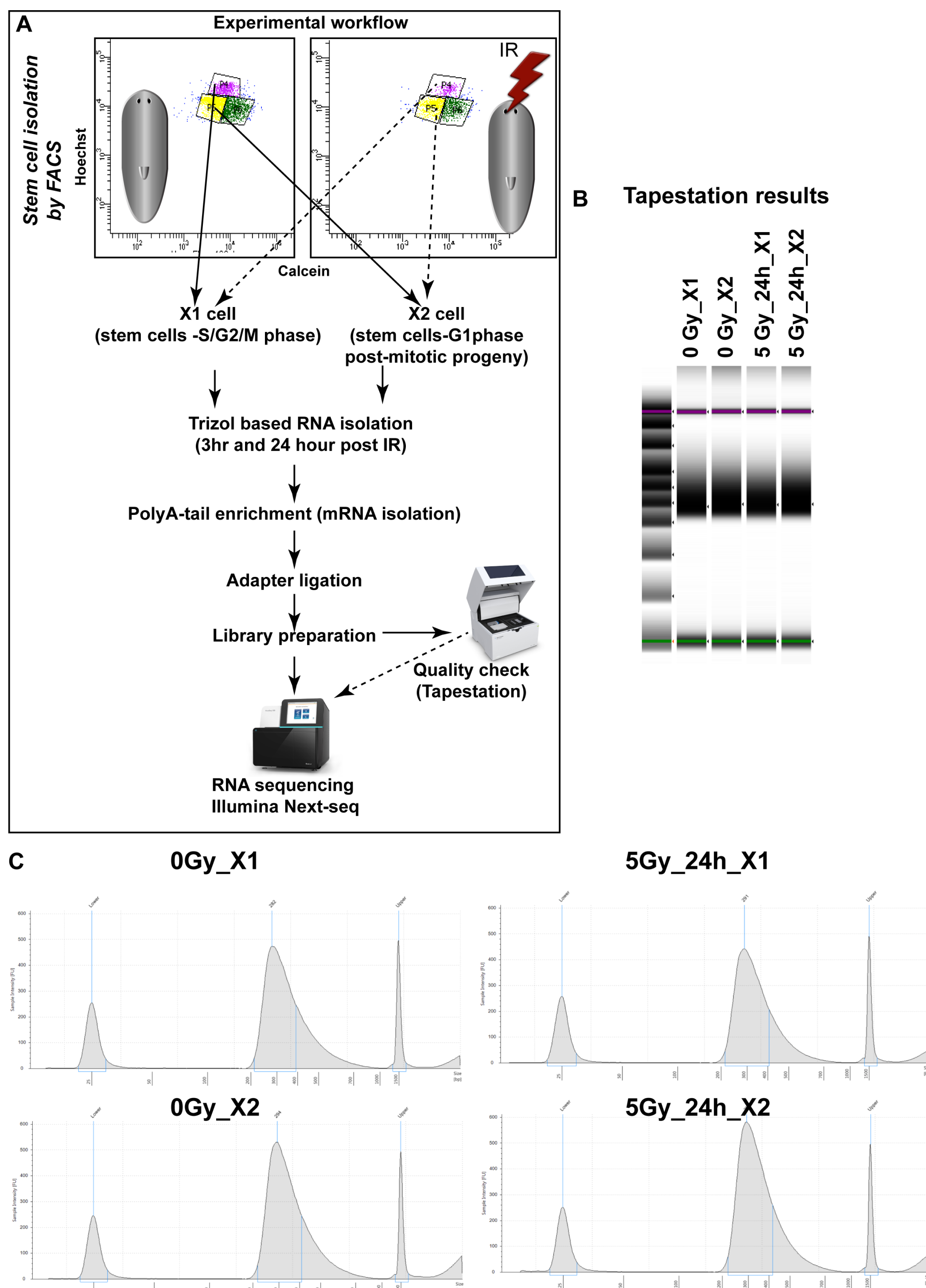

Figure. 5.2. Experimental strategy to understand the transcriptional response to γ-irradiation in planarian stem cells. (A) Stem cells were isolated based on nuclear to cytoplasmic content. X1 (cells from S/G2/M phase) and X2 (G1stem cells, post mitotic progenies) population were separately collected from 5Gy IR worms and unirradiated control worms. RNA was isolated, libraries were prepared and sequenced in the Nextseq 550 machine. **(B, C)** Quality control of libraries using Agilient Tape-station. The electrophenogram showing a clean band ~280 bp with no adapter dimers from one of the experimental replicates.

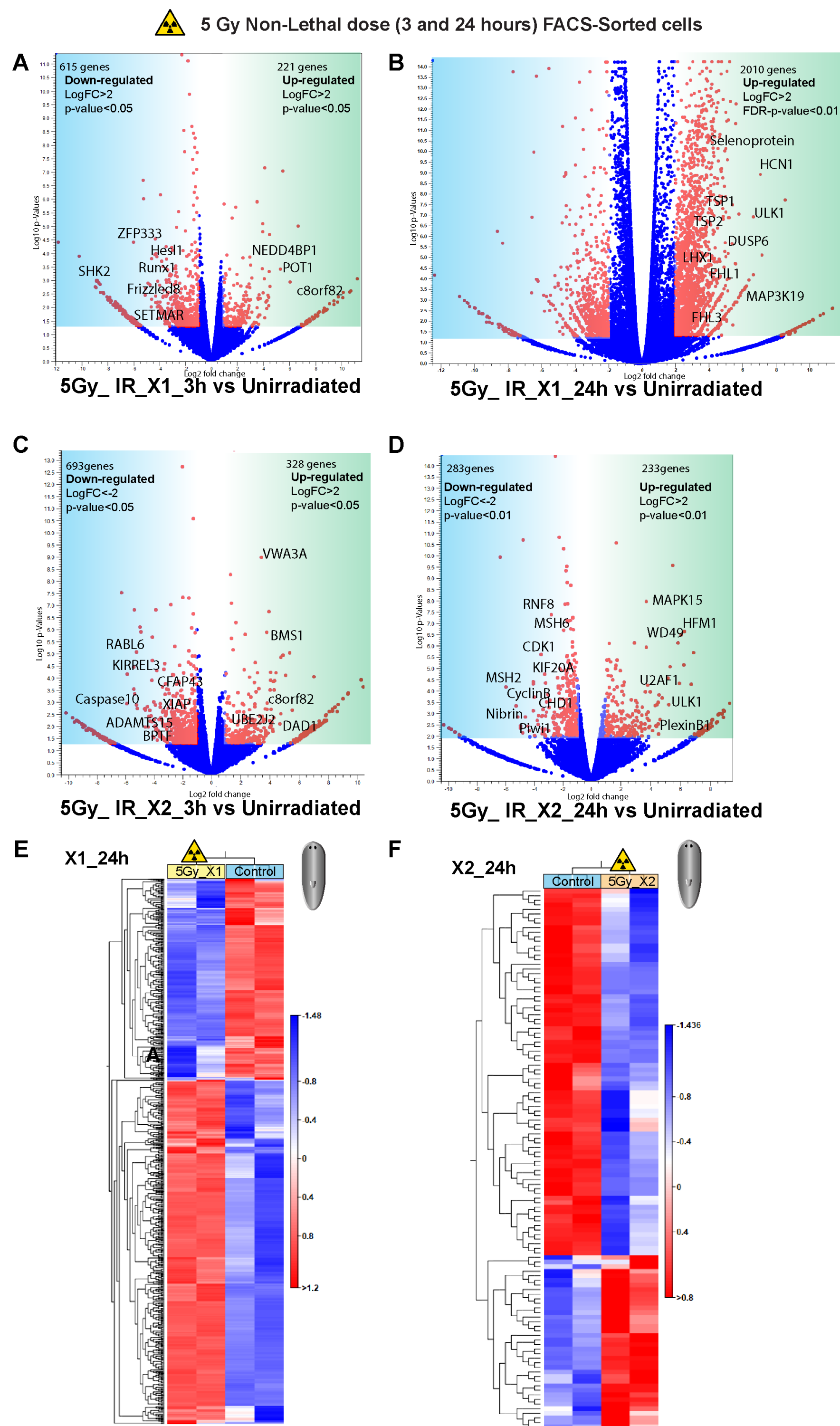

Figure. 5.3. Transcriptional response to γ-irradiation in planarian stem cells. (A-D) Volcano plots showing the differentially expressed transcripts in X1 and X2 cells after 3 hours and 24 hours post irradiation respectively. The X-axis represents the log (Fold change) and the Y-axis represent the Log (p values). **(E-F)** The hierarchical clustering of differentially expressed genes in X1 and X2 cells after 24 hours post-irradiation, based on Euclidean distance and single linkage. Statistical significance was calculated using Walds test FDR p-value<0.01 as a part of CLC genomics package.

A key therapeutic strategy currently being employed to treat cancer is to couple autophagic pathways along with radiotherapy (Levy et al., 2017; Tam et al., 2017). The role of autophagy in DNA repair has not been extensively studied and the role of *beclin1* has just been identified to regulate DSB repair independent of autophagy (Xu et al., 2017a). Low dose irradiation (~0.02 Gy) leads to an increase in oxidative stress, ROS generation in hematopoietic stem cells (HSC) and upregulation of ULK1 have been observed to trigger autophagy and mitophagy (Rodrigues-Moreira et al., 2017). Upregulation of NF-κB in response to IR plays a major role in apoptotic signalling leading to increased survival in human neuroblastoma cells (Veeraraghavan et al., 2011) and hematopoietic stem cells (Kim et al., 2014a).

We observed upregulation of TNF signalling pathway genes, encoding for TNF (tumour necrosis factor), chemokines, and interleukins, along with MAPK (mitogen-activated protein kinase) phosphatases in planarian SCs post-IR. TNF receptor associated factors (TRAFs) are a family of proteins involved in antiviral responses and apoptosis. TRAFs have been greatly expanded in planarians (Swapna et al., 2018) and our dataset identified four different TRAFs (*TRAF-1,2,3, 6*) that are upregulated in stem cells in response to IR. NF-κB-TNF signalling activation mediates IR-induced expression of cell death inhibitors which enhances cell survival and induce radiation resistance in several cancers (Veeraraghavan et al., 2011; Yu et al., 2017). The activation of TNF signalling and MAPK pathway in planarians in response to IR could be a survival strategy employed by the stem cells to resist such a high dose of IR. Our data also correlates with a previous study using radioresistant non-small-lung cancer cell line, showing upregulation of MAPK, solute carrier family genes involved in ion transport, membrane-bound proteins, TNF signalling pathway genes (Yang et al., 2013).

IR is a stressful response to living cells that induces several stress-responsive proteins like Heat shock proteins (HSPs). HSPs are evolutionarily conserved proteins that assists in refolding or degradation of other proteins and interfere with anti-apoptotic pathways or elicit anti-cancer immunity. HSPs are typically

based on their molecular weight and classified into five major families: HSP100, HSP70, HSP60 and small HSPs. These molecular chaperones are known to be upregulated in flies in response to irradiation (Moskalev et al., 2015), and recently HSPs have been characterized in planarians (*D. japonica*) to be critical for stem cell maintenance during regeneration (Isolani et al., 2012). Our RNA-seq. analysis revealed upregulation of *hsp40/ DnaJ*, *hsp60, hsp83, hsp90*, in stem cells in response to IR and this could play a major role in cell survival. The functional role of HSPs in response to IR and how it regulates SC survival post-IR is still unknown and requires experimental characterization in the future.

Several genes involved in metabolic processes were upregulated in X1 stem cells in response to IR. There are three arginine-glycine amidino-transferases (*AGAT-1,2,3*) that catalyse the first step in creatine biosynthesis to yield ornithine. IR induces the activation of these three AGATs along with antizymes Ornithine decarboxylase (ODC) and cytochrome P450 (CYP450). Polyamines are well known for their role in tumour suppression or DNA repair after the discovery of ODC as a transcriptional target of *MYC* oncogene (Bello-Fernandez et al., 1993). Dysregulated polyamine biosynthesis is considered to be the hallmark of several cancer like leukaemia, neuroblastoma, and breast cancer (Funakoshi-Tago et al., 2013; Hogarty et al., 2008). Elevated ODC and polyamine production promote increased proliferation in tumour cells and polyamines are currently being used as biomarkers for several cancers. Targeting the polyamine metabolism led to the development of ODC inhibitors that are recently implemented in cancer prevention (Casero et al., 2018). ODCs catalyse the first rate-limiting step in polyamine synthesis and 6 ODCs have been identified in planarians (Cassella et al., 2017). ODC1 gets activated during wounding (Wenemoser et al., 2012; Wurtzel et al., 2015) and its inhibition leads to failure in SC proliferation and differentiation. It is currently unknown whether ODCs are activated in stem cells near the wound site and how it regulates neoblast proliferation requires further characterization. ODCs are induced in response to UV irradiation in mouse keratinocytes and have been reported to play a major role in DNA double-stranded break repair (Rosen et al., 1990; Tsuji et al., 2007). These metabolic genes like *AGAT-1,2,3* and antizymes like *ODC* were highly expressed in

planarian epidermal progeny (Eisenhoffer et al., 2008; Tu et al., 2015). Although very little is known regarding the function of these metabolic genes in *Schmidtea,* it has been hypothesized that *AGAT*⁺ cells synthesize creatinine which is taken up by neighbouring muscle and neuronal cells (Eisenhoffer et al., 2008; Tu et al., 2015), but this requires further experimental evidence. Metabolic genes including polyamines are essential for cell growth, maintenance of chromatin conformation, gene regulation and ion channel regulation (Casero and Marton, 2007; Pegg, 2009). The upregulation of multiple metabolic genes in stem cells after irradiation suggests that despite these transcripts being lowly expressed in homeostatic condition, these genes play a significant role in stem cell survival post-irradiation.

Other genes that were upregulated in stem cells post IR include genes from notch signalling (*Jagged 1-like* and E3 ubiquitin ligase mindbomb 1 *(MIB1)),* Protein Phosphatases *(PTPRJ, PTPRN),* Matrix metalloproteinases *(MMP1, MMP2, MMPa, MMPb),* Limpet homeobox proteins *(FHL1, FHL2, FHL3, LHX1),* transcription factors *(EGR1-like and EGR4-like)* along with novel genes with domains of unknown function [c14orf166, c10orf11]. Two novel genes downregulated in response to IR include c8orf45 and c10orf2. Although in this study, we focused on characterizing genes with homology to mammals, irradiation also induced a multitude of flatworm and *S. mediterranea* specific genes. A similar study using low dose IR in another flatworm *D. japonica* also revealed upregulation of *Plexin-B*, Ornithine decarboxylase (*ODC1*), *Rab7*, *Tetraspanin CD63*, Ras-related C3 Botulinum toxin (*Rac1*), *Astacin* after 4 and 7-days post-irradiation. All of these genes are common to the *Schmidtea* irradiation transcriptome dataset that suggests a conserved response to IR exists among the flatworms. Although *D. japonica* dataset was performed using whole worms (technical limitation to isolate stem cells), the qPCR data revealed lethal dose of IR does not lead to upregulation of these genes. This data explains the upregulation of the metabolic genes could be in the *D. japonica* stem cells is similar to what we observe in X1-FACS sorted stem cells post IR.

5.3.2. Functional characterization of IR-responsive genes

We next wanted to study the role of the differentially upregulated genes in response to IR (as described in section 5.3.1), to identify genes that are involved in stem cell survival and DNA repair. Our RNA-seq. dataset revealed upregulation of two Tspan family genes were induced (Tspan18_1003 and TspanCD63_440) in X1 stem cells after 24 hours post IR. Tspan CD63 has been shown to be up-regulated after low dose radiation in *Dugesia japonica* (Rossi et al., 2007, 2018) but whether it regulates stem cell repopulation post IR still remain unknown. The tetraspanin family of genes have a broad role in cancer initiation, metastasis, cell adhesion and immune signalling (Charrin et al., 2014; Hemler, 2014; Zöller, 2009). Tetraspanins (TSPAN) are a family of small transmembrane integral proteins expressed by plants and all metazoans, with 33 members in mammals, 37 in *Drosophila*, 20 in *C. elegans* and 48 in *Schmidtea mediterranea* (Huang et al., 2005; Zeng et al., 2018)*.* Tetraspanins (Tspan) are a diverse family of membrane proteins that regulate cellular interactions with other cells or stroma/matrix along with some Tspan with more specialized functions like uroplakins in the bladder and retinal outer segment membrane protein (ROM1) in the retinal photoreceptors. These integral membrane proteins modulate cell signalling during cell motility by interacting with growth factor receptors or integrins (Lazo, 2007). For example, CD63 (also called melanoma associated antigen) was the first tetraspanin to be related to the invasive property of human melanomas and colon carcinoma cell line (Radford et al., 1995).

Using FISH, we checked the expression of the two Tspan identified in our RNA-seq. dataset and observed TspanCD63 is mostly expressed in the gut branches and Tspan18-like in the parenchymal cells. The single-cell RNA-seq. dataset (Fincher et al., 2018) is also consistent with our FISH showing the expression of *TSPCD63* and *Tspan18-like* in intestine and parenchymal cells respectively. [Fig. 5.4]. TSPCD63 has also been shown to be upregulated in the gut branches of *D. japonica* in response to low dose IR and is hypothesized to play a major role in stem cell survival and proliferation near the gut branches (Rossi et al., 2018).

Next, we investigated the role of LIM homeobox transcription factors (TFs), FHL-1 in stem cell survival post IR. The four and a half LIM (FHL) proteins comprises of 4 complete LIM (an acronym derived from LIN-11, ISL-1 and MEC-3) domains with zinc finger motifs preceded by an N-terminal half LIM domain. These proteins play a diverse role in cell migration, proliferation, differentiation and apoptosis (Johannessen et al., 2006). The role of FHL proteins in carcinogenesis is debatable as upregulation of FHLs has been reported in ovarian and gastrointestinal cancers and downregulation in rhabdomyosarcoma (Johannessen et al., 2006). FHL1/2 and 3 regulate TGF-β mediated transcription via interaction with Smad proteins to suppress tumour growth (Ding et al., 2009).

Many of the upregulated transcripts in neoblasts following IR correspond to genes that in wild-type animals have expression enrichment in the differentiated cells (Xins compartment). We therefore hypothesized that these genes could play a role in stem cell survival/repopulation post IR. We silenced the expression of TFs like FHL-1, and the two tetraspanin genes in our sub-lethal IR assay (as described in chapter 3) and stem cell repopulation was scored using *smedwi-1* FISH. Knockdown of these genes does not affect the regeneration capability suggesting cell proliferation does not get affected. But the expression of these genes was significantly upregulated in SCs after 24 hours post- IR. To validate the role of these genes in stem cell survival post-IR we silenced the expression of FHL-1, Tetraspanin-CD63 (TSPCD63) and Tetraspanin-18-like followed by exposure to 15 Gy of IR and checked for stem cell repopulation post IR. We performed FISH using the pan stem cell marker *smedwi-1* and observed a significant decrease in stem cell repopulation in *FHL-1, TSP18 like* and *TSPCD63* (RNAi) worms after 7 days post-IR [Fig. 5.5. A - B]. This data suggests the role of these genes is not required for homeostatic SC turnover but involved in the survival and repopulation of SCs post IR. Future work should focus to perform RNAi screen of other upregulated genes to understand the role of these genes in SC survival post IR.

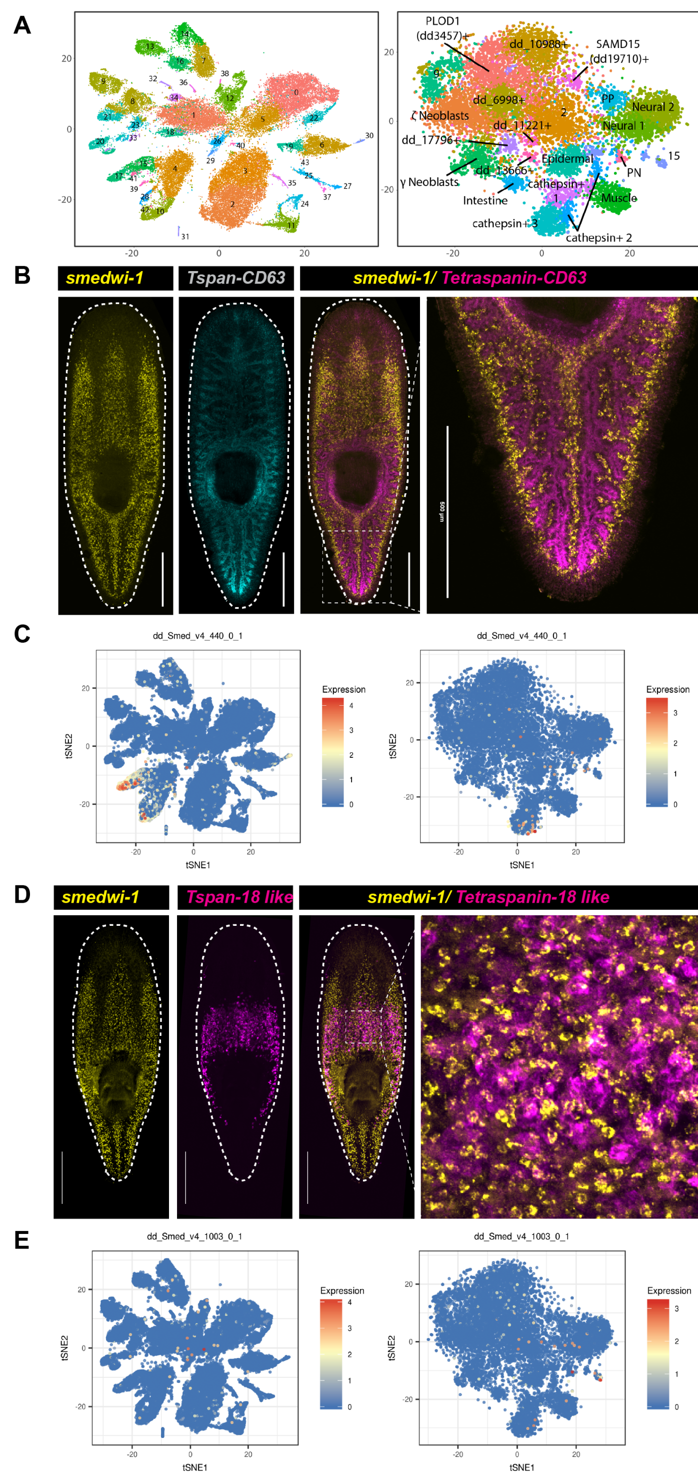

Figure. 5.4. Expression pattern of Tetraspanin group genes in planarians. (A) Cell type transcriptome atlas from https://digiworm.wi.mit.edu/ **(B)** Double FISH with a pan stem cell marker *smedwi-1* (Yellow) and *tetraspanin CD63* (expressed in the gut, Cyan, Magenta) after 24 hours post-5 Gy IR. We did not observe upregulation of these transcripts in *smedwi-1*$^{+}$ stem cells **(C,E)** Seurat map showing tSNE plot showing the expression of tetraspanin transcripts from single-cell-sequencing dataset (https://digiworm.wi.mit.edu/) **(D)** Double FISH with *smedwi-1* (Yellow) and *tetraspanin 18 like* (expressed in the parenchymal cells, Magenta) after 24 hours post-5 Gy IR.

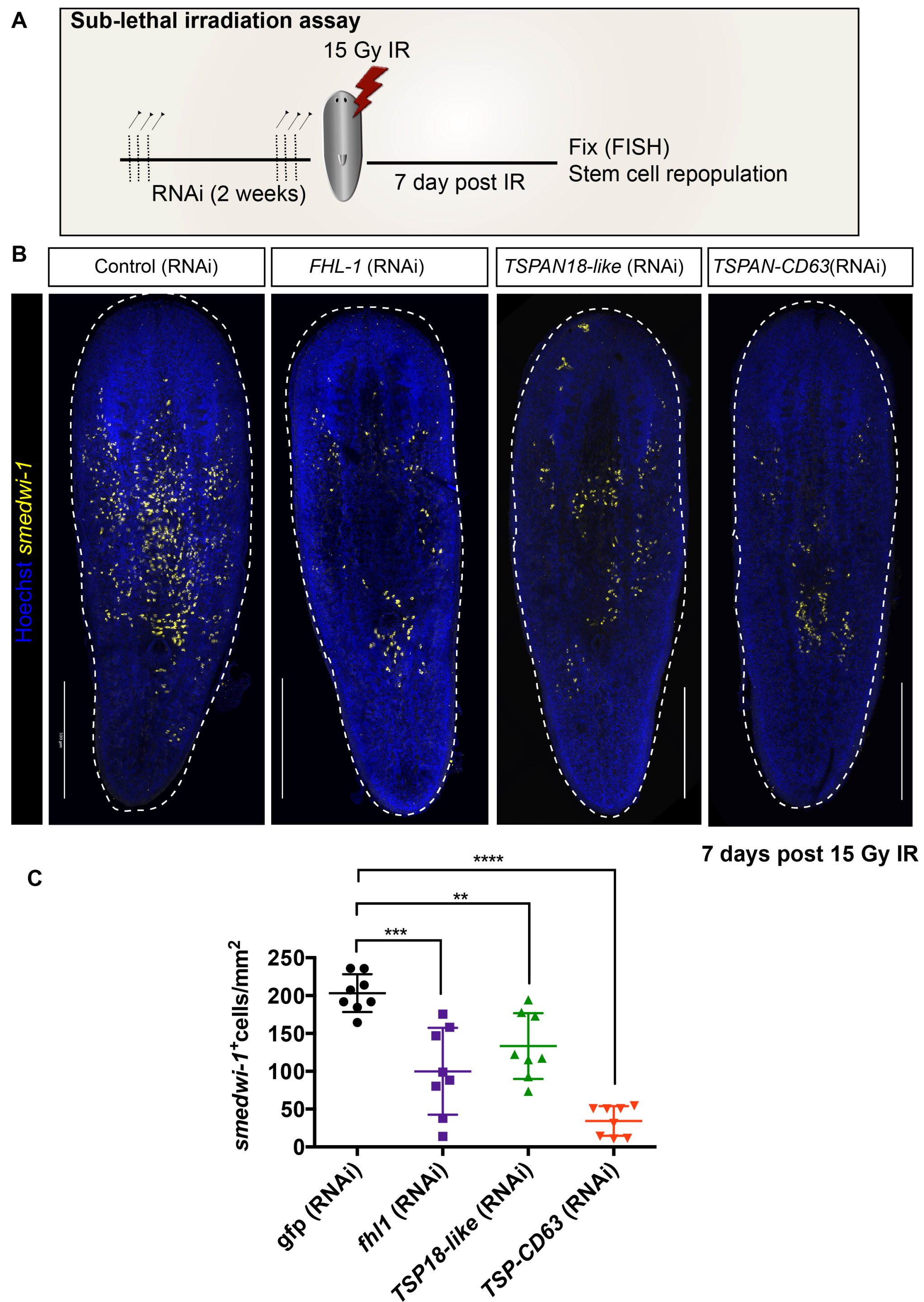

Figure. 5.5. Role of FHL and Tetraspanin in stem cell repopulation post IR. (A) Experimental schematic showing the loss of function strategy to understand the role of IR induced transcripts in stem cell survival/ repopulation post irradiation. **(B)** *smedwi-1* FISH showing the repopulation of stem cells after knockdown of FHL1, Tetraspanin 18 like and tetraspanin-CD63, after 7 days post 15 Gy IR. **(C)** Graph showing the repopulation of stem cells after knockdown compared to gfp RNAi (control). Each dot represents the *smedwi-1*$^{+}$ cells/ mm^{2} in individual worm, n = 8 worms/ RNAi condition, Unpaired students' t-test, (**p-value<0.001,***p-value<0.0001,****p-value<0.00001).

5.3.3. Evolutionarily conserved responses to ionizing radiation in human cancer cells*

S. mediterranea can tolerate a high dose of IR and are considered to be radiation resistant. Similarly, most of the human cancers are considered to be resistant to radiotherapy and understanding the mechanism behind this radiation resistance is crucial for developing therapies to target cancer cells. Therefore, investigating the transcriptional responses to IR in a wide range of evolutionary diverse range of species is important. The current study examines the radiation response of a human fibrosarcoma HT1080 cell line. To date, the transcriptome of this cell line post-irradiation has not been characterized and therefore provides exciting insights into the radiation response of cancer cells *in-vitro*. Here we perform a comparative analysis between *S. mediterranea* and HT1080 RNA-seq. data sets to identify genes with conserved and differential profiles between the two datasets.

5.3.3.1. γ-H2AX immunostaining show IR-induced DNA damage in HT1080 cells.

To understand the DNA repair mechanism in HT1080 cells and optimise a clinical dose that leads to DNA damage we performed γ-H2AX immunostaining after exposure to IR. HT1080 cells were grown on fibronectin-coated coverslips in 6-well tissue culture treated plates until they reached 75% confluency. The cells were irradiated with either 0 Gy (Un-irradiated control), 2 Gy, 4 Gy, and 8 Gy of gamma IR and were fixed after 2 hours to detect IR-induced DNA damage foci. γ-H2AX staining was performed to identify a relevant dose that induces DNA damage in the cells [Fig. 5.6. A-D].

*This section was performed as a part of M. Sc. thesis of Mr. Talal Syed (TS) (Oncology) associated with this project. HT1080 cells were kindly provided by Dr. Geoffrey Higgins (Oncology). Maintenance of cell line and preparation of RNA-seq. libraries of HT1080 cells were done by TS with the help of Sounak Sahu (SS). Anish Dattani helped in sequencing the RNA-seq. libraries. All data presented in this section including RNA-sequencing analysis was independently performed by the author.

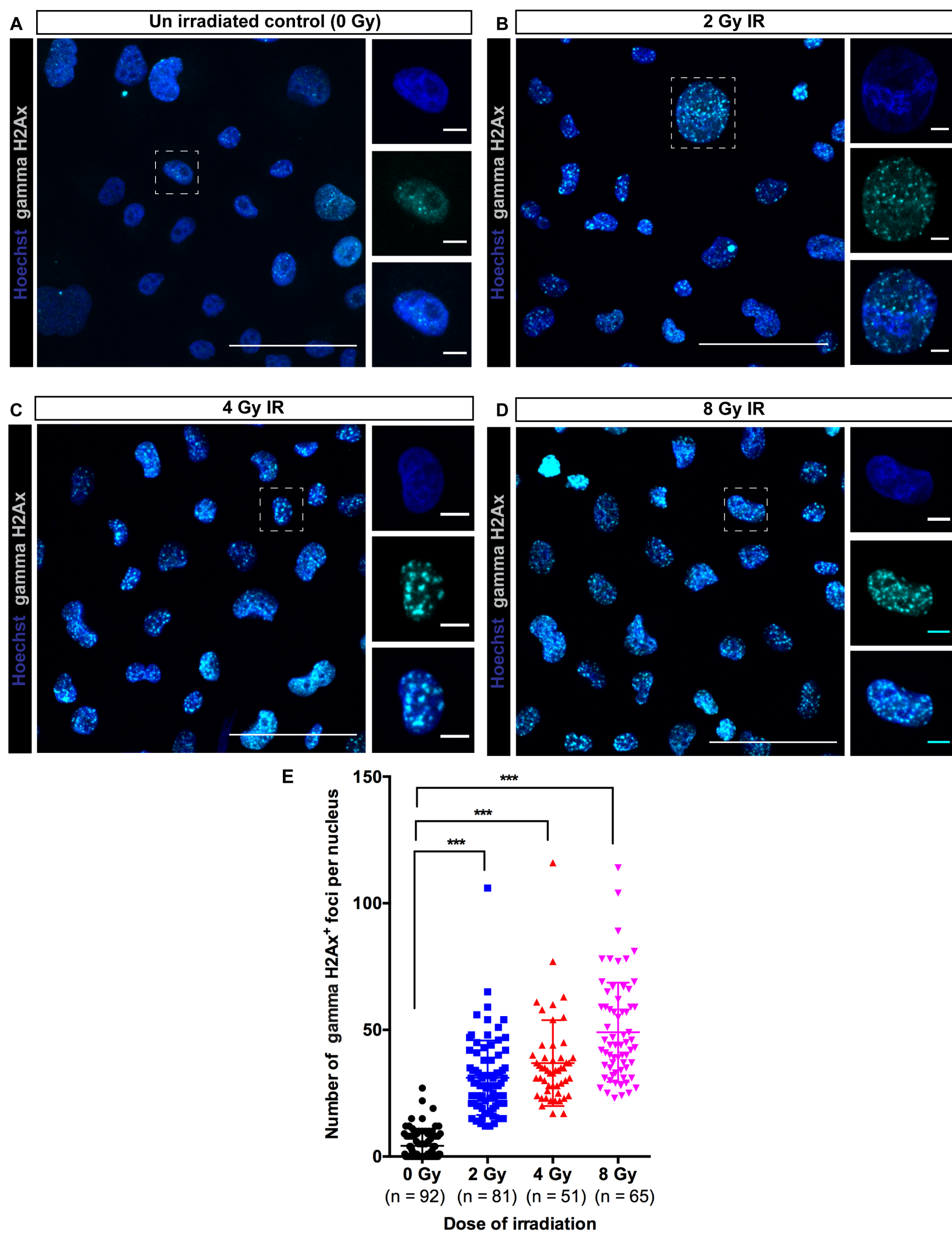

Figure. 5.6. γ-H2AX immunostaining show IR-induced DNA damage in HT1080 cells. HT1080 cells were exposed to 2, 4 and 8 Gy of γ-irradiation and fixed after 2 hours. **(A-D)** Immunostaining was performed using a DNA damage marker γ-H2Ax (Cyan) to detect damage foci in individual cells. DAPI was used to stain the nucleus (Blue). **(E)** Quantification of γ-H2Ax foci showing a significant increase in DNA damage foci after different dose of irradiation. N number in parenthesis denotes the number of cells counted per condition. (students t-test was performed to check for significance, **p-value <0.01, ***p-value <0.001).

Some un-irradiated HT1080 cells also show baseline DNA damage foci, due to intrinsic genome instability in cancer cells (Inset figure under 0 Gy) [Fig. 5.6. A]. Based on this result, 2 Gy was sufficient to induce DNA damage [Fig. 5.6. E]. and a clinically relevant dose that are used to treat human cancer. We next performed RNA-sequencing on HT1080 cells exposed to 2 Gy along with the unirradiated controls at different time points to get a global transcriptomic profile over a 24-hour post IR time course.

5.3.3.2. IR induces DNA protective proteins, anti-apoptotic and matrix remodelling proteins in HT1080 cells

HT1080 fibrosarcoma cell line was exposed to 2 Gy of γ-irradiation and total RNA was isolated after 3-hours, 6 hours and 24 hours (hr) post-IR [Fig. 5.7. A]. Differential gene expression analysis using Walds test was performed between the irradiated and control samples. We have identified 767 differentially expressed genes (DEG) within 3 hours, 6 hours and 24 hours datasets compared to un-irradiated control. Out of these 767 DEGs, 308 genes were unique to the 3-hr dataset, 128 to the 6-hr dataset and 4 were unique to the 24-hr dataset. The highest number of DEGs were identified after 3 hours post IR, suggesting a major transcriptional response occur immediately as a response to IR, which decreases within 24 hours. The PCA plot demonstrated the clustering of 24 hr irradiated dataset with the un-irradiated control and expression of very few differentially expressed genes [Fig. 5.7. B-C]. This suggests cells resume normal transcriptional activity after 24 hours post-IR and this has been reported recently by a reduction in γ-H2Ax foci after 24 hours post-IR in HT1080 cells (Bhattacharya et al., 2017). The genes that are differentially up-regulated post IR includes up-regulation of Protein phosphatases like *DUSP10, SMAD9, FGFR3, GATA2 and ID1/2/3, RNF43* and down-regulation of *OPN3, PDE2A, ADOR1, DEPP1, PECAM, ALDH1L2, PTGS2, KDM7A, PAPPA2* [Fig. 5.7. D].

Gene ontology analysis identified two genes induced in response to IR belong to the DNA protection category, *CBS* (Cystathionine beta-synthase) and an endonuclease *SLX1A*. Studies using tumour samples reported the upregulation

of CBS contributes to drug resistance and promotes carcinogenesis (Bhattacharyya et al., 2013; Phillips et al., 2017; Szczesny et al., 2016; Vanzin et al., 2014). We lack any knowledge of a role for *SLX1A* in DNA repair, but it's sustained up-regulation up to 24 hr post-IR suggests it may have a role in cell survival post-irradiation.

After 3-hr and 6-hr post irradiation, *ID3* (Inhibitors of DNA binding and cell differentiation) genes were upregulated and this family of Helix-loop-Helix (H-L-H) transcription factors are often linked to cancer invasion, tumour growth and drug resistance (Roschger and Cabrele, 2017). ID proteins are mostly involved in cellular pathways regulating proliferation and differentiation. Dysregulation of cell proliferation often leads to oncogenic transformation and therefore it is not surprising to identify Id proteins in the HT1080 fibrosarcoma cell line. However, these proteins may also regulate DNA repair or promote IR-induced differentiation. A recent study reported the phosphorylation of ID3 by ATM is required to recruit MDC1 to γ-H2AX to facilitate DNA repair (Lee et al., 2017).

Gene Set Enrichment Analysis (GSEA) revealed a set of genes differentially upregulated in HT1080 cells post-IR [Fig. 5.8]. The top highly upregulated GSEA category includes up-regulation of DNA protective mechanisms or DNA repair along with an up-regulation of genes involved in the negative regulation of apoptosis (*GDF5, IFIT2, MMP9*, and *TNFRSF6B*), modulation of hypoxia response (*ARNT2, EPAS1*) and generation of reactive oxygen species. In response to IR, HT1080 cells upregulate genes involved in the negative regulation of apoptosis-like *GDF15, IFIT2,* and *TNFRSF6B (DcR3). TNFRSF6B,* also known as *Decoy Receptor 3 (DcR3)* belong to the Tumour Necrosis Factor (TNF) superfamily that act as an immunomodulator in tumour growth and a regulator of EMT in cancer (Hsieh and Lin, 2017; Liu et al., 2016). The role of *TNFRSF6B* is to inhibit apoptosis thereby provide radiation resistance in lung cancer (Pitti et al., 1998; Sung et al., 2010). Conversely, upregulation of a pro-apoptotic *IFIT2* (Interferon induced protein 2) gene in HT1080 cells suggest a regulatory interplay exists between anti and pro-apoptotic gene to promote survival of HT1080 cells post IR.

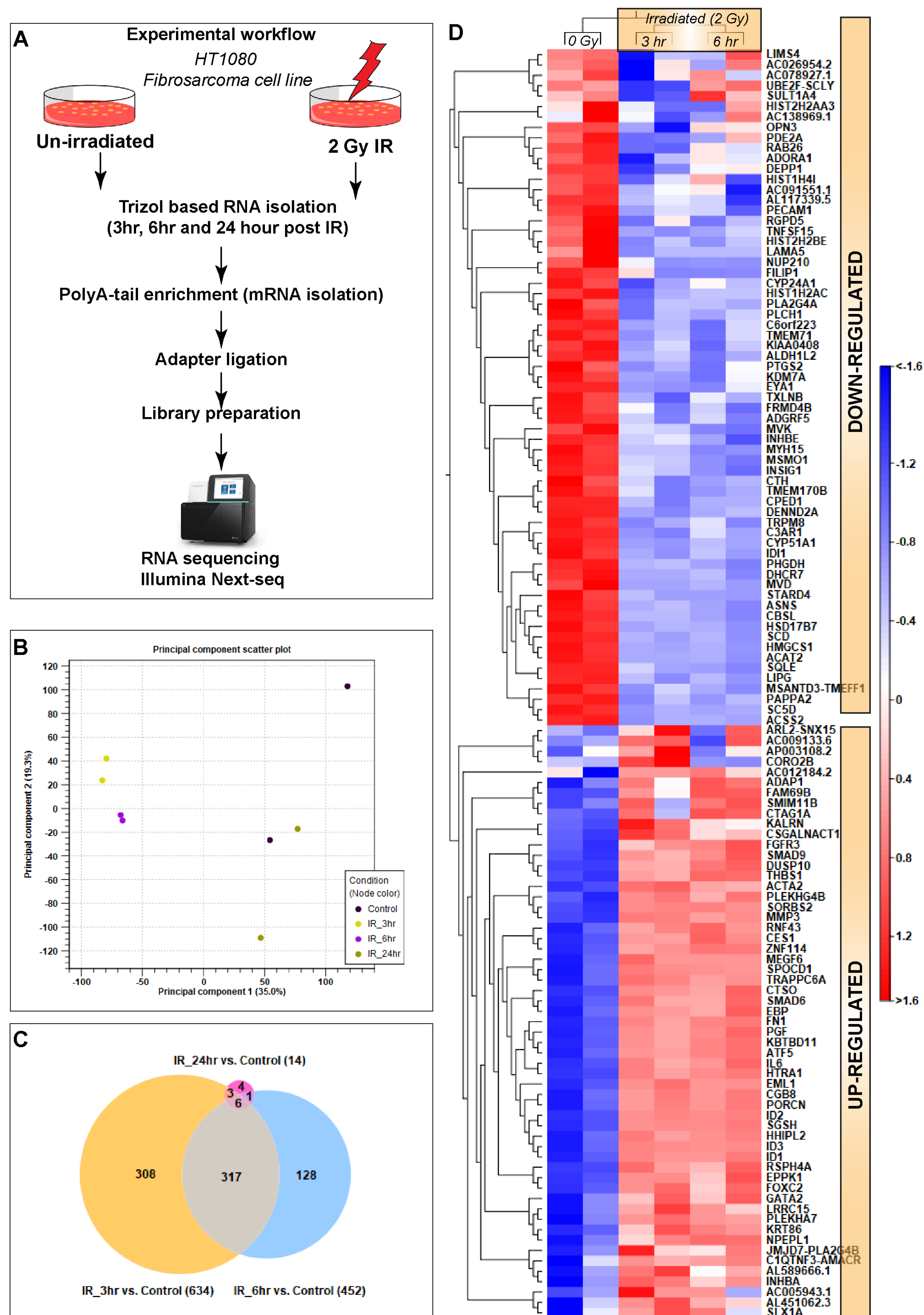

Figure. 5.7. Transcriptional response of HT1080 fibrosarcoma cells in response to gamma irradiation. (A) Experimental schematic showing confluent HT1080 cells were exposed to 2 Gy of γ-irradiation and RNA was isolated after 3-hour, 6 hour and 24-hours post-IR in duplicates. **(B)** The PCA plot showing the clustering of the different replicates of the RNA-seq. libraries. **(C)** Venn diagram showing the number of genes in common to 3hr, 6hr and 24 hr dataset compared to unirradiated controls. **(D)** Hierarchical clustering of the differentially expressed genes that were upregulated/downregulated in HT1080 cell line after 3 hour and 6-hours post-irradiation compared to unirradiated (0 Gy) controls.

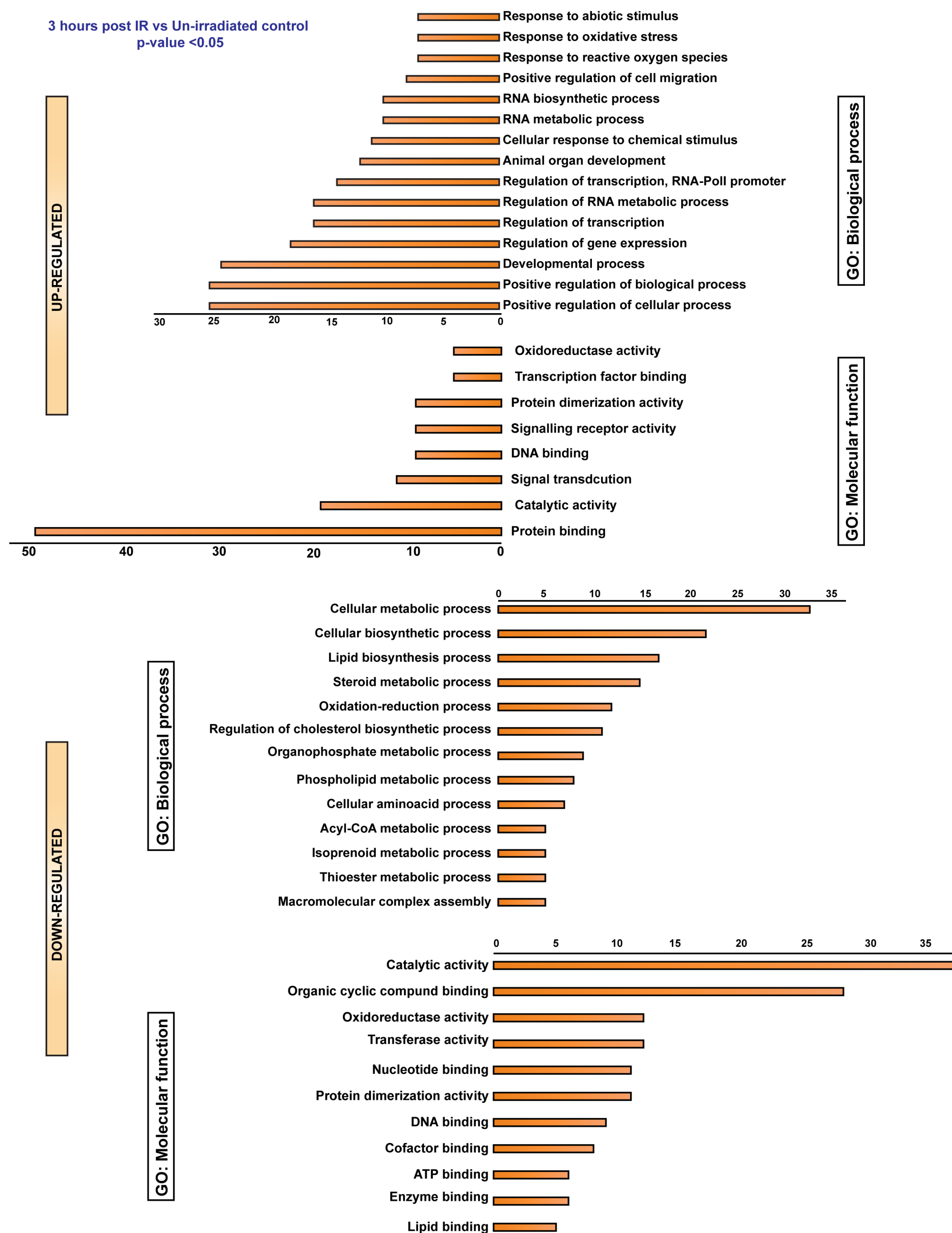

Figure. 5.8. Gene ontology (GO) analysis of differentially expressed genes in HT1080 fibrosarcoma cell line after exposure to 2 Gy of γ-irradiation. The X-Axis represents the number of genes in the subset that are differentially expressed (p-value<0.05)

5.3.3.3. Evolutionarily conserved responses between planarian stem cell and HT1080 fibrosarcoma cell line.

We have identified 767 DEGs at 3-hour, 6 hour and 24-hours post-IR and these were compared with the radiation transcriptome of planarian stem cells. Comparative analysis between the two RNA-seq. datasets identified 139 radiation responsive genes, of which 77 genes had similar expression profiles in response to radiation. Some of these genes that are common to both the datasets like *Four and a half LIM homeobox (FHL), Protein tyrosine phosphatase receptor (PTPR*) *Wnt 5, Annexin* have well-characterized roles in radiation response (Omerovic et al., 2010; Xu et al., 2017b; Zhao et al., 2018). We looked into genes with functional orthologs that were not studied previously in the context of radiation or DNA damage response. For example, *MEGF6* (Multiple EGF-like domain 6) is upregulated post IR in planarian stem cells and HT1080 cells has been recently identified to induce EMT in colorectal cancer (Hu et al., 2018).

Like MEGF6, several of these common genes are direct targets of TGFβ/SMAD signalling and include genes like *LTBP* (*latent TGFβ binding protein*), tumour suppressor gene - *Tropomyosin1* (*TPM1*) which has been previously linked to cancer progression and metastasis (Hu et al., 2018; Massagué, 2008; Zhu et al., 2007). Another common upregulated gene is Ras-oncogene family protein *RAB27B,* a regulator of vesicle exocytosis and a marker for breast cancer is reported to correlate with tumour invasion and metastasis (Hendrix et al., 2010a, 2010b). Forkhead box transcription factor (FOXO4) involved in cell cycle arrest was a conserved response to irradiation between planarian stem cells and HT1080 (Huang and Tindall, 2007; Lüpertz et al., 2008; Zhang et al., 2012). Additionally, the cytoskeletal protein *PDLIM7* (PDZ and LIM domain-containing protein 7), a positive regulator of *Mdm2* is reported to promote cell survival and chemo-resistance in cancer cell line by inhibiting p53-mediated apoptosis (Jung et al., 2010; Klein et al., 2018).

5.4. Conclusion

It is evident that there exists a robust transcriptional response to irradiation that regulates a diverse range of biological processes. Many of these processes involve regulation of apoptosis, cell metabolism, migration and DNA repair. The comparative study between an invertebrate radioresistant model planarian and a human cancer cell line (HT1080) prove to be informative to the development of targeted approaches to overcome radiation resistance in cancer cells. In this study we have put together a dataset of evolutionary conserved radiation responsive genes that can be functionally analysed in the future to predict potential biomarkers of radio-resistance and identify novel factors responsible for cell survival/DNA repair post-IR. Future functional studies are required to understand the mechanistic role of these genes in radiation sensitivity/tolerance. Although the majority of the genes still remain functionally unexplored, this work involving global gene-expression profiling holds great promise for unravelling the mechanisms that control DNA repair and cell survival.

Table.5.1. Mapping statistics of RNA-sequencing data used in this study

5Gy IR transcriptome (sorted planarian cells)

[X1 represents FACS sorted planarian neoblast at S/G2/M phase of cell cycle, X2 represents FACS sorted stem cells at G1 phase and post mitotic progeny]

X1 FACS sorted cells	Replicate	Number of reads (Paired)	Percentage of reads mapped	Mapped in pairs	Percentage
0Gy_X1	1	137494710	95.74	96783952	70.39
	2	62278820	98.19	46785248	75.12
5Gy_24hr_X1	1	148028772	97.13	92801022	62.59
	2	152705236	96.5	982599356	64.35
5Gy_3hr_X1	1	185771234	96.81	127797680	68.79
	2	152082588	96.62	108835948	71.56
X2 FACS sorted cells					
0Gy_X2	1	67,856,194	94.53	47357504	69.79
	2	172,352,496	97.97	124101958	72
5Gy_24hr_X2	1	66,601,850	97.4	42,782,604	64.24
	2	69,148,278	94.62	48,213,896	69.73
5Gy_3hr_X2	1	75,534,084	97.25	54,448,212	72.08
	2	66,676,784	96.45	45,939,766	68.9

Chapter 6

Discussion and future directions

6.1. Discussion

Cells are under constant assault from a multitude of genotoxic stresses leading to disruption of the stability of the genome. The preservation of the genome is therefore crucial for the survival and well-being of all organisms. Erroneous repair of DNA lesions often leads to chromosomal re-arrangements and loss of heterozygosity, which potentiates the development of various diseases such as cancer. Organisms have evolved with different repair strategies to preserve genome stability and cellular fitness for successive generations. The process needs to be well regulated and monitored, thus understanding the evolution of DNA repair machinery for cell survival is critical to elucidate novel mechanistic insights into genome-maintenance. DNA damage signalling is considered to be an intricate network of responses involving DNA repair, apoptosis, chromatin remodelling, transcriptional regulation, cell cycle progression, and metabolic control. A significant amount of research using yeast, *Drosophila*, *C. elegans* and mammalian species (along with immortalized cell lines) has contributed to our understanding of DNA damage response and how genome-instability can lead to oncogenic transformation. Here, we have begun to develop planarians as a model system for these studies.

Chapter 1 provided an overview of recent advancements in our knowledge of planarian stem cell biology and how genome integrity is maintained in response to DNA damage by different stem cells throughout metazoans. Planarians are an amazing model showing negligible signs of ageing or natural cancers (Sahu et al., 2017). This inherent longevity suggests the existence of a robust genome-maintenance mechanism. A fine balance must exist to monitor stem cell proliferation and differentiation and also protect from genotoxic stress to inhibit oncogenic transformation. Cancer occurrence is pervasive in metazoans and may be unavoidable in animals with highly dividing cells. This predicts animals with larger body-mass imposes an increased risk of developing cancer than small-bodied organism. However, the incidence of cancer does not correlate with the number of cells (Peto’s paradox) (Peto et al., 1975). In fact, recent evidence suggests larger and long-lived animals have a lower-than-expected chance of

getting cancer. For example, cancer resistance in elephants is linked to copy number expansion of tumour suppressor p53 (twenty copies in elephants compared to one in humans/other mammals) (Abegglen et al., 2015; Sulak et al., 2016) or duplication of the pro-apoptotic gene, LIF (Vazquez et al., 2018). On the other hand, there is no evidence that long-lived gigantic bowhead whales evolved extra copies of any tumour suppressor genes (Keane et al., 2015). Every organism in the animal kingdom has evolved with their own secrets to supress oncogenic transformation and induce cellular longevity. For example, hyaluronic acid and CDKN2A tumour suppressive gene that limit over-proliferation of naked-mole rat cells. If cancer suppression has repeatedly evolved as a trait, then basic research into the life history and cell biology of animals will provide better therapeutic approaches to treat human cancers. We believe regenerative animals have an extra advantage when it comes to combatting cancer, as they are able to induce a regenerative outcome if a single cell becomes transformed. The damage caused by a transformed cell cycling inappropriately can be repaired by other highly proliferative but healthy stem cells, thereby protecting them from naturally occurring cancer.

The primary goal of this research is to understand the genome maintenance mechanisms and DNA repair strategies in adult stem cells. This brings a regenerative flatworm with well-developed molecular biology tools and techniques (described in **chapter 2**) along with an array of Next- generation sequencing methods to study DNA repair and cell survival after IR exposure.

In **Chapter 3,** we have identified the different DNA repair pathways and their role in the survival of stem cell survival post-irradiation, first of its kind in the planarian literature. The recent genome sequencing identified the loss of several important regulators of DDR signalling by sequence analysis (for example BRCA1-BARD1-PALB2 complex, some regulators of NHEJ and the core Fanconi anaemia pathway genes). Several vertebrate-specific protein complexes have been identified to regulate DNA repair machinery. The most recent example includes the discovery of the “shieldin” complex comprising of REV7 and three previously uncharacterized proteins RINN1, RINN2 (FAM35A), RINN3 (c20orf96). Shieldin

is recruited via ATM-53BP1-RIF1 complex to promote NHEJ-dependent-DSB repair and sensitises BRCA1 mutant cells to PARP inhibitors (Dev et al., 2018; Gupta et al., 2018; Noordermeer et al., 2018). The reduced complexity of DDR proteins in invertebrates particularly in worms, flies or flatworms is an advantage to understand the underlying fundamental mechanism of DNA repair.

Over the last few decades, studies shed light on various endogenous sources of mutation that promote genome instability, the recent being the cellular microenvironment. Most somatic and adult stem cells in the human body do not exist in isolation but in the presence of spatial-mechanical constraints that often deform the cells and change their shape/size. Therefore, the underlying extra-cellular matrix (ECM) and the associated cellular-cytoskeleton regulates the nuclear morphology. Abnormalities in the nuclear-organization or alterations in nuclear-mechanotransduction are hallmarks of many diseases including cancer (Tubbs and Nussenzweig, 2017; Uhler and Shivashankar, 2018). ECM plays a major role in cell-migration through interstitial tissues and the impact of mechanical stress during migration may be a previously unappreciated source of genome instability (Denais et al., 2016; Irianto et al., 2017a; Raab et al., 2016). **Chapter 4** revealed the importance of DDR signalling and the role of DNA repair factors during stem cell migration. Using an *in-vivo* assay where the stem cells are required to migrate over long distances to a distal wound site (Abnave et al., 2017) we looked into the relationship between cell migration and DNA damage after wounding. Recent *in vitro* studies using cancer cell lines and dendritic cells have shown that mechanical stress on nuclei during migration through microcapillaries is a source of genome instability (Denais et al., 2016; Irianto et al., 2017a; Raab et al., 2016). The nucleus being the largest and stiffest cellular organelle act as a mechanosensor for cell-cycle progression and cell fate choices. The size and mechanical properties of the nucleus thus play a significant role in the behaviour of motile cells. Interestingly, planarian stem cells characterised by a higher nucleus to cytoplasmic ratio are migratory (in response to wound-stimulus) and therefore prone to mechanical damage from the underlying ECM and the associated cytoskeleton. We observed a significant nuclear deformity during migration. The extended actin-rich cytoplasmic

protrusion exerts mechanical stress to deform the nucleus, and this could be a major source of DNA damage during migration. Nuclear deformation leads to changes in gene expression and can induce differentiation (Connelly et al., 2010; Jain et al., 2013; Roy et al., 2018; Trappmann et al., 2012). With the discovery of a DNA repair protein ATR to translocate to the nuclear membrane in response to mechanical stress (Kumar et al., 2014), it is plausible to hypothesize that stem cells may undergo differentiation in response to mechanical damage to limit genome instability. Future experiments should aim to understand if a planarian stem cells are forced to differentiate due to mechanical stress during migration to reduce genome instability. We observed migratory stem cells have increased sensitivity to IR indicative of accumulating DNA damage during migration and therefore require active DNA repair machinery to migrate. These experiments also reveal that pre-loading stem cells with DNA damage delays migration until the damage is repaired suggesting a potential co-regulatory link between cell migration and DNA repair. Our observation is strengthened by some recent studies that potentially links the role of DNA repair genes with Epithelial-mesenchymal Transition (EMT) (Lee et al., 2016; Weyemi et al., 2016; Zhang et al., 2014). Using a combination of epigenomics and transcriptomics, we can now look into the regulatory changes in stem cells during migration and identify novel molecules that maintain genomic integrity during cell migration. It will also help us to understand how adult stem cells perceive spatial and mechanical cues from their immediate environment and translates into cell fate decisions, including DNA repair mechanism during migration. Unravelling these basic principles could provide new protein targets to modulate stem cell behaviours for the development of regenerative medicine and also effectively target migratory cancer cells undergoing metastasis.

Whole-body exposure to 10 Gy of IR is lethal to most vertebrates including humans, but surprisingly some species including bacteria, archaea and bdelloid rotifers are known to show exceptional resistance to ionising radiation (Gladyshev and Meselson, 2008; Harris et al., 2009; Krisko and Radman, 2013). Numerous studies over the years conducted by environmental radiation biologists have determined that invertebrates are capable of tolerating acute doses of IR, several

folds greater than maximum tolerable doses for humans and can maintain genomic and reproductive integrity. For example, Tardigrades can resist a high dose up to 5000 Gy, and a recent study identified a tardigrade specific protein named Dsup (Damage suppressor) that act as a shield to resist a high dose of IR. Furthermore, this study demonstrated this histone-binding protein Dsup rapidly localises to the nucleus in response to IR. Overexpression of tardigrade specific *Dsup* in human cells leads to increased survival and significantly reduced DNA damage post-IR.

Despite the loss of several DDR genes, the reduced complexity of gene structure/function makes invertebrates a unique model organism to study basic mechanisms of radiation resistance. For example, understanding the molecular mechanisms that allows planarian stem cells to tolerate such a high dose will allow to draw parallels with radiation response in mammals. With this idea, we focussed **chapter 5** on understanding the transcriptional response to IR in planarians, and how this response is conserved in a human cancer cell model. The overarching aim was to identify novel factors that are important for stem cell survival post IR in planarians.

Improvements in sequencing technology have benefited planarian research in the last few years. With an aim to understand the transcriptional response to IR, we used RNA sequencing on planarian stem cells after irradiation. We have identified some novel genes encoding proteins with domain of unknown function (DUF) along with lots of flatworm/planarian specific genes that were upregulated in response to IR. Using an RNAi-based screening we have identified *tetraspanin* family of genes responsible for stem cell repopulation post IR. Whether these proteins function in regulating DNA damage signalling or act as a transducer to initiate DNA repair will require further investigation. Our study gives an overview of the potential of a flatworm model to study the radiation response to stem cells and perform high-throughput robust screening on adult stem cells to identify biomarkers for radiation resistance. The prediction of radiation response is a critical step in cancer therapy and any knowledge regarding the role of these radiation-responsive genes could be verified using a mammalian model. We also

extended our investigation by performing a comparative analysis of the transcriptional response to IR in a radiation tolerant planarian and a human cancer cell line model of fibrosarcoma. We have identified evolutionarily conserved responses which might contribute to the survival of stem cells after IR and high radiation resistance in human cancers. For example, our data revealed that LIM homeobox domain containing gene, *FHL1* was upregulated in planarians and in HT1080 cancer cell line in response to IR. IR-inducible LIM proteins regulate G2/M checkpoint via CDC25 regulation. Cell cycle checkpoint proteins are well known regulators that are responsible for increased radiation tolerance in cancer cells (Ding et al., 2009; Xu et al., 2017b). *FHL2* has also been shown to regulate radio-resistance in pancreatic cells (Zienert et al., 2015) via regulating cyclin B.

Apart from damaging the chromatin, IR also leads to tissue damage (Kim et al., 2014b; Vorotnikova et al., 2010; Zhao et al., 2014). In response to IR-induced injury, stem cells and adjacent other cell types could activate a wound-like response to elicit proper healing. Multiple studies have been done to understand the gene activation program and we now have a firm understanding on the different wound-induced transcripts that coordinate regeneration in planarians (Wenemoser et al., 2012; Wurtzel et al., 2015). In future, we can look if the wound response transcripts overlap with our irradiation transcriptome dataset. As upregulation of these transcripts may contribute to the mechanisms that lead to increased SC survival post IR, we can investigate whether amputation to activate wound response could enhance SC survival post IR. An understanding of this phenomenon will help us to draw parallels between the IR-responsive genes that might have common effectors with generic stress and wound-responsive genes for SC survival.

6.2. Future directions

Although regenerating new body parts is not necessary for humans but daily wear and tear demands constant replenishment of lost cells. This is mainly regulated and replenished by the stem cells. Planarian stem cells have conserved genetic and epigenetic regulation of stem cell maintenance with humans (Dattani et al., 2018a, 2018b; Önal et al., 2012). Knowledge of their basic biological properties including DDR mechanism and radiation tolerance will provide mechanistic insights into how stem cells may be used for regenerative medicine and to develop effective therapeutic strategies to treat cancer and other age-related diseases. With the discovery of a heterogeneous stem cell population with a small proportion being pluripotent (Wagner et al., 2011; Zeng et al., 2018), future progress will require investigation to understand the DNA repair mechanisms in the different subclasses of stem cells.

An essential aspect of DDR signalling is the modulation of chromatin to provide access to the DNA repair machinery. How chromatin modulation occurs during DDR signalling is an outstanding question. The development of robust ChIP-sequencing methodologies on different histone marks to study the epigenetic regulation in adult stem cells in *Schmidtea* (Dattani et al., 2018a; Mihaylova et al., 2018), now gives us a better platform to answer some of these fundamental questions in flatworms. It will be particularly interesting to understand histone modifications during DNA damage signalling and how it changes with loss of DDR factors in stem cells. Future work should also aim to develop antibodies that can detect DNA damage *in vivo* in stem cells. Although *Schmidtea* specific H2Ax (developed by proteintech, described in chapter-3) failed to give any specific signal, future work should focus on developing other DDR sensors like RPA, 53BP1 or MDC1 that are known to form DNA damage foci in response to DNA breaks in mammalian cells. Using these DNA damage antibodies and performing a ChIP-sequencing will provide a comprehensive mapping of histone modifications at DNA double stranded breaks. Although, ionizing radiation lead to non-clustered breaks in the genome and in a very randomised fashion (compared to locus-specific restriction-enzyme based DSB generation in mammalian cells), it can be challenging to interpret the DSB break site. The

histone modifications at DSB sites will reveal the existence of any hotspots in the planarian genome that are more prone to DNA breaks. Active genes are considered to be fragile loci and frequently experience DSBs (Marnef et al., 2017) therefore performing ATAC-seq. after irradiation (to detect chromatin accessibility at open/closed chromatin) coupled with H3K27me3 (at active promoter) could be an alternative to identify DSB /translocation hotspots in the planarian genome. Another approach that can be employed to understand changes in genomic landscape in response to replication stress/other DNA damaging agents is to label the DNA breaks followed by sequencing (direct *in situ* breaks labelling, enrichment on streptavidin and next-generation sequencing, also known as BLESS) (Crosetto et al., 2013). BLESS is a powerful technology to detect specifically DSBs and prevents labelling of artificially formed DSBs during genomic DNA extraction. This technique has been successfully employed to identify hotspots in the HeLa genome, human and mouse cells and can be used for planarian stem cells. Future work with the development of genome editing strategies in planarian stem cells, we can also try to map DSB site at any particular locus [For review on Breaks Labelling *In Situ* and Sequencing (BLISS) read (Iannelli et al., 2017 and Yan et al., 2017)].

Recent advances using Next-generation sequencing have developed novel methods to detect DSBs and understand genome-wide changes at DNA breaks. The frequency of DSBs is generally higher in nucleosome-depleted regions at transcriptional start sites (TSS) of active genes and mostly in actively transcribed genes (Schwer et al., 2016). Despite such improvements in our knowledge of DDR signaling, a highly debated concept in the field is the coexistence of transcription and DNA repair. What is the fate of elongating RNA-polymerase II (RNAPII) after encountering a double-stranded break? How do chromatin modulation, transcription and RNA processing are regulated on the same stretch of damaged chromatin? Multiple studies looked into the concept of global transcription shutdown even in gene loci that are not damaged, but the exact mechanism is still not very well understood. These are some fundamental questions that need to be addressed to understand this transcription dilemma of the damaged chromatin. It has been hypothesised that DSBs result in the

localised shutdown of transcription around the damage site (Shanbhag et al., 2010) while base damage results in temporary pausing of elongating RNA polymerase (RNA Pol) II (Charlet-Berguerand et al., 2006). We are able to distinguish between paused and elongating RNA Pol II, owing to differences in serine phosphorylation in the deeply conserved heptad YSPTSPS repeat of the C-terminal domain of the largest subunit of RNA Pol II. With the conservation of RNA-Pol II in planarians (Dattani et al., 2018a) we can now perform ChIP-seq on both the paused (Ser5P) and elongating (Ser2P) form of RNA Pol II to understand the genome-wide dynamics of RNA transcription following irradiation in planarian stem cells.

The intricate network of DDR signalling is tightly regulated in a spatio-temporal manner mediated by numerous reversible post-translational modifications (PTMs) like phosphorylation, ubiquitination, SUMOylation, acetylation, ADP-ribosylation and NEDDylation that regulates DDR signalling at DNA breaks. It will be of great interest to perform phospho-proteomics in irradiated cells to understand the post-translational modifications of DNA repair proteins after irradiation. Stable Isotope Labelling by Amino acids in Cell culture (SILAC) proteomics have been employed in planarians to understand the proteome of the stem cell component (Böser et al., 2013). The identification/quantification of phosphorylation sites in the differentially regulated proteins post IR will provide novel targets for radiotherapy. The comprehensive insight into the radiation-induced phospho-proteome landscape of stem cells will broaden our understanding of the intricate signalling network of DDR factors and will improve better therapeutic interventions in cancer patients. These finding will provide insights into how PTMs regulate DDR factors, which otherwise trigger genomic instability, a hallmark of cancer progression.

In summary, we explored the potential of a freshwater planarian *Schmidtea mediterranea* as an experimentally accessible organism to study DNA repair. The extraordinary capacity to resist a high dose of irradiation and the accessibility to its pluripotent adult stem cell system provides an opportunity to study DDR in the context of stem cell regulation. While the present study

catalogued the role of different DNA repair genes in planarian stem cells and understanding the transcriptomic changes to IR in stem cells, future work should look into the mechanistic insights of radiation resistance and understand the post-translational modifications after IR. Planarian research over the last few years has seen extraordinary technical advancement in the field of stem cell and regenerative biology. The remaining mysteries to understand how these flatworms might accomplish their astounding regenerative feat and resist high dose of irradiation make this an exciting era for research in radiation biology. An exciting opportunity for the future would be to identify and answer fundamental questions related to *in-vivo* regulation of pluripotency, DNA repair and genome maintenance using the regenerative flatworm as a model.

Chapter 7

Appendix

7.1. Appendix A: Details of the reagents used in this study

7.1.1. Molecular biology techniques (PCR, cloning, *in-vitro* transcription)

Components	Company	Catalogue Number
rNTPs- UTP, ATP, GTP, CTP	Roche	11140949001, 11140965001, 11140957001, 11140922001,
dNTPs- dATP, dTTP, dCTP, dGTP	Roche	11934511001, 11934546001, 11934520001, 11051466001
Digoxigenin-11-UTP	Roche	11209256910
Fluorescein RNA labelling mix	Roche	11685619910
Hyclone Water	GE	SH30538.01
Phusion Hi-Fidelity DNA polymerase	NEB	M0530S
Red-Taq ready mix	Sigma	R2523-20RXN
Superscript IV reverse transcriptase	Invitrogen	Trial kit
TURBO DNAse	Thermo fisher	
RNAseOUT Ribonuclease inhibitor	Invitrogen	10777-019
pPR244 cloning vector	Jochen Rink lab	
DH5alpha competent cells (Bronze efficiency)	Bioline	BIO-85025
Wizard SV plus gel extraction kit	Promega	A9282
Wizard SV plus miniprep plasmid isolation kit	Promega	A1460
SP6 RNA polymerase	NEB	M0207S
T7 RNA polymerase	Roche	10881767001
T4 DNA polymerase	NEB	M0203S
TRIZOL	Invitrogen	15596-026
Chloroform	Fluka Analytical	25669-2.5L
Isopropanol	Sigma	I9516-500ml
Sodium Acetate	Applichem	A3947,0100
Glycogen		
Lithium chloride	Ambion	AM9480
Ultrapure water	Ambion	AM9937
Kanamycin sulfate	Fisher scientific	BP906-5

7.1.2. Fluorescence In-situ Hybridization (FISH) & Immunohistochemistry (IHC)

Components	Company	Catalogue Number
N-acetyl-L cysteine (NAC)	Sigma	A7250
Formaldehyade	Sigma	252549-1L
Phosphate Buffered Saline (PBS)	Sigma	P4417
Hydrogen Peroxide	Sigma	H1009
Formamide	Sigma	F7503-2.5L
20X SSC	Calbiochem	8310

Yeast RNA (10mg/ml)	Ambion	AM7118
Dextran sulfate	Sigma	D8906
Proteinase-K	Sigma	P4850-5ML
Ultrapure 10% SDS	Invitrogen	15553-035
Hoechst 33342 (for Insitu and Immunostaining)	Sigma	B2261-25MG
Pasteur pipettes	Appleton	KS230
Ethanol	Sigma	32221-2.5L-M
Methanol	Sigma	322213-2.5L-M
Hydrogen chloride	Sigma	H1758-500ML
Sodium hydroxide (NaOH) pellets	Sigma	71690-500G
Tween20	Sigma	P9416-100ML
TritonX-100	Sigma	T8787-250ML

7.1.3. Antibodies used in Immunohistochemistry (IHC) and Western blot (WB)

Primary Antibody	Company	Catalogue number	Dilution
Anti-H3-phosphorylated ser10, Rabbit polyclonal	Millipore	09-797	1:1000 (IHC) 1:2000 (WB)
Anti-RAD-51; Guineapig Polyclonal	Scott Hawley Lab	-	1:500 (IHC) 1:1000 (WB)
Anti-PAR, Rabbit Polyclonal	Trevigen	4336-BPC-100	1:250 (IHC)
Anti-Tubulin, Mouse monoclonal (E7)	DSHB	E7 (AB 2315513)	1:2000 (IHC) 1:2000(WB)
Anti-mouse IgG HRP linked antibody	Cell signalling	7076P2	1:2000 (IHC) 1:4000 (WB)
Anti-rabbit IgG HRP linked antibody	Cell signalling	7074P2	1:2000 (IHC) 1:4000 (WB)
Anti-PAR (Clone 10 H), Mouse Monoclonal	Santacruz	SC-56198	1:500 (IHC)
Anti-GammaH2AX, Rabbit Polyclonal	Thermo fisher	LF-PA0025	1:500 (IHC) 1:1000 (WB)
Anti- Drosophila H2Av, Mouse monoclonal	DSHB	UNC93-5.2.1	1:500 (IHC) 1:1000 (WB)

7.1.4. Western Blot

Components	Company	Catalogue Number
cOmplete Protease inhibitor	Roche, Sigma	11697498001
NuPAGE Novex 4-12% Bis-Tris protein gels	Thermo Fisher scientific (Invitrogen)	NP0327
NuPAGE MES SDS Running buffer (20X)	Thermo Fisher scientific (Invitrogen)	NP0002-02
Ponceau S solution	Sigma	P7170-1L
Qubit protein assay kit	Thermo Fisher	Q33211

Laemmli buffer 2X	Sigma	S3401-10VL
SeeBlue Pre stained protein standard	Thermo Fisher	LC5625
SuperSignal West Pico	Thermo Fisher	34079
Dried Skimmed milk	TESCO	N/A
Western blocking reagent	Roche	11921673001
Bovine serum albumin (BSA) fraction V	Roche	10735078001

7.1.5. Planarian cell dissociation protocol

Components	Company	Catalogue Number
Papain	Sigma	P4762-100MG
Hoechst 34580	Sigma	63493-5MG
Trypsin Inhibitor from chicken egg white	Sigma	T9253
Calcein (in DMSO)	Sigma	C1359
Propidium iodide (PI)	Sigma	P4864-10ML
NaH2PO4	VWR International	102454R
KCl	VWR	101985M
NaHCO3	VWR	102475W
NaOH Pellets	Fisher chemical	S/4880/53
Glucose	Fisher chemical	G/0500/53
L-cysteine hydrochloride	Merck	K47440335606
HEPES	Sigma	H3375-100G
BSA Fraction V	Roche	10735078001
0.5M EDTA	Promega	V4231
Eppendorf safe lock DNA lo bind tubes	Eppendorf (Fisher)	0030108051
Eppendorf DNA lo-bind tbes (0.5ml) for storage of libraries	Sigma	Z666521-250EA
Molecular grade nuclease free water	Thermo	SH30538.03
Filter tips	Starlab	S1121-3810

7.1.6. RNA-sequencing reagents

Components	Company	Catalogue Number
RNA later (100ml)	Thermo fisher	AM7020
Trizol	Ambion Invitrogen	15596026
RNA clean and concentrator-5 with DNAseI	Zymo	R1013
RNAsin RNAse inhibitor	Promega	N2111
Superscript-II reverse transcriptase(2000U)	Life technologies	
Agencourt AMPure XP 5ml	Beckman coulter	A63880
Ethanol 200 proof (Absolute)	Sigma Fisher Scientific	E7023 10644795
KAPA library quantification kit (KK4835)	Roche	07960204001
Truseq stranded mRNA LT set A	RS-122-2101	Illumina
NextSeq v2. Flow cell (75 cycles)	FC-404-2005	Illumina

7.1.7. Planarian maintenance

Components	Company	Catalogue Number
Instant Ocean (Planarian culture)	Aquatic biosystem	N/A
Chloretone (worm immobilization) [$C_4H_7Cl_3O.5H_2O$]	Sigma	112054-250G
Mineral oil	Fisher scientific	BP2629-1

7.1.8. Paraffin sectioning

Components	Company	Catalogue Number
Paraffin	Sigma	76244
Xylene Substitute	Sigma	A5597
Paraffin moulds		
Microtome blades	AccuEdge	4689
Poly-lysine coated slides	Sigma	P0425-72EA

7.1.9. COMET Assay

Components	Company	Catalogue Number
Superfrost slides	Thermo Scientific	
Coverslip	Thermo scientific	
Normal melting Agarose		
Low melting Agarose	Sigma	A2576-5G
SYBR Green	Molecular probes	4689

7.1.10. Software

Details	URL link
Fiji	https://fiji.sc/
Graphpad-Prism	https://www.graphpad.com/scientific-software/prism/
Adobe Illustrator	https://www.adobe.com/uk/illustrator
Adobe Photoshop	https://www.adobe.com/uk/photoshop
Primer3Plus	http://www.bioinformatics.nl/cgi-bin/primer3plus/primer3plus.cgi
Microsoft office	https://www.office.com/
Olympus FV1000	https://www.olympus-lifescience.com/en/support/downloads/
ZEN imaging (Airyscan)	https://www.zeiss.com/microscopy/int/confocal.html
Nikon NIS element	https://www.nikoninstruments.com/Products/Software
Andor KOMET	https://andor.oxinst.com/products/komet-software/komet-7
CLC genomics	https://www.qiagenbioinformatics.com/products/clc-genomics-workbench/

7.2. Appendix B: Details of primer sequences

ADAPTER SEQUENCES	**Forward**	**CATTACCATCCCG**
	Reverse	**CCAATTCTACCCG**
ATR	ATR_F	GCGCAGGAATTCAGAAACTC
	ATR_R	GACGGTCACCGAGACCTAAA
ATM	ATM_Fw_1	ATTCACTGGGCCAACGTTGA
	ATM_Re_1	TCTTCCCTCGACACCAAACG
BRCA2	BRCA2_Fw_1	ATGGACGGGATGTGATGAGC
	BRCA2_Re_1	ATGCACCTTCCACGAGCAAT
PARP1	PARP1_Fw_2	AACGTGCAATGCTGGAGTTT
	PARP1_Re_2	TCCTACCCCTTTGCAACTGT
PARP2	PARP2_Fw_2	TGACTGGCAAGATCGTCAGA
	PARP2_Re_2	AGTTGTTCTTGAACCGTGCC
PARP3	PARP3_F1	AACTCTTGTGGCATGGAACC
	PARP3_R1	CGCAGAGTTCGTGAAATGAA
PARG	PARG_F	GACAAAACCAATTCCGCTGT
	PARG_R	CAGCGAATTGCTGACTACCA
XRCC1	XRCC1_F	CCTGAAATTAATCCTGCCAAA
	XRCC1_R	TTCATCATTGCGGCTATTCA
FANCD2	Smed_FANCD2_F	GAGGTTTCGATTCCGTTGAA
	Smed_FANCD2_R	TGGCATTTGGTGGGTTAAAT
FANCM	Smed_FANCM_F	AGCATTACAACACGGCCTTC
	Smed_FANCM_R	GTGCCTTTGGGTTCTGATGT
FANCI	Smed_FANCI_F	CAAGCTGGGATTCAGATGGT
	Smed_FANC_R	CAAAAGTGGGAGGTTTTCCA
MRE11	Smed_Mre11_F	GCATGCAGCGAAGAATTACA
	Smed_Mre11_R	TTGTCGATTGACAGCCTCAG
FANCJ_1	Smed_FANCJ_1_F	TCGTGCCTAATGGAATATTGA
	Smed_FANCJ_1_R	TGTTGCCTTTTTGGAATAGGA
PNK	Smed_PNK_F	CGTGCGATTTCACTGTGAGT
	Smed_PNK_R	TTGTAGCAACGGCATACTCG
MSH6	Smed_msh6_F	CGGATCATCCAGATTCTCGT
	Smed_msh6_R	CCCCGTCTAAACCACGACTA
MSH2	Smed_msh2_F	TCGGTTCATTGCACCAGTTA
	Smed_msh2_R	TGCCTTGGCTACCTCGATAC
p53BP1	Smed_p53BP1_F	CCGCTCGGTGTAACCATTAT
	Smed_p53BP1_R	TCAATAACGCACCCATTGTG
FANCJ (BRIP)	Smed_FANCJ_1_F	AGCGGAAAGGAAGACTGTCA
	Smed_FANCJ_1_R	TAGGCACGACTTCACTGCAC

7.3. Appendix C: Amino-acid sequences of DNA repair genes used in this study

Smed-ATR
>dd_Smed_v6_8754_0_1

```
MNLLKDYLESKETIPFDEAFKSLLLNVVNHCNWSWEHQSISAIVAMFRICFQSSAIKLQY
DCRLIIFEFAKKLVCPNQPWPLTQQALANIFEELIDKNNSKIIRPVIYSLESLLKIVPIR
TLGIFIRLICKIAYFPDQKVVTLLRNTVGRVLVYREISEEQLVKQWSIVIVEVLCSEPDF
QQWMVNRLSEIFNLSYTNFYKMLLPHIFIYFVIKGGYESHQSIQRAFQFVTWVNQNEDHF
NRVIQTVVLPESIVHFYLNFSNERFNEIKNFLNDHFSMTLEKLILYNDVSRTIHSFMVYL
SEKFANVLAGIKWIALDVIQVQGIVDRLSIRKDFNDDKISKFLREYSVGILEHFKLQLLD
NKLPSQEHERVISSLQHFIRLIKNDLKNIHIMCSSILKTCLKFTSPSLMEKSYTTWYEFI
TLLDFADLEGLLVESIAVLLFIENPLINRIKDILLYIFNNENYLKTKILDLHFILELPSL
SEFHDKLLRLISADNQSDSFISILKCCNRNLHHENSCVRYLSANHLFTVLSSNLVKLSML
MAVFKLENETNTDNMDLIHSLNHSLMSSITEEIGDNKLVFSRCLGLLGAVDSGRYRELTV
SGNHSTSMEFVTSPRFSYEIMCELGKFYLGITTTTQMDAMCITIQELIKTFKISKPSYDC
SDSKKFKTQDSYPCAFDGMITGHLLWEMIPGPIKEIFQPFLNSRYKLLITVDWSHITIPL
LTLSDGMKLDNWICTWTGYLVHLMKNSGHISVFTHFQILIKNDAKFAKYILRHVILALLI
ENNPDVVSNINLEIISIFKSISRVSDEESHFNVEKILNNSSSVNLSEIHNFNNENTKILQ
SAGQIIFKVLDYLQLWLNMTRNEIEKLGKDQPKSLILANNLELIKTFVRSIPNSLLAVCS
FKCGSLARSVKHWMLAYRCDINAEEDAMLKTRKRKEIIIGILQVYSALHDSDEITGYLST
FKSELEPFAQTLKLEYEGKYDLALSIYEQQLLEHQRKNQDLLFSKESIDLHRSSFRCQLF
NISALPSIIARTNCCLNDPNFPLEYYESMNSIQVEALYKIGDWKRLETSLNMADENDDNW
TISVTKALCQAKNQKLEVSQINIDAIWKKTITNLEVSSVEGFDYERVHTDLSRFARLTEI
EMILATKEICAINTLSMNNKMKYFKKMRLKNLPTFFNQRYKLSETNFVNQESLLTSHFNL
FQLISDSQMQSDNKSKSNLNANFLNNEIGQIWLQRCKIARRAGLFASAMACLMNVEKMDF
IEFSIEKGKLFWKMGRVEESLGHLDEVIENISPLRVNNCARTNKKYNMDRFWKLLLLRAH
LTDVTCRHDFKTTKEMYKAVFEFESQSEVAHFRFAHFLDETLKLTKDYEETLSNCLMEYG
NALMYGCKFVYQSMPRLLSLWLDKKAKSKNLGSINAIMKKNIKVIPKFQFYVALYQIISR
LCHEEDNEILTLLNDLVVQLMILFPQQTIWSLICLNGSSIKVRRNKFDLIFAHIKNQKKE
MQEFIHKMINLSNALREIGDVEESFFVKMQLNLKKCGKSFDHLLKPGIYSGVILPLYHQL
FGTLPTPATFKDSYLPFPSKLVCISHMEESADVLPSLTKPKKMIWIGTDGKKYIMIVKPK
DDLRRDCRIMELNGMFNRLMRRNSETRHRLLYIRTYAVTPLGEKSGLIEWVNNTESFRQV
VVDLHIQRNNPIIWQKLHARYAQRGDSFEKKLMKFTKEVLPLYPVVFNKWFLQKFPEPNA
WYRSVQKYCRSVAVMSMVGYILGLGDRHIENILFDHTSGDVVHIDYNCLFNHGKTLEWPE
VVPFRLTRNMQDGLGPCGENNGLFRSSCVATLNLLRNEIEPIMAVFKPMYYDTLTEVKDP
LIKSNKQSNAVTMTENKLEEMENRLKGKVNQLPLSVEGEVNYLIAQAIDEKLLCQMYMGW
GSFI
```

Smed ATM
>dd_Smed_v6_14586_0_1

```
MEIFPSLKSPETSDAIISCLMYLKLLLPQYHISPNQQLAIVGKFDQDPVISDQIDLLYHL
SIICLQDFGNRSWCSYLSLCSLYQSINTSKNKFLTDILSLFHPEKNNKKINIIYEKNPDF
PAILKFLENSIPFCPHTQWRCELTKMLAVRSSKPVYNRCHPELVSSVASISFYCLPRIFA
TVEFSTEETRILSQVINRILHEQHYCESRKIVLVDCVVKKLEYIIIEEGNCRNNWEDIDF
FKAAEVAYCGKMYTATLLLLDKLWLKESNTEMNAGIVNLYYKTFKSLASQEDLTADRFLI
GSSSQYNDYGDGDGDCNDLLWLIKNGKFKVLHRLLKAEKNSDIFSFKPEAKIDILWKLSR
WGDEEKLEINNLSQENVCSLAMYDFLYSRSEHVSEFYRNHVVDSCKISWDQEACFRPLIE
RATLFGNETSLPTILESLIRIANKSNIDQLDSSIVWALIRSNRFARNLEIVNQQLLGISD
LAKRCKRHEYIDFIRDMLNLHKVDNSILKCSGESSLFRTIDIFSQKTETEETKKSFLQLE
QFIYDSQKHILTCQQIKRNHDLFFKLYFKAVSKICAWNQEYPVHSVSHIRTKILEPAMGV
FGKSLKQESDMLSTMSTFSYQQYTHINQYMRSSEYENRVKILTESKRDVSYLVDLRGKCP
LRKILEKQSEVDWDELNNLSQDRERFLLSAAISCSECLQNEDGNDFKIFHLMSMWLSNES
NEKLNNIISDVIGKIETHKFLVLMPQLCARLNSENNKSFEINLEKLIKRIILDHPFHSIY
NLLAIRNANRDSELEKSKKSIKEANDKMNSRISVAYTMVEQLVKESQSDIIRDADILTTA
```

YIHWANVDMSAFKQDIHKKLKFPLNCSLLRIAKQVKLPVPTLSIPIDRSLKYSLDRLPLI
VGFDDVYSLQGGINLPKIVWCQSSDGLKRRQLVKSNDDLRQDSVMQQVFSVVNSLLGNKG
SITYKANSIKSSDWSAFIYNRMISIRTYKVIPMTQTSGIIEWCEDTVPLGDWLANDKTGA
HQRYRPQDSTPLQCRKRLQISAEENIKKRIETFKDILTKIQPVLGYFHFEKFPESQRWFK
AKKSYANSLAINSIVGFILGLGDRHVQNILLDVNTAELIHIDFGIAFDLGKLMPTQERVP
FRLTRDLVHGLGPFGVEGRFKTTCCDVLNLLRSQKDIILTLIEVLLHDPLHSWKLNPQHA
RVLHTKREADNDCNNTSNTSSKTIEGFDNKSRPGSSQNQMAERVILEMSRKFAGAVDSSY
LNCEGHVNYLIQTASNVENLARMFHGWQAYL

Smed BRCA2
>dd_Smed_v6_12551_0_1

MNSEDDLFDFDYSQKDNSNINSTTSVLNDIFEVTQKQIKMNANIVNLTKKCAINTLLNSE
FNYKKFIYPSNDDIIKEMEDTKNPNINCKSVVPDETCSQLDPEILRQFDIPMTLPHENIE
TRYENSPVHEISKELNKNIYVNSDFEVDLDLSIVSEENQKEIEFDNQEIFSDFKTETRKR
KAIPFNEHSIEESEYISEVTNNKMACFGFKTGTGKQVSISKLAEQKAKQLFEEIEEKEII
VDQDESINLNRIVFNPSTNTDNQISKTKSTLIHKETSSRNVSSSTVTVGFATATGRIIPK
SKSALNQAKKLLNEIEEYGHENIFEPVEFKSNLAEPFCPSKMSGIEIETNSNQSHSNKEN
KEFIGFKTGTGRAISVSESAKLTYQRMLENVAKEISFEESAVSKETPHLNTTENLGDTDS
IYKFDSDKAATIIHPDNGGTVSKLSKEQLLETDLIMKEVENMECSWDYVETSDSWNNDRT
VNCLSNLIQSPIINKTAGSITNQKAHLLSSTPIRKSKPDIHVRSINSFSENFDVESNSLA
NRVNASIKLQEATASKCITEISPNAGRFSRLRLNRSQLFPMRKLFKLAAPASVEEAAGEH
IDFMSCIHVRFYCDQSVVSLDVGDNGVIVPDEGGYIGLPQFIDSFMGLPNVDPKLISAEW
IKNHYQMILWKLMALDMRYRQYLADDWLSPHHIMLQLKYRYDKEIDLAKRPCLRKICEQD
DTANKRLVLVVAFIEKIENDSFKVFVSDGWYCVPAIFDKFLKDQIINKKIKPGTKLVSCN
AVWTGCDEPLVLPVDHFPPGCGLKLHGNSTRRARAFAKLGYQSNLKPFPVTLGSLNPNGG
TASLINVVINRIYPLQYMETIYHPNQDIPQRVFRNERAEEFSRKQFDLLKENIINTTLEK
MMSSVSTNKKRYHLGQKKDKVTDLCNGEDIMNWLNNSMDQESALTELSFNQQNMLRIYRE
NLVSDALQEKCPNRNVVTLLRILVGGCLAVDVDSNQVAIFTLWKPNDDLMTLLVEGASIK
LYSVGVTHGKLDAQFSASSSASVALNSISTTRFERNKEIHENLISKIYQSRQLFSITNAC
QFLSDTSTACEIDCIGIVIAFSKVNTTSNDSWQHVVLSDPDDMDNGIIILVKLWGGLKGNF
LTSVIEIGNFVKFFNLQYRKSVYSKFNPNSKIPAFECHYNTHSNVVYVSRKWDFHAMKQS
IGEKLEKCLPAFEIFTNDKYNSIKSLSSRTLSPLTPKNKLIKNHGNSLNVSELKSNLSLN
IAASTPKRLGLSSKRILKTTTLETIFQKNELLKSTGIEESKIQTDIPKPSNSSSYNYHDS
FGMDSSIAELVKIRKRTSTVNASYFINKKK

Smed BRCA1 interacting protein (BRIP/ FANC-J)
>dd_Smed_v6_16638_0_2

MVEFKLSDVPVTFPIEPYPQQLYMMRRIINSINKSENCLMELPTGSGKTIALLCSTLGWL
KQYQSQLLLNSRNDECKENAKQVKIFFGTRTHKQIGQVIRELKKSAYSNTRMSILSGRNL
SCLNQEVLMSKEIDQNCKDLCKKMGCIYKIDNQPHPETTWDIESISMKLKKVKICPYFQF
KSWMKSADIVFCPYNYILNPFIRKSMGVNLENNIIILDEAHNIEDICREGASMSISLKDI
DYLKMLLPHILKKSGKEDCQHDLLTMLEKMHEVIELLSSKLFYKDEDVLKKTWDLESFVQ
LLKNCQLDLENIKNFENHLAKLRNEIRVNGEITDSTSEIPSSFMQLIDSFIMLVKLMMDS
DKTKQNDFSIVITEGEKYAEPINEKVASGEWISCKKRKADALNNNFVLNIWCMNPGIVFK
QISDISRSIILTSGTLSPVVSFEKELNCKFSAIFQAGHVVQPEKTFLASIGNGPSGNAMK
AVFSTTSKLSFQDELGQMLLKCSEVVPNGILIFLSSFALIELFMQRWTNTGLINEIRKHK
SIFIEPRQTSEMNECIDAYFKHVKDGALLLAVFRGKASEGVDFADEAARLVITVGIPYPS
IADPKVVLKMNYNTNKKKHFDDQLLSGNEWYNIQAFRALNQALGRCIRHREDWGAMIMID
SRLDGSNPTYSGGLCGWIQKRKIDFRNCEDLYVSLQLFIDLHCQVDIDKLPID

Smed PARP1
>dd_Smed_v6_10338_0_1

MEKDYPYMTEYAKSSRSCCKLCKISITKDSLRMAKMCQSPHFDGKIPNWYHFDCFFNKFK
LNCLGDINNVDTLRWEDQENIKMKLNEAVSEPPYHLTIEYSKAKNKCNGCKEKINKGDIR

ILIMEKVNNTSRVKKSWYHINCFIDLKNEIIKEATFDIEKINGFDSLSEDDKQILSKFKT
SNRSKKRPVKDDSEPFTIIKKPKLEDELDNQLKEQNLLLWDVRDKINAEVSKAALVHLLE
INKQHIPIGEANLLNSVADCMVFGCLNACPECGGQLHYSSSRYKCKSMVNEWSKCLYTSR
EVIRSPFVISEEYMEADILKNYRYKKLTRILPPESEECSNINPLKGYYVTIDQVNFPEEF
GKLQIQNRIKELGGRCNKTLTTSSLILISTIEGLKTKKSHKTKAENYGVDVVSAEFLINV
KNADLVEAIKKNSLVNWGRSKDEIATLYNSGERTADKDNWQIQTIKGGAAVDPDSGLIDK
AHLYQDRKTRDPLNAILGTADIITGSNSFYKIQLLESDKLSKWWVFRSWGRIGTAIGSNK
LELFHDLDSAIKNFCGIYLEKTGNKWENRNEFKKCPYKFVPLDIDYGNRAKVIENITEES
SNLPQTVEGLIRFIFDVESMKRAMLEFKIDSNKMPLGKVSQKQIDISYTILKELQDLLIN
SNPTKTKLCELSNRFYTMMPHNFGMMSPPLINSLSMVKDKCEMIESLMEIEVAYKLMEAE
KGKNIIDSQYEKLHNCISPLDKSSDVYKRLETYLQNTHAPTHNYKIMIEDIFDVSREGES
NRYHSFKRLPNRMMLWHGSRRTNWAGILSQGLRIAPPEAPVTGYMFGKGVYFADVVSKSA
NYCHSSSTSPDGILLLCEVALGKMTERYQADSNIVLKPGEHSCKGVGLTEPDPNGNFDDN
GVIYPMGKLVQQDIKSSLLYNEYIVYDIGQIKQRYLFKVKFIYK

Smed PARP2
>dd_Smed_v6_6154_0_1

MRKCEKSTICNNSNKRPKIIVKLDNLSMDSQEDTYKSFIIKRSEHVKDESCVDSPDLNSD
CKSSKRETRKIKKLISSESSDVISNKRKRKFTEPPKENFSTKNLKQRLTERKNILKCNNK
IHAIAIDEEKKKAKTISSKNKENLLSNDLSVALSPVITEHGRYPTRRKIVQEVELNISNK
VHKNRVIKKNLKIVKSPVKTSKRLVNSVNSNPNQSNDSDSSIKAKKSKIIVSKDDKKSKS
AKLNKKVKIENQTIKENGSITVGMEKLDIPVDKECKELSCKAKIYVENSEVFDVMLNQTN
LQFNNNKFYIIQLLKDEKEPIYYVWMRWARVGKIGQMKLTRFYNNLAAAKECFMKKFYDK
TKNDWQDRQKFEKINGKYDLVQIDYCKKEILETNKIASQVKLEPIESKLEEKLQVDKMN

Smed PARP3
>dd_Smed_v6_2611_0_1

MPPKRKASAKLKKAPVKKKVKNEFDSIKTALTKGPSFRKKIHTIDKFAATLFHGGIVVDD
YDCMLNQTNIDGNNNKYYVIQMIQYNGKYFVWTRWGRVGENGATLKLGPYNTKEDAHKQF
DKKFQDKTKNHWDNRDNFKSVKGKYTLLEMGVEDEDETSEVLVTNSDASEKFSPSKLAKE
TQFLVDLIFQTDMFNHALAQLKLDTKKLPLGKLSKPQIMKGFEVLEELQNEISKNKTAKL
SELSSKFYTIIPHDFGRTVPPKITTLDTVREKMDMLLVLTDIESTQALLKTKKT

Smed RAD51
>dd_smed_v6_8626_0_1

MAAKQMVQADVAQEEECMGPLPLKKLEGAGISAQDIKKLIEAGYHSIESIQYVPKKTLASIK
GLSEPKVDKIVEAASKLVPLGFTTAAEFHQKRSEIIQLTTGSKEFDKLLQGGVETGSITEIF
GEFRTGKTQICHSLAVTCQLPVDLGGGEGKCLYIDTEGTFRPERLLAVAERYGLSGTEVLEN
VAYARAYNTDHQNELLVQAAAMMSESRYALLVVDSATALYRTDYSGRGELSARQMHLARFLR
ALLRLADEFGVAVVITNQVVAQVDGASMFTADPKKPIGGNIMAHASTTRLYLRKGRGETRIC
KIYDSPCLPESEAMFAILPDGIGDAKE

Smed 53BP1
>dd_smed_v6_12961_0_1

MTEINISSQNTLESIETSESLSIKMFKENEFSHDSNKSKSSNSKQYCTGCLLLNLSFHGY
QLNKVIEADGENIDQAMKNIKENMKVLDTYVDNFKSLIDERLMSADRRTNGNKQNSGNMK
SETDCALLSLPNTREFKYPNLELSDNFKRRLTSSSSSSNRPGSSIVNRYSTASSNAFSGF
SEYAVKTDSEELISETSDSEQEPLGVTIIEQEEESEYIKIYAKWKTDKYYYSGKVKDIYS
NENWEVLFDDGTVETVKRGDILQMCLFPEGTEVSVDTEGDGNFLRNFVISEHLDIKVNFG
KKPERGCRVLNKLTGEYFTVTRNRISIHSAVAKKLMSLFGDVNISLTENSESGNISVDNI
VTEKRTLKRKRYSQYITLDDIKSKRCPSPSIFNMSTPNRAKSIFPNTKHHIPKSESNLFT
NCFFMITGVKNGDETGNDLTKDSLEKIIYKHNGCVIEQPTQAHVEKNKNKQYRLILIVLG

DVTQTAKFMMALAVGQMPIVNDKWIHECSDQSKFLDYGPFLLFRGIDEEGQIIPLNLTNI
NQPGIFINKYILIVTDNVLTFGKIWQYILELAGAETFLMDTLFNKPSISSDCCDFAVIDK
DGVTNNRINKLKNSNILVLDILYATKCLVLNELIDNKDFILXXXXIFGYINL

Smed 53BP2
>dd_smed_v6_8443_0_1

MFSDKNRDPYQKNESRRTGKEAPIEVELMKNRNRNTSRDVQVNKVDVSDKNKVQRSSLSS
SAGSMHNSNPTFEIFNTHTLVAKANPSTAKSSKSTLIKSRTGNLLQPQQPVITLKPHYNN
NTMVVNSSDINPKITRHQFNPQEEKRSMSAVVKSQSRPDMGYKSSSVKSTHPIISKSQIR
TLSATSKSNNHSYNTNNYDSLNRSRNKNANRSNDQNNDPNLIYYSLPRKSKSHIPAESKP
SNRTKPIIISTDMSKKHKLPLDTAATIATDVSDANPINFSTTLAKAATNSPPIKRRSSSL
IHSPNPRMPARFASRSTINDIYTSKNFKEYQEKYKRAASEILRENLALKFGPNASFLNQN
NIEAAQSRSSISSASSSSSSTSTSSGTDQQISISSIPHDDIPLEIPLKNGSFPKPKENVP
ILLLPSHIQNKKEEEPVNEIVQGMVMFDDNIKKDADVVHVSDEDNDEYDEYSVDDQSSSG
SYSSDSNEDIENLKKKFIPLYEIERMDDDFVIQNEISGLPDHQHSQSFRVENTSVASNTE
VFVHKESLQRAKNALKIEPNRGILSLKYLESSENLKVKKRKAIFDPHILLLDACLEPDFE
LVKELVPKVPNLSKKTIDGITALHNAVCSADPKLVLFLLQSGADVNASDADGWTPLHCAA
CCNNKQISKILVEHGASLFSITLSDFEIPSQKCNKASQEDTQCEEYLFWEQENLGVCNKG
IAYALFHYEPQKEDELPLVPNQILKILDTNPHGESGWFFAEDLSQIVAVSRKGFVAAAYV
SVYPLIIPQKRSDLIHRS

Smed MSH2
>dd_smed_v6_11434_0_1

MDELTNSFSLFWNSLGDKPNSTIRFFDRQDYYTVHFEDAEMLARSYYKSMEILKYFRRDS
VSSPYINISKSNSDGVFKYLLIANQYKVEVYSNNKSHDSWDLDFVATPGNLEKYQDILFK
DVELVSSNSLLGLNIKRINDDYRIFLGFCDLDNGIFMIGGFEESFTGYEQLANLSSALFQ
LNCRECLIPNDTRPELLAVKNAVQSAGLLVTEVKKSFFSSENVMNSILKLICKTKLNNEN
TVLKLVDTEGAETIGCLGSVITYLDLANDESFFNFFDVQTFKLDNYMRVGEQCSRALNIL
PSPNDLRKHDSLYGLLNCCRTASGERLLLQWIKQPLMDVNLINNRLDIVESLINDNKLRG
CLYEENLRRIPDLQRITRRLQRNKGNLQDIYKLYVALRQASDMLNLLNEHNGPYKCIIQS
ELSSVIQEILKDTENFIQMFTSFFDFEAVKNHEFKVKCDVDESLKECENSMITLKSQMET
ESSRVSDKLGIESTKQLKFESSNSLGYYMRVSRKDENVLRNKSFISIIETLKDGVKFHST
QMTLMNESYLQHRRDYEEYERSIIEEIMKITNKYVGSLHQLSSIIAKLDVLCSLATMVCG
APGTYARPKVVDDCKTRVFKVKNCRHPLVEMQNNMSYIANDISFDESRTFQIITGPNMGG
KSTYIRSIGLISVMAQIGSFVPCDGAEISIFDRIMTRIGAGDCQLTGVSTFMAEMLDISW
ILKTATSKSLIIIDELGRGTSTFDGFGLAWSISEHIATELKAFSAFATHFHELTDLSKIH
CNVNNLHVTAQTIGNELIFMYKVEEGPAVRSYGIEVAKASGLPDESIKLAKLKLSEYENL
MEWDSNHSEKLAATRNALMEFCLKDLVKDSIDFPVFVKMLRDKL

Smed MSH6
>dd_smed_v6_15463_0_1

MQKSILSFFPKTPSSKNKQTDILNIETANSKSKVNKTDKIKFKDNDSMPSTDNKDSDDFR
NNSRKSFKRLKALSEDDESDKENSLIFSTNKKIKVKPNYESPPMTKTENEFLSGIRKNVN
ASTPHKKKPTKDEKSINDSTKALLSSFSINANDSNIETNISQVIEDDFKNDIESYEHFSY
EFLKKENIRDAQRRKPDHPDYDPTTLFIPESFMMSLIQSKLTPGLKQWWKIKANGNMETI
FFFKVGKFYELYHMDAVTAVSELGLTYMRGNYAHSGFPEIAFSKMADQLGFKVARVEQTE
TVEAMTERIKHESSKNKVVNREICQVITPGTRGFSLRNRTCRETGQEGSEELGYIEDAGG
LLYSFKESLIEENVKGKLKNTVNIGVALIAQFADDDQRSRFRTLISRFQPNEIIYLKGNL
SKNTQHVFNSCLAATKKECFTNNKQFLSSEDTLSRLMSSDYFAEAPANKLSRFGLPNGLT
KTLNEADNLGRSSSKEYELAVSCLGALLYYLGKCLIDKYLVSIADFNLYYPSDGDCIQPH
QLAIDDKEPFYTHQSHMIIDSNTLTNLDLLKNSSLGGIDGTLLERLDFSLTAFGRRLLIQ

WIATPLCDPDKIIERQKAIKELIELDANLSNIKNNLKSCPDLEKLVAKIHVLGLSKSVSD
HPDSRAVLYEGLLYSRRKITDFVNTLTAFDNIIKIQLEFTRMHVEQNIQSKLLRKIMLHS
KDSKIGEFPDISEIISFFKTAFDQENAKKNGKIIPESGIDADYDESVALIKEIERDLAEY
LEKQKKIINSNVLINFFGTGKNRFQLEIPESKCSKVPSTYIASSQRKGFKRYLTVEIEGL
LKKLINAEDKRDLVLKNIMSKIFAKFDEHYFQWTQVINSIAQFDALLSLTSFSRGLDGGP
MTRPEIRHINPGDKPFLIITEGRFPCKAKTQSGEFISNTIKLGSLLMNSNRNLDNPVMLL
TGPNMGGKSTLMRQTALIIILSQLGCYVPAEGPVILTPVDRLFTRQGANDSIGSGQSTLQ
VEMNEAALILSYMSPHSFLLIDELGRGTATYDGCALAFSILKRIADSCSPRTIFSTHFHK
LLEEKEIGDNLQISHMACMIEDDNDDDVGNNECHLDNNLKLQNITFLYKLTHGGCPKSYG
FNAARLANIPEQIILNGLKKAKIFEEETLIMEFR

Smed FANCD2
>dd_smed_v6_12881_0_1

MRNDDLQSLNHILSICGIEFDLNFVQKRPTNVVLENIIDLLNKGIVSNYAKFQEMIRGIE
TNRINFTQFLQPVKSNYDLYLFSTPKSLCQICLMIPKLNDFLIEMLVNKICECSLTNDDE
DNELAILCLNQFKWNVYNKNMNEIVDKLLDVGYIANNFVQNHLISIFPDICQDKCNPRLA
EKLHDWMSSNNYLITSSLDTISKLNLPTSFLKEIELLVMNMLDSATMGMLPSLITFLIKN
TDKNNLVELIDKIRINVEFENLNSMFNSAVSSTPLMHVRNESSCGVKLINSLKINLQFNP
YLRKAWLKSISTKSDSVRSPSFDFIILLIIFNEYKVEMHVITNIIKSKITKEQFTQQTIE
TVFKYHFSILKPIYRGFLTIINSIMISDKGLLLDFAKEAYYNAFMNPNKDFIIDQIFEYL
IADISTKPKSNINAILEVLKHLAENCRNKIQLFYTQISGLLSNNLEFNSIQIYNIYSIFG
IIAFKDISENDDIFGDEKQIRNHVILLVKKQLQNPNFLIKRNGGIGAVTLMKYLCNVDVN
TDSTVNAITNLLNSAGGVLNDTEEEQQSQMTNSQKIVSKILKLLLSYSETVPELIIVVFD
ELYRLISTGEITEINVEKIIEKIISDSFLYNFTSEIDEIDEIDKKDRHLLFGVGVGLDYC
EIAVIVSQSNSSSNLIGKTAKIHLPAHFRLLALLELRNKKSLCEINALFGCPVRFVGGFD
SVEAVELQTVINWLIEVVNAFSSDINNGGGIDNFRLKMVQRMKLIVEQVSNLQSMLLLSV
QSKPTKLPIIQASNVGYGVVGVGGGGGGGSHLLINVTEIIIKKVSVKRKTVKKKKKSKKS
KQNHDNNNNNKTTTVGNSIQESDESEELFETDKIENATTSVRCKLLEENLRFCFRELDLS
VFTMLSSLTKSDLVLFDHNSELLGWKELKYYLSDLWLKVEHCFRDRNELPNGFNPPNANK
NGMLFRNIDQVDNLTILENIISMQDLFKLIISKSIEFCLSDEILENVDDPCFLVFEFVLK
ILSKIFHYLKNNLTDSGDEMIKRLLDGLSPVNYSKSLLKQILSIREKIPSINIAAAYCEF
VSELLTITSDNESEVSMLDLTAKFLGTKWISTNMTIYKSSVLRLFEIHLLLLSDKWFEVI
VSAILPEMQTIVTRNIDDNESEPVYACLDKTTILGVFKLVSDFILKKCKNLSKVSYSQRN
TLEMLESWEKIVVIVKLFTIVISNNKESNMILSFIKFSREFIKFIIKNLMPILDNMLRHE
NAQVIKLLTEIQFVTRFIQRLCTHCKQKNNLSSASLVPQVRRYLETFMFRVKKMLCINKC
SGDSINILFLANKDIHGRRIEESVQSENEEEDEDNEEEVCTDVSEELNACSDDVENESLN
E

Smed FANCI
>dd_smed_v6_8024_0_1

MIREDSNTIFIKVLKFFWTLESKNFDSYIYIFINSLANFNVAASYSILDSLKEILNEVTL
VQECVLSSIPVLVENIRRNDSLFTGYIDVTKINERPENIIPLVKVLREMNTLTGSEKNLL
IKNLLEMITTIDLEFCPGLVNEILHLCGKNNFQFCVGAVVNFFNQRTISCSQLSQSNINV
DSRRLISIQTSVLHHYYEIAKNNNEFVKEILKLCKNNNALYSISGFMCIILLNLAGLEFI
KAQILDMMTSCITSCYKDTKLFIESAFIRESVFENFDMDSLLMNSIKYCCISEREHISKS
LLELGFLLIKSGLPRSKITSLKSGTSNKKGGDILISEMCNNDINMNTAQRVGQAGIQMVI
QLFKRLPRLRQLIIDNIQNFILKESHKVSVFVYLELFADLISLMPTEIFDFIDEATTGQP
IFELLCHFREDVAVALVNAMLPLIRYSSTIRNNLISIIMNNILSGRSQSRLICVESALTL
LKYLRITVEQFGTENVASSNSYLTQCSQFACTQIAADSKPLPVDNFNNDEICSQILQIIN
ESSLQYPDTKSLIYKGLLQVIEKNYYFAGRVVMFLLEKLQSVVTNISDSNNISDNNPFVF
SKILSDTNVLENLPLLVSCLAESVRQCRKNMPENDLLSAAVEENACISQAVSKAEKTLDQ
LSLYLSRHDILKICQLSNEISASNHQMFVEQFIDFYEVLLVHFMCSNNQENNEKIEKLFQ
HKELALKSLKTDRKPKKSNTGSVISLTSLIAAIRYLFDSLLNEAKTTDSNRVPNLSQRRF

RTTQAIATEISIENNNSNSIHRNIVENVDSTSMAGLLNEKVSIYLLNKAINTVKTIGSPE
YRISYRNRKDICILLRDFVSICLDYYVNCLRRENIDTIPAYQRQIMQHSITLYCLSINKA
ILFCSKSLDIFLENLFEVTDHIKSLQASIGLISLDEEFSSTAEKNQVSMSSFVRLHKYMV
SMILIGGVRKLYGDIDSILNATLNIAIFCGIEDARKSGGSDFAYGTNHLNVLLLTNLNAW
SYNILKSSKLHFKTKTGEIVKNIELSDTHVCRCLFYICMVTSRAAIPDSVNTLEKFVIDM
SVKIGSYSGVAQETPKLTFEFIVHPTDLLVDLINALTLALDDVDCLLFKWKCSWQGFKQR
KAINNSQLSNINSTPSDFVEESLSVITDQERLLFEQLFPLCTMLNKLIGCAVTNIPRLQS
LIKLCTRIFDQLTTLVKQYISLIKSKMGCFASNFEKLVRISGGTLSFQASQFIVYNQKN

Smed FANCM
>dd_smed_v6_11718_0_1

MKQTTLFDFKLQKLENKSNTLDNDFKYPEHKLKKLLYKPSAVDSDIIEGFDASKSNWIYP
INFPIRDYQLQIVQECLFKNTLVCLPTGLGKTFIASVVMYNFYLWYPKGKLIFVAPTRPL
VNQQMYACQETIPIYSSDIVEMTGSINQGLRINLWKEKRVFFLTAQVLVNDLISKICPGK
SIVFIVLDEAHKASKNHAYCQIIRELTGVNFNNRLFRIIGLSATPGNELETIQDVIKNLL
ISHIELRTDECKDIKIYSHERLIEEIIVPLGSDVIDIRDRLLAICSPILDRLKAAGAIRA
MNSNHCFSKFGLLKMKDEYRMTTGGYKSHSVLTDFSQAISIYYAIELVQQHGIKSTFLYL
SNAISNSQANPQILYLIQNKEFMDFFELLQQKVSSESFTFSHPKLKRLHDIVKDHFSNKT
EENRKKSRVIIFSQIRDSVGEIMELLKKLEPLIRPIAFMGQTKNVSQKEQMEAMRLFTEG
TANVLVSTCIGEEGLDIGEVDLIICFDSQKSPIRLVQRAGRTGRKKEGRVVMLLSEGKEV
SNYRTSLSKKSRIHSAIFEGYKHLVFYPDNPRMVPLGFEPTVSFQKVIISKSPTKKTRKS
LKQKDITECIGNIPQKLKFKTEFNDCDSMRFLNELPISGSETFTQRFHCNRYKNSFYQLQ
TTINIEHSELTVNLISILKLKELHNRGKTNIIFHLSNLRILDIDEPMTQIDEEFSQHSSK
SFSVSVSSNESDSKDDNLTEKECLIKLGNSFIISPFLQLFQPNLSNKMFNGFLEKLNNSK
PDLISFLDQKIKEIDHKSIIENNQKKLGISDDKFSLNEFDDINQEILDQFSPVKDLKSTI
ALYTSTPISSNFRQSNLNNILTSFNISKSAPKLPINQSLLRSFKISPGSISSIKKENKLG
MESALKFFEEKSVLCCELSSDLFSDCESSYQNDQSNGVSVHCQQNVTDSVITISSNESDS
SIETDLVGKVGTIKELECQNKNNKNIDLKSDDDLFSDDFELYSPASDSESLSFDNEKNKN
ENPRNQWSSDLPGSFLVSIEPNLNRHLTLTQNPISTLTENDEIANEEANKSRSPSFESNV
SSENGFSENEPQNKVNQNPVKEFFFSQAEIYRNKEYKSNEIDDDEEDNNDSEQQLLASSF
INDKDTSGVVSHTQMQQIYLQSIKSPSMKRNLYEIQSNRKQPIYSQTSSLDDDDDYIMDS
FVIPDDYITPKRKRPNRLKRQINSSENPMMTFKRLKSITDSPD

Smed XRCC1
>dd_smed_v6_18657_0_1

MPEINPAKIISFSSEDQLYPVKNLLKGSSLYQWKCKNTSEIEGYVEFQFEKLTRFTRIEI
GNQSSAFIEIKVSRSMDDQDYKVLLGQTSLMSPSESLKFENLNRVKYFKDFNFSTELSQE
KWDIVRVILTQPFNKTLQFGLSFIKFFGELDSVIHVDETENNTIDQKIDISKLLNSRNDE
EFKPGSLFANRKKADEFSKLKEIKIESESVSHSSSSSIDIIPTDSNTLSEKDKKKQIKQL
SSEVTNDENNTKSNEDITLKSDKSIDKLKKLSEKSSLLLTTKRPIQDSGNKLSSQCKRPK
LDSIPNENVKAKLTPCSSSLSQSSDHHNSISKKKSLDLSSNNIFKDVIFVLSGYLNPFRN
ELRDKALSLGAKYRTSWTDDSTHLICAYNNTPKFNEVCGKGIIVSEKWIIQSYNQKKLLN
WRDFRLKGATSPPKIINSSKRSYSNSISSVGNDISNYSDIKDAPSTSKDKYSSCDKTENE
DNVDSINTLPPLPDIFEGLNFFFYGNFENKDLRFFKRIIVTFGGVIHEYMDSAVRIVITN
SSWDHNFDEALESNPGLKFIRSSWLNACDEQNFLVSFDDFEMKKE

7.4. Appendix D

Publications during the course of D. Phil.

Review

Sahu, S., Dattani, A., and Aboobaker, A.A. (2017). Secrets from immortal worms: What can we learn about biological ageing from the planarian model system? Semin. Cell Dev. Biol. *70*, 108–121.

Article

Lai, A.G., Pouchkina-Stantcheva, N., Di Donfrancesco, A., Kildisiute, G., Sahu, S., and Aboobaker, A.A. (2017). The protein subunit of telomerase displays patterns of dynamic evolution and conservation across different metazoan taxa. BMC Evol. Biol. *17*, 107.

Lai, A.G., Kosaka, N., Abnave, P., Sahu, S., and Aboobaker, A.A. (2018). The abrogation of condensin function provides independent evidence for defining the self-renewing population of pluripotent stem cells. Dev. Biol. *433*, 218–226.

Dattani, A., Kao, D., Mihaylova, Y., Abnave, P., Hughes, S., Lai, A., Sahu, S., and Aboobaker, A. (2018). Epigenetic analyses of planarian stem cells demonstrate conservation of bivalent histone modifications in animal stem cells. Genome Res. 122135.

In preparation

Sahu S**,** Abnave P, Kosaka N, Dattani A, Thompson J M, Hill M A , Aboobaker AA, Ongoing repair of migration-coupled DNA damage is required for stem cells to reach wound sites*. (Under review)*

Abegglen, L.M., Caulin, A.F., Chan, A., Lee, K., Robinson, R., Campbell, M.S., Kiso, W.K., Schmitt, D.L., Waddell, P.J., Bhaskara, S., et al. (2015). Potential Mechanisms for Cancer Resistance in Elephants and Comparative Cellular Response to DNA Damage in Humans. JAMA *314*, 1850–1860.

Abnave, P., Aboukhatwa, E., Kosaka, N., Thompson, J., Hill, M.A., and Aboobaker, A.A. (2017). Epithelial-mesenchymal transition transcription factors control pluripotent adult stem cell migration in vivo in planarians. Development *144*, 3440–3453.

Aboobaker, A.A. (2011). Planarian stem cells: a simple paradigm for regeneration. Trends Cell Biol. *21*, 304–311.

Aboobaker, A.A., and Kao, D. (2012). A lack of commitment for over 500 million years: conserved animal stem cell pluripotency. EMBO J. *31*, 2747–2749.

Adamo, A., Collis, S.J., Adelman, C.A., Silva, N., Horejsi, Z., Ward, J.D., Martinez-Perez, E., Boulton, S.J., and La Volpe, A. (2010). Preventing nonhomologous end joining suppresses DNA repair defects of Fanconi anemia. Mol. Cell *39*, 25–35.

Adams, P.D., Jasper, H., and Rudolph, K.L. (2015). Aging-Induced Stem Cell Mutations as Drivers for Disease and Cancer. Cell Stem Cell *16*, 601–612.

Adler, C.E., and Sánchez Alvarado, A. (2015). Types or States? Cellular Dynamics and Regenerative Potential. Trends Cell Biol. *25*, 687–696.

Ahmed, S.U., Carruthers, R., Gilmour, L., Yildirim, S., Watts, C., and Chalmers, A.J. (2015). Selective Inhibition of Parallel DNA Damage Response Pathways Optimizes Radiosensitization of Glioblastoma Stem-like Cells. Cancer Res. *75*, 4416–4428.

Ahnesorg, P., Smith, P., and Jackson, S.P. (2006). XLF Interacts with the XRCC4-DNA Ligase IV Complex to Promote DNA Nonhomologous End-Joining. Cell *124*, 301–313.

Ahuja, A.K., Jodkowska, K., Teloni, F., Bizard, A.H., Zellweger, R., Herrador, R., Ortega, S., Hickson, I.D., Altmeyer, M., Mendez, J., et al. (2016). A short G1 phase imposes constitutive replication stress and fork remodelling in mouse embryonic stem cells. Nat. Commun. *7*, 1–11.

Al-Ejeh, F., Pajic, M., Shi, W., Kalimutho, M., Miranda, M., Nagrial, A.M., Chou, A., Biankin, A. V, Grimmond, S.M., Australian Pancreatic Cancer Genome Initiative, et al. (2014). Gemcitabine and CHK1 inhibition potentiate EGFR-directed radioimmunotherapy against pancreatic ductal adenocarcinoma. Clin. Cancer Res. *20*, 3187–3197.

Alié, A., Leclère, L., Jager, M., Dayraud, C., Chang, P., Le Guyader, H., Quéinnec, E., and Manuel, M. (2011). Somatic stem cells express Piwi and Vasa genes in an adult ctenophore: ancient association of “germline genes” with stemness. Dev. Biol. *350*, 183–197.

Alié, A., Hayashi, T., Sugimura, I., Manuel, M., Sugano, W., Mano, A., Satoh, N., Agata, K., and Funayama, N. (2015). The ancestral gene repertoire of animal stem cells. Proc. Natl. Acad. Sci. U. S. A. *112*, E7093-100.

Almuedo-Castillo, M., Saló, E., and Adell, T. (2011). Dishevelled is essential for neural connectivity and planar cell polarity in planarians. Proc. Natl. Acad. Sci. U. S. A. *108*, 2813–2818.

Alt, F.W., Zhang, Y., Meng, F.-L., Guo, C., and Schwer, B. (2013). Mechanisms of programmed DNA lesions and genomic instability in the immune system. Cell *152*, 417–429.

Álvarez-Quilón, A., Serrano-Benítez, A., Lieberman, J.A., Quintero, C., Sánchez-Gutiérrez, D., Escudero, L.M., and Cortés-Ledesma, F. (2014). ATM specifically mediates repair of double-strand breaks with blocked DNA ends. Nat. Commun. *5*, 3347.

Aman, A., and Piotrowski, T. (2010). Cell migration during morphogenesis. Dev. Biol. *341*, 20–33.

Amundson, S.A., Do, K.T., Vinikoor, L., Koch-Paiz, C.A., Bittner, M.L., Trent, J.M., Meltzer, P., and Fornace, A.J. (2005). Stress-specific signatures: expression profiling of p53 wild-type and -null human cells. Oncogene *24*, 4572–4579.

Apostolou, E., and Hochedlinger, K. (2013). Chromatin dynamics during cellular reprogramming. Nature *502*, 462–471.

Aravin, A.A., Sachidanandam, R., Bourc'his, D., Schaefer, C., Pezic, D., Toth, K.F., Bestor, T., and Hannon, G.J. (2008). A piRNA pathway primed by individual transposons is linked to de novo DNA methylation in mice. Mol. Cell *31*, 785–799.

Argueso, J.L., Westmoreland, J., Mieczkowski, P.A., Gawel, M., Petes, T.D., and Resnick, M.A. (2008). Double-strand breaks associated with repetitive DNA can reshape the genome. Proc. Natl. Acad. Sci. U. S. A. *105*, 11845–11850.

Arya, R., and Bassing, C.H. (2017). V(D)J Recombination Exploits DNA Damage Responses to Promote Immunity. Trends Genet. *33*, 479–489.

Awasthi, P., Foiani, M., and Kumar, A. (2015). ATM and ATR signaling at a glance. J. Cell Sci. *128*, 4255–4262.

Bakkenist, C.J., and Kastan, M.B. (2003). DNA damage activates ATM through intermolecular autophosphorylation and dimer dissociation. Nature *421*, 499–506.

Bao, S., Wu, Q., McLendon, R.E., Hao, Y., Shi, Q., Hjelmeland, A.B., Dewhirst, M.W., Bigner, D.D., and Rich, J.N. (2006). Glioma stem cells promote radioresistance by preferential activation of the DNA damage response. Nature *444*, 756–760.

Barghouth, P.G., Thiruvalluvan, M., LeGro, M., and Oviedo, N.J. (2018). DNA damage and tissue repair: What we can learn from planaria. Semin. Cell Dev. Biol. pii: S1084-9521(17)30237-9. doi: 10.1016/j.semcdb.2018.04.013. [Epub ahead of print]

Barker, N. (2014). Adult intestinal stem cells: critical drivers of epithelial homeostasis and regeneration. Nat. Rev. Mol. Cell Biol. *15*, 19–33.

Barry, E.R., Morikawa, T., Butler, B.L., Shrestha, K., de la Rosa, R., Yan, K.S., Fuchs, C.S., Magness, S.T., Smits, R., Ogino, S., et al. (2013). Restriction of intestinal stem cell expansion and the regenerative response by YAP. Nature *493*, 106–110.

Bartucci, M., Svensson, S., Romania, P., Dattilo, R., Patrizii, M., Signore, M., Navarra, S., Lotti, F., Biffoni, M., Pilozzi, E., et al. (2012). Therapeutic targeting of Chk1 in NSCLC stem cells during chemotherapy. Cell Death Differ. *19*, 768–778.

Bello-Fernandez, C., Packham, G., and Cleveland, J.L. (1993). The ornithine decarboxylase gene is a transcriptional target of c-Myc. Proc. Natl. Acad. Sci. U. S. A. *90*, 7804–7808.

Beltrán-Pardo, E., Jönsson, K.I., Wojcik, A., Haghdoost, S., Harms-Ringdahl, M., Bermúdez-Cruz, R.M., and Bernal Villegas, J.E. (2013). Effects of Ionizing Radiation on Embryos of the Tardigrade Milnesium cf. tardigradum at Different Stages of Development. PLoS One *8*, 1–6.

Beltrán-Pardo, E., Jönsson, K.I., Harms-Ringdahl, M., Haghdoost, S., and Wojcik, A. (2015). Tolerance to Gamma Radiation in the Tardigrade Hypsibius dujardini from Embryo to Adult Correlate Inversely with Cellular Proliferation. PLoS One *10*, e0133658.

Bely, A.E., Zattara, E.E., and Sikes, J.M. (2014). Regeneration in spiralians: evolutionary patterns and developmental processes. Int. J. Dev. Biol. *58*, 623–634.

Bennett, R.R., Pfeifer, C.R., Irianto, J., Xia, Y., Discher, D.E., and Liu, A.J. (2017). Elastic-Fluid Model for DNA Damage and Mutation from Nuclear Fluid Segregation Due to Cell Migration. Biophys. J. *112*, 2271–2279.

Bernhard, E.J., Stanbridge, E.J., Gupta, S., Gupta, A.K., Soto, D., Bakanauskas, V.J., Cerniglia, G.J., Muschel, R.J., and McKenna, W.G. (2000). Direct evidence for the contribution of activated N-ras and K-ras oncogenes to increased intrinsic radiation resistance in human tumor cell lines. Cancer Res. *60*, 6597–6600.

Bhargava, R., Onyango, D.O., and Stark, J.M. (2016). Regulation of Single-Strand Annealing and its Role in Genome Maintenance. Trends Genet. *32*, 566–575.

Bhattacharjee, S., and Nandi, S. (2017). Synthetic lethality in DNA repair network: A novel avenue in targeted cancer therapy and combination therapeutics. IUBMB Life *69*, 929–937.

Bhattacharya, S., Srinivasan, K., Abdisalaam, S., Su, F., Raj, P., Dozmorov, I., Mishra, R., Wakeland, E.K., Ghose, S., Mukherjee, S., et al. (2017). RAD51 interconnects between DNA replication, DNA repair and immunity. Nucleic Acids Res. *45*, 4590–4605.

Bhattacharyya, S., Saha, S., Giri, K., Lanza, I.R., Nair, K.S., Jennings, N.B., Rodriguez-Aguayo, C., Lopez-Berestein, G., Basal, E., Weaver, A.L., et al. (2013). Cystathionine beta-synthase (CBS) contributes to advanced ovarian cancer progression and drug resistance. PLoS One *8*, e79167.

Bieging, K.T., Mello, S.S., and Attardi, L.D. (2014). Unravelling mechanisms of p53-mediated tumour suppression. Nat. Rev. Cancer *14*, 359–370.

Blanpain, C., and Fuchs, E. (2009). Epidermal homeostasis: a balancing act of stem cells in the skin. Nat. Rev. Mol. Cell Biol. *10*, 207–217.

Blanpain, C., Mohrin, M., Sotiropoulou, P.A., and Passegué, E. (2011). DNA-damage response in tissue-specific and cancer stem cells. Cell Stem Cell *8*, 16–29.

Blythe, M.J., Kao, D., Malla, S., Rowsell, J., Wilson, R., Evans, D., Jowett, J., Hall, A., Lemay, V., Lam, S., et al. (2010). A dual platform approach to transcript discovery for the planarian Schmidtea mediterranea to establish RNAseq for stem cell and regeneration biology. PLoS One *5*, e15617.

Boehler, C., Gauthier, L.R., Mortusewicz, O., Biard, D.S., Saliou, J.-M., Bresson, A., Sanglier-Cianferani, S., Smith, S., Schreiber, V., Boussin, F., et al. (2011). Poly(ADP-ribose) polymerase 3 (PARP3), a newcomer in cellular response to DNA damage and mitotic progression. Proc. Natl. Acad. Sci. U. S. A. *108*, 2783–2788.

Te Boekhorst, V., Preziosi, L., and Friedl, P. (2016). Plasticity of Cell Migration In Vivo and In Silico. Annu. Rev. Cell Dev. Biol. *32*, 491–526.

Bonner, W.M., Redon, C.E., Dickey, J.S., Nakamura, A.J., Sedelnikova, O.A., Solier, S., and Pommier, Y. (2008). GammaH2AX and cancer. Nat. Rev. Cancer *8*, 957–967.

Böser, A., Drexler, H.C.A., Reuter, H., Schmitz, H., Wu, G., Schöler, H.R., Gentile, L., and Bartscherer, K. (2013). SILAC proteomics of planarians identifies Ncoa5 as a conserved component of pluripotent stem cells. Cell Rep. *5*, 1142–1155.

Botuyan, M.V., Lee, J., Ward, I.M., Kim, J.-E., Thompson, J.R., Chen, J., and Mer, G. (2006). Structural basis for the methylation state-specific recognition of histone H4-K20 by 53BP1 and Crb2 in DNA repair. Cell *127*, 1361–1373.

Brandl, H., Moon, H., Vila-Farré, M., Liu, S.-Y., Henry, I., and Rink, J.C. (2016). PlanMine--a mineable resource of planarian biology and biodiversity. Nucleic Acids Res. *44*, D764-73.

Brandsma, I., and Gent, D.C. (2012). Pathway choice in DNA double strand break repair: observations of a balancing act. Genome Integr. *3*, 9.

Brennecke, J., Aravin, A.A., Stark, A., Dus, M., Kellis, M., Sachidanandam, R., and Hannon, G.J. (2007). Discrete small RNA-generating loci as master regulators of transposon activity in Drosophila. Cell *128*, 1089–1103.

Brockes, J.P., and Gates, P.B. (2014). Mechanisms underlying vertebrate limb regeneration: lessons from the salamander. Biochem. Soc. Trans. *42*, 625–630.

Brough, R., Wei, D., Leulier, S., Lord, C.J., Rong, Y.S., and Ashworth, A. (2008). Functional analysis of Drosophila melanogaster BRCA2 in DNA repair. DNA Repair (Amst). *7*, 10–19.

Brown, D.D.R., and Pearson, B.J. (2015). One FISH, dFISH, Three FISH: Sensitive Methods of Whole-Mount Fluorescent In Situ Hybridization in Freshwater Planarians. (Humana Press, New York, NY), pp. 127–150.

Brown, F.D., Keeling, E.L., Le, A.D., and Swalla, B.J. (2009). Whole body regeneration in a colonial ascidian, Botrylloides violaceus. J. Exp. Zool. B. Mol. Dev. Evol. *312*, 885–900.

Brubacher, J.L., Vieira, A.P., and Newmark, P. a (2014). Preparation of the planarian Schmidtea mediterranea for high-resolution histology and transmission electron microscopy. Nat. Protoc. *9*, 661–673.

Bryant, H.E., Schultz, N., Thomas, H.D., Parker, K.M., Flower, D., Lopez, E., Kyle, S., Meuth, M., Curtin, N.J., and Helleday, T. (2005). Specific killing of BRCA2-deficient tumours with inhibitors of poly(ADP-ribose) polymerase. Nature *434*, 913–917.

Buffenstein, R. (2008). Negligible senescence in the longest living rodent, the naked mole-rat: insights from a successfully aging species. J. Comp. Physiol. B. *178*, 439–445.

Bunting, S.F., Callén, E., Wong, N., Chen, H.T., Polato, F., Gunn, A., Bothmer, A., Feldhahn, N., Fernandez-Capetillo, O., Cao, L., et al. (2010). 53BP1 inhibits homologous recombination in brca1-deficient cells by blocking resection of DNA breaks. Cell *141*, 243–254.

Burkhalter, M.D., Rudolph, K.L., and Sperka, T. (2015). Genome instability of ageing stem cells—Induction and defence mechanisms. Ageing Res. Rev. *23*, 29–36.

Campisi, J. (1997). Aging and cancer: the double-edged sword of replicative senescence. J. Am. Geriatr. Soc. *45*, 482–488.

Capozzo, I., Iannelli, F., Francia, S., and d'Adda di Fagagna, F. (2017). Express or repress? The transcriptional dilemma of damaged chromatin. FEBS J. *284*, 2133–2147.

Carlson, B.M. (2005). Some principles of regeneration in mammalian systems. Anat. Rec. B. New Anat. *287*, 4–13.

Casero, R.A., and Marton, L.J. (2007). Targeting polyamine metabolism and function in cancer and other hyperproliferative diseases. Nat. Rev. Drug Discov. *6*, 373–390.

Casero, R.A., Murray Stewart, T., and Pegg, A.E. (2018). Polyamine metabolism and cancer: treatments, challenges and opportunities. Nat. Rev. Cancer *18*, 681–695.

Cassella, L., Salvetti, A., Iacopetti, P., Ippolito, C., Ghezzani, C., Gimenez, G., Ghigo, E., and Rossi, L. (2017). Putrescine independent wound response phenotype is produced by ODC-like RNAi in planarians. Sci. Rep. *7*, 9736.

Ceccaldi, R., Rondinelli, B., and D'Andrea, A.D. (2016). Repair Pathway Choices and Consequences at the Double-Strand Break. Trends Cell Biol. *26*, 52–64.

Chang, H.H.Y., and Lieber, M.R. (2016). Structure-Specific nuclease activities of Artemis and the Artemis: DNA-PKcs complex. Nucleic Acids Res. *44*, 4991–4997.

Chapman, J.R., Barral, P., Vannier, J.B., Borel, V., Steger, M., Tomas-Loba, A., Sartori, A.A., Adams, I.R., Batista, F.D., and Boulton, S.J. (2013). RIF1 Is Essential for 53BP1-Dependent Nonhomologous End Joining and Suppression of DNA Double-Strand Break Resection. Mol. Cell.

Charlet-Berguerand, N., Feuerhahn, S., Kong, S.E., Ziserman, H., Conaway, J.W., Conaway, R., and Egly, J.M. (2006). RNA polymerase II bypass of oxidative DNA damage is regulated by transcription elongation factors. EMBO J. *25*, 5481–5491.

Charras, G., and Paluch, E. (2008). Blebs lead the way: how to migrate without lamellipodia. Nat. Rev. Mol. Cell Biol. *9*, 730–736.

Charrin, S., Jouannet, S., Boucheix, C., and Rubinstein, E. (2014). Tetraspanins at a glance. J. Cell Sci. *127*, 3641–3648.

Chen, J., Guo, L., Zhang, L., Wu, H., Yang, J., Liu, H., Wang, X., Hu, X., Gu, T., Zhou, Z., et al. (2013). Vitamin C modulates TET1 function during somatic cell reprogramming. Nat. Genet. *45*, 1504–1509.

Chen, W.-T., Ebelt, N.D., Stracker, T.H., Xhemalce, B., Van Den Berg, C.L., and Miller, K.M. (2015). ATM regulation of IL-8 links oxidative stress to cancer cell migration and invasion. Elife *4*, e07270.

Cheng, L., Tu, K.C., Seidel, C.W., Robb, S.M.C., Guo, F., and Sánchez Alvarado, A. (2018). Cellular, ultrastructural and molecular analyses of epidermal cell development in the planarian Schmidtea mediterranea. Dev. Biol. *433*, 357–373.

Chiou, S.-H., Kao, C.-L., Chen, Y.-W., Chien, C.-S., Hung, S.-C., Lo, J.-F., Chen, Y.-J., Ku, H.-H., Hsu, M.-T., and Wong, T.-T. (2008). Identification of CD133-positive radioresistant cells in atypical teratoid/rhabdoid tumor. PLoS One *3*, e2090.

Chiruvella, K.K., Liang, Z., and Wilson, T.E. (2013). Repair of double-strand breaks by end joining. Cold Spring Harb. Perspect. Biol. *5*, a012757.

Cho, S., Irianto, J., and Discher, D.E. (2017). Mechanosensing by the nucleus: From pathways to scaling relationships. J. Cell Biol. 1–11.

Chow, K.-H., Factor, R.E., and Ullman, K.S. (2012). The nuclear envelope environment and its cancer connections.

Chung, W.-H., Zhu, Z., Papusha, A., Malkova, A., and Ira, G. (2010). Defective Resection at

DNA Double-Strand Breaks Leads to De Novo Telomere Formation and Enhances Gene Targeting. PLoS Genet. *6*, e1000948.

Ciccia, A., and Elledge, S.J. (2010). The DNA Damage Response: Making It Safe to Play with Knives. Mol. Cell *40*, 179–204.

Citarelli, M., Teotia, S., and Lamb, R.S. (2010). Evolutionary history of the poly(ADP-ribose) polymerase gene family in eukaryotes. BMC Evol. Biol. *10*, 308.

Clauson, C., Schärer, O.D., and Niedernhofer, L. (2013). Advances in understanding the complex mechanisms of DNA interstrand cross-link repair. Cold Spring Harb. Perspect. Biol. *5*, a012732.

Clejan, I., Boerckel, J., and Ahmed, S. (2006). Developmental modulation of nonhomologous end joining in Caenorhabditis elegans. Genetics *173*, 1301–1317.

Collins, J.J., Wendt, G.R., Iyer, H., and Newmark, P.A. (2016). Stem cell progeny contribute to the schistosome host-parasite interface. Elife *5*, e12473.

Connelly, J.T., Gautrot, J.E., Trappmann, B., Tan, D.W.-M., Donati, G., Huck, W.T.S., and Watt, F.M. (2010). Actin and serum response factor transduce physical cues from the microenvironment to regulate epidermal stem cell fate decisions. Nat. Cell Biol. *12*, 711–718.

Cordaux, R., and Batzer, M.A. (2009). The impact of retrotransposons on human genome evolution. Nat. Rev. Genet. *10*, 691–703.

Cortez, D., Guntuku, S., Qin, J., and Elledge, S.J. (2001). ATR and ATRIP: partners in checkpoint signaling. Science *294*, 1713–1716.
Crane, G.M., Jeffery, E., and Morrison, S.J. (2017). Adult haematopoietic stem cell niches. Nat. Rev. Immunol. *17*, 573–590.

Crosetto, N., Mitra, A., Silva, M.J., Bienko, M., Dojer, N., Wang, Q., Karaca, E., Chiarle, R., Skrzypczak, M., Ginalski, K., et al. (2013). nucleotide-resolution dnA double-strand break mapping by next-generation sequencing. Artic. Nat. Methods *10*, 361.

Currie, K.W., Brown, D.D.R., Zhu, S., Xu, C., Voisin, V., Bader, G.D., and Pearson, B.J. (2016). HOX gene complement and expression in the planarian Schmidtea mediterranea. Evodevo *7*, 7.

D’Alessandro, G., and d’Adda di Fagagna, F. (2017). Transcription and DNA Damage: Holding Hands or Crossing Swords? J. Mol. Biol. *429*, 3215–3229.

Dalyell, J.G. (1814). Observations on Some Interesting Phaenomena in Animal Physiology Exhibited by Several Species of Planariae.

Dannenmann, B., Lehle, S., Hildebrand, D.G., Kübler, A., Grondona, P., Schmid, V., Holzer, K., Fröschl, M., Essmann, F., Rothfuss, O., et al. (2015). Stem Cell Reports High Glutathione and Glutathione Peroxidase-2 Levels Mediate Cell-Type- Specific DNA Damage Protection in Human Induced Pluripotent Stem Cells. Stem Cell Reports *4*, 886–898.

Dattani, A., Kao, D., Mihaylova, Y., Abnave, P., Hughes, S., Lai, A., Sahu, S., and Aboobaker, A. (2018a). Epigenetic analyses of planarian stem cells demonstrate conservation of bivalent histone modifications in animal stem cells. Genome Res. 122135.

Dattani, A., Sridhar, D., and Aziz Aboobaker, A. (2018b). Planarian flatworms as a new model system for understanding the epigenetic regulation of stem cell pluripotency and

differentiation. Semin. Cell Dev. Biol. pii: S1084-9521(17)30441-X. doi:10.1016/j.semcdb.2018.04.007. [Epub ahead of print]

Davis, A.J., and Chen, D.J. (2013). DNA double strand break repair via non-homologous end-joining. Transl. Cancer Res. *2*, 130–143.

Denais, C.M., Gilbert, R.M., Isermann, P., McGregor, A.L., te Lindert, M., Weigelin, B., Davidson, P.M., Friedl, P., Wolf, K., and Lammerding, J. (2016). Nuclear envelope rupture and repair during cancer cell migration. Science *352*, 353–358.

Deng, W., Henriet, S., and Chourrout, D. (2018). Prevalence of Mutation-Prone Microhomology-Mediated End Joining in a Chordate Lacking the c-NHEJ DNA Repair Pathway. Curr. Biol. *28*, 3337–3341.e4.

Dengg, M., Garcia-Muse, T., Gill, S.G., Ashcroft, N., Boulton, S.J., and Nilsen, H. (2006). Abrogation of the CLK-2 checkpoint leads to tolerance to base-excision repair intermediates. EMBO Rep. *7*, 1046–1051.

Desai, A., Webb, B., and Gerson, S.L. (2014). CD133+ cells contribute to radioresistance via altered regulation of DNA repair genes in human lung cancer cells. Radiother. Oncol. *110*, 538–545.

Dev, H., Chiang, T.-W.W., Lescale, C., de Krijger, I., Martin, A.G., Pilger, D., Coates, J., Sczaniecka-Clift, M., Wei, W., Ostermaier, M., et al. (2018). Shieldin complex promotes DNA end-joining and counters homologous recombination in BRCA1-null cells. Nat. Cell Biol. *20*, 954–965.

Ding, L., Wang, Z., Yan, J., Yang, X., Liu, A., Qiu, W., Zhu, J., Han, J., Zhang, H., Lin, J., et al. (2009). Human four-and-a-half LIM family members suppress tumor cell growth through a TGF-beta-like signaling pathway. J. Clin. Invest. *119*, 349–361.

Ding, X., Chaudhuri, A.R., Callen, E., Pang, Y., Biswas, K., Klarmann, K.D., Martin, B.K., Burkett, S., Cleveland, L., Stauffer, S., et al. (2016). Synthetic viability by BRCA2 and PARP1/ARTD1 deficiencies. Nat. Commun. *7*, 12425.

Duncan, E.M., Chitsazan, A.D., Seidel, C.W., and Sánchez Alvarado, A. (2015). Set1 and MLL1/2 Target Distinct Sets of Functionally Different Genomic Loci In Vivo. Cell Rep. *13*, 2741–2755.

Egger, B., Gschwentner, R., and Rieger, R. (2007). Free-living flatworms under the knife: past and present. Dev. Genes Evol. *217*, 89–104.

Eisenhoffer, G.T., Kang, H., and Sánchez Alvarado, A. (2008). Molecular analysis of stem cells and their descendants during cell turnover and regeneration in the planarian Schmidtea mediterranea. Cell Stem Cell *3*, 327–339.

Elliott, S.A., and Sánchez Alvarado, A. (2013). The history and enduring contributions of planarians to the study of animal regeneration. Wiley Interdiscip. Rev. Dev. Biol. *2*, 301–326.

Ermolaeva, M.A., Segref, A., Dakhovnik, A., Ou, H.-L., Schneider, J.I., Utermöhlen, O., Hoppe, T., and Schumacher, B. (2013). DNA damage in germ cells induces an innate immune response that triggers systemic stress resistance. Nature *501*, 416–420.

Esteban, M.A., Wang, T., Qin, B., Yang, J., Qin, D., Cai, J., Li, W., Weng, Z., Chen, J., Ni, S., et al. (2010). Vitamin C enhances the generation of mouse and human induced pluripotent stem cells. Cell Stem Cell *6*, 71–79.

Falck, J., Mailand, N., Syljuåsen, R.G., Bartek, J., and Lukas, J. (2001). The ATM-Chk2-Cdc25A checkpoint pathway guards against radioresistant DNA synthesis. Nature *410*, 842–847.

Farmer, H., McCabe, N., Lord, C.J., Tutt, A.N.J., Johnson, D.A., Richardson, T.B., Santarosa, M., Dillon, K.J., Hickson, I., Knights, C., et al. (2005). Targeting the DNA repair defect in BRCA mutant cells as a therapeutic strategy. Nature *434*, 917–921.

Felgentreff, K., Du, L., Weinacht, K.G., Dobbs, K., Bartish, M., Giliani, S., Schlaeger, T., DeVine, A., Schambach, A., Woodbine, L.J., et al. (2014). Differential role of nonhomologous end joining factors in the generation, DNA damage response, and myeloid differentiation of human induced pluripotent stem cells. Proc. Natl. Acad. Sci. U. S. A. *111*, 8889–8894.

Feng, Z., Scott, S.P., Bussen, W., Sharma, G.G., Guo, G., Pandita, T.K., and Powell, S.N. (2011). Rad52 inactivation is synthetically lethal with BRCA2 deficiency. Proc. Natl. Acad. Sci. U. S. A. *108*, 686–691.

Fincher, C.T., Wurtzel, O., de Hoog, T., Kravarik, K.M., and Reddien, P.W. (2018). Cell type transcriptome atlas for the planarian Schmidtea mediterranea. Science *360*.

Findlay, S., Heath, J., Luo, V.M., Malina, A., Morin, T., Coulombe, Y., Djerir, B., Li, Z., Samiei, A., Simo-Cheyou, E., et al. (2018). SHLD2/FAM35A co-operates with REV7 to coordinate DNA double-strand break repair pathway choice. EMBO J. *37*.

Finkel, T., and Holbrook, N.J. (2000). Oxidants, oxidative stress and the biology of ageing. Nature *408*, 239–247.

Fire, A., Xu, S., Montgomery, M.K., Kostas, S.A., Driver, S.E., and Mello, C.C. (1998). Potent and specific genetic interference by double-stranded RNA in Caenorhabditis elegans. Nature *391*, 806–811.

Fokas, E., Prevo, R., Hammond, E.M., Brunner, T.B., McKenna, W.G., and Muschel, R.J. (2014). Targeting ATR in DNA damage response and cancer therapeutics. Cancer Treat. Rev. *40*, 109–117.

Fortini, P., Ferretti, C., Pascucci, B., Narciso, L., Pajalunga, D., Puggioni, E.M.R., Castino, R., Isidoro, C., Crescenzi, M., and Dogliotti, E. (2012a). DNA damage response by single-strand breaks in terminally differentiated muscle cells and the control of muscle integrity. Cell Death Differ. *19*, 1741–1749.

Fortini, P., Chiara, F., and Eugenia, D. (2012b). The Plasticity of DNA Damage Response during Cell Differentiation: Pathways and Consequences. In The Cellular Response to the Genotoxic Insult: The Question of Threshold for Genotoxic Carcinogens, R.A. Helmut Greim, ed. (Royal Society of Chemistry)

Friedl, P., and Gilmour, D. (2009). Collective cell migration in morphogenesis, regeneration and cancer. Nat. Rev. Mol. Cell Biol. *10*, 445–457.

Friedl, P., and Wolf, K. (2010). Plasticity of cell migration: A multiscale tuning model. J. Cell Biol. *188*, 11–19.

Friedl, P., Borgmann, S., and Bröcker, E. (2001). Amoeboid leukocyte crawling through extracellular matrix: lessons from the Dictyostelium paradigm of cell movement. J. Leukoc. Biol. *70*, 491–509.

Friedl, P., Wolf, K., and Lammerding, J. (2011). Nuclear mechanics during cell migration. Curr. Opin. Cell Biol. *23*, 55–64.

Friedländer, M.R., Adamidi, C., Han, T., Lebedeva, S., Isenbarger, T.A., Hirst, M., Marra, M., Nusbaum, C., Lee, W.L., Jenkin, J.C., et al. (2009). High-resolution profiling and discovery of planarian small RNAs. Proc. Natl. Acad. Sci. *106*, 11546–11551.

Fuchs, E. (2016). Epithelial Skin Biology: Three Decades of Developmental Biology, a Hundred Questions Answered and a Thousand New Ones to Address. Curr. Top. Dev. Biol. *116*, 357–374.

Funakoshi-Tago, M., Sumi, K., Kasahara, T., and Tago, K. (2013). Critical roles of Myc-ODC axis in the cellular transformation induced by myeloproliferative neoplasm-associated JAK2 V617F mutant. PLoS One *8*, e52844.

Funayama, N., Nakatsukasa, M., Mohri, K., Masuda, Y., and Agata, K. (2010). Piwi expression in archeocytes and choanocytes in demosponges: insights into the stem cell system in demosponges. Evol. Dev. *12*, 275–287.

Gahan, J.M., Bradshaw, B., Flici, H., and Frank, U. (2016). The interstitial stem cells in Hydractinia and their role in regeneration. Curr. Opin. Genet. Dev. *40*, 65–73.

Galliot, B. (2012). Hydra, a fruitful model system for 270 years. Int. J. Dev. Biol. *56*, 411–423.

Galloni, M. (2012). Global irradiation effects, stem cell genes and rare transcripts in the planarian transcriptome. Int. J. Dev. Biol. *56*, 103–116.

Gao, S., Feng, S., Ning, S., Liu, J., Zhao, H., Xu, Y., Shang, J., Li, K., Li, Q., Guo, R., et al. (2018). An OB-fold complex controls the repair pathways for DNA double-strand breaks. Nat. Commun. *9*, 3925.

Gartner, A., Milstein, S., Ahmed, S., Hodgkin, J., and Hengartner, M.O. (2000). A conserved checkpoint pathway mediates DNA damage--induced apoptosis and cell cycle arrest in C. elegans. Mol. Cell *5*, 435–443.

Gehrke, A.R., and Srivastava, M. (2016). Neoblasts and the evolution of whole-body regeneration. Curr. Opin. Genet. Dev. *40*, 131–137.

Ghysen, A., and Dambly-Chaudière, C. (2004). Development of the zebrafish lateral line. Curr. Opin. Neurobiol. *14*, 67–73.

Gibbs-Seymour, I., Fontana, P., Rack, J.G.M., and Ahel, I. (2016). HPF1/C4orf27 Is a PARP-1-Interacting Protein that Regulates PARP-1 ADP-Ribosylation Activity. Mol. Cell *62*, 432–442.

Gibson, B. a., and Kraus, W.L. (2012). New insights into the molecular and cellular functions of poly(ADP-ribose) and PARPs. Nat. Rev. Mol. Cell Biol. *13*, 411–424.

Gladyshev, E., and Meselson, M. (2008). Extreme resistance of bdelloid rotifers to ionizing radiation. Proc. Natl. Acad. Sci. U. S. A. *105*, 5139–5144.

Golding, S.E., Rosenberg, E., Valerie, N., Hussaini, I., Frigerio, M., Cockcroft, X.F., Chong, W.Y., Hummersone, M., Rigoreau, L., Menear, K.A., et al. (2009). Improved ATM kinase inhibitor KU-60019 radiosensitizes glioma cells, compromises insulin, AKT and ERK prosurvival signaling, and inhibits migration and invasion. Mol. Cancer Ther. *8*, 2894–2902.

Gong, W., Guo, M., Han, Z., Wang, Y., Yang, P., Xu, C., Wang, Q., Du, L., Li, Q., Zhao, H., et al. (2016). Mesenchymal stem cells stimulate intestinal stem cells to repair radiation-induced intestinal injury. Cell Death Dis. *7*, e2387.

González-estévez, C., Felix, D.A., Rodríguez-esteban, G., and Aboobaker, A.A. (2012). Decreased neoblast progeny and increased cell death during starvation-induced planarian degrowth. 83–91.

González-Estévez, C., Felix, D.A., Smith, M.D., Paps, J., Morley, S.J., James, V., Sharp, T. V, and Aboobaker, A.A. (2012). SMG-1 and mTORC1 act antagonistically to regulate response to injury and growth in planarians. PLoS Genet. *8*, e1002619.

Goodell, M.A., and Rando, T.A. (2015). Stem cells and healthy aging. Science *350*, 1199–1204.

Gorbunova, V., Seluanov, A., Zhang, Z., Gladyshev, V.N., and Vijg, J. (2014). Comparative genetics of longevity and cancer: insights from long-lived rodents. Nat. Rev. Genet. *15*, 531–540.

Gregorieff, A., Liu, Y., Inanlou, M.R., Khomchuk, Y., and Wrana, J.L. (2015). Yap-dependent reprogramming of Lgr5(+) stem cells drives intestinal regeneration and cancer. Nature *526*, 715–718.

Grillari, J., Katinger, H., and Voglauer, R. (2007). Contributions of DNA interstrand cross-links to aging of cells and organisms. Nucleic Acids Res. *35*, 7566–7576.

Grillo, M., Konstantinides, N., and Averof, M. (2016). Old questions, new models: Unraveling complex organ regeneration with new experimental approaches. Curr. Opin. Genet. Dev. *40*, 23–31.

Grinnell, F. (2003). Fibroblast biology in three-dimensional collagen matrices. Trends Cell Biol. *13*, 264–269.

Grohme, M.A., Schloissnig, S., Rozanski, A., Pippel, M., Young, G.R., Winkler, S., Brandl, H., Henry, I., Dahl, A., Powell, S., et al. (2018). The genome of Schmidtea mediterranea and the evolution of core cellular mechanisms. Nature *554*, 56–61.

Grudniewska, M., Mouton, S., Simanov, D., Beltman, F., Grelling, M., Mulder, K. De, and Arindrarto, W. (2016). Transcriptional signatures of somatic neoblasts and germline cells in Macrostomum lignano. 1–23.

Guedelhoefer, O.C., and Sánchez Alvarado, A. (2012). Amputation induces stem cell mobilization to sites of injury during planarian regeneration. Development *139*, 3510–3520.

Gunawardane, L.S., Saito, K., Nishida, K.M., Miyoshi, K., Kawamura, Y., Nagami, T., Siomi, H., and Siomi, M.C. (2007). A slicer-mediated mechanism for repeat-associated siRNA 5' end formation in Drosophila. Science *315*, 1587–1590.

Guo, T., Peters, A.H.F.M., and Newmark, P.A. (2006). A bruno-like Gene Is Required for Stem Cell Maintenance in Planarians. Dev. Cell *11*, 159–169.

Gupta, R., Somyajit, K., Narita, T., Maskey, E., Stanlie, A., Kremer, M., Typas, D., Lammers, M., Mailand, N., Nussenzweig, A., et al. (2018). DNA Repair Network Analysis Reveals Shieldin as a Key Regulator of NHEJ and PARP Inhibitor Sensitivity. Cell *173*, 972–988.e23.

Güttinger, S., Laurell, E., and Kutay, U. (2009). Orchestrating nuclear envelope disassembly and reassembly during mitosis. Nat. Rev. Mol. Cell Biol. *10*, 178–191.

Hall, A.E., Lu, W.-T., Godfrey, J.D., Antonov, A. V, Paicu, C., Moxon, S., Dalmay, T., Wilczynska, A., Muller, P.A.J., and Bushell, M. (2016). The cytoskeleton adaptor protein

ankyrin-1 is upregulated by p53 following DNA damage and alters cell migration. Cell Death Dis. *7*, e2184.

Hardee, M.E., Marciscano, A.E., Medina-Ramirez, C.M., Zagzag, D., Narayana, A., Lonning, S.M., and Barcellos-Hoff, M.H. (2012). Resistance of glioblastoma-initiating cells to radiation mediated by the tumor microenvironment can be abolished by inhibiting transforming growth factor-β. Cancer Res. *72*, 4119–4129.

Harfouche, G., Vaigot, P., Rachidi, W., Rigaud, O., Moratille, S., Marie, M., Lemaitre, G., Fortunel, N.O., and Martin, M.T. (2010). Fibroblast growth factor type 2 signaling is critical for DNA repair in human keratinocyte stem cells. Stem Cells *28*, 1639–1648.

Harris, D.R., Pollock, S. V., Wood, E.A., Goiffon, R.J., Klingele, A.J., Cabot, E.L., Schackwitz, W., Martin, J., Eggington, J., Durfee, T.J., et al. (2009). Directed evolution of ionizing radiation resistance in Escherichia coli. J. Bacteriol. *191*, 5240–5252.

Hashimoto, T., Horikawa, D.D., Saito, Y., Kuwahara, H., Kozuka-Hata, H., Shin-I, T., Minakuchi, Y., Ohishi, K., Motoyama, A., Aizu, T., et al. (2016). Extremotolerant tardigrade genome and improved radiotolerance of human cultured cells by tardigrade-unique protein. Nat. Commun. *7*, 12808.

Hayashi, T., Asami, M., Higuchi, S., Shibata, N., and Agata, K. (2006). Isolation of planarian X-ray-sensitive stem cells by fluorescence-activated cell sorting. Dev. Growth Differ. *48*, 371–380.

He, Y.J., Meghani, K., Caron, M.-C., Yang, C., Ronato, D.A., Bian, J., Sharma, A., Moore, J., Niraj, J., Detappe, A., et al. (2018). DYNLL1 binds to MRE11 to limit DNA end resection in BRCA1-deficient cells. Nature *563*, 522–526.

van Helvert, S., Storm, C., and Friedl, P. (2018). Mechanoreciprocity in cell migration. Nat. Cell Biol. *20*, 8–20.

Hemler, M.E. (2014). Tetraspanin proteins promote multiple cancer stages. Nat. Rev. Cancer *14*, 49–60.

Hendrix, A., Braems, G., Bracke, M., Seabra, M., Gahl, W., De Wever, O., and Westbroek, W. (2010a). The secretory small GTPase Rab27B as a marker for breast cancer progression. Oncotarget *1*, 304–308.

Hendrix, A., Maynard, D., Pauwels, P., Braems, G., Denys, H., Van den Broecke, R., Lambert, J., Van Belle, S., Cocquyt, V., Gespach, C., et al. (2010b). Effect of the secretory small GTPase Rab27B on breast cancer growth, invasion, and metastasis. J. Natl. Cancer Inst. *102*, 866–880.

Herraiz, C., Calvo, F., Pandya, P., Cantelli, G., Rodriguez-Hernandez, I., Orgaz, J.L., Kang, N., Chu, T., Sahai, E., and Sanz-Moreno, V. (2016). Reactivation of p53 by a Cytoskeletal Sensor to Control the Balance between DNA Damage and Tumor Dissemination. J. Natl. Cancer Inst. *108*, 1–14.

Hill, E.M., and Petersen, C.P. (2015). Wnt/Notum spatial feedback inhibition controls neoblast differentiation to regulate reversible growth of the planarian brain. Development *142*, 4217–4229.

Hoeijmakers, J.H. (2001). Genome maintenance mechanisms for preventing cancer. Nature *411*, 366–374.

Hoeijmakers, J.H.J. (2009). DNA Damage, Aging, and Cancer. N. Engl. J. Med. *361*, 1475–

1485.

Hogarty, M.D., Norris, M.D., Davis, K., Liu, X., Evageliou, N.F., Hayes, C.S., Pawel, B., Guo, R., Zhao, H., Sekyere, E., et al. (2008). ODC1 is a critical determinant of MYCN oncogenesis and a therapeutic target in neuroblastoma. Cancer Res. *68*, 9735–9745.
Hollenbach, J.P., Resch, A.M., Palakodeti, D., Graveley, B.R., and Heinen, C.D. (2011). Loss of DNA mismatch repair imparts a selective advantage in planarian adult stem cells. PLoS One *6*, e21808.

Horikawa, D.D., Sakashita, T., Katagiri, C., Watanabe, M., Kikawada, T., Nakahara, Y., Hamada, N., Wada, S., Funayama, T., Higashi, S., et al. (2006). Radiation tolerance in the tardigrade Milnesium tardigradum. Int. J. Radiat. Biol. *82*, 843–848.

Horikawa, D.D., Cumbers, J., Sakakibara, I., Rogoff, D., Leuko, S., Harnoto, R., Arakawa, K., Katayama, T., Kunieda, T., Toyoda, A., et al. (2013). Analysis of DNA repair and protection in the Tardigrade Ramazzottius varieornatus and Hypsibius dujardini after exposure to UVC radiation. PLoS One *8*, e64793.

Hovinga, K.E., Shimizu, F., Wang, R., Panagiotakos, G., Van Der Heijden, M., Moayedpardazi, H., Correia, A.S., Soulet, D., Major, T., Menon, J., et al. (2010). Inhibition of Notch Signaling in Glioblastoma Targets Cancer Stem Cells via an Endothelial Cell Intermediate. Stem Cells *28*, 1019–1029.

Hsieh, S.-L., and Lin, W.-W. (2017). Decoy receptor 3: an endogenous immunomodulator in cancer growth and inflammatory reactions. J. Biomed. Sci. *24*, 39.

Hu, H., Wang, M., Wang, H., Liu, Z., Guan, X., Yang, R., Huang, R., Tang, Q., Zou, C., Wang, G., et al. (2018). MEGF6 Promotes the Epithelial-to-Mesenchymal Transition via the TGFβ/SMAD Signaling Pathway in Colorectal Cancer Metastasis. Cell. Physiol. Biochem. *46*, 1895–1906.

Hua, G., Thin, T.H., Feldman, R., Haimovitz-Friedman, A., Clevers, H., Fuks, Z., and Kolesnick, R. (2012). Crypt base columnar stem cells in small intestines of mice are radioresistant. Gastroenterology *143*, 1266–1276.

Huang, H., and Tindall, D.J. (2007). Dynamic FoxO transcription factors. J. Cell Sci. *120*, 2479–2487.

Huang, S., Yuan, S., Dong, M., Su, J., Yu, C., Shen, Y., Xie, X., Yu, Y., Yu, X., Chen, S., et al. (2005). The phylogenetic analysis of tetraspanins projects the evolution of cell-cell interactions from unicellular to multicellular organisms. Genomics *86*, 674–684.

Huang, X.A., Yin, H., Sweeney, S., Raha, D., Snyder, M., and Lin, H. (2013). A major epigenetic programming mechanism guided by piRNAs. Dev. Cell *24*, 502–516.

Huertas, P., and Jackson, S.P. (2009). Human CtIP mediates cell cycle control of DNA end resection and double strand break repair. J. Biol. Chem. *284*, 9558–9565.

Hustedt, N., and Durocher, D. (2017). The control of DNA repair by the cell cycle. Nat Cell Biol *19*, 1–9.

Iannelli, F., Galbiati, A., Capozzo, I., Nguyen, Q., Magnuson, B., Michelini, F., D'Alessandro, G., Cabrini, M., Roncador, M., Francia, S., et al. (2017). A damaged genome's transcriptional landscape through multilayered expression profiling around in situ-mapped DNA double-strand breaks. Nat. Commun. *8*, 15656.

Iismaa, S.E., Kaidonis, X., Nicks, A.M., Bogush, N., Kikuchi, K., Naqvi, N., Harvey, R.P.,

Husain, A., and Graham, R.M. (2018). Comparative regenerative mechanisms across different mammalian tissues. NPJ Regen. Med. *3*, 6.
Irianto, J., Xia, Y., Pfeifer, C.R., Athirasala, A., Ji, J., Alvey, C., Tewari, M., Bennett, R.R., Harding, S.M., Liu, A.J., et al. (2017a). DNA Damage Follows Repair Factor Depletion and Portends Genome Variation in Cancer Cells after Pore Migration. Curr. Biol. *27*, 210–223.

Irianto, J., Xia, Y., Pfeifer, C.R., Greenberg, R.A., and Discher, D.E. (2017b). As a Nucleus Enters a Small Pore, Chromatin Stretches and Maintains Integrity, Even with DNA Breaks. Biophys. J. *112*, 446–449.

Isermann, P., and Lammerding, J. (2017). Consequences of a tight squeeze: Nuclear envelope rupture and repair. Nucleus *8*, 00–00.

Isolani, M.-E., Conte, M., Deri, P., and Batistoni, R. (2012). Stem cell protection mechanisms in planarians: the role of some heat shock genes. Int. J. Dev. Biol. *56*, 127–133.

Iwabuchi, K., Bartel, P.L., Li, B., Marraccino, R., and Fields, S. (1994). Two cellular proteins that bind to wild-type but not mutant p53. Proc. Natl. Acad. Sci. U. S. A. *91*, 6098–6102.

Jackson, S.P., and Bartek, J. (2009). The DNA-damage response in human biology and disease. Nature *461*, 1071–1078.

Jain, N., Iyer, K.V., Kumar, A., and Shivashankar, G. V (2013). Cell geometric constraints induce modular gene-expression patterns via redistribution of HDAC3 regulated by actomyosin contractility. Proc. Natl. Acad. Sci. U. S. A. *110*, 11349–11354.

Jen, K.-Y., and Cheung, V.G. (2003). Transcriptional response of lymphoblastoid cells to ionizing radiation. Genome Res. *13*, 2092–2100.

Jen, K.-Y., and Cheung, V.G. (2005). Identification of novel p53 target genes in ionizing radiation response. Cancer Res. *65*, 7666–7673.

Jiang, Q., and Greenberg, R.A. (2015). Deciphering the BRCA1 Tumor Suppressor Network. J. Biol. Chem. *290*, 17724–17732.

Johannessen, M., Møller, S., Hansen, T., Moens, U., and Van Ghelue, M. (2006). The multifunctional roles of the four-and-a-half-LIM only protein FHL2. Cell. Mol. Life Sci. *63*, 268–284.

Johnson, J. (1822). Observations on the genus Planaria. PhilTrans R Soc L. *112*, 437–447.

Jones, B.C., Wood, J.G., Chang, C., Tam, A.D., Franklin, M.J., Siegel, E.R., and Helfand, S.L. (2016). A somatic piRNA pathway in the Drosophila fat body ensures metabolic homeostasis and normal lifespan. Nat. Commun. *7*, 13856.

Juliano, C.E., Swartz, S.Z., and Wessel, G.M. (2010). A conserved germline multipotency program. Development *137*, 4113–4126.

Juliano, C.E., Reich, A., Liu, N., Gotzfried, J., Zhong, M., Uman, S., Reenan, R.A., Wessel, G.M., Steele, R.E., and Lin, H. (2014). PIWI proteins and PIWI-interacting RNAs function in Hydra somatic stem cells. Proc Natl Acad Sci U S A *111*, 337–342.

Jun, S., Jung, Y.-S., Suh, H.N., Wang, W., Kim, M.J., Oh, Y.S., Lien, E.M., Shen, X., Matsumoto, Y., McCrea, P.D., et al. (2016). LIG4 mediates Wnt signalling-induced radioresistance. Nat. Commun. *7*, 10994.

Jung, C.-R., Lim, J.H., Choi, Y., Kim, D.-G., Kang, K.J., Noh, S.-M., and Im, D.-S. (2010).

Enigma negatively regulates p53 through MDM2 and promotes tumor cell survival in mice. J. Clin. Invest. *120*, 4493–4506.

Kahn, J., Hayman, T.J., Jamal, M., Rath, B.H., Kramp, T., Camphausen, K., and Tofilon, P.J. (2014). The mTORC1/mTORC2 inhibitor AZD2014 enhances the radiosensitivity of glioblastoma stem-like cells. Neuro. Oncol. *16*, 29–37.

Kamisugi, Y., Whitaker, J.W., and Cuming, A.C. (2016). The Transcriptional Response to DNA-Double-Strand Breaks in Physcomitrella patens. PLoS One *11*, e0161204.

Kang, E., Wang, X., Tippner-Hedges, R., Ma, H., Folmes, C.D.L., Gutierrez, N.M., Lee, Y., Van Dyken, C., Ahmed, R., Li, Y., et al. (2016). Age-Related Accumulation of Somatic Mitochondrial DNA Mutations in Adult-Derived Human iPSCs. Cell Stem Cell *18*, 625–636.

Kao, D., Felix, D., and Aboobaker, A. (2013). The planarian regeneration transcriptome reveals a shared but temporally shifted regulatory program between opposing head and tail scenarios. BMC Genomics *14*, 797.

Karanam, K., Kafri, R., Loewer, A., and Lahav, G. (2012). Quantitative live cell imaging reveals a gradual shift between DNA repair mechanisms and a maximal use of HR in mid S phase. Mol. Cell *47*, 320–329.

Kastenhuber, E.R., and Lowe, S.W. (2017). Putting p53 in Context. Cell *170*, 1062–1078.

Kaushik, S., and Cuervo, A.M. (2015). Proteostasis and aging. Nat. Med. *21*, 1406–1415.

Kaushik, G., Venugopal, A., Ramamoorthy, P., Standing, D., Subramaniam, D., Umar, S., Jensen, R.A., Anant, S., and Mammen, J.M. V (2015). Honokiol inhibits melanoma stem cells by targeting notch signaling. Mol. Carcinog. *54*, 1710–1721.

Keane, M., Semeiks, J., Webb, A.E., Li, Y.I., Quesada, V., Craig, T., Madsen, L.B., van Dam, S., Brawand, D., Marques, P.I., et al. (2015). Insights into the evolution of longevity from the bowhead whale genome. Cell Rep. *10*, 112–122.

Kenyon, J., and Gerson, S.L. (2007). The role of DNA damage repair in aging of adult stem cells. Nucleic Acids Res. *35*, 7557–7565.

Keren, K., Pincus, Z., Allen, G.M., Barnhart, E.L., Marriott, G., Mogilner, A., and Theriot, J.A. (2008). Mechanism of shape determination in motile cells. Nature *453*, 475–480.

Khanna, K.K., and Jackson, S.P. (2001). DNA double-strand breaks: signaling, repair and the cancer connection. Nat. Genet. *27*, 247–254.

Kidd, J.M., Cooper, G.M., Donahue, W.F., Hayden, H.S., Sampas, N., Graves, T., Hansen, N., Teague, B., Alkan, C., Antonacci, F., et al. (2008). Mapping and sequencing of structural variation from eight human genomes. Nature *453*, 56–64.

Kim, E.B., Fang, X., Fushan, A.A., Huang, Z., Lobanov, A. V, Han, L., Marino, S.M., Sun, X., Turanov, A.A., Yang, P., et al. (2011). Genome sequencing reveals insights into physiology and longevity of the naked mole rat. Nature *479*, 223–227.

Kim, J.-H., Thimmulappa, R.K., Kumar, V., Cui, W., Kumar, S., Kombairaju, P., Zhang, H., Margolick, J., Matsui, W., Macvittie, T., et al. (2014a). NRF2-mediated Notch pathway activation enhances hematopoietic reconstitution following myelosuppressive radiation. J. Clin. Invest. *124*, 730–741.

Kim, J.H., Jenrow, K.A., and Brown, S.L. (2014b). Mechanisms of radiation-induced normal tissue toxicity and implications for future clinical trials. Radiat. Oncol. J. *32*, 103–115.

King, R.S., and Newmark, P.A. (2013). In situ hybridization protocol for enhanced detection of gene expression in the planarian Schmidtea mediterranea. BMC Dev. Biol. *13*, 8.

Klein, M.E., Dickson, M.A., Antonescu, C., Qin, L.-X., Dooley, S.J., Barlas, A., Manova, K., Schwartz, G.K., Crago, A.M., Singer, S., et al. (2018). PDLIM7 and CDH18 regulate the turnover of MDM2 during CDK4/6 inhibitor therapy-induced senescence. Oncogene *37*, 5066–5078.

Kniss, J.S., Jiang, L., and Piotrowski, T. (2016). Insights into sensory hair cell regeneration from the zebrafish lateral line. Curr. Opin. Genet. Dev. *40*, 32–40.

Kondo, M., and Akasaka, K. (2010). Regeneration in crinoids. Dev. Growth Differ. *52*, 57–68.

Korbel, J.O., Urban, A.E., Affourtit, J.P., Godwin, B., Grubert, F., Simons, J.F., Kim, P.M., Palejev, D., Carriero, N.J., Du, L., et al. (2007). Paired-end mapping reveals extensive structural variation in the human genome. Science *318*, 420–426.

Kramer, N., Walzl, A., Unger, C., Rosner, M., Krupitza, G., Hengstschläger, M., and Dolznig, H. (2013). In vitro cell migration and invasion assays. Mutat. Res. - Rev. Mutat. Res. *752*, 10–24.

Krause, M., Dubrovska, A., Linge, A., and Baumann, M. (2017). Cancer stem cells: Radioresistance, prediction of radiotherapy outcome and specific targets for combined treatments. Adv. Drug Deliv. Rev. *109*, 63–73.

Kreso, A., and Dick, J.E. (2014). Evolution of the cancer stem cell model. Cell Stem Cell *14*, 275–291.

Krishnakumar, R., and Kraus, W.L. (2010). PARP-1 regulates chromatin structure and transcription through a KDM5B-dependent pathway. Mol. Cell *39*, 736–749.

Krisko, A., and Radman, M. (2013). Biology of extreme radiation resistance: the way of Deinococcus radiodurans. Cold Spring Harb. Perspect. Biol. *5*, 1–12.

Kulkarni, A., McNeill, D.R., Gleichmann, M., Mattson, M.P., and Wilson, D.M. (2008). XRCC1 protects against the lethality of induced oxidative DNA damage in nondividing neural cells. Nucleic Acids Res. *36*, 5111–5121.

Kumar, A., Mazzanti, M., Mistrik, M., Kosar, M., Beznoussenko, G. V., Mironov, A.A., Garrè, M., Parazzoli, D., Shivashankar, G. V., Scita, G., et al. (2014). ATR mediates a checkpoint at the nuclear envelope in response to mechanical stress. Cell *158*, 633–646.

Labbé, R.M., Irimia, M., Currie, K.W., Lin, A., Zhu, S.J., Brown, D.D.R., Ross, E.J., Voisin, V., Bader, G.D., Blencowe, B.J., et al. (2012). A comparative transcriptomic analysis reveals conserved features of stem cell pluripotency in planarians and mammals. Stem Cells *30*, 1734–1745.

Lagunas-Rangel, F.A., and Chávez-Valencia, V. (2017). Learning of Nature: the Curious Case of the Naked Mole Rat. Mech. Ageing Dev. *164*, 76–81.

Lai, A.G., and Aboobaker, A.A. (2018). EvoRegen in animals: Time to uncover deep conservation or convergence of adult stem cell evolution and regenerative processes. Dev. Biol. *433*, 118–131.

Lai, A.G., Kosaka, N., Abnave, P., Sahu, S., and Aboobaker, A.A. (2018). The abrogation of condensin function provides independent evidence for defining the self-renewing population of pluripotent stem cells. Dev. Biol. *433*, 218–226.

Lake, C.M., Holsclaw, J.K., Bellendir, S.P., Sekelsky, J., and Hawley, R.S. (2013). The development of a monoclonal antibody recognizing the Drosophila melanogaster phosphorylated histone H2A variant (γ-H2AV). G3 (Bethesda). *3*, 1539–1543.

Lamm, N., Ben-David, U., Golan-Lev, T., Storchová, Z., Benvenisty, N., and Kerem, B. (2016). Genomic Instability in Human Pluripotent Stem Cells Arises from Replicative Stress and Chromosome Condensation Defects. Cell Stem Cell *18*, 253–261.

Lapan, S.W., and Reddien, P.W. (2011). dlx and sp6-9 Control optic cup regeneration in a prototypic eye. PLoS Genet. *7*, e1002226.

Latella, L., Lukas, J., Simone, C., Puri, P.L., and Bartek, J. (2004). Differentiation-induced radioresistance in muscle cells. Mol. Cell. Biol. *24*, 6350–6361.

Lazo, P.A. (2007). Functional implications of tetraspanin proteins in cancer biology. Cancer Sci. *98*, 1666–1677.

Lee, H.-J., Li, C.-F., Ruan, D., Powers, S., Thompson, P.A., Frohman, M.A., and Chan, C.-H. (2016). The DNA Damage Transducer RNF8 Facilitates Cancer Chemoresistance and Progression through Twist Activation. Mol. Cell *63*, 1021–1033.

Lee, J.-H., Park, S.-J., Hariharasudhan, G., Kim, M.-J., Jung, S.M., Jeong, S.-Y., Chang, I.-Y., Kim, C., Kim, E., Yu, J., et al. (2017). ID3 regulates the MDC1-mediated DNA damage response in order to maintain genome stability. Nat. Commun. *8*, 903.

Lee, K.Y., Chung, K.Y., and Koo, H.S. (2010). The involvement of FANCM, FANCI, and checkpoint proteins in the interstrand DNA crosslink repair pathway is conserved in C. elegans. DNA Repair (Amst). *9*, 374–382.

Lee, S.E., Pellicioli, A., Vaze, M.B., Sugawara, N., Malkova, A., Foiani, M., and Haber, J.E. (2003). Yeast Rad52 and Rad51 recombination proteins define a second pathway of DNA damage assessment in response to a single double-strand break. Mol. Cell. Biol. *23*, 8913–8923.

Lee, Y., Katyal, S., Li, Y., El-Khamisy, S.F., Russell, H.R., Caldecott, K.W., and McKinnon, P.J. (2009). The genesis of cerebellar interneurons and the prevention of neural DNA damage require XRCC1. Nat. Neurosci. *12*, 973–980.

Lehmann, R. (2012). Germline stem cells: origin and destiny. Cell Stem Cell *10*, 729–739.

Lei, K., Thi-Kim Vu, H., Mohan, R.D., McKinney, S.A., Seidel, C.W., Alexander, R., Gotting, K., Workman, J.L., and Sánchez Alvarado, A. (2016). Egf Signaling Directs Neoblast Repopulation by Regulating Asymmetric Cell Division in Planarians. Dev. Cell *38*, 413–429.

Levin, H.L., and Moran, J. V (2011). Dynamic interactions between transposable elements and their hosts. Nat. Rev. Genet. *12*, 615–627.

Levin-Zaidman, S., Englander, J., Shimoni, E., Sharma, A.K., Minton, K.W., and Minsky, A. (2003). Ringlike structure of the Deinococcus radiodurans genome: a key to radioresistance? Science *299*, 254–256.

Levy, J.M.M., Towers, C.G., and Thorburn, A. (2017). Targeting autophagy in cancer. Nat. Rev. Cancer *17*, 528–542.

Li, L., and Clevers, H. (2010). Coexistence of quiescent and active adult stem cells in mammals. Science *327*, 542–545.

Li, L., Chen, Z., Ding, X., Shan, Z., Liu, L., and Guo, J. (2015). Deep sequencing analysis of the Kineococcus radiotolerans transcriptome in response to ionizing radiation. Microbiol. Res. *170*, 248–254.

Li, M., He, Y., Dubois, W., Wu, X., Shi, J., and Huang, J. (2012). Distinct regulatory mechanisms and functions for p53-activated and p53-repressed DNA damage response genes in embryonic stem cells. Mol. Cell *46*, 30–42.

Liang, G., and Zhang, Y. (2013). Genetic and epigenetic variations in iPSCs: potential causes and implications for application. Cell Stem Cell *13*, 149–159.

Lieber, M.R. (2008). The mechanism of human nonhomologous DNA end joining. J. Biol. Chem. *283*, 1–5.

Lieber, M.R. (2010). The Mechanism of Double-Strand DNA Break Repair by the Nonhomologous DNA End-Joining Pathway. Annu. Rev. Biochem. *79*, 181–211.

Lim, R.S.M., Anand, A., Nishimiya-Fujisawa, C., Kobayashi, S., and Kai, T. (2014). Analysis of Hydra PIWI proteins and piRNAs uncover early evolutionary origins of the piRNA pathway. Dev. Biol. *386*, 237–251.

Lim, Y.C., Roberts, T.L., Day, B.W., Harding, A., Kozlov, S., Kijas, A.W., Ensbey, K.S., Walker, D.G., and Lavin, M.F. (2012). A role for homologous recombination and abnormal cell-cycle progression in radioresistance of glioma-initiating cells. Mol. Cancer Ther. *11*, 1863–1872.

Lin, T., Chao, C., Saito, S., Mazur, S.J., Murphy, M.E., Appella, E., and Xu, Y. (2005). p53 induces differentiation of mouse embryonic stem cells by suppressing Nanog expression. Nat. Cell Biol. *7*, 165–171.

Liu, J., and Heyer, W.-D. (2011). Who's who in human recombination: BRCA2 and RAD52. Proc. Natl. Acad. Sci. *108*, 441–442.

Liu, J.C., Guan, X., Ryan, J.A., Rivera, A.G., Mock, C., Agrawal, V., Agarwal, V., Letai, A., Lerou, P.H., and Lahav, G. (2013a). High mitochondrial priming sensitizes hESCs to DNA-damage-induced apoptosis. Cell Stem Cell *13*, 483–491.

Liu, S.-Y., Selck, C., Friedrich, B., Lutz, R., Vila-Farré, M., Dahl, A., Brandl, H., Lakshmanaperumal, N., Henry, I., and Rink, J.C. (2013b). Reactivating head regrowth in a regeneration-deficient planarian species. Nature *500*, 81–84.

Liu, Y., Burness, M.L., Martin-Trevino, R., Guy, J., Bai, S., Harouaka, R., Brooks, M.D., Shang, L., Fox, A., Luther, T.K., et al. (2017). RAD51 Mediates Resistance of Cancer Stem Cells to PARP Inhibition in Triple-Negative Breast Cancer. Clin. Cancer Res. *23*, 514–522.

Liu, Y.-P., Zhu, H.-F., Liu, D.-L., Hu, Z.-Y., Li, S.-N., Kan, H.-P., Wang, X.-Y., and Li, Z.-G. (2016). DcR3 induces epithelial-mesenchymal transition through activation of the TGF-β3/SMAD signaling pathway in CRC. Oncotarget *7*, 77306–77318.

Lodish, H., Berk, A., Zipursky, S.L., Matsudaira, P., Baltimore, D., and Darnell, J. (2004). Molecular Cell Biology (W. H. Freeman).

Lok, B.H., Carley, A.C., Tchang, B., and Powell, S.N. (2013). RAD52 inactivation is synthetically lethal with deficiencies in BRCA1 and PALB2 in addition to BRCA2 through

RAD51-mediated homologous recombination. Oncogene *32*, 3552–3558.

Lombardo, Y., Scopelliti, A., Cammareri, P., Todaro, M., Iovino, F., Ricci-Vitiani, L., Gulotta, G., Dieli, F., de Maria, R., and Stassi, G. (2011). Bone morphogenetic protein 4 induces differentiation of colorectal cancer stem cells and increases their response to chemotherapy in mice. Gastroenterology *140*, 297–309.

López-Otín, C., Blasco, M.A., Partridge, L., Serrano, M., and Kroemer, G. (2013). The hallmarks of aging. Cell *153*, 1194–1217.

Lovejoy, C.A., and Cortez, D. (2009). Common mechanisms of PIKK regulation. DNA Repair (Amst). *8*, 1004–1008.

Lu, K.L., and Yamashita, Y.M. (2017). Germ cell connectivity enhances cell death in response to DNA damage in theDrosophila testis. Elife *6*. pii: e27960

Lu, T.-P., Hsu, Y.-Y., Lai, L.-C., Tsai, M.-H., and Chuang, E.Y. (2014). Identification of gene expression biomarkers for predicting radiation exposure. Sci. Rep. *4*, 6293.

Lüpertz, R., Chovolou, Y., Unfried, K., Kampkötter, A., Wätjen, W., and Kahl, R. (2008). The forkhead transcription factor FOXO4 sensitizes cancer cells to doxorubicin-mediated cytotoxicity. Carcinogenesis *29*, 2045–2052.

Ma, H., Rao, L., Wang, H.L., Mao, Z.W., Lei, R.H., Yang, Z.Y., Qing, H., and Deng, Y.L. (2013). Transcriptome analysis of glioma cells for the dynamic response to γ-irradiation and dual regulation of apoptosis genes: a new insight into radiotherapy for glioblastomas. Cell Death Dis. *4*, e895.

Ma, X., Han, Y., Song, X., Do, T., Yang, Z., Ni, J., and Xie, T. (2016). DNA damage-induced CHK2 activation compromises germline stem cell self-renewal and lineage differentiation. Development *41*, 4312–4323.

Maciejowski, J., Li, Y., Bosco, N., Campbell, P.J., and De Lange, T. (2015). Chromothripsis and Kataegis Induced by Telomere Crisis. Cell *163*, 1641–1654.

Madabhushi, R., Pan, L., and Tsai, L.-H. (2014). DNA damage and its links to neurodegeneration. Neuron *83*, 266–282.

Malik, H.S., and Henikoff, S. (2003). Phylogenomics of the nucleosome. Nat. Struct. Biol. *10*, 882–891.

Mandal, P.K., Blanpain, C., and Rossi, D.J. (2011). DNA damage response in adult stem cells: pathways and consequences. Nat. Rev. Mol. Cell Biol. *12*, 198–202.

Marion, R.M., Strati, K., Li, H., Tejera, A., Schoeftner, S., Ortega, S., Serrano, M., and Blasco, M.A. (2009). Telomeres acquire embryonic stem cell characteristics in induced pluripotent stem cells. Cell Stem Cell *4*, 141–154.

Marión, R.M., López de Silanes, I., Mosteiro, L., Gamache, B., Abad, M., Guerra, C., Megías, D., Serrano, M., and Blasco, M.A. (2017). Common Telomere Changes during In Vivo Reprogramming and Early Stages of Tumorigenesis. Stem Cell Reports *8*, 460–475.

Marnef, A., Cohen, S., and Legube, G. (2017). Transcription-Coupled DNA Double-Strand Break Repair: Active Genes Need Special Care. J. Mol. Biol. *429*, 1277–1288.

Martin, J.S., Winkelmann, N., Petalcorin, M.I.R., McIlwraith, M.J., and Boulton, S.J. (2005). RAD-51-dependent and -independent roles of a Caenorhabditis elegans BRCA2-related

protein during DNA double-strand break repair. Mol. Cell. Biol. *25*, 3127–3139.

Massagué, J. (2008). TGFbeta in Cancer. Cell *134*, 215–230.

Matsumura, H., Mohri, Y., Binh, N.T., Morinaga, H., Fukuda, M., Ito, M., Kurata, S., Hoeijmakers, J., and Nishimura, E.K. (2016). Hair follicle aging is driven by transepidermal elimination of stem cells via COL17A1 proteolysis. Science *351*, aad4395.

Mayshar, Y., Ben-David, U., Lavon, N., Biancotti, J.-C., Yakir, B., Clark, A.T., Plath, K., Lowry, W.E., and Benvenisty, N. (2010). Identification and classification of chromosomal aberrations in human induced pluripotent stem cells. Cell Stem Cell *7*, 521–531.

McAuliffe, S.M., Morgan, S.L., Wyant, G.A., Tran, L.T., Muto, K.W., Chen, Y.S., Chin, K.T., Partridge, J.C., Poole, B.B., Cheng, K.-H., et al. (2012). Targeting Notch, a key pathway for ovarian cancer stem cells, sensitizes tumors to platinum therapy. Proc. Natl. Acad. Sci. U. S. A. *109*, E2939-48.

Melguizo-Sanchis, D., Xu, Y., Taheem, D., Yu, M., Tilgner, K., Barta, T., Gassner, K., Anyfantis, G., Wan, T., Elango, R., et al. (2018). iPSC modeling of severe aplastic anemia reveals impaired differentiation and telomere shortening in blood progenitors. Cell Death Dis. *9*, 128.

Ménissier de Murcia, J., Ricoul, M., Tartier, L., Niedergang, C., Huber, A., Dantzer, F., Schreiber, V., Amé, J.-C., Dierich, A., LeMeur, M., et al. (2003). Functional interaction between PARP-1 and PARP-2 in chromosome stability and embryonic development in mouse. EMBO J. *22*, 2255–2263.

Michelini, F., Pitchiaya, S., Vitelli, V., Sharma, S., Gioia, U., Pessina, F., Cabrini, M., Wang, Y., Capozzo, I., Iannelli, F., et al. (2017). Damage-induced lncRNAs control the DNA damage response through interaction with DDRNAs at individual double-strand breaks. Nat. Cell Biol. *19*.

Mihaylova, Y., Abnave, P., Kao, D., Hughes, S., Lai, A., Jaber-Hijazi, F., Kosaka, N., and Aboobaker, A.A. (2018). Conservation of epigenetic regulation by the MLL3/4 tumour suppressor in planarian pluripotent stem cells. Nat. Commun. *9*, 3633.

Milyavsky, M., Gan, O.I., Trottier, M., Komosa, M., Tabach, O., Notta, F., Lechman, E., Hermans, K.G., Eppert, K., Konovalova, Z., et al. (2010). A distinctive DNA damage response in human hematopoietic stem cells reveals an apoptosis-independent role for p53 in self-renewal. Cell Stem Cell *7*, 186–197.

Mirman, Z., Lottersberger, F., Takai, H., Kibe, T., Gong, Y., Takai, K., Bianchi, A., Zimmermann, M., Durocher, D., and de Lange, T. (2018). 53BP1-RIF1-shieldin counteracts DSB resection through CST- and Polα-dependent fill-in. Nature *560*, 112–116.

Moehrle, B.M., Nattamai, K., Brown, A., Florian, M.C., Ryan, M., Vogel, M., Bliederhaeuser, C., Soller, K., Prows, D.R., Abdollahi, A., et al. (2015). Stem Cell-Specific Mechanisms Ensure Genomic Fidelity within HSCs and upon Aging of HSCs. Cell Rep. *13*, 2412–2424.

Mohrin, M., Bourke, E., Alexander, D., Warr, M.R., Barry-Holson, K., Le Beau, M.M., Morrison, C.G., and Passegué, E. (2010). Hematopoietic stem cell quiescence promotes error-prone DNA repair and mutagenesis. Cell Stem Cell *7*, 174–185.

Molinaro, A.M., and Pearson, B.J. (2016). In silico lineage tracing through single cell transcriptomics identifies a neural stem cell population in planarians. Genome Biol. *17*, 87.

Momcilovic, O., Knobloch, L., Fornsaglio, J., Varum, S., Easley, C., and Schatten, G. (2010). DNA damage responses in human induced pluripotent stem cells and embryonic stem cells. PLoS One *5*, e13410.

Montell, D.J. (2003). Border-cell migration: The race is on. Nat. Rev. Mol. Cell Biol. *4*, 13–24.

Morgan, T.H. (1898). Experimental studies of the regeneration of Planaria maculata. Arch. Für Entwickelungsmechanik Der Org. *7*, 364–397.

Morgan, T.H. (1901). Regeneration (New york: Macmillan).

Morita, M., Best, J.B., and Noel, J. (1969). Electron microscopic studies of planarian regeneration. I. Fine structure of neoblasts in Dugesia dorotocephala. J. Ultrastruct. Res. *27*, 7–23.

Morrison, S.J., and Spradling, A.C. (2008). Stem cells and niches: mechanisms that promote stem cell maintenance throughout life. Cell *132*, 598–611.

Moskalev, A., Zhikrivetskaya, S., Krasnov, G., Shaposhnikov, M., Proshkina, E., Borisoglebsky, D., Danilov, A., Peregudova, D., Sharapova, I., Dobrovolskaya, E., et al. (2015). A comparison of the transcriptome of Drosophila melanogaster in response to entomopathogenic fungus, ionizing radiation, starvation and cold shock. BMC Genomics *16 Suppl 1*, S8.

Mouton, S., Willems, M., Back, P., Braeckman, B.P., and Borgonie, G. (2009). Demographic analysis reveals gradual senescence in the flatworm Macrostomum lignano. Front. Zool. *6*, 15.

De Mulder, K., Kuales, G., Pfister, D., Willems, M., Egger, B., Salvenmoser, W., Thaler, M., Gorny, A.-K., Hrouda, M., Borgonie, G., et al. (2009). Characterization of the stem cell system of the acoel Isodiametra pulchra. BMC Dev. Biol. *9*, 69.

Munoz, I.M., Jowsey, P.A., Toth, R., and Rouse, J. (2007). Phospho-epitope binding by the BRCT domains of hPTIP controls multiple aspects of the cellular response to DNA damage. Nucleic Acids Res. *35*, 5312–5322.

Murina, O., von Aesch, C., Karakus, U., Ferretti, L.P., Bolck, H.A., Hänggi, K., and Sartori, A.A. (2014). FANCD2 and CtIP cooperate to repair DNA interstrand crosslinks. Cell Rep. *7*, 1030–1038.

Nacu, E., and Tanaka, E.M. (2011). Limb regeneration: a new development? Annu. Rev. Cell Dev. Biol. *27*, 409–440.

Narciso, L., Fortini, P., Pajalunga, D., Franchitto, A., Liu, P., Degan, P., Frechet, M., Demple, B., Crescenzi, M., and Dogliotti, E. (2007). Terminally differentiated muscle cells are defective in base excision DNA repair and hypersensitive to oxygen injury. Proc. Natl. Acad. Sci. U. S. A. *104*, 17010–17015.

Newmark, P.A., and Sánchez Alvarado, A. (2000). Bromodeoxyuridine specifically labels the regenerative stem cells of planarians. Dev. Biol. *220*, 142–153.

Newmark, P.A., and Sánchez Alvarado, A. (2002). Not your father’s planarian: a classic model enters the era of functional genomics. Nat. Rev. Genet. *3*, 210–219.

Newmark, P.A., Reddien, P.W., Cebrià, F., and Sánchez Alvarado, A. (2003). Ingestion of bacterially expressed double-stranded RNA inhibits gene expression in planarians. Proc.

Natl. Acad. Sci. U. S. A. *100 Suppl*, 11861–11865.

Noordermeer, S.M., Adam, S., Setiaputra, D., Barazas, M., Pettitt, S.J., Ling, A.K., Olivieri, M., Álvarez-Quilón, A., Moatti, N., Zimmermann, M., et al. (2018). The shieldin complex mediates 53BP1-dependent DNA repair. Nature *560*, 117–121.

O'Neil, N.J., Bailey, M.L., and Hieter, P. (2017). Synthetic lethality and cancer. Nat. Rev. Genet. *18*, 613–623.

Ochs, F., Somyajit, K., Altmeyer, M., Rask, M.-B., Lukas, J., and Lukas, C. (2016). 53BP1 fosters fidelity of homology-directed DNA repair. Nat. Struct. Mol. Biol. *23*, 714–721.

Oderberg, I.M., Li, D.J., Scimone, M.L., Gaviño, M.A., and Reddien, P.W. (2017). Landmarks in Existing Tissue at Wounds Are Utilized to Generate Pattern in Regenerating Tissue. Curr. Biol. *27*, 733–742.

Oh, J., Lee, Y.D., and Wagers, A.J. (2014). Stem cell aging: mechanisms, regulators and therapeutic opportunities. Nat. Med. *20*, 870–880.

Oliver, L., Hue, E., Séry, Q., Lafargue, A., Pecqueur, C., Paris, F., and Vallette, F.M. (2013). Differentiation-related response to DNA breaks in human mesenchymal stem cells. Stem Cells *31*, 800–807.

Omerovic, J., Clague, M.J., and Prior, I.A. (2010). Phosphatome profiling reveals PTPN2, PTPRJ and PTEN as potent negative regulators of PKB/Akt activation in Ras-mutated cancer cells. Biochem. J. *426*, 65–72.

Önal, P., Grün, D., Adamidi, C., Rybak, A., Solana, J., Mastrobuoni, G., Wang, Y., Rahn, H.-P., Chen, W., Kempa, S., et al. (2012). Gene expression of pluripotency determinants is conserved between mammalian and planarian stem cells. EMBO J. *31*, 2755–2769.

Oviedo, N.J., Pearson, B.J., Levin, M., and Sánchez Alvarado, A. (2008). Planarian PTEN homologs regulate stem cells and regeneration through TOR signaling. Dis. Model. Mech. *1*, 131–43; discussion 141.

Özpolat, B.D., and Bely, A.E. (2016). Developmental and molecular biology of annelid regeneration: a comparative review of recent studies. Curr. Opin. Genet. Dev. *40*, 144–153.

Pace, P., Mosedale, G., Hodskinson, M.R., Rosado, I. V, Sivasubramaniam, M., and Patel, K.J. (2010). Ku70 corrupts DNA repair in the absence of the Fanconi anemia pathway. Science *329*, 219–223.

Pajerowski, J.D., Dahl, K.N., Zhong, F.L., Sammak, P.J., and Discher, D.E. (2007). Physical plasticity of the nucleus in stem cell differentiation. Proc. Natl. Acad. Sci. U. S. A. *104*, 15619–15624.

Pajonk, F., Vlashi, E., and McBride, W.H. (2010). Radiation resistance of cancer stem cells: the 4 R's of radiobiology revisited. Stem Cells *28*, 639–648.

Pal, S., and Tyler, J.K. (2016). Epigenetics and aging. Sci. Adv. *2*, e1600584.

Palakodeti, D., Smielewska, M., Lu, Y.-C., Yeo, G.W., and Graveley, B.R. (2008). The PIWI proteins SMEDWI-2 and SMEDWI-3 are required for stem cell function and piRNA expression in planarians. RNA (New York, NY) *14*, 1174–1186.

Panier, S., and Boulton, S.J. (2014). Double-strand break repair: 53BP1 comes into focus. Nat. Rev. Mol. Cell Biol. *15*, 7–18.

Pardo, B., Gómez-González, B., and Aguilera, A. (2009). DNA repair in mammalian cells: DNA double-strand break repair: how to fix a broken relationship. Cell. Mol. Life Sci. *66*, 1039–1056.

Pathania, R., Ramachandran, S., Mariappan, G., Thakur, P., Shi, H., Choi, J.-H., Manicassamy, S., Kolhe, R., Prasad, P.D., Sharma, S., et al. (2016). Combined Inhibition of DNMT and HDAC Blocks the Tumorigenicity of Cancer Stem-like Cells and Attenuates Mammary Tumor Growth. Cancer Res. *76*, 3224–3235.

Paul, K., Wang, M., Mladenov, E., Bencsik-Theilen, A., Bednar, T., Wu, W., Arakawa, H., and Iliakis, G. (2013). DNA ligases I and III cooperate in alternative non-homologous end-joining in vertebrates. PLoS One *8*, e59505.

Pearson, B.J., and Sánchez Alvarado, A. (2008). Regeneration, stem cells, and the evolution of tumor suppression. Cold Spring Harb. Symp. Quant. Biol. *73*, 565–572.

Pearson, B.J., and Sánchez Alvarado, A. (2010). A planarian p53 homolog regulates proliferation and self-renewal in adult stem cell lineages. Development *137*, 213–221.
Pegg, A.E. (2009). Mammalian polyamine metabolism and function. IUBMB Life *61*, 880–894.

Peiris, T.H., Weckerle, F., Ozamoto, E., Ramirez, D., Davidian, D., García-Ojeda, M.E., and Oviedo, N.J. (2012). TOR signaling regulates planarian stem cells and controls localized and organismal growth. J. Cell Sci. *125*, 1657–1665.

Peiris, T.H., Ramirez, D., Barghouth, P.G., Ofoha, U., Davidian, D., Weckerle, F., and Oviedo, N.J. (2016). Regional signals in the planarian body guide stem cell fate in the presence of genomic instability. Development *143*, 1697–1709.

Perina, D., Mikoč, A., Ahel, J., Ćetković, H., Žaja, R., and Ahel, I. (2014). Distribution of protein poly(ADP-ribosyl)ation systems across all domains of life. DNA Repair (Amst). *23*, 4–16.

Perrat, P.N., DasGupta, S., Wang, J., Theurkauf, W., Weng, Z., Rosbash, M., and Waddell, S. (2013). Transposition-driven genomic heterogeneity in the Drosophila brain. Science *340*, 91–95.

Petersen, C.P., and Reddien, P.W. (2008). Smed-Bcatenin-1 Is Required for Anteroposterior Blastema Polarity in Planarian Regeneration. Science *319*, 327–330.

Petersen, C.P., and Reddien, P.W. (2009). Wnt Signaling and the Polarity of the Primary Body Axis. Cell *139*, 1056–1068.

Petersen, C.P., and Reddien, P.W. (2011). Polarized notum activation at wounds inhibits Wnt function to promote planarian head regeneration. Science *332*, 852–855.

Peto, R., Roe, F.J., Lee, P.N., Levy, L., and Clack, J. (1975). Cancer and ageing in mice and men. Br. J. Cancer *32*, 411–426.

Pfeifer, C.R., Alvey, C.M., Irianto, J., and Discher, D.E. (2017). Genome variation across cancers scales with tissue stiffness – An invasion-mutation mechanism and implications for immune cell infiltration. Curr. Opin. Syst. Biol. *2*, 103–114.

Pfeifer, C.R., Xia, Y., Zhu, K., Liu, D., Irianto, J., García, V.M.M., Millán, L.M.S., Niese, B., Harding, S., Deviri, D., et al. (2018). Constricted migration increases DNA damage and independently represses cell cycle. Mol. Biol. Cell *29*, 1948–1962.

Phillips, C.M., Zatarain, J.R., Nicholls, M.E., Porter, C., Widen, S.G., Thanki, K., Johnson, P., Jawad, M.U., Moyer, M.P., Randall, J.W., et al. (2017). Upregulation of Cystathionine-β-Synthase in Colonic Epithelia Reprograms Metabolism and Promotes Carcinogenesis. Cancer Res. *77*, 5741–5754.

Pitti, R.M., Marsters, S.A., Lawrence, D.A., Roy, M., Kischkel, F.C., Dowd, P., Huang, A., Donahue, C.J., Sherwood, S.W., Baldwin, D.T., et al. (1998). Genomic amplification of a decoy receptor for Fas ligand in lung and colon cancer. Nature *396*, 699–703.
Plass, M., Solana, J., Wolf, F.A., Ayoub, S., Misios, A., Glažar, P., Obermayer, B., Theis, F.J., Kocks, C., and Rajewsky, N. (2018). Cell type atlas and lineage tree of a whole complex animal by single-cell transcriptomics. Science *360*.

Proietti-De-Santis, L., Drané, P., and Egly, J.-M. (2006). Cockayne syndrome B protein regulates the transcriptional program after UV irradiation. EMBO J. *25*, 1915–1923.

Raab, M., Gentili, M., de Belly, H., Thiam, H.R., Vargas, P., Jimenez, A.J., Lautenschlaeger, F., Voituriez, R., Lennon-Duménil, A.M., Manel, N., et al. (2016). ESCRT III repairs nuclear envelope ruptures during cell migration to limit DNA damage and cell death. Science *352*, 359–362.

Radford, K.J., Mallesch, J., and Hersey, P. (1995). Suppression of human melanoma cell growth and metastasis by the melanoma-associated antigen CD63 (ME491). Int. J. Cancer *62*, 631–635.

Radman, M. (2016). Protein damage, radiation sensitivity and aging. DNA Repair (Amst). *44*, 186–192.

Rashi-Elkeles, S., Warnatz, H.-J., Elkon, R., Kupershtein, A., Chobod, Y., Paz, A., Amstislavskiy, V., Sultan, M., Safer, H., Nietfeld, W., et al. (2014). Parallel profiling of the transcriptome, cistrome, and epigenome in the cellular response to ionizing radiation. Sci. Signal. *7*, rs3.

Ray Chaudhuri, A., Callen, E., Ding, X., Gogola, E., Duarte, A.A., Lee, J.-E., Wong, N., Lafarga, V., Calvo, J.A., Panzarino, N.J., et al. (2016). Replication fork stability confers chemoresistance in BRCA-deficient cells. Nature *535*, 382–387.

Reddien, P.W. (2018). The Cellular and Molecular Basis for Planarian Regeneration. Cell *175*, 327–345.

Reddien, P.W., and Sánchez Alvarado, A. (2004). Fundamentals of planarian regeneration. Annu. Rev. Cell Dev. Biol. *20*, 725–757.

Reddien, P.W., Bermange, A.L., Murfitt, K.J., Jennings, J.R., and Sánchez Alvarado, A. (2005a). Identification of genes needed for regeneration, stem cell function, and tissue homeostasis by systematic gene perturbation in planaria. Dev. Cell *8*, 635–649.

Reddien, P.W., Oviedo, N.J., Jennings, J.R., Jenkin, J.C., and Sánchez Alvarado, A. (2005b). SMEDWI-2 is a PIWI-like protein that regulates planarian stem cells. Science *310*, 1327–1330.

Rich, J.N. (2007). Cancer stem cells in radiation resistance. Cancer Res. *67*, 8980–8984.

Ridley, A.J., Schwartz, M.A., Burridge, K., Firtel, R.A., Ginsberg, M.H., Borisy, G., Parsons, J.T., and Horwitz, A.R. (2003). Cell migration: integrating signals from front to back. Science *302*, 1704–1709.

Rijkers, T., Van Den Ouweland, J., Morolli, B., Rolink, A.G., Baarends, W.M., Van Sloun, P.P., Lohman, P.H., and Pastink, A. (1998). Targeted inactivation of mouse RAD52 reduces homologous recombination but not resistance to ionizing radiation. Mol. Cell. Biol. *18*, 6423–6429.

Rink, J.C. (2013). Stem cell systems and regeneration in planaria. Dev. Genes Evol. *223*, 67–84.

Rink, J.C., Gurley, K.A., Elliott, S.A., and Sánchez Alvarado, A. (2009). Planarian Hh signaling regulates regeneration polarity and links Hh pathway evolution to cilia. Science *326*, 1406–1410.

Rinkevich, Y., Voskoboynik, A., Rosner, A., Rabinowitz, C., Paz, G., Oren, M., Douek, J., Alfassi, G., Moiseeva, E., Ishizuka, K.J., et al. (2013). Repeated, long-term cycling of putative stem cells between niches in a basal chordate. Dev. Cell *24*, 76–88.

Robb, S.M.C., Gotting, K., Ross, E., and Sánchez Alvarado, A. (2015). SmedGD 2.0: The Schmidtea mediterranea genome database. Genesis *53*, 535–546.

Roberts-Galbraith, R.H., and Newmark, P.A. (2013). Follistatin antagonizes Activin signaling and acts with Notum to direct planarian head regeneration. Proc. Natl. Acad. Sci. *110*, 1363–1368.

Robinton, D.A., and Daley, G.Q. (2012). The promise of induced pluripotent stem cells in research and therapy. Nature *481*, 295–305.

Rockx, D.A., Mason, R., van Hoffen, A., Barton, M.C., Citterio, E., Bregman, D.B., van Zeeland, A.A., Vrieling, H., and Mullenders, L.H. (2000). UV-induced inhibition of transcription involves repression of transcription initiation and phosphorylation of RNA polymerase II. Proc. Natl. Acad. Sci. U. S. A. *97*, 10503–10508.

Rodier, F., and Campisi, J. (2011). Four faces of cellular senescence. J. Cell Biol. *192*, 547–556.

Rodrigues-Moreira, S., Moreno, S.G., Ghinatti, G., Lewandowski, D., Hoffschir, F., Ferri, F., Gallouet, A.-S., Gay, D., Motohashi, H., Yamamoto, M., et al. (2017). Low-Dose Irradiation Promotes Persistent Oxidative Stress and Decreases Self-Renewal in Hematopoietic Stem Cells. Cell Rep. *20*, 3199–3211.

Rogakou, E.P., Pilch, D.R., Orr, A.H., Ivanova, V.S., and Bonner, W.M. (1998). DNA Double-stranded Breaks Induce Histone H2AX Phosphorylation on Serine 139. J. Biol. Chem. *273*, 5858–5868.

Romero, B.T., Evans, D.J., and Aboobaker, A.A. (2012). FACS analysis of the planarian stem cell compartment as a tool to understand regenerative mechanisms. Methods Mol. Biol. *916*, 167–179.

Roschger, C., and Cabrele, C. (2017). The Id-protein family in developmental and cancer-associated pathways. Cell Commun. Signal. *15*, 7.

Rosen, C.F., Gajic, D., and Drucker, D.J. (1990). Ultraviolet radiation induction of ornithine decarboxylase in rat keratinocytes. Cancer Res. *50*, 2631–2635.

Rosner, A., Moiseeva, E., Rinkevich, Y., Lapidot, Z., and Rinkevich, B. (2009). Vasa and the germ line lineage in a colonial urochordate. Dev. Biol. *331*, 113–128.

Rossi, L., Salvetti, A., Marincola, F.M., Lena, A., Deri, P., Mannini, L., Batistoni, R., Wang,

E., and Gremigni, V. (2007). Deciphering the molecular machinery of stem cells: a look at the neoblast gene expression profile. Genome Biol. *8*, R62.

Rossi, L., Cassella, L., Iacopetti, P., Ghezzani, C., Tana, L., Gimenez, G., Ghigo, E., and Salvetti, A. (2018). Insight into stem cell regulation from sub-lethally irradiated worms. Gene *662*, 37–45.

Van Roten, A., Barakat, A.Z.A.-Z., Wouters, A., Tran, T.A., Mouton, S., Noben, J.-P., Gentile, L., and Smeets, K. (2018). A carcinogenic trigger to study the function of tumor suppressor genes in Schmidtea mediterranea. Dis. Model. Mech. *11*.

Roy, B., Venkatachalapathy, S., Ratna, P., Wang, Y., Jokhun, D.S., Nagarajan, M., and Shivashankar, G. V (2018). Laterally confined growth of cells induces nuclear reprogramming in the absence of exogenous biochemical factors. Proc. Natl. Acad. Sci. U. S. A. *115*, E4741–E4750.

Rozanski, A., Moon, H., Brandl, H., Martín-Durán, J.M., Grohme, M.A., Hüttner, K., Bartscherer, K., Henry, I., and Rink, J.C. (2018). PlanMine 3.0-improvements to a mineable resource of flatworm biology and biodiversity. Nucleic Acids Res.

Ruiz, S., Lopez-Contreras, A.J., Gabut, M., Marion, R.M., Gutierrez-Martinez, P., Bua, S., Ramirez, O., Olalde, I., Rodrigo-Perez, S., Li, H., et al. (2015). Limiting replication stress during somatic cell reprogramming reduces genomic instability in induced pluripotent stem cells. Nat. Commun. *6*, 8036.

Ruzankina, Y., Pinzon-Guzman, C., Asare, A., Ong, T., Pontano, L., Cotsarelis, G., Zediak, V.P., Velez, M., Bhandoola, A., and Brown, E.J. (2007). Deletion of the developmentally essential gene ATR in adult mice leads to age-related phenotypes and stem cell loss. Cell Stem Cell *1*, 113–126.

Ryu, J.-S., Kang, S.J., and Koo, H.-S. (2013). The 53BP1 homolog in C. elegans influences DNA repair and promotes apoptosis in response to ionizing radiation. PLoS One *8*, e64028.

Saha, S., Aranda, E., Hayakawa, Y., Bhanja, P., Atay, S., Brodin, N.P., Li, J., Asfaha, S., Liu, L., Tailor, Y., et al. (2016). Macrophage-derived extracellular vesicle-packaged WNTs rescue intestinal stem cells and enhance survival after radiation injury. Nat. Commun. *7*, 13096.

Sahu, S., Dattani, A., and Aboobaker, A.A. (2017). Secrets from immortal worms: What can we learn about biological ageing from the planarian model system? Semin. Cell Dev. Biol. *70*, 108–121.

Sánchez Alvarado, A. (2012). Cellular hyperproliferation and cancer as evolutionary variables. Curr. Biol. *22*, 772–778.

Sánchez Alvarado, A., and Newmark, P.A. (1999). Double-stranded RNA specifically disrupts gene expression during planarian regeneration. Proc. Natl. Acad. Sci. U. S. A. *96*, 5049–5054.

Lo Sardo, V., Ferguson, W., Erikson, G.A., Topol, E.J., Baldwin, K.K., and Torkamani, A. (2017). Influence of donor age on induced pluripotent stem cells. Nat. Biotechnol. *35*, 69–74.

Sartori, A.A., Lukas, C., Coates, J., Mistrik, M., Fu, S., Bartek, J., Baer, R., Lukas, J., and Jackson, S.P. (2007). Human CtIP promotes DNA end resection. Nature *450*, 509.

Sasaki, M., Lange, J., and Keeney, S. (2010). Genome destabilization by homologous recombination in the germ line. Nat. Rev. Mol. Cell Biol. *11*, 182–195.

Scarpa, E., and Mayor, R. (2016). Collective cell migration in development. J. Cell Biol. *212*, 143–155.

Schaible, R., Scheuerlein, A., Danko, M.J., Gampe, J., Martinez, D.E., and Vaupel, J.W. (2015). Constant mortality and fertility over age in Hydra. Proc Natl Acad Sci U S A *112*, 15701–15706.

Schlacher, K., Wu, H., and Jasin, M. (2012). A distinct replication fork protection pathway connects Fanconi anemia tumor suppressors to RAD51-BRCA1/2. Cancer Cell *22*, 106–116.

Schneider, L., Fumagalli, M., and d'Adda di Fagagna, F. (2012). Terminally differentiated astrocytes lack DNA damage response signaling and are radioresistant but retain DNA repair proficiency. Cell Death Differ. *19*, 582–591.

Schultz, M.B., and Sinclair, D.A. (2016). When stem cells grow old: phenotypes and mechanisms of stem cell aging. Development *143*, 3–14.

Schwer, B., Wei, P.-C., Chang, A.N., Kao, J., Du, Z., Meyers, R.M., and Alt, F.W. (2016). Transcription-associated processes cause DNA double-strand breaks and translocations in neural stem/progenitor cells. Proc. Natl. Acad. Sci. U. S. A. *113*, 2258–2263.

Sekelsky, J. (2017). DNA repair in Drosophila: Mutagens, models, and missing genes. Genetics *205*, 471–490.

Seluanov, A., Hine, C., Bozzella, M., Hall, A., Sasahara, T.H.C., Ribeiro, A.A.C.M., Catania, K.C., Presgraves, D.C., and Gorbunova, V. (2008). Distinct tumor suppressor mechanisms evolve in rodent species that differ in size and lifespan. Aging Cell *7*, 813–823.

Sen, P., Shah, P.P., Nativio, R., and Berger, S.L. (2016). Epigenetic Mechanisms of Longevity and Aging. Cell *166*, 822–839.

Sfeir, A., and Symington, L.S. (2015). Microhomology-Mediated End Joining: A Back-up Survival Mechanism or Dedicated Pathway? Trends Biochem. Sci. *40*, 701–714.

Shackleton, M., Vaillant, F., Simpson, K.J., Stingl, J., Smyth, G.K., Asselin-Labat, M.-L., Wu, L., Lindeman, G.J., and Visvader, J.E. (2006). Generation of a functional mammary gland from a single stem cell. Nature *439*, 84–88.

Shah, P., Wolf, K., and Lammerding, J. (2017). Bursting the Bubble - Nuclear Envelope Rupture as a Path to Genomic Instability? Trends Cell Biol. *27*, 546–555.

Shanbhag, N.M., Rafalska-Metcalf, I.U., Balane-Bolivar, C., Janicki, S.M., and Greenberg, R.A. (2010). ATM-dependent chromatin changes silence transcription in cis to DNA double-strand breaks. Cell *141*, 970–981.

Sharp, A.J., Cheng, Z., and Eichler, E.E. (2006). Structural Variation of the Human Genome. Annu. Rev. Genomics Hum. Genet. *7*, 407–442.

Shechter, D., Chitta, R.K., Xiao, A., Shabanowitz, J., Hunt, D.F., and Allis, C.D. (2009). A distinct H2A.X isoform is enriched in Xenopus laevis eggs and early embryos and is phosphorylated in the absence of a checkpoint. Proc. Natl. Acad. Sci. U. S. A. *106*, 749–754.
Shibata, N., Kashima, M., Ishiko, T., Nishimura, O., Rouhana, L., Misaki, K., Yonemura, S., Saito, K., Siomi, H., Siomi, M.C., et al. (2016). Inheritance of a Nuclear PIWI from Pluripotent Stem Cells by Somatic Descendants Ensures Differentiation by Silencing Transposons in Planarian. Dev. Cell *37*, 226–237.

Shiloh, Y., and Ziv, Y. (2013). The ATM protein kinase: regulating the cellular response to

genotoxic stress, and more. Nat. Rev. Mol. Cell Biol. *14*, 197–210.

Shinohara, A., and Ogawa, T. (1998). Stimulation by Rad52 of yeast Rad51- mediated recombination. Nature *391*, 404–407.

Sienski, G., Dönertas, D., and Brennecke, J. (2012). Transcriptional silencing of transposons by Piwi and maelstrom and its impact on chromatin state and gene expression. Cell *151*, 964–980.

Sikes, J.M., and Newmark, P.A. (2013). Restoration of anterior regeneration in a planarian with limited regenerative ability. Nature *500*, 77–80.

Simkin, J., Sammarco, M.C., Dawson, L.A., Schanes, P.P., Yu, L., and Muneoka, K. (2015). The mammalian blastema: regeneration at our fingertips. Regen. (Oxford, England) *2*, 93–105.

Singh, N.P., McCoy, M.T., Tice, R.R., and Schneider, E.L. (1988). A simple technique for quantitation of low levels of DNA damage in individual cells. Exp. Cell Res. *175*, 184–191.

Smerdon, M.J. (1991). DNA repair and the role of chromatin structure. Curr. Opin. Cell Biol. *3*, 422–428.

Smoyer, C.J., and Jaspersen, S.L. (2014). Breaking down the wall: the nuclear envelope during mitosis. Curr. Opin. Cell Biol. *26*, 1–9.

Solana, J. (2013). Closing the circle of germline and stem cells: the Primordial Stem Cell hypothesis. Evodevo *4*, 2.

Solana, J., Lasko, P., and Romero, R. (2009). Spoltud-1 is a chromatoid body component required for planarian long-term stem cell self-renewal. Dev. Biol. *328*, 410–421.

Solana, J., Kao, D., Mihaylova, Y., Jaber-Hijazi, F., Malla, S., Wilson, R., and Aboobaker, A. (2012). Defining the molecular profile of planarian pluripotent stem cells using a combinatorial RNA-seq, RNAi and irradiation approach. Genome Biol. *13*, R19.

Solana, J., Irimia, M., Ayoub, S., Orejuela, M.R., Zywitza, V., Jens, M., Tapial, J., Ray, D., Morris, Q., Hughes, T.R., et al. (2016). Conserved functional antagonism of CELF and MBNL proteins controls stem cell-specific alternative splicing in planarians. Elife *5*, 1–29.

Song, M.S., Salmena, L., and Pandolfi, P.P. (2012). The functions and regulation of the PTEN tumour suppressor. Nat. Rev. Mol. Cell Biol. *13*, 283–296.

Soria, G., Polo, S.E., and Almouzni, G. (2012). Prime, repair, restore: the active role of chromatin in the DNA damage response. Mol. Cell *46*, 722–734.

Soteriou, D., and Fuchs, Y. (2018). A matter of life and death: stem cell survival in tissue regeneration and tumour formation. Nat. Rev. Cancer *18*, 187–201.

Sotiropoulou, P.A., Karambelas, A.E., Debaugnies, M., Candi, A., Bouwman, P., Moers, V., Revenco, T., Rocha, A.S., Sekiguchi, K., Jonkers, J., et al. (2013). BRCA1 deficiency in skin epidermis leads to selective loss of hair follicle stem cells and their progeny. Genes Dev. *27*, 39–51.

Soussi, T., Kroemer, G., Iwabuchi, K., al., et, Sullivan, A., Lu, X., Panier, S., Boulton, S.J., Zimmermann, M., Lange, T. de, et al. (2016). TP53 and 53BP1 Reunited. Trends Cell Biol. *0*, 1693–1696.

Sperka, T., Wang, J., and Rudolph, K.L. (2012). DNA damage checkpoints in stem cells, ageing and cancer. Nat. Rev. Mol. Cell Biol. *13*, 579–590.

Spradling, A., Fuller, M.T., Braun, R.E., and Yoshida, S. (2011). Germline stem cells. Cold Spring Harb. Perspect. Biol. *3*, a002642.

Sprangers, R., Groves, M.R., Sinning, I., and Sattler, M. (2003). High-resolution X-ray and NMR structures of the SMN Tudor domain: conformational variation in the binding site for symmetrically dimethylated arginine residues. J. Mol. Biol. *327*, 507–520.

Steffen, K.K., and Dillin, A. (2016). A Ribosomal Perspective on Proteostasis and Aging. Cell Metab. *23*, 1004–1012.

Stergiou, L., and Hengartner, M.O. (2004). Death and more: DNA damage response pathways in the nematode C. elegans. Cell Death Differ. *11*, 21–28.

Stergiou, L., Eberhard, R., Doukoumetzidis, K., and Hengartner, M.O. (2011). NER and HR pathways act sequentially to promote UV-C-induced germ cell apoptosis in Caenorhabditis elegans. Cell Death Differ. *18*, 897–906.

Stingl, J., Eirew, P., Ricketson, I., Shackleton, M., Vaillant, F., Choi, D., Li, H.I., and Eaves, C.J. (2006). Purification and unique properties of mammary epithelial stem cells. Nature *439*, 993–997.

Sulak, M., Fong, L., Mika, K., Chigurupati, S., Yon, L., Mongan, N.P., Emes, R.D., and Lynch, V.J. (2016). TP53 copy number expansion is associated with the evolution of increased body size and an enhanced DNA damage response in elephants. Elife *5*, 1–30.

Sung, H.Y., Wu, H.-G., Ahn, J.-H., and Park, W.-Y. (2010). Dcr3 inhibit p53-dependent apoptosis in gamma-irradiated lung cancer cells. Int. J. Radiat. Biol. *86*, 780–790.

Swapna, L.S., Molinaro, A.M., Lindsay-Mosher, N., Pearson, B.J., and Parkinson, J. (2018). Comparative transcriptomic analyses and single-cell RNA sequencing of the freshwater planarian Schmidtea mediterranea identify major cell types and pathway conservation. Genome Biol. *19*, 124.

Szczesny, B., Marcatti, M., Zatarain, J.R., Druzhyna, N., Wiktorowicz, J.E., Nagy, P., Hellmich, M.R., and Szabo, C. (2016). Inhibition of hydrogen sulfide biosynthesis sensitizes lung adenocarcinoma to chemotherapeutic drugs by inhibiting mitochondrial DNA repair and suppressing cellular bioenergetics. Sci. Rep. *6*, 36125.

Takaki, T., Montagner, M., Serres, M.P., Le Berre, M., Russell, M., Collinson, L., Szuhai, K., Howell, M., Boulton, S.J., Sahai, E., et al. (2017). Actomyosin drives cancer cell nuclear dysmorphia and threatens genome stability. Nat. Commun. *8*, 16013.

Takubo, K., Ohmura, M., Azuma, M., Nagamatsu, G., Yamada, W., Arai, F., Hirao, A., and Suda, T. (2008). Stem cell defects in ATM-deficient undifferentiated spermatogonia through DNA damage-induced cell-cycle arrest. Cell Stem Cell *2*, 170–182.

Tam, S.Y., Wu, V.W.C., and Law, H.K.W. (2017). Influence of autophagy on the efficacy of radiotherapy. Radiat. Oncol. *12*, 57.

Tan, T.C.J., Rahman, R., Jaber-Hijazi, F., Felix, D.A., Chen, C., Louis, E.J., and Aboobaker, A. (2012). Telomere maintenance and telomerase activity are differentially regulated in asexual and sexual worms. Proc. Natl. Acad. Sci. U. S. A. *109*, 4209–4214.

Tanaka, E.M., and Reddien, P.W. (2011). The cellular basis for animal regeneration. Dev.

Cell *21*, 172–185.

Tasaki, J., Uchiyama-Tasaki, C., and Rouhana, L. (2016). Analysis of Stem Cell Motility In Vivo Based on Immunodetection of Planarian Neoblasts and Tracing of BrdU-Labeled Cells After Partial Irradiation. Methods Mol. Biol. *1365*, 323–338.

Tejada-Romero, B., Carter, J.-M., Mihaylova, Y., Neumann, B., and Aboobaker, A.A. (2015). JNK signalling is necessary for a Wnt- and stem cell-dependent regeneration programme. Development *142*, 2413–2424.

Thatcher, T.H., and Gorovsky, M.A. (1994). Phylogenetic analysis of the core histones H2A, H2B, H3, and H4. Nucleic Acids Res. *22*, 174–179.

Theveneau, E., and Mayor, R. (2012). Neural crest delamination and migration: From epithelium-to-mesenchyme transition to collective cell migration. Dev. Biol. *366*, 34–54.
Thiery, J.P. (2002). Epithelial–mesenchymal transitions in tumour progression. Nat. Rev. Cancer *2*, 442–454.

Thiery, J.P. (2003). Epithelial–mesenchymal transitions in development and pathologies. Curr. Opin. Cell Biol. *15*, 740–746.

Thiruvalluvan, M., Barghouth, P.G., Tsur, A., Broday, L., and Oviedo, N.J. (2017). SUMOylation controls stem cell proliferation and regional cell death through Hedgehog signaling in planarians. Cell. Mol. Life Sci.

Le Thomas, A., Rogers, A.K., Webster, A., Marinov, G.K., Liao, S.E., Perkins, E.M., Hur, J.K., Aravin, A.A., and Tóth, K.F. (2013). Piwi induces piRNA-guided transcriptional silencing and establishment of a repressive chromatin state. Genes Dev. *27*, 390–399.

Tomczyk, S., Fischer, K., Austad, S., and Galliot, B. (2015). Hydra, a powerful model for aging studies. Invertebr. Reprod. Dev. *59*, 11–16.

Tomida, J., Takata, K.-I., Bhetawal, S., Person, M.D., Chao, H.-P., Tang, D.G., and Wood, R.D. (2018). FAM35A associates with REV7 and modulates DNA damage responses of normal and BRCA1-defective cells. EMBO J. *37*.

Török, A., Schiffer, P.H., Schnitzler, C.E., Ford, K., Mullikin, J.C., Baxevanis, A.D., Bacic, A., Frank, U., and Gornik, S.G. (2016). The cnidarian Hydractinia echinata employs canonical and highly adapted histones to pack its DNA. Epigenetics Chromatin *9*, 36.

Tothova, Z., Kollipara, R., Huntly, B.J., Lee, B.H., Castrillon, D.H., Cullen, D.E., McDowell, E.P., Lazo-Kallanian, S., Williams, I.R., Sears, C., et al. (2007). FoxOs are critical mediators of hematopoietic stem cell resistance to physiologic oxidative stress. Cell *128*, 325–339.

Trappmann, B., Gautrot, J.E., Connelly, J.T., Strange, D.G.T., Li, Y., Oyen, M.L., Cohen Stuart, M.A., Boehm, H., Li, B., Vogel, V., et al. (2012). Extracellular-matrix tethering regulates stem-cell fate. Nat. Mater. *11*, 642–649.

Tsuji, T., Katsurano, M., Ibaragi, S., Shima, K., Sasaki, A., and Hu, G.-F. (2007). Ornithine decarboxylase antizyme upregulates DNA-dependent protein kinase and enhances the nonhomologous end-joining repair of DNA double-strand breaks in human oral cancer cells. Biochemistry *46*, 8920–8932.

Tu, K.C., Cheng, L.-C., Tk Vu, H., Lange, J.J., McKinney, S.A., Seidel, C.W., and Sánchez Alvarado, A. (2015). Egr-5 is a post-mitotic regulator of planarian epidermal differentiation. Elife *4*, 1–5.

Tubbs, A., and Nussenzweig, A. (2017). Endogenous DNA Damage as a Source of Genomic Instability in Cancer. Cell *168*, 644–656.

Tulin, A., Stewart, D., and Spradling, A.C. (2002). The Drosophila heterochromatic gene encoding poly(ADP-ribose) polymerase (PARP) is required to modulate chromatin structure during development. Genes Dev. *16*, 2108–2119.

Uhler, C., and Shivashankar, G. V (2018). Nuclear Mechanopathology and Cancer Diagnosis. Trends in Cancer *4*, 320–331.

Unno, J., Itaya, A., Taoka, M., Sato, K., Tomida, J., Sakai, W., Sugasawa, K., Ishiai, M., Ikura, T., Isobe, T., et al. (2014). FANCD2 binds CtIP and regulates DNA-end resection during DNA interstrand crosslink repair. Cell Rep. *7*, 1039–1047.

Vahidi Ferdousi, L., Rocheteau, P., Chayot, R., Montagne, B., Chaker, Z., Flamant, P., Tajbakhsh, S., and Ricchetti, M. (2014). More efficient repair of DNA double-strand breaks in skeletal muscle stem cells compared to their committed progeny. Stem Cell Res. *13*, 492–507.

Valdez, B.C., Li, Y., Murray, D., Liu, Y., Nieto, Y., Champlin, R.E., and Andersson, B.S. (2018). Combination of a hypomethylating agent and inhibitors of PARP and HDAC traps PARP1 and DNMT1 to chromatin, acetylates DNA repair proteins, down-regulates NuRD and induces apoptosis in human leukemia and lymphoma cells. Oncotarget *9*, 3908–3921.

Valenzano, D.R., Aboobaker, A., Seluanov, A., and Gorbunova, V. (2017). Non-canonical aging model systems and why we need them. EMBO J. e201796837.

Vanzin, C.S., Manfredini, V., Marinho, A.E., Biancini, G.B., Ribas, G.S., Deon, M., Wyse, A.T. de S., Wajner, M., and Vargas, C.R. (2014). Homocysteine contribution to DNA damage in cystathionine β-synthase-deficient patients. Gene *539*, 270–274.
Vasilyev, A., Liu, Y., Mudumana, S., Mangos, S., Lam, P.-Y., Majumdar, A., Zhao, J., Poon, K.-L., Kondrychyn, I., Korzh, V., et al. (2009). Collective Cell Migration Drives Morphogenesis of the Kidney Nephron. PLoS Biol. *7*, e1000009.

Vazquez, J.M., Sulak, M., Chigurupati, S., and Lynch, V.J. (2018). A Zombie LIF Gene in Elephants Is Upregulated by TP53 to Induce Apoptosis in Response to DNA Damage. Cell Rep. *24*, 1765–1776.

Veeraraghavan, J., Natarajan, M., Aravindan, S., Herman, T.S., and Aravindan, N. (2011). Radiation-triggered tumor necrosis factor (TNF) alpha-NFkappaB cross-signaling favors survival advantage in human neuroblastoma cells. J. Biol. Chem. *286*, 21588–21600.

Venere, M., Hamerlik, P., Wu, Q., Rasmussen, R.D., Song, L.A., Vasanji, A., Tenley, N., Flavahan, W.A., Hjelmeland, A.B., Bartek, J., et al. (2014). Therapeutic targeting of constitutive PARP activation compromises stem cell phenotype and survival of glioblastoma-initiating cells. Cell Death Differ. *21*, 258–269.

Venkata Narayanan, I., Paulsen, M.T., Bedi, K., Berg, N., Ljungman, E.A., Francia, S., Veloso, A., Magnuson, B., di Fagagna, F. d'Adda, Wilson, T.E., et al. (2017). Transcriptional and post-transcriptional regulation of the ionizing radiation response by ATM and p53. Sci. Rep. *7*, 43598.

Venkitaraman, A.R. (2014). Cancer suppression by the chromosome custodians, BRCA1 and BRCA2. Science *343*, 1470–1475.

Vermezovic, J., Stergiou, L., Hengartner, M.O., and d'Adda di Fagagna, F. (2012). Differential regulation of DNA damage response activation between somatic and germline

cells in Caenorhabditis elegans. Cell Death Differ. *19*, 1847–1855.

Vilenchik, M.M., and Knudson, A.G. (2006). Radiation dose-rate effects, endogenous DNA damage, and signaling resonance. Proc. Natl. Acad. Sci. U. S. A. *103*, 17874–17879.

Di Virgilio, M., Callen, E., Yamane, A., Zhang, W., Jankovic, M., Gitlin, A.D., Feldhahn, N., Resch, W., Oliveira, T.Y., Chait, B.T., et al. (2013). Rif1 prevents resection of DNA breaks and promotes immunoglobulin class switching. Science *339*, 711–715.

Vishavkarma, R., Raghavan, S., Kuyyamudi, C., Majumder, A., Dhawan, J., and Pullarkat, P.A. (2014). Role of Actin Filaments in Correlating Nuclear Shape and Cell Spreading. PLoS One *9*, e107895.

Vitale, I., Manic, G., De Maria, R., Kroemer, G., and Galluzzi, L. (2017). DNA Damage in Stem Cells. Mol. Cell *66*, 306–319.

Vorotnikova, E., Rosenthal, R.A., Tries, M., Doctrow, S.R., and Braunhut, S.J. (2010). Novel synthetic SOD/catalase mimetics can mitigate capillary endothelial cell apoptosis caused by ionizing radiation. Radiat. Res. *173*, 748–759.

Wagner, D.E., Wang, I.E., and Reddien, P.W. (2011). Clonogenic neoblasts are pluripotent adult stem cells that underlie planarian regeneration. Science *332*, 811–816.

Wagner, D.E., Ho, J.J., and Reddien, P.W. (2012). Genetic regulators of a pluripotent adult stem cell system in planarians identified by RNAi and clonal analysis. Cell Stem Cell *10*, 299–311.

Walter, M., Teissandier, A., Pérez-Palacios, R., and Bourc'his, D. (2016). An epigenetic switch ensures transposon repression upon dynamic loss of DNA methylation in embryonic stem cells. Elife *5*, 7250–7257.

Wang, H., and Xu, X. (2017). Microhomology-mediated end joining: new players join the team. Cell Biosci. *7*, 6.

Wang, B., Matsuoka, S., Carpenter, P.B., and Elledge, S.J. (2002). 53BP1, a mediator of the DNA damage checkpoint. Science *298*, 1435–1438.

Wang, J., Wakeman, T.P., Lathia, J.D., Hjelmeland, A.B., Wang, X.-F., White, R.R., Rich, J.N., and Sullenger, B.A. (2010a). Notch promotes radioresistance of glioma stem cells. Stem Cells *28*, 17–28.

Wang, Y., Stary, J.M., Wilhelm, J.E., and Newmark, P. a (2010b). A functional genomic screen in planarians identifies novel regulators of germ cell development. Genes Dev. *24*, 2081–2092.

Ward, I.M., Minn, K., van Deursen, J., and Chen, J. (2003). p53 Binding protein 53BP1 is required for DNA damage responses and tumor suppression in mice. Mol. Cell. Biol. *23*, 2556–2563.

Weick, E.-M., and Miska, E.A. (2014). piRNAs: from biogenesis to function. Development *141*, 3458–3471.

Wenemoser, D., and Reddien, P.W. (2010). Planarian regeneration involves distinct stem cell responses to wounds and tissue absence. Dev. Biol. *344*, 979–991.

Wenemoser, D., Lapan, S.W., Wilkinson, A.W., Bell, G.W., and Reddien, P.W. (2012). A molecular wound response program associated with regeneration initiation in planarians.

Genes Dev. *26*, 988–1002.

Weyemi, U., Redon, C.E., Choudhuri, R., Aziz, T., Maeda, D., Boufraqech, M., Parekh, P.R., Sethi, T.K., Kasoji, M., Abrams, N., et al. (2016). The histone variant H2A.X is a regulator of the epithelial-mesenchymal transition. Nat. Commun. *7*, 10711.

van Wolfswinkel, J.C. (2014). Piwi and potency: PIWI proteins in animal stem cells and regeneration. Integr. Comp. Biol. *54*, 700–713.

van Wolfswinkel, J.C., Wagner, D.E., and Reddien, P.W. (2014). Single-cell analysis reveals functionally distinct classes within the planarian stem cell compartment. Cell Stem Cell *15*, 326–339.

Woodward, W.A., Chen, M.S., Behbod, F., Alfaro, M.P., Buchholz, T.A., and Rosen, J.M. (2007). WNT/beta-catenin mediates radiation resistance of mouse mammary progenitor cells. Proc. Natl. Acad. Sci. U. S. A. *104*, 618–623.

Worbs, T., Hammerschmidt, S.I., and Förster, R. (2017). Dendritic cell migration in health and disease. Nat. Rev. Immunol. *17*, 30–48.

Wudarski, J., Simanov, D., Ustyantsev, K., de Mulder, K., Grelling, M., Grudniewska, M., Beltman, F., Glazenburg, L., Demircan, T., Wunderer, J., et al. (2017). Efficient transgenesis and annotated genome sequence of the regenerative flatworm model Macrostomum lignano. Nat. Commun. *8*, 2120.

Wurtzel, O., Cote, L.E., Poirier, A., Satija, R., Regev, A., and Reddien, P.W. (2015). A Generic and Cell-Type-Specific Wound Response Precedes Regeneration in Planarians. Dev. Cell *35*, 632–645.

Wurtzel, O., Oderberg, I.M., and Reddien, P.W. (2017). Planarian Epidermal Stem Cells Respond to Positional Cues to Promote Cell-Type Diversity. Dev. Cell *40*, 491–504.e5.

Xia, B., Sheng, Q., Nakanishi, K., Ohashi, A., Wu, J., Christ, N., Liu, X., Jasin, M., Couch, F.J., and Livingston, D.M. (2006). Control of BRCA2 cellular and clinical functions by a nuclear partner, PALB2. Mol. Cell *22*, 719–729.

Xia, Y., Ivanovska, I.L., Zhu, K., Smith, L., Irianto, J., Pfeifer, C.R., Alvey, C.M., Ji, J., Liu, D., Cho, S., et al. (2018). Nuclear rupture at sites of high curvature compromises retention of DNA repair factors. J. Cell Biol. 1–13.

Xiang, Y., Miller, D.E., Ross, E.J., Sánchez Alvarado, A., and Hawley, R.S. (2014). Synaptonemal complex extension from clustered telomeres mediates full-length chromosome pairing in Schmidtea mediterranea. Proc. Natl. Acad. Sci. *111*, E5159–E5168.

Xu, F., Fang, Y., Yan, L., Xu, L., Zhang, S., Cao, Y., Xu, L., Zhang, X., Xie, J., Jiang, G., et al. (2017a). Nuclear localization of Beclin 1 promotes radiation-induced DNA damage repair independent of autophagy. Sci. Rep. *7*, 45385.

Xu, X., Fan, Z., Liang, C., Li, L., Wang, L., Liang, Y., Wu, J., Chang, S., Yan, Z., Lv, Z., et al. (2017b). A signature motif in LIM proteins mediates binding to checkpoint proteins and increases tumour radiosensitivity. Nat. Commun. *8*, 14059.

Yamazaki, S., Iwama, A., Takayanagi, S., Morita, Y., Eto, K., Ema, H., and Nakauchi, H. (2006). Cytokine signals modulated via lipid rafts mimic niche signals and induce hibernation in hematopoietic stem cells. EMBO J. *25*, 3515–3523.

Yan, W.X., Mirzazadeh, R., Garnerone, S., Scott, D., Schneider, M.W., Kallas, T., Custodio,

J., Wernersson, E., Li, Y., Gao, L., et al. (2017). BLISS is a versatile and quantitative method for genome-wide profiling of DNA double-strand breaks. Nat. Commun. *8*, 15058.

Yang, H.J., Kim, N., Seong, K.M., Youn, H., and Youn, B. (2013). Investigation of radiation-induced transcriptome profile of radioresistant non-small cell lung cancer A549 cells using RNA-seq. PLoS One *8*, e59319.

Yang, X., Wang, H., and Jiao, B. (2017). Mammary gland stem cells and their application in breast cancer. Oncotarget *8*, 10675–10691.

Yazinski, S.A., and Zou, L. (2016). Functions, Regulation, and Therapeutic Implications of the ATR Checkpoint Pathway. Annu. Rev. Genet. *50*, 155–173.

Yin, S., Huang, Y., Zhangfang, Y., Zhong, X., Li, P., Huang, J., Liu, D., and Songyang, Z. (2016). SmedOB1 is Required for Planarian Homeostasis and Regeneration. Sci. Rep. *6*, 34013.

Yoshida, Y., Takahashi, K., Okita, K., Ichisaka, T., and Yamanaka, S. (2009). Hypoxia enhances the generation of induced pluripotent stem cells. Cell Stem Cell *5*, 237–241.

Yoshida-Noro, C., and Tochinai, S. (2010). Stem cell system in asexual and sexual reproduction of Enchytraeus japonensis (Oligochaeta, Annelida). Dev. Growth Differ. *52*, 43–55.

Youds, J.L., Barber, L.J., Ward, J.D., Collis, S.J., O 'neil, N.J., Boulton, S.J., and Rose, A.M. (2008). DOG-1 Is the Caenorhabditis elegans BRIP1/FANCJ Homologue and Functions in Interstrand Cross-Link Repair. Mol. Cell. Biol. *28*, 1470–1479.

Yousefi, M., Li, N., Nakauka-Ddamba, A., Wang, S., Davidow, K., Schoenberger, J., Yu, Z., Jensen, S.T., Kharas, M.G., and Lengner, C.J. (2016). Msi RNA-binding proteins control reserve intestinal stem cell quiescence. J. Cell Biol. *215*, 401–413.

Yu, H., Aravindan, N., Xu, J., and Natarajan, M. (2017). Inter- and intra-cellular mechanism of NF-kB-dependent survival advantage and clonal expansion of radio-resistant cancer cells. Cell. Signal. *31*, 105–111.

Yuan, M., Eberhart, C.G., and Kai, M. (2014). RNA binding protein RBM14 promotes radio-resistance in glioblastoma by regulating DNA repair and cell differentiation. Oncotarget *5*, 2820–2826.

Yun, M. (2015). Changes in Regenerative Capacity through Lifespan. Int. J. Mol. Sci. *16*, 25392–25432.

Yun, M.H., and Hiom, K. (2009). CtIP-BRCA1 modulates the choice of DNA double-strand-break repair pathway throughout the cell cycle. Nature *459*, 460–463.

Zahradka, K., Slade, D., Bailone, A., Sommer, S., Averbeck, D., Petranovic, M., Lindner, A.B., and Radman, M. (2006). Reassembly of shattered chromosomes in Deinococcus radiodurans. Nature *443*, 569–573.

Zeng, A., Li, H., Guo, L., Gao, X., McKinney, S., Wang, Y., Yu, Z., Park, J., Semerad, C., Ross, E., et al. (2018). Prospectively Isolated Tetraspanin+ Neoblasts Are Adult Pluripotent Stem Cells Underlying Planaria Regeneration. Cell *173*, 1593–1608.e20.

Zhang, C.-Z., Spektor, A., Cornils, H., Francis, J.M., Jackson, E.K., Liu, S., Meyerson, M., and Pellman, D. (2015). Chromothripsis from DNA damage in micronuclei. Nature *522*, 179–184.

Zhang, M., Atkinson, R.L., and Rosen, J.M. (2010). Selective targeting of radiation-resistant tumor-initiating cells. Proc. Natl. Acad. Sci. U. S. A. *107*, 3522–3527.

Zhang, P., Wei, Y., Wang, L., Debeb, B.G., Yuan, Y., Zhang, J., Yuan, J., Wang, M., Chen, D., Sun, Y., et al. (2014). ATM-mediated stabilization of ZEB1 promotes DNA damage response and radioresistance through CHK1. Nat. Cell Biol. *16*, 864–875.

Zhang, Y., Xing, Y., Zhang, L., Mei, Y., Yamamoto, K., Mak, T.W., and You, H. (2012). Regulation of cell cycle progression by forkhead transcription factor FOXO3 through its binding partner DNA replication factor Cdt1. Proc. Natl. Acad. Sci. U. S. A. *109*, 5717–5722.

Zhao, X., Yang, H., Jiang, G., Ni, M., Deng, Y., Cai, J., Li, Z., Shen, F., and Tao, X. (2014). Simvastatin attenuates radiation-induced tissue damage in mice. J. Radiat. Res. *55*, 257–264.

Zhao, Y., Yi, J., Tao, L., Huang, G., Chu, X., Song, H., and Chen, L. (2018). Wnt signaling induces radioresistance through upregulating HMGB1 in esophageal squamous cell carcinoma. Cell Death Dis. *9*, 433.

Zhou, L., Zhang, Y., Chen, S., Kmieciak, M., Leng, Y., Lin, H., Rizzo, K.A., Dumur, C.I., Ferreira-Gonzalez, A., Dai, Y., et al. (2015). A regimen combining the Wee1 inhibitor AZD1775 with HDAC inhibitors targets human acute myeloid leukemia cells harboring various genetic mutations. Leukemia *29*, 807–818.

Zhu, S.J., and Pearson, B.J. (2013). The Retinoblastoma pathway regulates stem cell proliferation in freshwater planarians. Dev. Biol. *373*, 442–452.

Zhu, S., Si, M.-L., Wu, H., and Mo, Y.-Y. (2007). MicroRNA-21 targets the tumor suppressor gene tropomyosin 1 (TPM1). J. Biol. Chem. *282*, 14328–14336.

Zhu, S.J., Hallows, S.E., Currie, K.W., Xu, C., and Pearson, B.J. (2015). A mex3 homolog is required for differentiation during planarian stem cell lineage development. Elife *4*.

Zienert, E., Eke, I., Aust, D., and Cordes, N. (2015). LIM-only protein FHL2 critically determines survival and radioresistance of pancreatic cancer cells. Cancer Lett. *364*, 17–24.

Zimmermann, M., Lottersberger, F., Buonomo, S.B., Sfeir, A., and de Lange, T. (2013). 53BP1 regulates DSB repair using Rif1 to control 5’ end resection. Science *339*, 700–704.

Zink, D., Fischer, A.H., and Nickerson, J.A. (2004). Nuclear structure in cancer cells. Nat. Rev. Cancer *4*, 677–687.

Zöller, M. (2009). Tetraspanins: push and pull in suppressing and promoting metastasis. Nat. Rev. Cancer *9*, 40–55.

Zou, L., and Elledge, S.J. (2003). Sensing DNA damage through ATRIP recognition of RPA-ssDNA complexes. Science *300*, 1542–1548.